THE GENESIS AND CONTROLS OF GOLD MINERALIZATION SOUTH OF REHOBOTH, NAMIBIA

by

DEREK WHITFIELD B.Sc Hons

Project presented in partial fulfilment
of the requirements for the degree of
M.Sc. Economic Geology
in the
Department of Geology,
Rhodes University,
Grahamstown.
November, 1990

DECLARATION

All work presented in this mini-thesis is the original work of the author except where specific acknowledgement is made to the work of others.

No portion of this thesis may be reproduced or published without written permission of the author, or the Head of the Geology Department of this University.

Date: 14./ 12 / 90.

Signed: D.K. Whitfield

D.K. Whitfield

CONTENTS

Abstract

Gold mineralization is hosted within gossanous quartz-haematite veins in volcano-sedimentary lithologies of the Klein Aub - Rehoboth basin of the Irumide Belt, Namibia. Mineralization and hydrothermal alteration are restricted to deformed lithologies particularly the metasediments.

Lithological relationships, geochemistry and metallogenic characteristics of the Irumide Belt suggest an intra-continental rift setting. Copper mineralization is well known along the length of the belt, from Klein Aub in the southwest to Ghanzi in the northeast, whereas gold mineralization appears restricted to the Klein Aub - Rehoboth basin. The gold is envisaged ashaving being leached initially from graben fill sequences during rift closure and basin dewatering. Location of the mineralization is strongly controlled by structure and lithological contact zones. Such zones are percieved as having acted as conduit zones for escaping mineralized fluids during basin closure and deformation.

Apart from the lack of an effective mineralizing trap, all features consistent with the development of an ore deposit are present. The largest mineralization traps within the area studied are shear zones followed by lithological contact zones. The Mebi and Blanks gold mines are developed over large shear zones while the Swartmodder and Neuras gold mines are situated over mineralized lithological contacts. The Swartmodder copper mine yielded ore from a mineralized schist enclave within granite. Copper and gold occurrences are attributed to two contrasting styles of mineralization. Copper mineralization is suggested to have developed during initial rifting of the belt (ie. stratabound sedimentary exhalative type), while the gold and minor copper resulted from rift closure and basin dewatering.

Although no economical orebody was realized during the course of this study a model is proposed for the development of mineralization within the Irumide basement lithologies as a working hypothesis for future exploration.

LIST OF FIGURES

pg.

LIST OF TABLES

LIST OF PLATES

LIST OF FIGURES - APPENDIX 1

LIST OF PLATES - APPENDIX 1

pg.

1 INTRODUCTION

The study area, Neuras grant M46/3/1658, is located in the Rehoboth Baster Gebiet of Namibia. The area is situated some 90 km SW of Windhoek, the capital of Namibia, and 8 km SW of the town of Rehoboth. The area studied is bounded by latitudes 23°20'55'' S, 23°28'53'' S and 17°00'00'' E, 17°07'08''E which encompasses an area of about 400 Km². This area is within a semi-reserve occupied by the Baster (coloured) people prior to the German settlement of 1885. The capital of the proclaimed 'Gebiet' is Rehoboth (4th largest town in Namibia). This is centrally situated and serviced by a road and rail network from Windhoek.

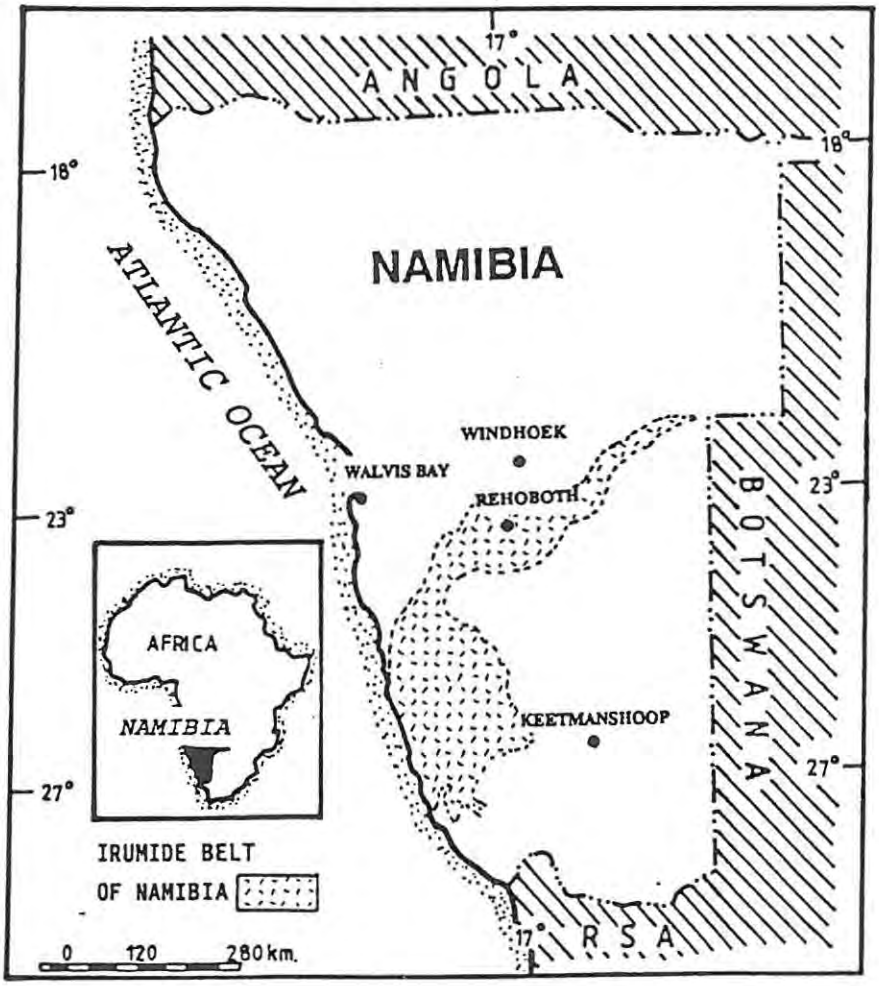

Figure 1: A regional locality map.

1.1 Thesis Objectives

The intention of the study was to investigate the potential of the area for a low-tonnage, low grade gold deposit, which may have been missed or ignored by earlier workers. In order to obtain a clear perspective of the

occurrences and controls of mineralization, it was necessary to characterise the tectonic setting of the area. A hypothesis, based largely on lithological associations, trace element geochemistry and metallogenic characteristics, is proposed for the area studied. The basic premise of the study is to determine the genesis and control of gold mineralization within the Irumide basement lithologies.

The study area was mapped and lithologically sampled at a scale of 1 : 25000 and target areas of specific intrest, were covered at a scale of 1 : 1000. From the mapping exercise it became apparent that the mineralization within the area can be classified into two categories, base metal (copper) and precious metal (gold) mineralization.

The study was carried out during a period of four months field mapping and a further six months laboratory work. This was followed up by the collation of a number of "in-house" Gold Fields Namibia (GFN) reports and relevant literature.

1.2 Discovery, History and Production

Gold mineralization in the Rehoboth Province was first discovered in 1888. Exploitation, however, only occurred in the early part of the following century culminating in the 'pegging boom' of 1933-34. Despite the opening of numerous mines and prospects, documentation is limited and only a small amount was published, the most important being De Kock (1934), Reuning (1937), Burg (1942) and Martin (1965).

Mining traditionally took place on a small scale. Narrow shafts were sunk to depths generally less than 30m, although it is recorded that a shaft in excess of 70 m was sunk at the Neuras Gold Mine. Access was usually by ladders and ore appears to have been hoisted by means of bucket and winch. Most shafts were sunk down dip of a mineralized zone and mining appears to have been generally short lived, probably as a result of highly irregular grades and the impersistent nature of the mineralization.

Numerous mines operated within the study area. They include Blank's Mine, Swartmodder Mine, Neuras Mine and Mebi Mine (currently operational) which primarily mined gold while Raabies and Swartmodder Mines primarily mined copper. Swartmodder and Neuras gold mines were economically the most important of the gold mines. The first shafts were sunk at the Neuras Mine

by the Hanseatische Minengesellschaft in 1910. Subsequently devaluation of the pound, in 1932, gave new impetus to gold mining and another three shafts were sunk. Four shafts were sunk on the Swartmodder Gold Mine during 1937 but limited reserves finally led to the closure of mines soon afterwards.

Documentation of grades, production and ore reserves is scarce in the literature. Very few records of mines within the study area were unearthed during an extensive literature search. The Swartmodder Gold mine is recorded as having yielded 32.5 kg of Au (Cooke, 1965). The only figure recorded for Neuras mine is an average grade of the concentrate of 68.5 g/t. The Mebi mine, currently in production since 1979, is reported as having mined between 30 000 and 50 000 t at an average grade of 2.2 g/t (Siebeck, 1989 pers comm.).

2. THE GEOLOGY OF THE IRUMIDE BELT IN NAMIBIA AND BOTSWANA

2.1 Introduction

Four main tectonometamorphic cycles characterise the Precambrian evolution of Southern and Central Africa. These are :

Limpopo - Liberia tectonometamorphic	(2700 ± 200 Ma)
Eburnian tectonometamorphic	(2000 ± 200 Ma)
Kibaran or Irumide tectonometamorphic	(1100 ± 200 Ma)
Pan African tectonometamorphic	(600 ± 150 Ma)

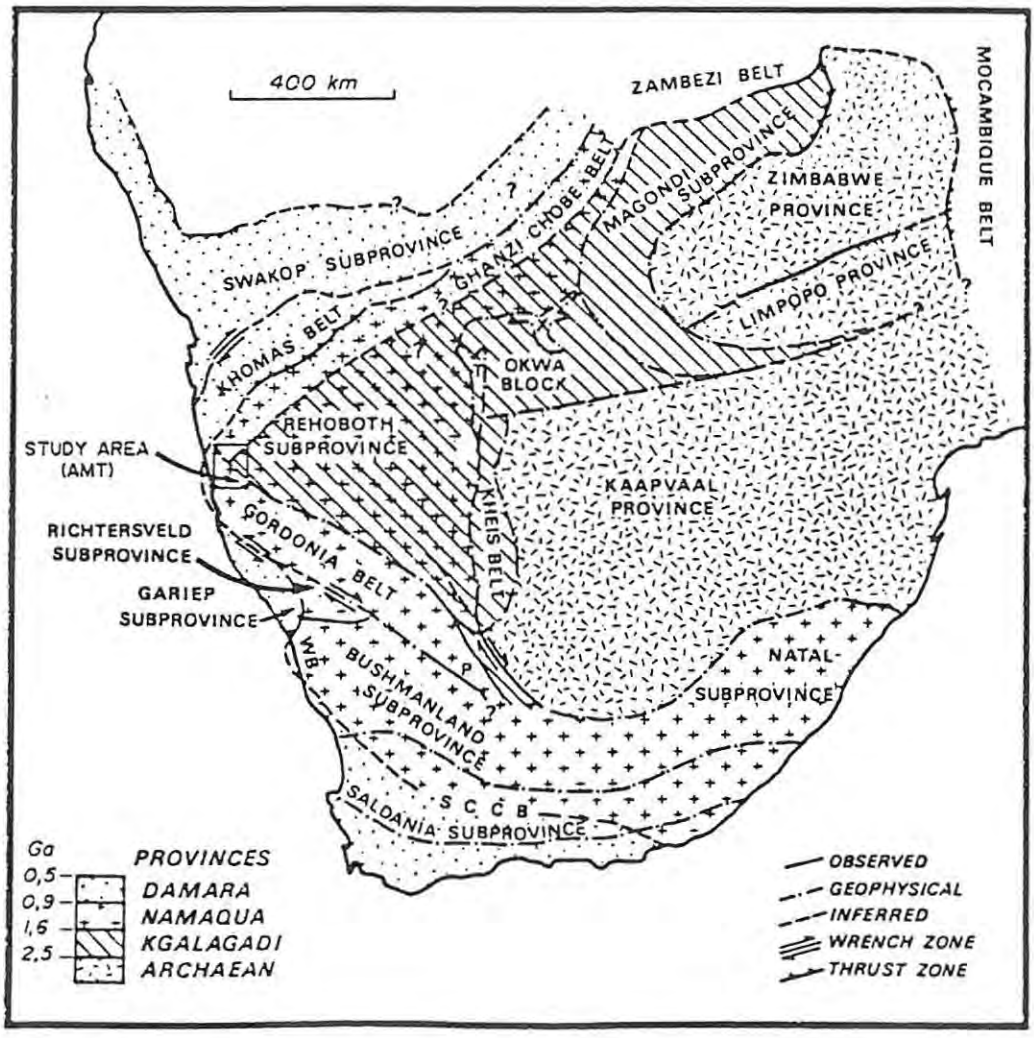

Figure 2.1(a): Major tectonic provinces of Southern Africa (after Hartnady et al., 1985).

Of these cycles the Irumide tectonogenesis affected comparatively small portions of the African continent. Three major mobile belts evolved during the Kibaran event, namely the Kibarides (Cahen, 1970), the Rehoboth - Irumide Belt (Ackerman, 1960) and Namaqua-Natal belts (Figure 2.1(a)). Significantly, these belt transect older shield areas and terminate within them, thus excluding their origin through continental accretion (Kröner, 1976).

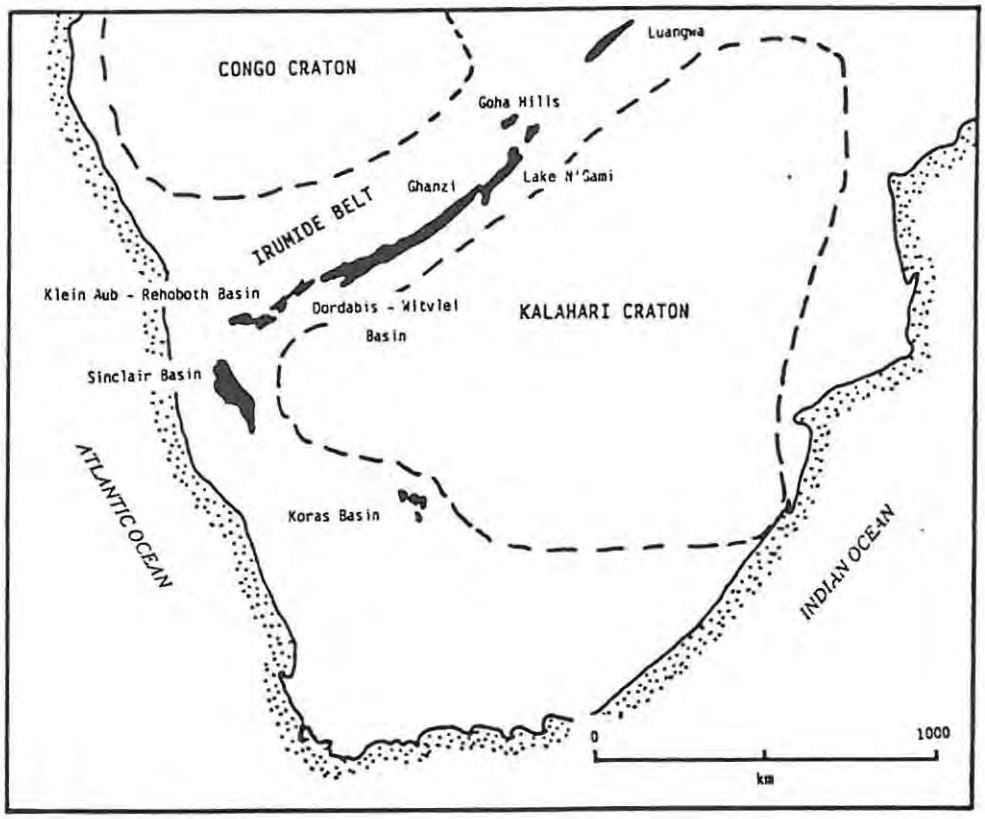

Figure 2.1(b): The Irumide Belt of Southern Africa (modified after Borg, 1988).

The term Irumide was first applied by Ackermann (1960) to a belt of north-easterly trending, strongly folded rocks which occur to the east and north-east of Broken Hill in Zambia. Recent research and exploration indicates that the northeast - trending Irumide Belt extends from Namibia, through northwestern Botswana, Zambia and terminates in Malawi (Bloomfield, 1981). According to Bloomfield (op sit.), the NE-trending Irumide belt, in Malawi, is a 120 km -wide zone of basal granite gneisses overlain by more than 10000m of banded metasiltstones and metaquartzites. In Zambia the Irumide belt becomes extensively overprinted by the Zambesi and Mozambique Belts and appears to form the southeastern margin of the stable Bengwelu block. The Irumide belt represents a linear zone of much sheared metasediments and metavolcanic units whose inter-relationship is poorly known. Deformation was polycyclic and resulted in intense faulting and folding accompanied by widespread migmatization and crustal melting.

This section deals with a sector of the Irumide belt, from Namibia to Botswana. The Irumide belt in Namibia forms the southwestern strike continuation of the Zambian Irumide. It has been proposed that the southern extension of the Irumide belt in turn forms part of the Natal - Namaqua Mobile Belt (Hartnady et al.,1985). Lithostratigraphic relationships are confusing; uncertainty is attributed to the rapid facies changes, lack of geochronological data (SACS, 1980; Watters, 1982), limited outcrops and complex contact relationships caused by superimposed thrusting and shearing. Facies variation and ratios of sedimentary:volcanic rocks in different parts of the Irumide Belt necessitate subdivision of the Irumide belt into various sub-basins. These are : The Koras basin, Sinclair-Helmeringhausen basin, Klein Aub-Rehoboth basin, Dordabis-Witvlei basin and the Ghanzi-Lake N'Gami basin (Borg, 1988). They are briefly discussed below.

2.2 The Koras Basin, Cape Province South Africa

The Koras basin occurs to the east of Upington and consists of volcano-sedimentary sequence known as the Koras Group (SACS, 1980). The lithologies of this group comprise a succession of immature, coarse clastic continental red-bed sediments and a suite of bimodal lavas. For a detailed description of the lithologies, the reader is referred to Grobler et al. (1977) and Sanderson (1983). The lithologies are thought to have been deposited in narrow yoked graben basins, whose deep-seated faults tapped magma sources.

2.3 The Sinclair - Helmeringhausen Basin

The Sinclair basin occupies the largest area of exposed late-middle Proterozoic rocks of the entire Irumide belt. The sedimentary and volcanic rocks of the Sinclair Sequence (SACS, 1980) crop out between the sand cover of the Namib desert to the west and the rocks of the late Precambrian Nama Group to the east. To the north they are overlain by Nama Group and the Naukluft Nappe Complex. In the south the Sinclair Sequence borders rocks of the Namaqualand Metamorphic Complex. The Sinclair Group in this area consists essentially of five distinct major volcanic and volcaniclastic units invaded extensively at intervals by high level, intermediate, granite bodies, a large syenite intrusion and dense swarms of basic and felsic dykes (Watters, 1977).

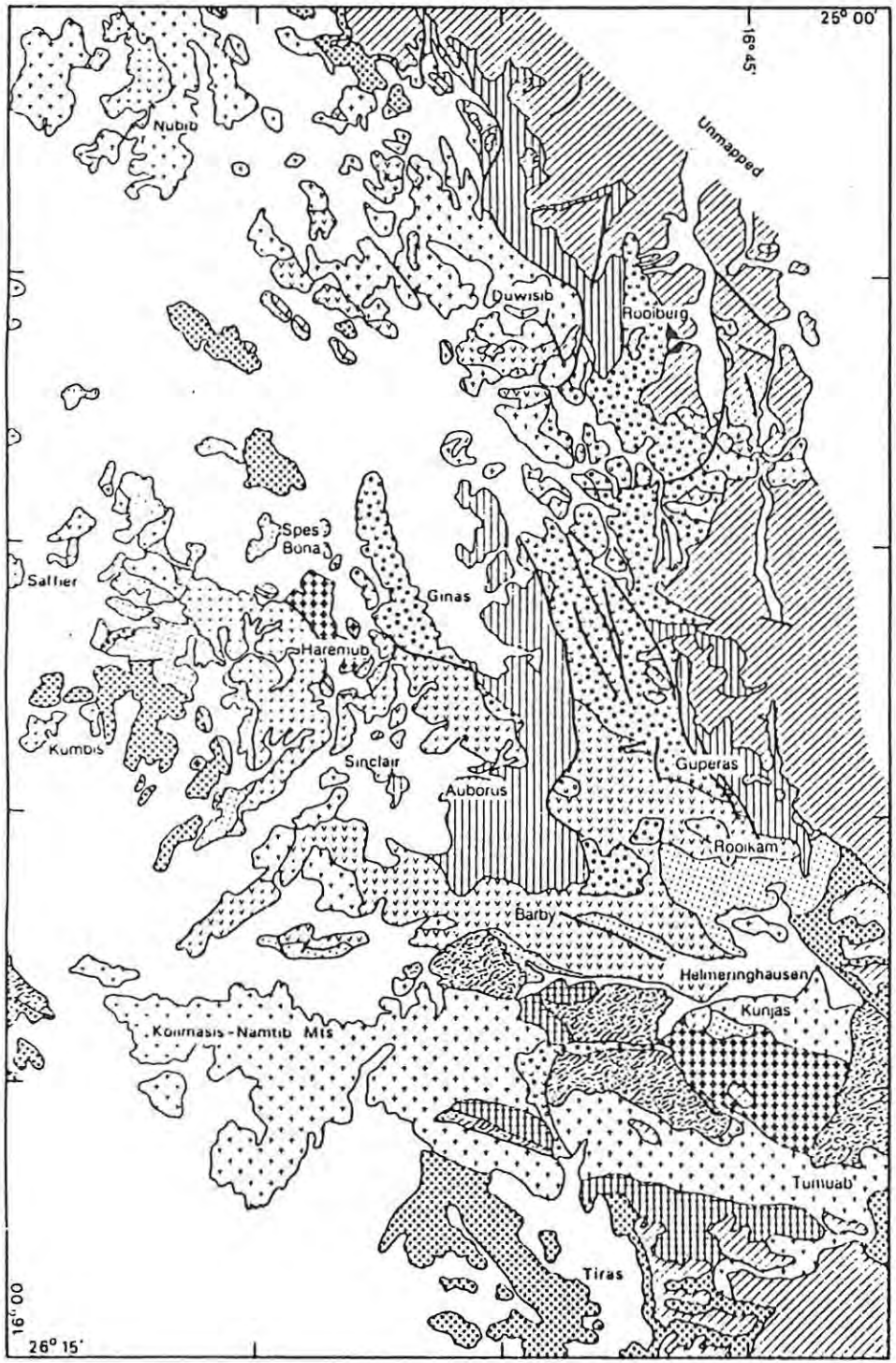

Figure 2.3(a): Geological map of the Sinclair-Helmeringhausen Area (after Watters, 1977).

FIGURE 1: GEOLOGICAL MAP OF THE SINCLAIR – HELMERINGHAUSEN AREA*

	Dunes, rock-waste, sand	
	Black limestone, quartzite, sandstone, conglomerate, shale	NAMA GROUP
	Red sandstone, conglomerate, shale	— AUBORUS FORMATION
	Red porphyritic-granophyric granite	— ROOIBERG GRANITE
	Rhyolitic and basic lava, intrusives and volcaniclastics, sandstone conglomerate	— GUPERAS FORMATION
	Red porphyritic-granophyric granite	— NUBIB GRANITE
	Grey syenite (Spes Bona syenite)	— BARBY FORMATION
	Basic lava and intrusives, rhyolitic lava, volcaniclastics, quartzite, conglomerate	— BARBY FORMATION
	Arkose, shale, grit, quartzite, conglomerate	— KUNJAS FORMATION
	Red-grey hybrid granite	— HAREMUB GRANITE
	Rhyolitic lava and volcaniclastics, basic lava, arkose, grit, shale	— NAGATIS FORMATION
		— GREY GRANODIORITE
	Amphibolite, gneiss, metabasalt, schist, metasediment,	— KUMBIS COMPLEX
	Major faults	

SINCLAIR GROUP

LOCALITY MAP

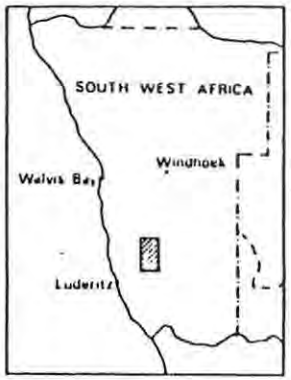

0 10 20 30 km

* Compiled from data published and unpublished by [illegible]

Tectonic activity in the Irumide Belt was accompanied by sporadic granite emplacement. Volcanic activity and related sedimentation appear to have been initially restricted to the Sinclair - Helmeringhausen area of Namibia (1300 - 1100 Ma) (Mason, 1981).

Characteristic of the Sinclair - Helmeringhausen area is a cyclic evolutionary pattern which commenced with the generation and emplacement of basic to intermediate magma followed by felsic magma (Figure 2.3(b)). Subsequent vertical tectonics led to the development of local elongate graben. Erosion of the earlier igneous and sedimentary units provided immature clastic debris which was deposited in the newly formed basins. The cycle then ended with a period of relatively mild faulting and tilting of the volcano-clastic sequences (Watters, 1977).

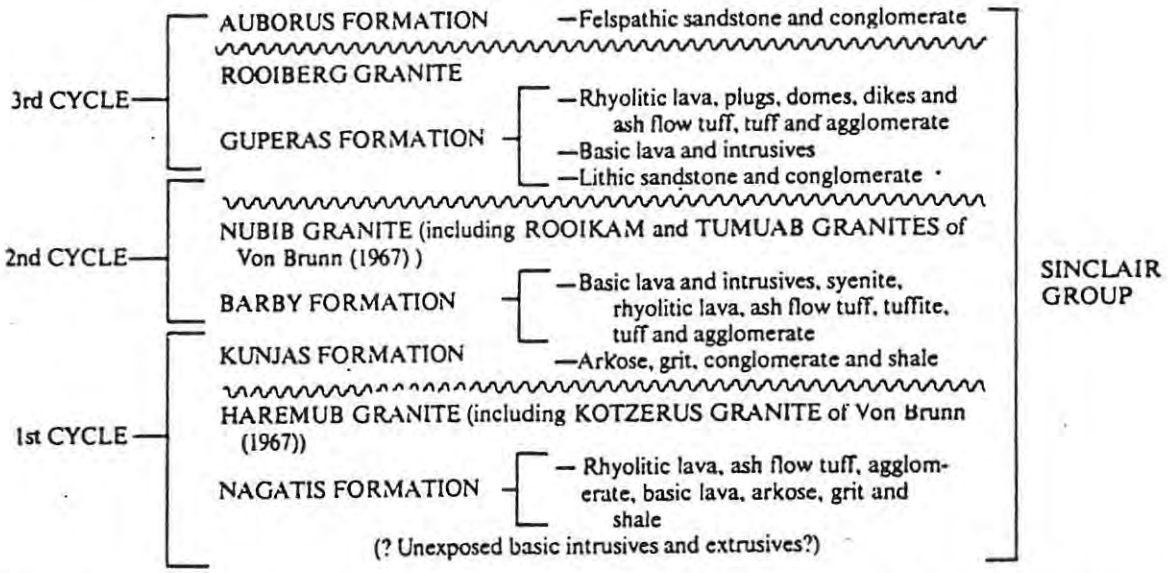

Figure 2.3(b): Evolutionary Cycles of the Sinclair Group (after Watters, 1976).

The majority of the faults, shear zones and foliation fabrics are parallel (ie. NW - trending) to the basin axis. Major faults are believed to have provided channelways for igneous intrusions/extrusions, and to have played an important role in basin subsidence. Thickness and distribution of the Guperas Formation indicate two northerly trending grabens while rhyolitic plugs of the same formation are interpreted as feeder channels to volcanic units.

2.4 The Klein Aub - Rehoboth Basin

Attempts to elucidate the pre-Damaran geological history of Namibia have often been based on unravelling the complex stratigraphic relations in the Rehoboth region. As a contribution to the timing of the pre-Damara igneous, sedimentary and metamorphic events in this important region, several granitoid suites have been isotopically and geochemically investigated (Ziegler & Stoessel, 1988; Stoessel and Ziegler, 1988; this study).

Two major periods of pre-Damara granitoid emplacement are indicated by Rb/Sr ages determined by Reid et al. (1986):

(1) an older 1800 - 1600 Ma event so far only recognised in a small part of the region near Rehoboth; and

(2) a younger 1200 - 1000 Ma event which is widespread throughout the region and represents a major magmatic episode, at least in terms of the volume of products involved (Reid et al., 1988).

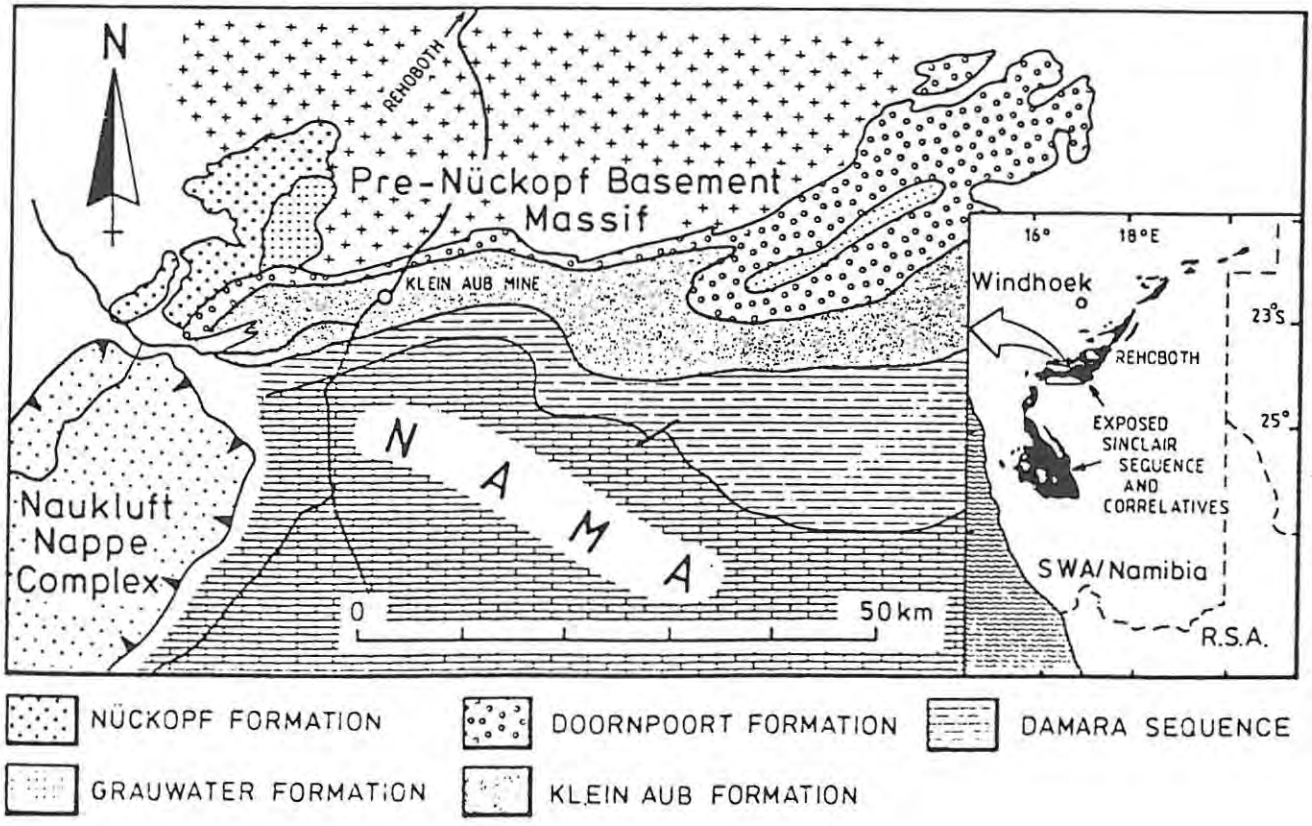

Figure 2.4(a): A geological sketch map of the Klein Aub and surrounding areas (after Borg & Maiden, 1986a).

The older granitoids include the Naub Diorite (1725 ± 52 Ma) and the Swartmodder Granite (1639 ± 25 Ma), whereas the voluminous younger granitoids are represented by Biesipoort Granite (1222 ± 45 Ma), Piksteel Granodiorite (1170 ± 20 Ma) and Gamsberg Granite (1079 ± 25 Ma). The Weener Quartz Diorite may also be part of the younger granitoid event (dated at 1207 ± 170 Ma), but an older age of about 1800 Ma cannot be ruled out (Reid et al., 1988).

The Klein Aub - Rehoboth basin contains a volcano-sedimentary succession with a total thickness of about 11000 m (Hoal, 1989). These mid/late Proterozoic formations are exposed between the igneous and metamorphic complexes of the Rehoboth inlier and Damara Sequences to the north, and the Nama Group sediments to the south. The metavolcano-metasedimentary lithologies of the Sinclair Group overlie a block-faulted basement. Predominant lithologies in the area include molasse-type red-bed sequences, conglomerates intercalated with aeolian, playa and lacustrine sediments, and minor mafic and felsic magmas (Handley, 1965; Ruxton, 1981, 1986). Major faults are thought to have tapped magma to produce the volcanic rocks of the Nukopf Formation. Continued displacement along the faults led to the development of graben sub-basins into which sediments and volcanic rocks of the Graafwater Formation were deposited. Major basement uplift in the vicinity accompanied deposition of the Doornpoort Formation, a widespread unit of red-bed alluvial-fan conglomerates which grade upwards into sheet-flood braided-stream-and aeolian sediments. After the cessation of faulting, deposition of the Kaigas Member of the Klein Aub Formation occurred in a shallow lacustrine environment (Borg and Maiden, 1986). The two palaeo-environments envisaged for the Doornpoort and Klein Aub Formations are illustrated in Figure 2.4(b).

The sequence of events can be summarized as follows:- (Borg & Maiden, 1986)

Stage 1: Strong block faulting along a north-northwest trending Nuwedam fault with displacements of 2 km resulting in an uneven basement floor which was infilled with Nukopf Formation.

Stage 2: Futher subsidence along the Nuwedam West fault allowed for deposition of the Grauwater Formation. Some faults tapped basic and acidic magmas during this phase.

Stage 3: Clastic sedimentation of the Doornpoort Formation in response to regional uplift also covered the basement horst blocks.

Stage 4: Deposition of medium to fine-grained lacustrine sediments occurred.

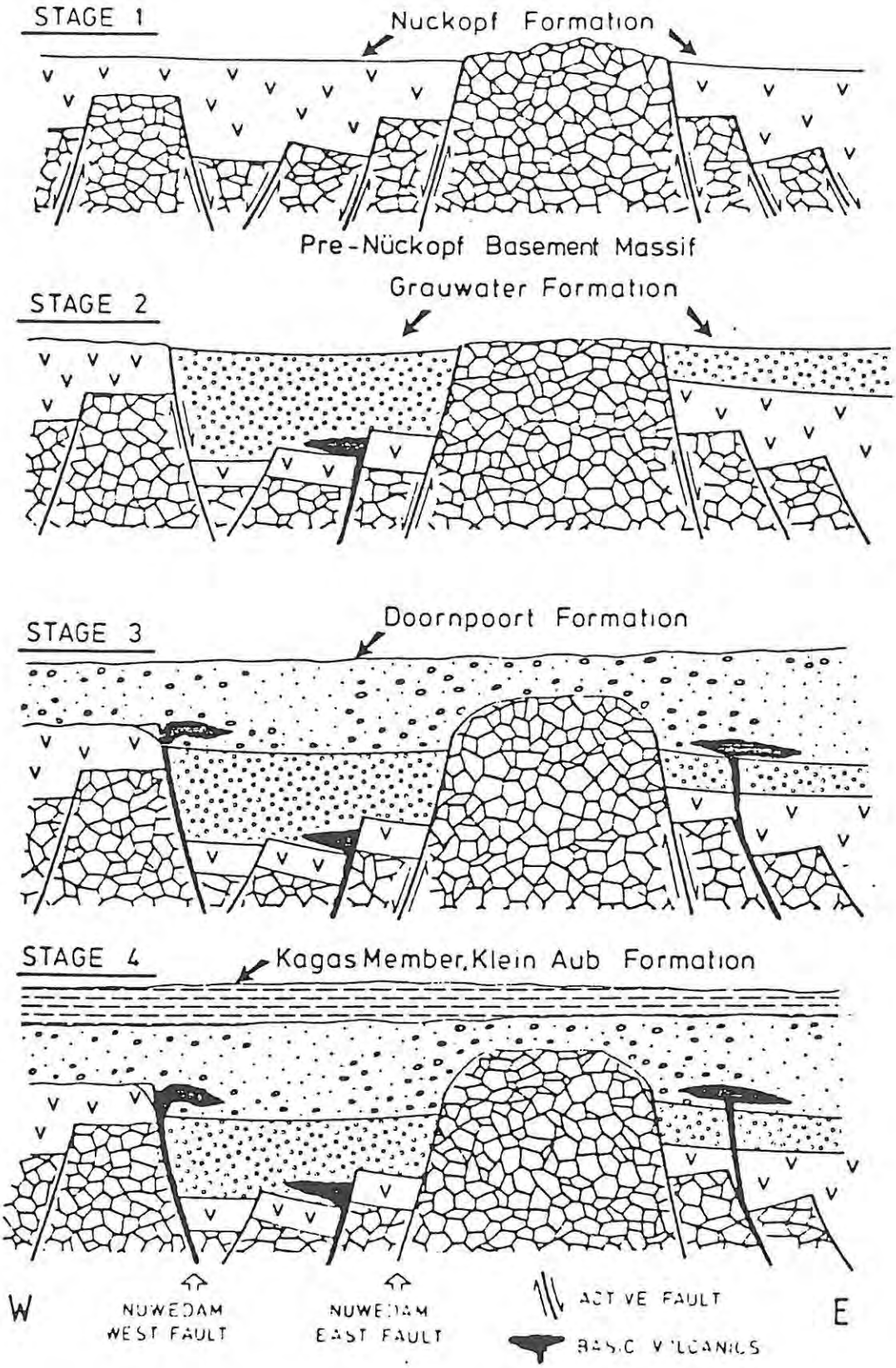

Figure 2.4(b): The tectonic, volcanic and sedimentological development of the Klein Aub basin from Nükopf to Klein Aub times (after Borg & Maiden, 1986).

Metamorphism and deformation affected these sequences during the Damaran Orogeny (Ahrendt et al., 1978), resulting in regional greenschist facies metamorphism. Ahrendt et al.(1978) determined that temperatures during metamorphism did not exceed 350° C (lower greenschist). A coherent age pattern shown by individual minerals and whole rock samples (489 - 532 Ma) from the Marienhof Formation also suggests that lower greenschist facies conditions (300° ± 50° C) were reached in the area around Rehoboth (Ziegler and Stoessel, 1988).

Deformation is indicated by a slaty cleavage with a dip of 70° to the NW; while in some regions of the Klein Aub area the rocks contain a second cleavage.

2.5 The Dordabis - Witvlei Basin

The late-Proterozoic rocks which are exposed between Dordabis and Witvlei occur as narrow thrust slices (Figure 2.5(a)). Outcrop is generally very poor due to Kalahari sand cover. The sequence in the Dordabis/Witvlei basin differs from that at Klein Aub, in that the alluvial fan deposits are thicker and have rapid lateral facies changes into aeolian, playa and lacustrine sediments. These rapid changes are attributed to localised uplift along major faults, with deposition through restricted entry points. The differences observed between the Klein Aub basin and the Dordabis/Witvlei basins are thus a function of tectonism and local facies changes. General similarities however support a correlation between the two areas.

Three alluvial fan centres have been recognised in this area, namely at Okasewa, Witvlei and Gobabis. Most of the surrounding area is overlain by the Duruchaus (shale, phyllite, and limestone) and Kamtsas (quartzite and shale) Formations of the Damara Supergroup. Two cycles of alluvial fan deposits are distinguished on the basis of conglomerate type, namely an earlier angular conglomerate followed by a more mature and extensive conglomerate (Ruxton and Clemmy, 1986).

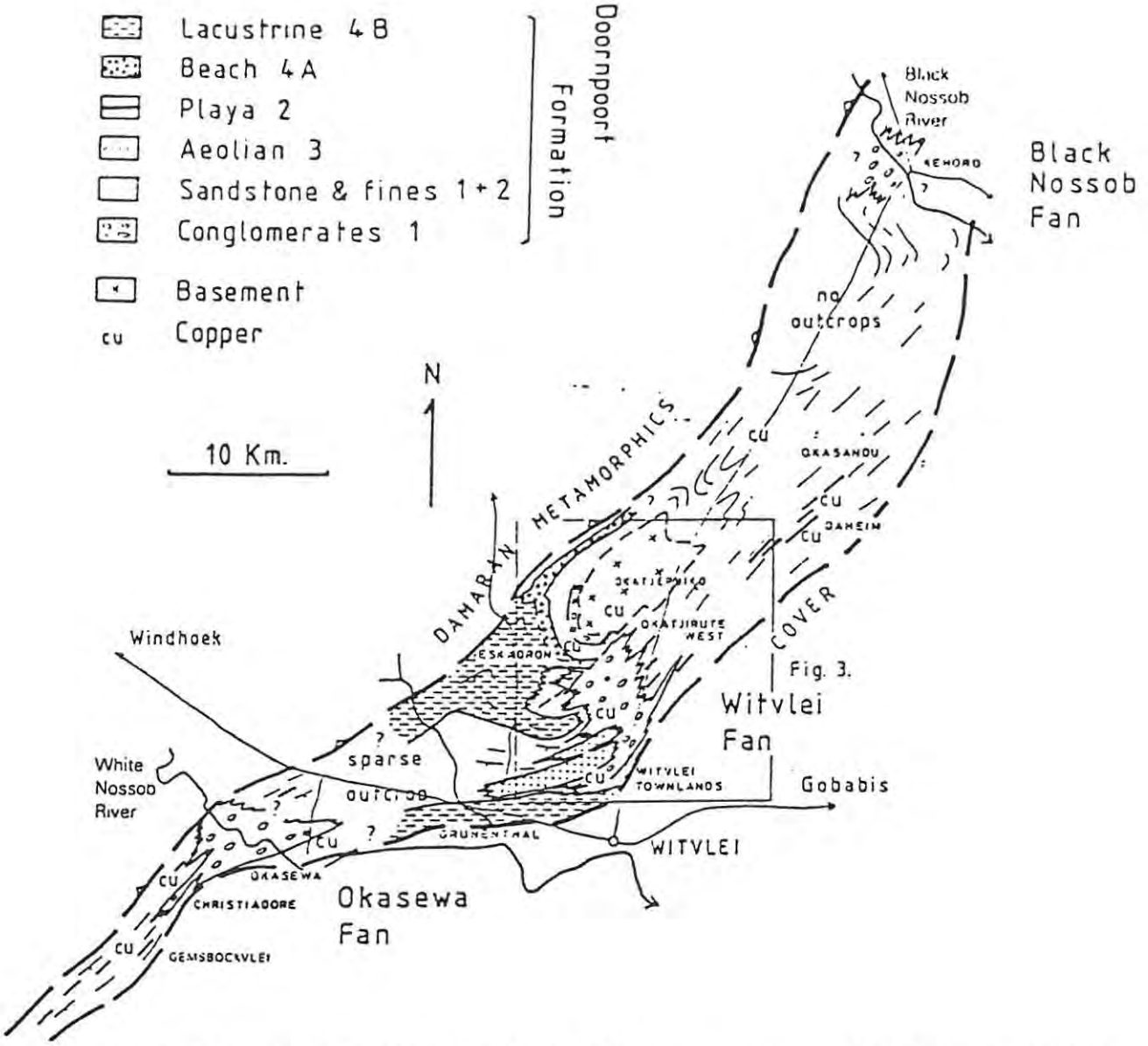

Figure 2.5(a): Sedimentary facies relations and copper distribution in the Doornpoort Formation of the Witvlei area (after Ruxton & Clemmey, 1986).

In contrast to the Klein Aub basin, the Dordabis - Witvlei region underwent intense folding, faulting and thrusting. Deformation resulted in north-east-trending fold axes within the thrust slices and caused the development of a strong cleavage.

Stratigraphic classification and correlation of sequences within and between different basin of the Irumide belt has been much debated due to rapid facies changes, faulting and poor outcrop. A tentative correlation of the Sinclair Group between the better known parts of the Irumide Belt is presented in Table 1.

Sinclair Group in Helmeringhausen, Sinclair and Awasib Areas.	SINCLAIR-HELMERING-HAUSEN AREA[1]	AWASIB MOUNTAINS AREA[2]	NAUCHAS AREA[3]	REHOBOTH AREA[4]	BOTSWANA[5]
	Tuboris Formation Red felspathic sandstone, conglomerate, shale		*Klein Aub Formation* Conglomerate, shale, quartzite	*Klein Aub Formation* Conglomerate, shale, quartzite	*Ghanzi Formation* Felspathic sandstone, shale, conglomerate
			Doornpoort Formation Red quartzites, conglomerate, slate, felsic volcanics, basic lava	*Doornpoort Formation* Red quartzites, conglomerate, slate, felsic volcanics, basic lava	*Kwebe Formation* Sandstone, tuffaceous sandstone, basic intrusives, felsic porphyry volcanics and intrusives (950 ± 37, 1 020 ± 50 Ma)
				Uitdraai Granophyre (932 ± 50 Ma)	
			Grauwater Formation (including Opdam Formation) Quartzite, basic lava, felsic volcanics and pyroclastics (1 030 ± 30 Ma from lowermost felsic unit)	*Grauwater Formation* (including Opdam Formation) Quartzite, basic lava, felsic volcanics and pyroclastics	---?---?---
			Gamsberg granite (1 078 ± 30 Ma), Abendrühe granite (1 089 ± 30 Ma), Koichas granite (1 104 ± 20 Ma), and granite from Kanaus South, Rehoboth District (1 064 ± 20 Ma)	Felsic lava and pyroclastics, conglomerate and quartzite (1 090 ± 90 Ma)	
	Rooiberg granite (1 270, 1 290 Ma)				
	Guperas Formation Lithic sandstone, conglomerate, rhyolite lava, ash-flow tuff, tuff, rhyolite plugs, quartz-porphyry dykes, basic lava, intrusives and dykes	*Guperas Formation* Non-volcanic facies — conglomerate, grit, sandstone, quartzite, shale, felsic porphyry intrusives		Basic and felsic lava, phyllite, conglomerate	
	Nubib granite (1 020 ± 80, 1 290 ± 80, 1 360 ± 50 Ma)	*Younger Awasib granite*	*Older (pre-Gamsberg) units of the Nauchas granite suite* (including Piksteel granodiorite)	*Piksteel and Suiderkruis granodiorites*	
	Barby Formation (including Spes Bona syenite) Porphyritic trachy-andesite and trachy-basalt, basalt, rhyolite, ash-flow tuff, tuff, volcanic conglomerate, quartzite, gabbroic, dioritic and monzonitic intrusives	*Barby Formation* Basic to intermediate lava, basic intrusives	*Alberta basic complex*		
	Kunjas Formation Basal conglomerate, arkose, shale		*Gauh Valley schists and conglomerates*	*Gauh Valley member* of the Older Abbabis Formation	
	Haremub granite	*Older Awasib granite*			
	Nagatis Formation Ash-flow tuff, felsic lava, basic lava, agglomerate, arkose, shale, grit				

References

[1] Von Brunn (1967), Watters (1974a)
[2] Watters (1974a), unpublished map by Consolidated Diamond Mines
[3] Martin (1965), De Waal (1966), Halbich (1970), Schalk (1973), Hugo and Schalk (1975), Burger and Coertze (1975).
[4] Schalk (1973), Hugo and Schalk (1975)
[5] Boocock (1968)

Table 1. Tentative stratigraphic correlations of the Irumide Belt (after Watters, 1977).

2.6 The Ghanzi/ Lake N'Gami Basin, Botswana

Northeast of the Witvlei area, towards the Botswana border, the Irumide rocks become hidden under a cover of Damara and Nama rocks and by sands of the Kalahari Desert. Irumide rocks in northwestern Botswana occur in a 30 to 40 km-wide belt known as the Ghanzi/Lake N'Gami belt. The lithologies represent a volcaniclastic sequence, known as the Kgwebe Porphyry Formation, dated at between 900 - 1000 Ma and are overlain by the Ghanzi Formation (Boocock, 1968; Thomas, 1973).

The Kgwebe Porphyry Formation consists of quartz porphyries and breccias, vesicular diabases, tuffaceous sediments and sandstones, grits and conglomerates. The unconformably overlying Ghanzi Formation crops out in two belts on either side of the central rift valley. The northern belt is made up of sandstones whereas the southern belt is made up of a succession of protoquartzites, calcareous sandstones, shales, argillites and limestones containing copper mineralization. The Ghanzi Formation is correlated with the earliest members of the Damara Sequence on the 1:1 000 000 Geological Survey map but has generally been considered to have accumulated in a similar environment to the rocks of the Klein Aub and Witvlei areas (Toens, 1975; Mason, 1981).

The Kgwebe and Ghanzi Formations are tightly folded in major upright folds with very tight closures (Mason, 1981). The Ghanzi basin is recognised as a distinctly linear and uniform magnetic entity from aeromagnetic data and suggests a correlation with the Muva rocks of Zambia (Reeves, 1979).

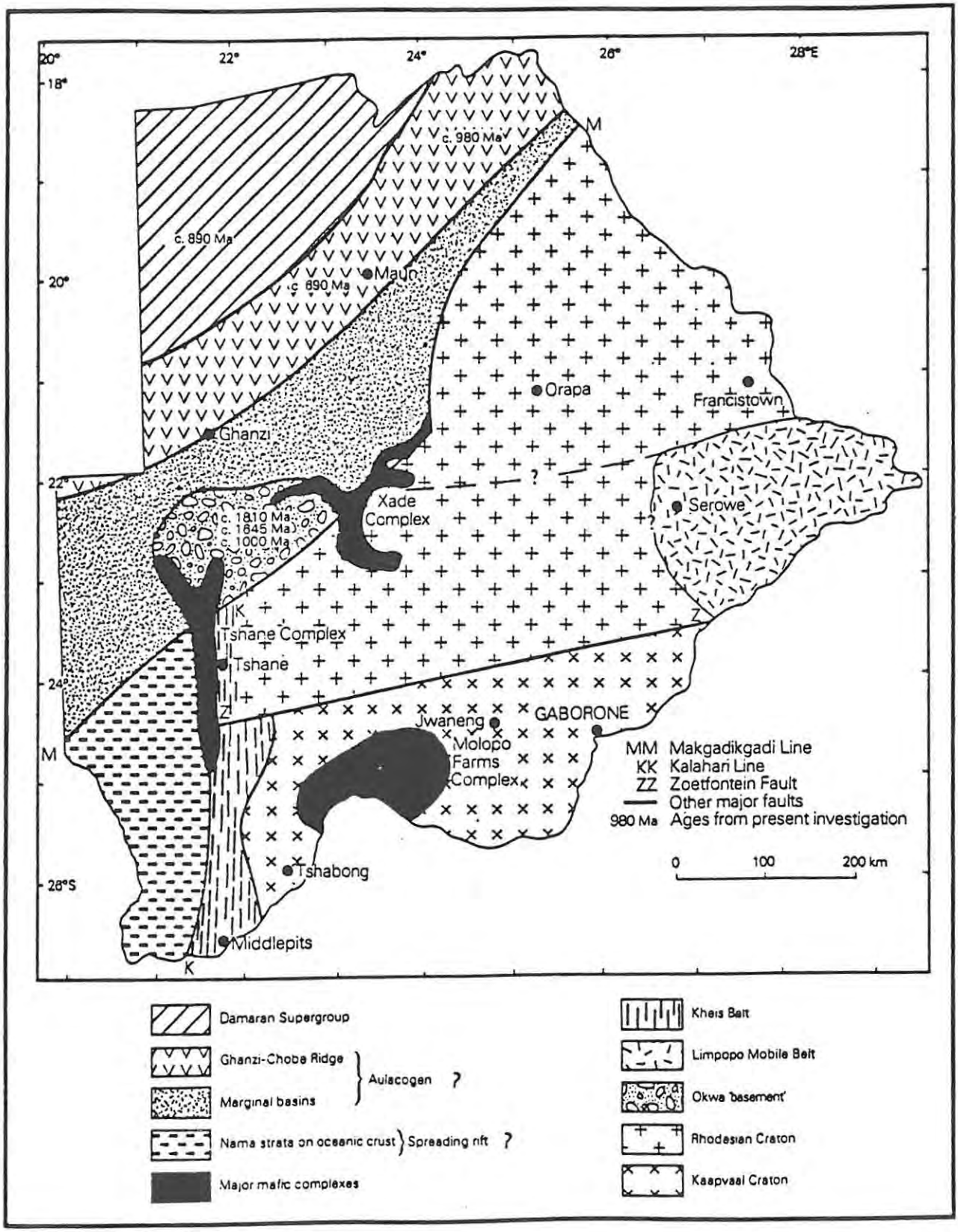

Figure 2.6: The Precambrian geological provinces of Botswana (after Reeves, 1978).

3 GEODYNAMIC EVOLUTION OF THE IRUMIDE PROVINCE

3.1 Lithological Evidence

Based on voluminous amounts of igneous rocks of calc-alkaline and shoshonitic affinities, Watters (1974, 1976, 1977) proposed, that the Sinclair Group represents a succession of lithologies which developed along a magmatic arc - referred to as the *Rehoboth Magmatic Arc*. He proposed that the magmatic arc developed along the western and northwestern margins of the Kalahari Craton as a result of consumption of ancient oceanic crust along an approximately southeast dipping subduction zone. The palaeoplate margin was tentatively located as illustrated in Figure 3.1.

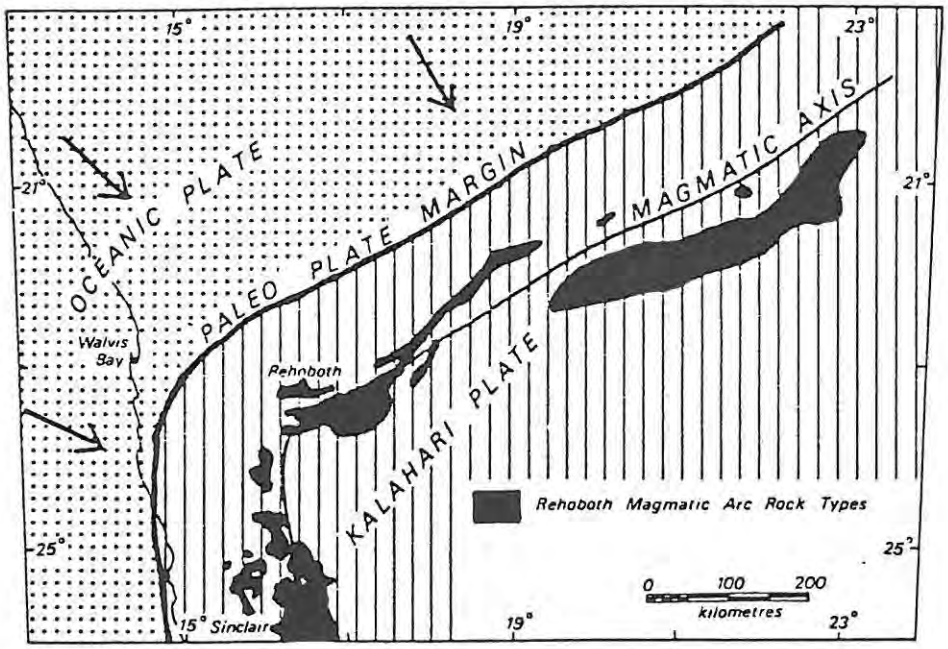

Figure 3.1: Suggested reconstruction of the geotectonic setting during the evolution of the late Precambrian Rehoboth Magmatic Arc (after Watters, 1976).

Watters (1974, 1976, 1977) cited the following as evidence for this view :

(1) An extensive and curvilinear distribution pattern.

(2) The arc separates the predominantly undeformed Precambrian deposits (Nama Group) of the Kalahari Craton from the highly deformed late Precambrian deposits of the Damara Orogenic Belt, suggesting that the arc occupied a marginal cratonic position.

(3) The trend of the arc and arc structures (faults etc..) parallels that of the Damaran structural trends - suggesting a possible relationship between the geotectonic development of the arc and Damaran Orogeny.

(4) The polarity of lava types, voluminous granites, tholeiitic extrusives, episodic magmatic activity and contemporaneous sedimentation.

The contention of Watters (1974, 1976, 1977) that the Rehobothan - Irumide lithologies represent a '*Magmatic Arc*' above a continentward dipping subduction zone, has not generally been accepted (Krøner, 1977; Mason, 1981; Cahen and Snelling, 1984; Borg and Maiden, 1986a, b and 1987a & b; Borg, 1988; Whitfield (this study). Martin and Porada (1977) and Martin (1983) have demonstrated that the arc-like distribution of the Irumide lithologies is controlled rather by faults and present outcrop. Krøner (op. cit.) argues that field evidence favours the deposition of undeformed Sinclair rocks in an intracratonic trough or aulacogen, probably related to tectonic activity in the Namaqualand Metamorphic Complex. Borg (1988) favours rift tectonics which may have resulted from an elongate mantle plume.

Problems of correlation of the Irumide formations are a manifestation of the lack of continuity between the relatively small, localized yoked basins, in a rift situation. The Irumide Cycle thus appears to have marked a long period of sporadic tectonic unrest with rifting, associated volcanic activity and the development of restricted intermontane yoked basins, which accomodated thick, but localized piles of clastic sediments, volcanic rocks and lacustrine deposits. The cycle is remarkably similar in these respects to the recent development of volcanic and sedimentary sequences in the East African Rift system. However, there is no such recent parallel there for the major granite emplacement events which appear to be a persistent feature of the entire Irumide Cycle (Mason, 1981).

3.2 Geochemical and Isotopic Evidence

Attempts to elucidate the Rehobothan - Irumide geological history have often been based on unravelling the complex stratigraphic relations. Much of the confusion relating to the origin of the Sinclair sequences is the result of a paucity of data especially geochemical and isotopic. Numerous attempts have been made to correlate the stratigraphic successions of the

various basins. Such correlations have been plagued by contradictory radiometric age dates. Borg (1988) suggests that the development of the various basins was in fact diachronous. Evolution of the rift is proposed to have proceeded from the south-west towards the north-east. Data illustrated in Figure 3.2 reveal a marked younging trend of the dated rocks towards the north-east.

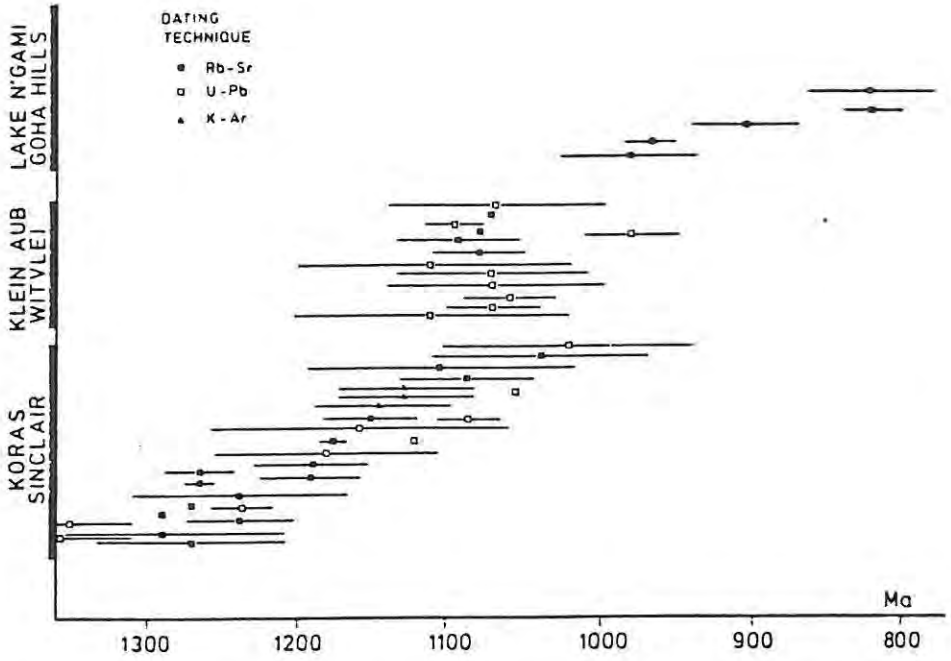

Figure 3.2: Radiometric age data from the different basins of the Irumide belt, displaying a younging trend from south to north (After Borg, 1988).

Age and geochemical data recently published by Ziegler & Stoessel (1988), Stoessel & Ziegler (1988) and Reid et al. (1988) must be regarded with a high degree of uncertainty. It appears that no field mapping was done by Ziegler & Stoessel (1988) who based their geochemical sampling on outdated and largely incorrect field maps (Hoffman, 1989 pers comm.). Reid et al. (1988) produce a locality map for Swartmodder Granite (Figure 3), showing sample collection sites. Mapping by the author shows that the area marked as locality 2 (Figure 3, Reid et al. 1988) in fact has no Swartmodder Granite outcrop but rather schist and quartz porphyry; also, grid references pertaining to the same figure lie a few kilometres to the south, again indicating an area devoid of Swartmodder Granite.

Stoessel and Ziegler (1988) propose that the geochemistry of the Rehoboth Granitoids (Gamsberg Granite Suite, Piksteel Intrusive Suite and Weener Intrusive Suite) are all peraluminous in character (according to the criteria of Chappell and White, 1974) as well as calc-alkaline, according

to the AFM diagram of Kuno (1968). A/CNK ratios indicate an S-type character for the Weener Granitoids, an S- or I-type origin for the Piksteel Granitoids and an I-type origin for the Gamsberg Granitoids (Stoessel and Ziegler, 1988). These results only partly coincide with isotopic data of Reid et al., (1988), Siefret (1986a, b) and this study, which favour I-type origins for almost all of the Rehoboth Granitoids. The high alumina saturation of most of the granitoid suites suggests that they are derived from upper continental crustal melts (Stoessel and Ziegler, 1988).

Geochemical analyses, in particular trace-element analyses, of the various igneous suites in the Rehoboth area have been incorporated in latest attempts to unravel the tectonic setting of the area (Stoessel and Ziegler, 1988; this study). Association of certain characteristic trace-element (Nb, Y, Th, Hf...) signatures with particular tectonic environments of eruption have been used, with varying degrees of success, since the early 1970's (Pearce and Cann, 1973; Floyd and Winchester, 1975; Pearce et al., 1984). By plotting Rb, Nb and Y trace-element signatures of the various granitoid- and mafic suites, on tectonic discrimination diagrams of Pearce et al. (1984), it can be seen that the majority of the granitoids are classified as being characteristic of *'Volcanic Arc Granites'*, *'syn-Collisional Granites'* and *'Continental tholeiites'* (Stoessel and Ziegler, 1988; this study). Some of these data appear to support Watters (1974, 1976, 1977) theory of a *magmatic arc*, tectonic setting for the Irumide belt.

Work done by Hoal et al., (1989) on the Kariab Complex of the Aswab Mountain Terrain (AMT) which forms part of the basement to the Sinclair Sequence, reveals calc-alkaline characteristics similar to "anomalous" Volcanic Arc Basalts. Within the cover sequences of the ATM, the Haiber Flats Formation (HFF) (which is correlated with the Sinclair Sequence) displays many of the geochemical characteristics thought to be typical of an island arc or active continental margin setting. Hoal et al. (1989) suggest that the bimodal nature of the HFF probably excludes their extrusion in a convergent arc setting, but is not incompatible with a back-arc setting. Geological evidence indicates extrusion of HFF volcanics in graben basins which is consistent with an extensional tectonic setting.

Arculus (1987) points out that there is accumulating data regarding tectonic misassignment and palaeotectonic inferences when using trace-element criteria alone. Twist and Harmer (1987) argue that trace-element

their tectonic setting per se, but rather point to the melting and crystallization histories of the source regions from which their parent magmas were extracted. The significant amount of tectonic misassignments (eg. volcanic arc) and calc-alkaline nature of many of the intrusives within the Rehoboth Sub-province is suggested as a result of their altered state and possibly from melting of basement sequences, whose tectonic history differs from that of the overlying sequences (eg. Sinclair). The tectonic signature (volcanic arc) thus appears to be inherited from melts derived from basement rocks of the Irumide lithologies, and do not reflect the tectonic setting into which they were emplaced.

Hence the majority of "magmatic" evidence thus far appears not to support Watters (1974, 1976, 1977) theory of a magmatic arc tectonic setting, but rather a rift - type setting for the Rehobothan - Irumide belt in Namibia.

3.3 Geophysical Constraints

Palaeomagnetic data from cratonic sequences of the Sahara - Congo Craton and the Kalahari Craton (ie. from both sides of the Kibaran Belts) define a single apparent polar wander path for the Kibaran tectonic period (Piper, 1974). Futhermore, Cahen and Lepersonne (1967) and Shackleton (1973) demonstrated the continuity of older structures through the Irumide belt, reinforcing a rift - type setting rather than a volcanic arc setting.

The various basins described in Chapter 2 are associated with a number of elongate gravity highs which produce a distinct linear feature in the southern part of Namibia. The positive gravity anomalies are caused by basaltic infill, of graben, by lavas and are flanked by negative gravity anomalies which are interpreted as granitic bodies (Borg, 1988).

Kröner (1976) suggests that basement inliers attest to the ensialic nature of the Irumide Belt. Pirajno and Jacob (1984), however, suggest the possibility that the Irumide represented a period of tectonism, that gave rise to pull-apart or strike-slip basins and associated sedimentation/volcanic activity. Broadly contemporaneous collisional tectonics between 1.2 Ga and 0.9 Ga in the Gordonia Belt of the Namaqua Metamorphic Province suggests that extension in the Irumide Belt may be related to continental convergence although not necessarily associated with an active continental margin. Hoal et al. (1989) suggest a similar tectonism to that of the Keweenawan "impactogen" as described by Gordon & Hempton (1986).

4 THE GEOLOGY OF THE NEURAS GRANT

4.1 Stratigraphy - an Overview

4.1.1 Introduction

This section summarises the authors findings on stratigraphic, petrographical and petrological findings from studies conducted on the various units in the Neuras Grant. When presented in full detail, such accounts usually distract the reader from an overall appreciation of lithological relations. For this reason details of each lithology and brief discussions are included in Appendix 1 and omitted from the body of the text. Conclusions presented here are drawn from the data presented in Appendix 1.

The mid- to late Proterozoic rocks within the Neuras Grant form a volcano-sedimentary sequence. The volcanic rocks have a bimodal (basalt-rhyolite) composition. The volcano-sedimentary sequences represent graben infill sequences. Deep-seated graben-related fractures are suggested as possible conduits for the mafic magmas. The acid volcanic rocks comprise rhyolitic lavas, tuffs and ignimbrites whereas the mafic rocks comprise dolerite dykes, metagabbros (sills) and basaltic lavas. Granitic plutons intrusive into the volcano-sedimentary pile may represent melting of basement sequences in response to the high geothermal gradient developed during extension of the crust as attested by their peraluminous character (Appendix 1). Plutons vary from high level intrusions to deep-seated and have varying compositions. Compressional deformation during the Irumide (D_1), possibly as a result of rift closure, resulted in an intense north-westward dipping foliation cleavage and south-eastward propagating thrusts. A younger swarm of mafic dyke and gabbroic intrusions - the Swartkoppies dyke swarm - is correlated with incipient rifting possibly related to the Damara event. The Gamsberg Granite suite, intruded the older deformed rocks and represents the final phase of magma emplacement. Both the Swartkoppie intrusions and Gamsberg Granites are undeformed and post-date the D_1 event. Regional *low-grade* metamorphism is suggested to have occured during the D_1 event and later overprinted by a similar grade, M_2, and subtle D_2 events tentatively correlated with the Damara event.

4.1.2 Possible Equivalents of the Elim Formation

A retrogressively metamorphosed gabbroic plug and a remnant portion of basaltic lava, constitute possible Elim Formation equivalents within the study area. Both units are intruded by the various younger granites. The remnant basaltic lava occurs only as blocky scree although it is a prominent feature on the Landsat image (Plate 4.1.2).

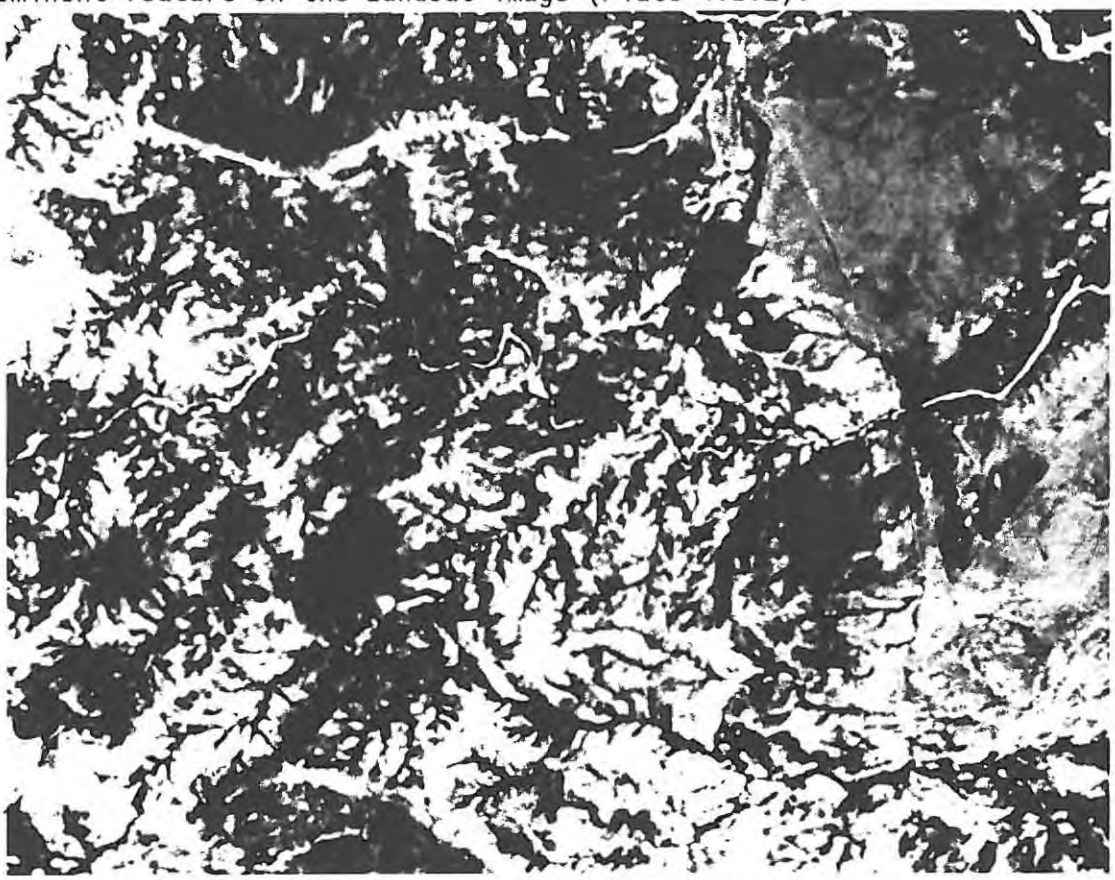

Plate 4.1.2: A Lansat - TM - image of the study area.

4.1.3 Marienhof Formation

The Marienhof Formation comprises a sequence of metasediments and bimodal volcanic rocks. The volcano-sedimentary package is thought to represent a major portion of the graben infill. The metasediments can be subdivided into schists, phyllites and quartzites. The acid volcanic rocks are dominated by rhyolitic lavas, tuffs and ignimbrites. Mafic rocks include sheared dolerite dykes and sills.

Deformation and metamorphism resulted in the complete destruction of internal sedimentary structures within the schists, although, remnant bedding within the phyllites is locally preserved. The rhyolites on the other hand are comparatively undeformed and internal flow banding is clearly visible. Lava flows are between 1 m and 2 m thick and are

interbedded with tuffaceous units which lack internal structure. Together these units form rhyolitic volcanic units up to 100m thick.

4.1.4 Acid and Basic Intrusives

Isotopic dating by Reid et al., (1988) gives an age of 1639 ± 25 Ma, which confirms the granite as being the oldest intrusive within the area. Field observations suggest that the Swartmodder Granite is the oldest intrusive unit within the area studied. Copper has, in the past, been mined from a schist enclave within the Swartmodder Granite. The Piksteel Granodiorite followed as the next voluminous intrusive phase. The granodiorite is the only granitoid which has an S-type geochemistry and is corundum normative (Appendix 1). The Piksteel Granodiorite is interpreted as large scale anatexis of metasedimentary units. A Rb/Sr age of 1170 ± 20 Ma is reported by Reid et al. (1988). Intrusive relationships and morphological characteristics suggest that both the Swartskaap and Neuras Granites post date the intrusion of the Piksteel Granodiorite. Both granites have poorly developed gneissic textures and like the other granites exhibit calc-alkaline and S-type affinities (Appendix 1). Melting of metasedimentary material is interpreted to have given rise to these granites.

A mafic dyke swarm, known as the Older sheared dyke swarm, has intruded the volcano-sedimentary units, Swartmodder Granite, Piksteel Granodiorite, Neuras Granite and Swartskaap Granites. Orientation of the mafic dykes is commonly NE - SW and all are foliated and altered. Gold mineralization is associated with the margins and is discussed at length in section 4.5.7. A high-level Granite intrusion, referred to as the quartz-feldspar porphyry in this study, has an I-type calc-alkaline geochemistry. This unit intruded after the Older sheared dyke swarm. The texture of this High Level Granite varies from being porphyritic in the northern part of the grant to fine grained granitic in the southern portion of the area. Quartz porphyry dykes are spatially restricted to the northern part of the grant suggesting that this area represents the roof zones of the intrusion and the southern part the lower, deeper seated portion.

A second and younger dyke swarm, the Swartkoppies mafic dyke swarm and associated gabbros, is manifested as undeformed metamorphosed dykes with roughly east-west trends. Outcrop of the Swartkoppies mafic dyke swarm is restricted to the southern part of the grant area. Geochemically the younger Swartkoppies mafic dykes are relatively depleted in incompatible trace-elements and thus are primitive in comparison with the Older sheared

dykes. Major- and trace-element analytical data of the two dyke swarms indicate a fractional crystallization trend, suggesting that they may have evolved from the same initial source. The Swartkoppie mafic dyke swarm is however unaltered and undeformed, which contrasts markedly from the Older sheared dykes. No isotopic ages are published for the Older sheared mafic dykes, however, a time gap of between 49 Ma and 140 Ma is suggested to exist between the two mafic swarms (Appendix 1). An explanation which accounts for the relative differences in major- and trace-element abundances is :-

Decompression partial melting of a 'fertile' (undepleted) mantle during Irumide rifting and emplacement of the melt as the Older Mafic dykes effectively depleted the mantle of incompatible trace elements. Initial rifting associated with the early rift development of the Damara again led to partial melting of the 'now depleted mantle' giving rise to magma which was relatively depleted in incompatible trace elements, the - Swartkoppies mafic dyke swarm.

Two granites, namely the Uitdraai pluton and the Kobos plutons, are collectively known as the Gamsberg Granite Suite. The Gamsberg suite is characteristically undeformed and appears to have been intruded last in the geological evolution of the study area. No isotopic ages of these plutons are published however an age of 1079 ± 29 Ma for other Gamsberg Granites in the Rehoboth area, are presented by Reid et al. (1988). Trace-element data for the Gamsberg Granites constantly plot on or near the 'Within-Plate Granite' field on tectonic descrimination diagrams.

4.2 STRUCTURE

4.2.1 Regional Structure

The regional structure of the Rehoboth Basement rocks is particularly poorly documented. Few, if any, studies have concentrated on unravelling the deceptively 'simple' deformation. Published material on the Basement rocks attributes all the observed deformation as being genetically linked to the Damara Orogen. Orientation data recorded in the field indicate a single compressive deformation, directed towards the south-east. Dating of various minerals, dominantly micas, yields ages of about 530 Ma (Ahrendt et al. 1978; Ziegler and Stoessel, 1988). Petrographic examination of thin sections reveals a dominant foliation which in places appears weakly crenulated. Orientation data reveal a dominant foliation which dips steeply towards the north-west and a moderately developed lineation which generally plunges towards west-north-west (Figures and Plates 4.2.1(a) & (b)). A combination of previous findings have been the basis upon which many authors have advocated a single deformation event related to the Damaran Orogeny.

Hoffman (pers. com., 1990) alternatively suggests that at least two separate deformation events, an Irumide and a younger Damara event, have affected the Rehoboth basement rocks. A major shear zone, the Areb shear zone, is believed to be a major oblique shear related to the Irumide deformation event. Regional salient features are suggested to highlight subtle yet strategic differences between the two deformation events.

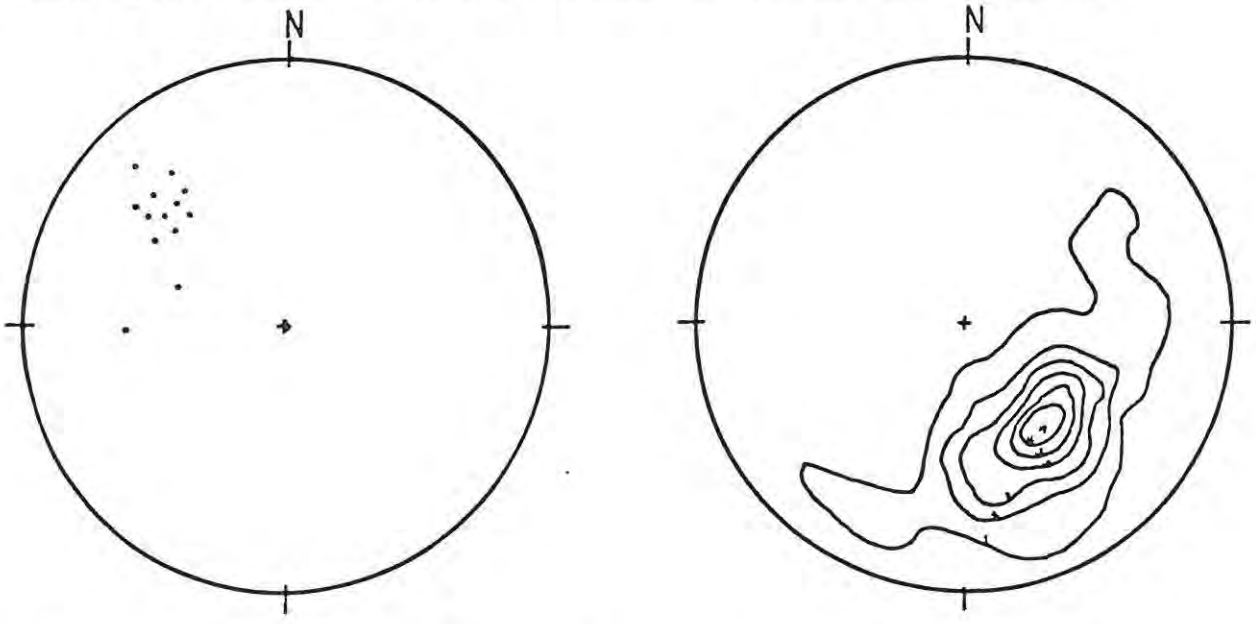

Figure 4.2.1(a) Plot of the regional lineation data.

Facts which support Hoffman's (pers comm., 1990) proposed multi-deformational history of the Rehoboth rocks include :

i) The structural fabric of the Irumide rocks rocks are <u>much</u> more deformed than the overlying Damara rocks.

ii) The structural trend of the Damara rocks differs from that of the Irumide basement rocks resulting in a fabric unconformity. Two differing foliations are developed within basement rocks near the contact between the Damara and Irumide Orogens.

iii) Gamsberg Suite plutons adjacent to the Damara margin are deformed, but plutons futher south (ie. around Rehoboth) are essentially undeformed. This suggests that deformation associated with the Damara event dissipated southwards and became effectively negligble within 40 km of the Southern Damara margin or south of the Areb shear zone.

Plate 4.2.1(a): Dominant foliation within granodiorite, note porphyroblasts in the areas of strain shadow.

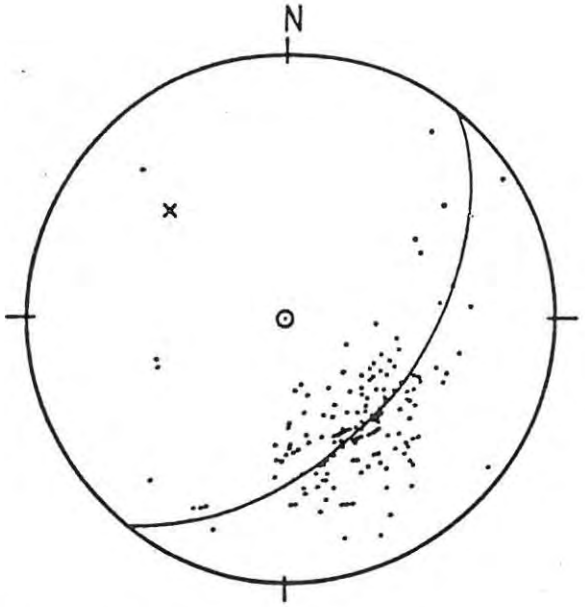

Figure 4.2.1(b) Poles to the regional foliation

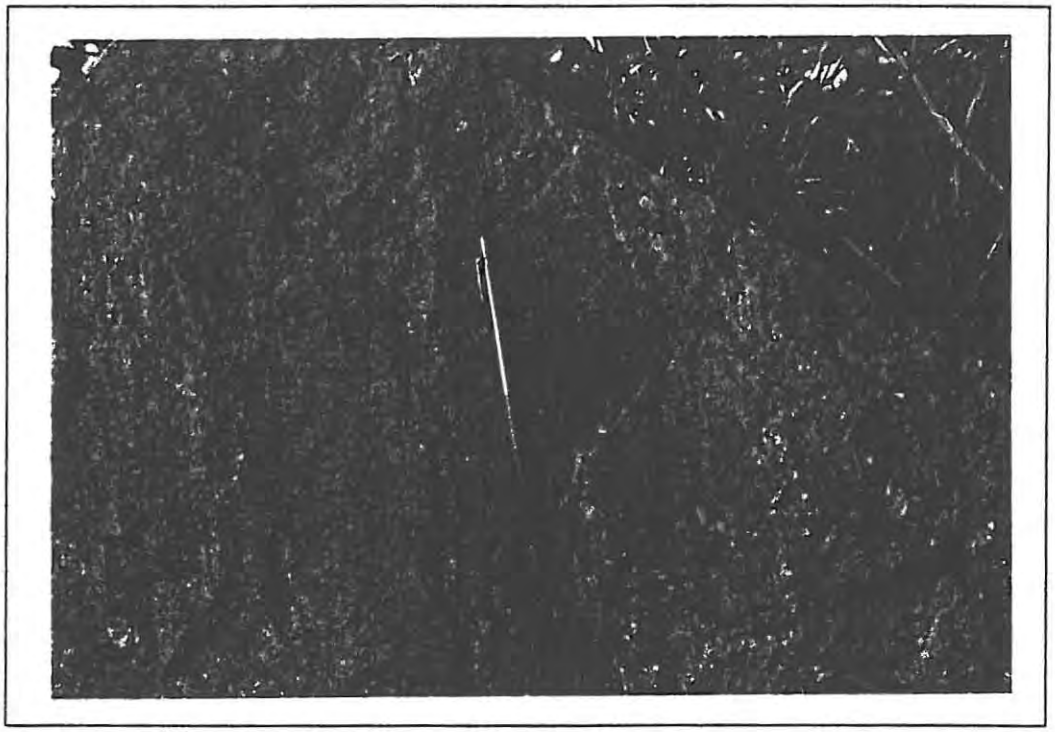

Plate 4.2.1(b): Prominent NEN trending lineation within ignimbrites.

4.2.2 Thrust Faulting

Thrust faulting within the Neuras grant is restricted to the northern region (Regional geological map). A prominent thrust plane, thought to represent the sole thrust of a series of imbricate thrusts which occur north thereof, strikes east-west. It is characterised by the development

of a melange and by hydrothermal carbonate and magnatite; it is devoid of any mineralization (Plate 4.2.2(a)).

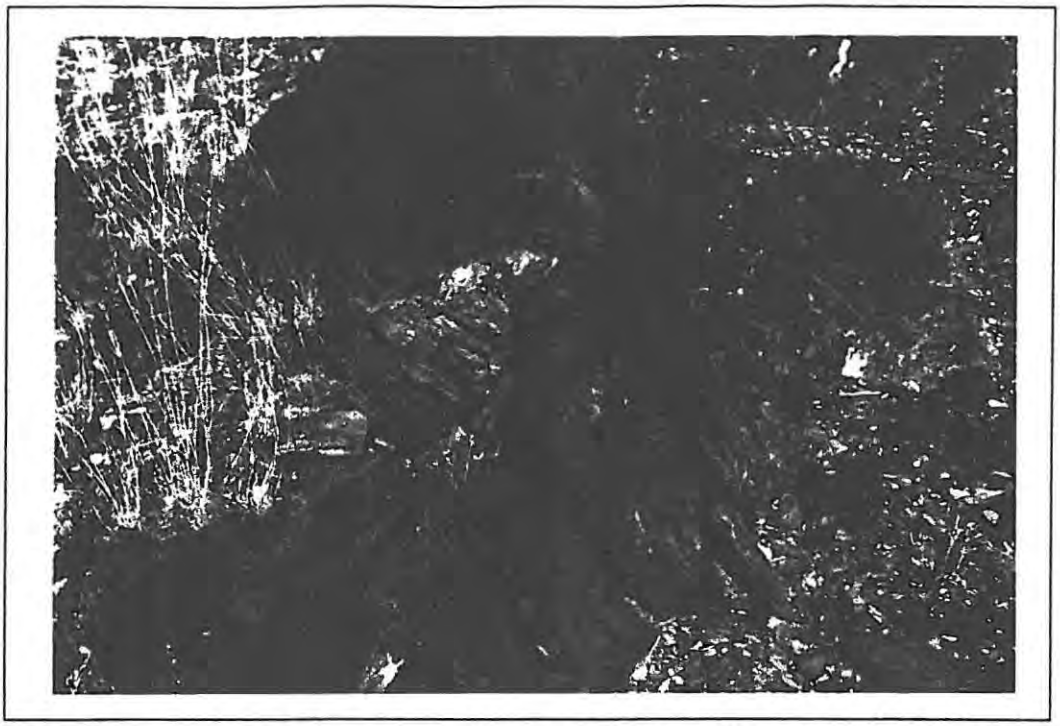

Plate 4.2.2(a): Hydrothermal carbonate within the sole thrust melange.

Detailed examination of thrust planes revealed micro thrusts within the plane of movement (Plate 4.2.2(b)).

Plate 4.2.2(b): Micro-thrusting within a thrust plane.

The thrusts generally dip at about 30° - 350° and a computer generated cross-section (A - B, Regional geological map) reveals that the phyllites in the western margin of the area form a Klippè (Figure 4.2.2).

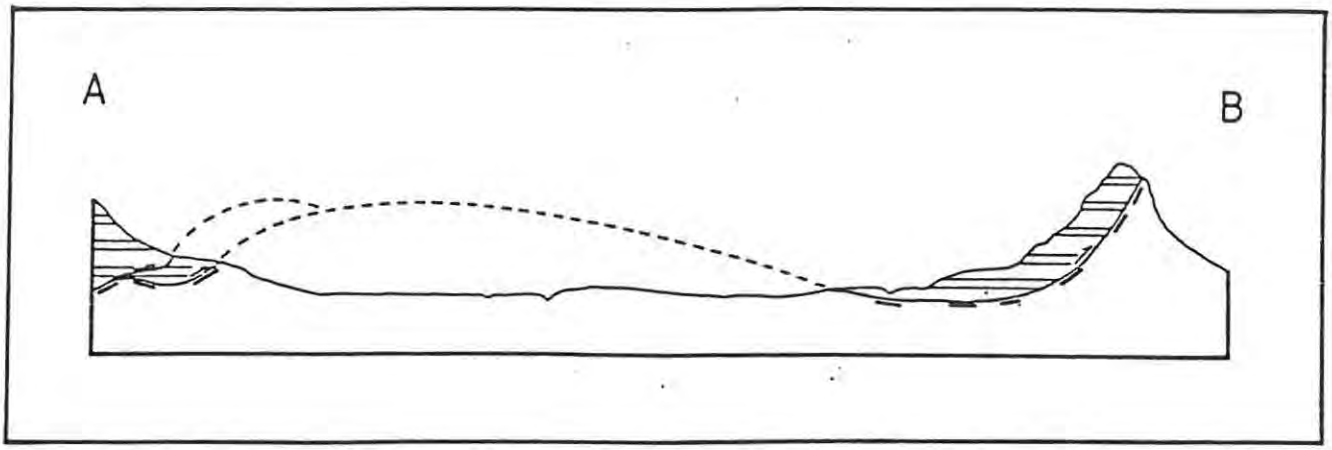

Figure 4.2.2: A computer generated cross-section through points A - B on the regional geological map.

4.2.3 Mebi Shear Zone

The Mebi Shear zone is approximately 1.5 - 2 km long and varies between 0.5 - 3m in width. Surface expression is generally poor and indicated by narrow ferruginised quartz-haematite veins at surface. Access to a depth of 60m within the shear is possible at the Mebi Gold Mine where numerous structural readings were obtained.

The shear zone is best developed within the Piksteel Granodiorite and extends for a few hundred metres into the Marienhof Schists before dying out. Quartz veins hosting sulphide and gold mineralization reach a maximum thickness of 3m at 60m below surface (Plate 4.2.3).

Structural data obtained from along the shear zone confirm the trend of the shear as defined by a lithosampling exercise. Lithosampling results revealed anomalous gold mineralization with a trend of 094° (section 5.3). Structural data obtained from within the mine are shown in (Figure 4.2.3) and reveal a trend of 090° and an average dip of 53° towards the north. The sense of movement along the shear appears to be reverse suggesting that the Mebi Shear zone is genetically related to the thrust faults situated further to the north.

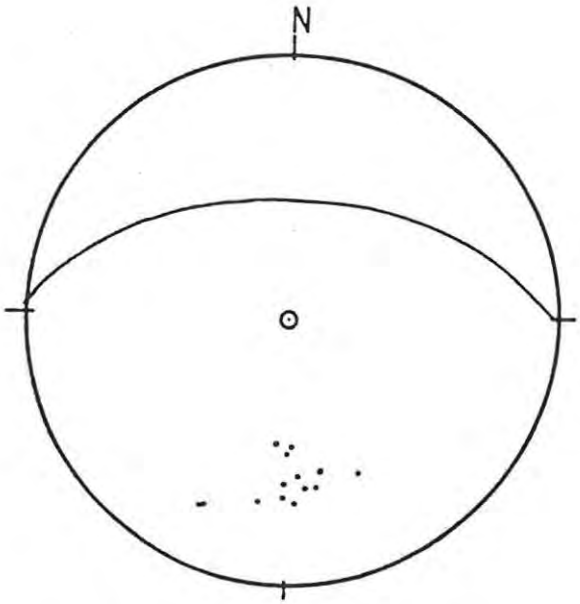

Figure 4.2.3: Shear plane orientation data from the Mebi Shear mine.

Plate 4.2.3: Mineralized quartz veins within the Mebi Shear zone.

4.3 METAMORPHISM

Metamorphism is defined by both Winkler (1979) and Turner (1981) as the process of mineralogical and structural adjustment of solid rocks to physical and chemical conditions that have been imposed at depths which differ from those conditions under which the rock in question originated.

The essential criteria for determining the grade (Winkler, 1979) and facies (Turner, 1981) of metamorphism in any given area are the identification of metamorphic minerals and characteristic mineral assemblages. Both the concepts of grade and facies are used in the determination of pressures and temperatures which prevailed over the area studied.

4.3.1 Metamorphism of the Pelitic Rocks

The metapelites in the grant area, namely schists and phyllites, consist predominantly of quartz, muscovite, chlorite with lesser amounts of plagioclase (albite), epidote, calcite, magnetite and sphene. The less-pelitic schist units and phyllites have typical blastopsammitic textures and display a schistose fabric, S_1, caused by elongated quartz grains and lepidoblastic mica. S_1 was produced during D_1 of the Irumide tectonogenesis. This foliation was then deformed into crenulation folds with the formation of an S_2 axial planar foliation in places. Quartz is the dominant mineral in these metapelites and occurs as xenoblastic elongated grains which exhibit an undulose extinction. The more psammitic units of the schists are characterized by a relatively high plagioclase (albite) content. The albite is generally subidioblastic in form and non-pervasively altered to sericite. The minerals muscovite, chlorite and calcite all appear to be in stable contact with one another.

Figures 4.3.1(a) and (b) depict the relationship between the mineral assemblages muscovite-epidote-calcite-chlorite and muscovite-chlorite-magnetite respectively.

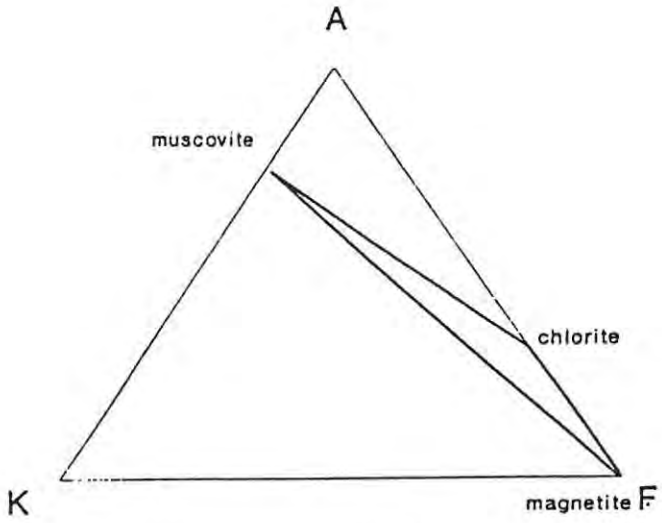

Figure 4.3.1(a): Mineral assemblage muscovite-epidote-calcite-chlorite.

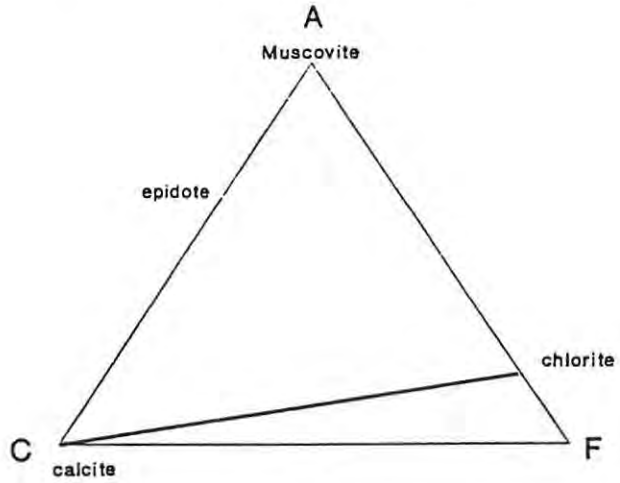

Figure 4.3.1(b): Mineral assemblage muscovite-chlorite-magnetite.

4.3.2 Metamorphism of the Mafic Rocks

Of the variety of mafic rocks recorded in the study area, the Swartkoppies dyke swarm and the various metagabbros proved to be most useful in the determination of metamorphic mineral assemblages. The Older mafic dyke swarm has completely altered to a mass of quartz, chlorite, oxides and sulphides. Dominant minerals in the mafic rocks include hornblende/actinolite, plagioclase (albite), epidote and clinozoisite with lesser amounts of quartz, chlorite, clinopyroxene (remnant), muscovite, calcite and opaque oxides. A brief description of each mafic lithology follows, for a more complete description of each rock type the reader is referred to Appendix 1.

The metagabbros of apparent Sinclair age characteristically show no remnant igneous texture and exhibit a decussate texture. Predominant minerals include actinolite, epidote - clinozoisite, albite and chlorite. The younger *Swartkoppie Metagabbros* have characteristic porphyroblastic textures. An amphibole, probably hornblende, is the dominant mineral and occurs as the large subidioblastic porphyroblasts. The formation of amphibole from clinopyroxene is a retrograde change. Its composition is initially that of hornblende followed at lower temperatures by actinolite. The matrix consists of subidioblastic laths of remnant clinopyroxene, hornblende/actinolite, plagioclase (albite) and sphene. The *Swartkoppie dyke swarm* is characterized by a blastophitic texture typical of dykes. Remnant clinopyroxene is rare and almost all has gone to actinolite. Subidioblastic laths of plagioclase (albite), epidote - clinozoisite and chlorite make up most of the rock.

The main changes of basaltic rocks to amphibolites from temps to the high-temperature part of *low-grade* metamorphism are :-

1). The formation of hornblende and almandine garnet (if pressure is high enough) mainly from clinopyroxenes and/or olivine.

2). The formation of less An - rich plagioclase (eventually albite), actinolite and commonly clinozoisite - epidote, from the breakdown of Ca-plagioclase.

3). In low grade metamorphism, chlorite and quartz are additional constituents to those in the above (after Winkler, 1979).

The *low-grade* metabasites are normally distinguished from the higher grade amphibolites by the presence of chlorite in the assemblage.

The chemographic diagram (Figure 4.3.3) depicts the high temperature mineral assemblages recorded in the Swartkoppie Metagabbros.

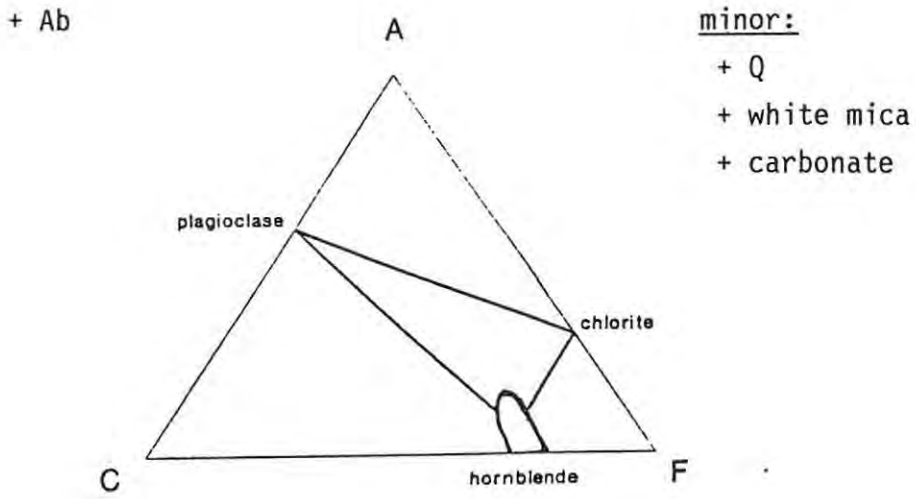

Figure 4.3.2(a): The high temperature mineral assemblage of the Swartkoppie Metagabbros.

The Sinclair-aged metagabbros, basic metalava and Swartkoppie dykes are characterised by the mineral assocciation *albite* - *actinolite* - *chlorite* and lack hornblende. This assemblage is indicative of the lower temperature (about 300°C) part of the low-grade greenschist facies. The chemographic diagram which best represents the above-mentioned assemblage is the ACF diagram depicted in figure 4.3.2(b).

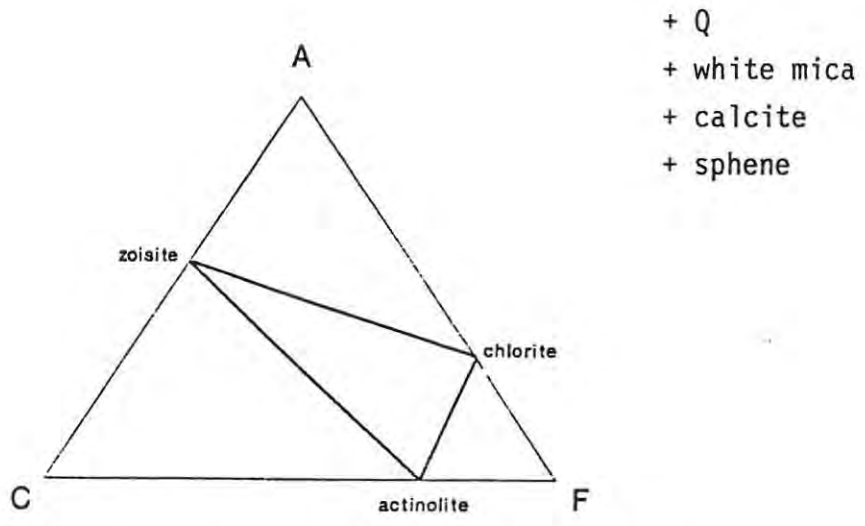

Figure 4.3.2(b): Low temperature mineral assemblage - Sinclair Metagabbro.

4.3.3 Contact Metamorphism

The effects of contact metamorphism are restricted to narrow zones within the schists bordering granitic intrusions. Contact aureoles are not readily recognised in the field, although thin-section studies of schists near granite intrusives contain biotite. Stubby laths of biotite are randomly orientated in contrast to the lepidoblastic nature of the pre-existing chlorite and muscovite. In the aureole the breakdown of muscovite + chlorite has led to the formation of biotite (Plate 4.3.3). The mineralogical assemblage of these contact zones is typically *quartz - muscovite - biotite - chlorite* and is assigned to the albite-epidote-hornfels facies of Turner (1981).

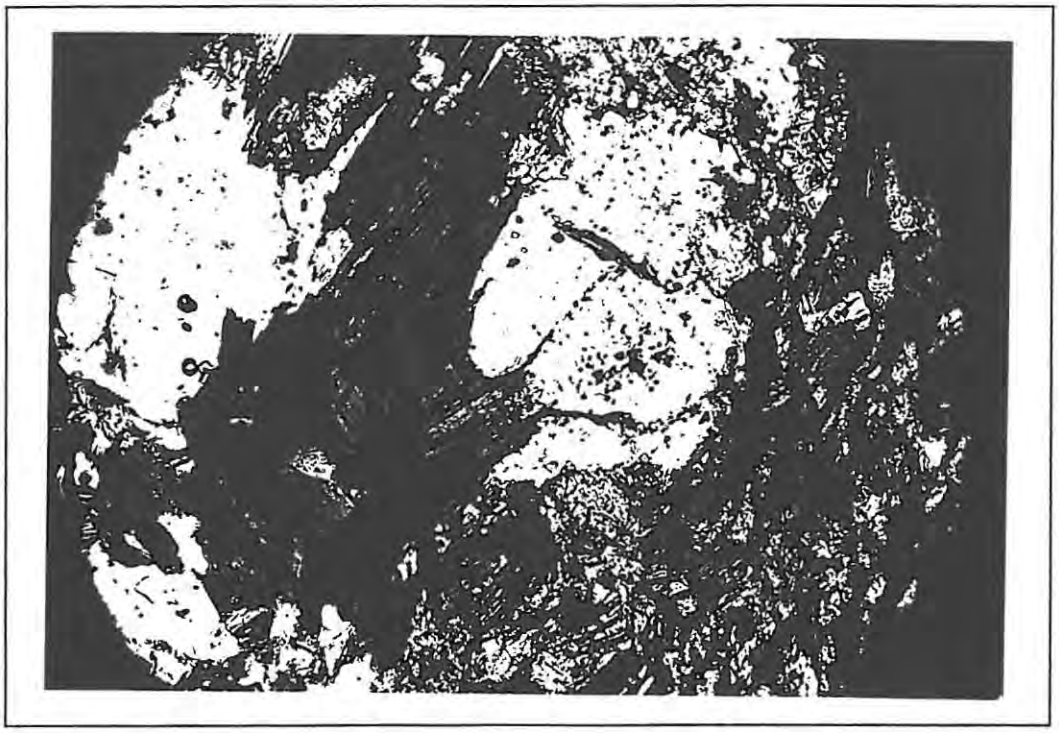

Plate 4.3.3: Biotite laths associated with contact metamorphism.

4.3.4 Relationship between Metamorphism and Structure

The strong lepidoblastic fabric of the micas in the various pelitic units indicates that mineral growth occurred syn-tectonically during the D_1 deformation event. Later deformation and metamorphic overprinting resulted in a crenulation of this S_1 fabric to form the S_2 fabric. The S_2 fabric is not associated with any futher development of metamorphic minerals and thus M_2 was not sufficiently severe to have resulted in recrystallization of the

minerals and thus M_2 was not sufficiently severe to have resulted in recrystallization of the minerals (in particular micas).

Microtextural observations of the rocks within the grant area suggest a single regional *low-grade* metamorphic event. Observations include :

i) all minerals are diagnostic of the same metamorphic grade and facies,

ii) only <u>one</u> generation of metamorphic minerals exists

iii) contact metamorphism from younger granitic intrusions post dates the regional S_1 fabric.

4.3.5 Pressure and Temperature Estimates

An accurate determination of the metamorphic conditions (temperature and pressure) is not possible from only studying mineral relationships. Experimental studies of various systems reveal the accurate conditions under which various reactions occur in chemical systems much simpler than natural rocks. Unfortunately such studies are restricted to a few chemical systems (ie. calcite-dolomite), which are not present in the area studied. Although pressures and temperatures deduced from mineral assemblages are not very accurate, the approximate estimates from this study are in agreement with isotopic studies presented by Ahrendt et al. (1978) and Ziegler and Stoessel (1988).

The mineral assemblages discussed in the previous section are all characteristic of the *low-grade greenschist facies*. The lower limit of the grade in question is marked by the elimination of pumpellyite in favour of epidote, while the upper limit is best recognised in metapelites by the diagnostic first appearance of staurolite or cordierite. This upper limit is also defined, in basic rocks, by the sudden incoming of oligoclase (An_{20}) accompanying or replacing albite (An_5) (Turner, 1981). Within this temperature range of about 200°C, reactions in pelitic rocks give rise to mineral assemblages of the classic Barrovian "*chlorite, biotite and garnet zones*". The presence or absence of the assemblage *biotite + muscovite* determines the boundary between the chlorite and biotite zones. No biotite was recorded in any of the regionally metamorphosed pelites (only muscovite + chlorite), hence the conditions of metamorphism seem to correlate well with those of the chlorite zone of the Barrovian assemblages.

Hornblende is present with clinozoisite, epidote, clinopyroxene and plagioclase (albite) within the Swartkoppie Metagabbros. At first the assemblage would seem to indicate conditions similar to those of the high temperature greenschist facies. On the contrary, the metapelite assemblages indicate conditions of metamorphism of the lower temperature part of the greenschist facies. The presence of clinopyroxene is due metastable persistence in this retrogressed mineral assemblage. Thus it is feasible to conclude that the mineral assemblages of the Swartkoppie Metagabbros did not fully equilibrate with the metamorphic conditions prevailing and thus imply higher conditions of metamorphism than actually prevailed. This conclusion is supported by the mineral assemblage of the 'older metagabbros', which have fully equilibrated to a low-temperature greenschist facies assemblage (actinolite-epidote-clinozoisite-quartz-plag (albite)).

Based on the above conclusions the conditions of metamorphism suggested were temperatures in the range of 300°- 350°C and a pressures of 3-4 kb (Figure 4.3.5).

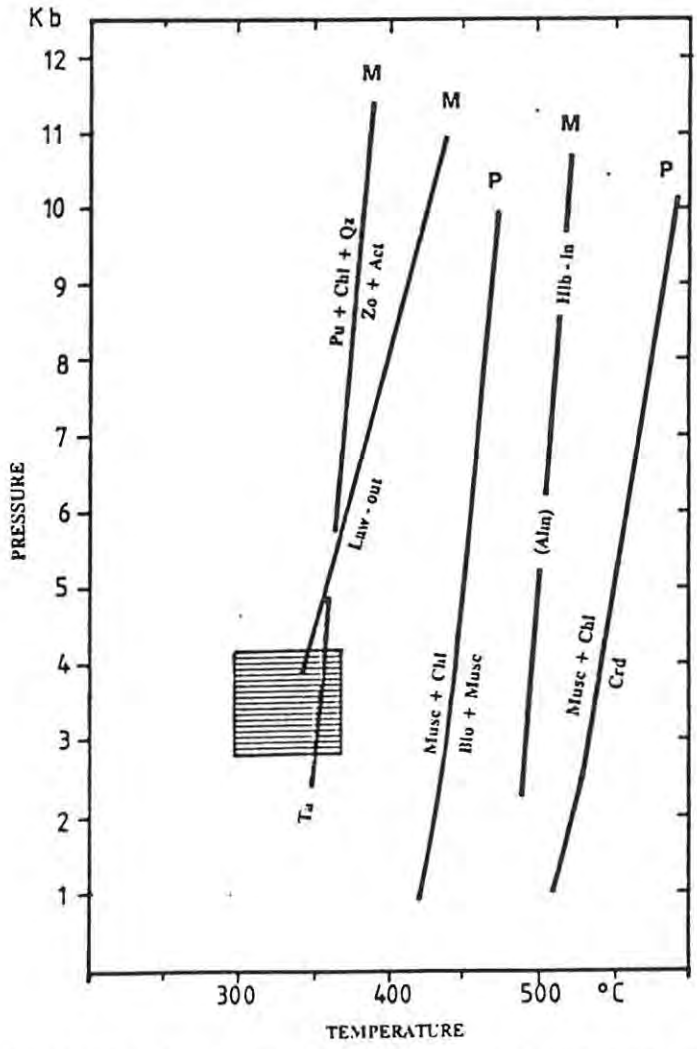

Figure 4.3.5(a): Pressure / Temperature estimates of the Neuras Grant.

The grade of metamorphism is known to increase from the Southern Margin of the Damara towards the centre. Lowest grades in the Southern Margin Zone are indicated by biotite grade conditions in the metapelites (Hartmann et. al., 1983). The first appearance of biotite together with stilpnomelane is recorded further south, in the Pre-Damara basement, of the Southern Margin (Hartman et al., 1983). The area studied lies some 40km south of the Southern Margin of the Damara and is devoid of any biotite. The investigations of this study show that Millers' (1983) map of metamorphic isograds, page 470, is more correct than that of Ahrendt et al. (1978). Figure 4.3.5(b) depicts a compilation of the various isograds proposed (including this study). Millers' (1983) and Ahrendt et al's. (1978) maps are presented on the following pages.

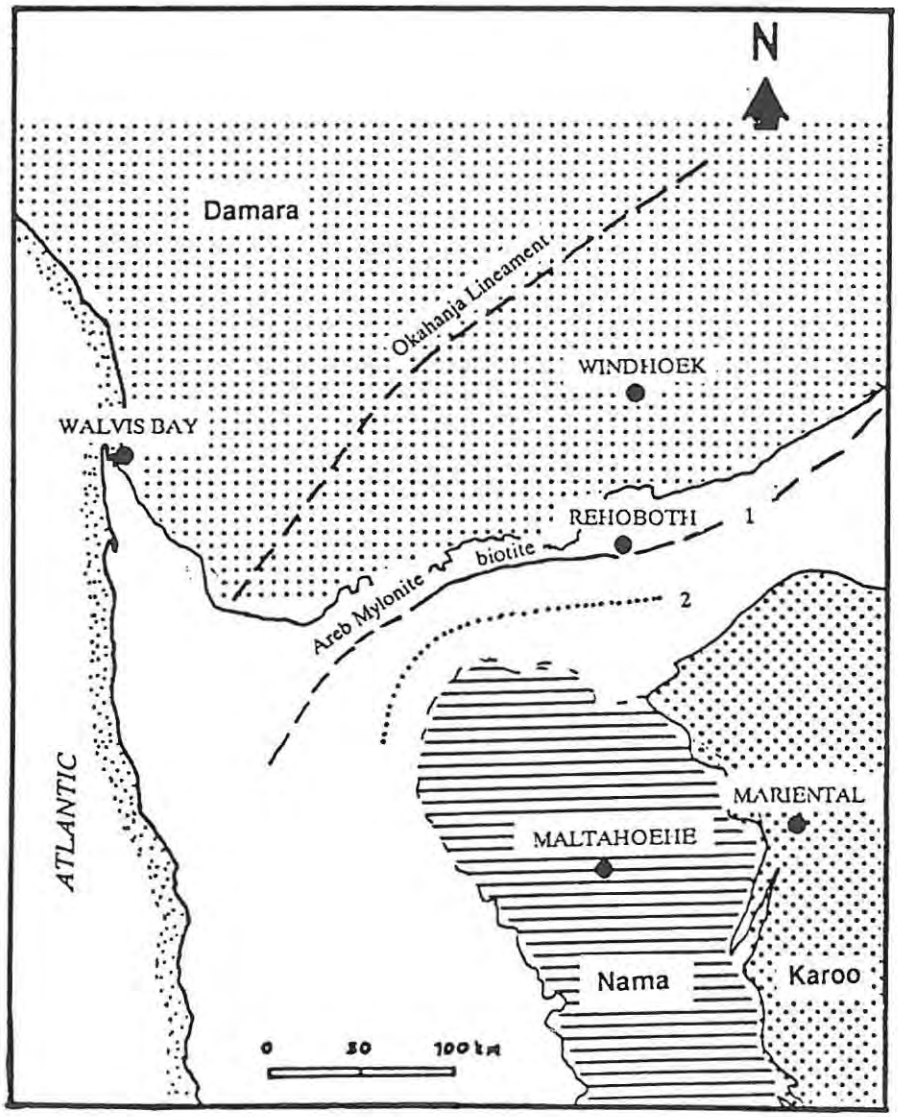

Figure 4.3.5(b): Metamorphic isograd map of the area studied.

1 = Millers' (1983) biotite isograd (supported by this study)

2 = Ahrendts' et al. (1978) biotite isograd (not supported by this study).

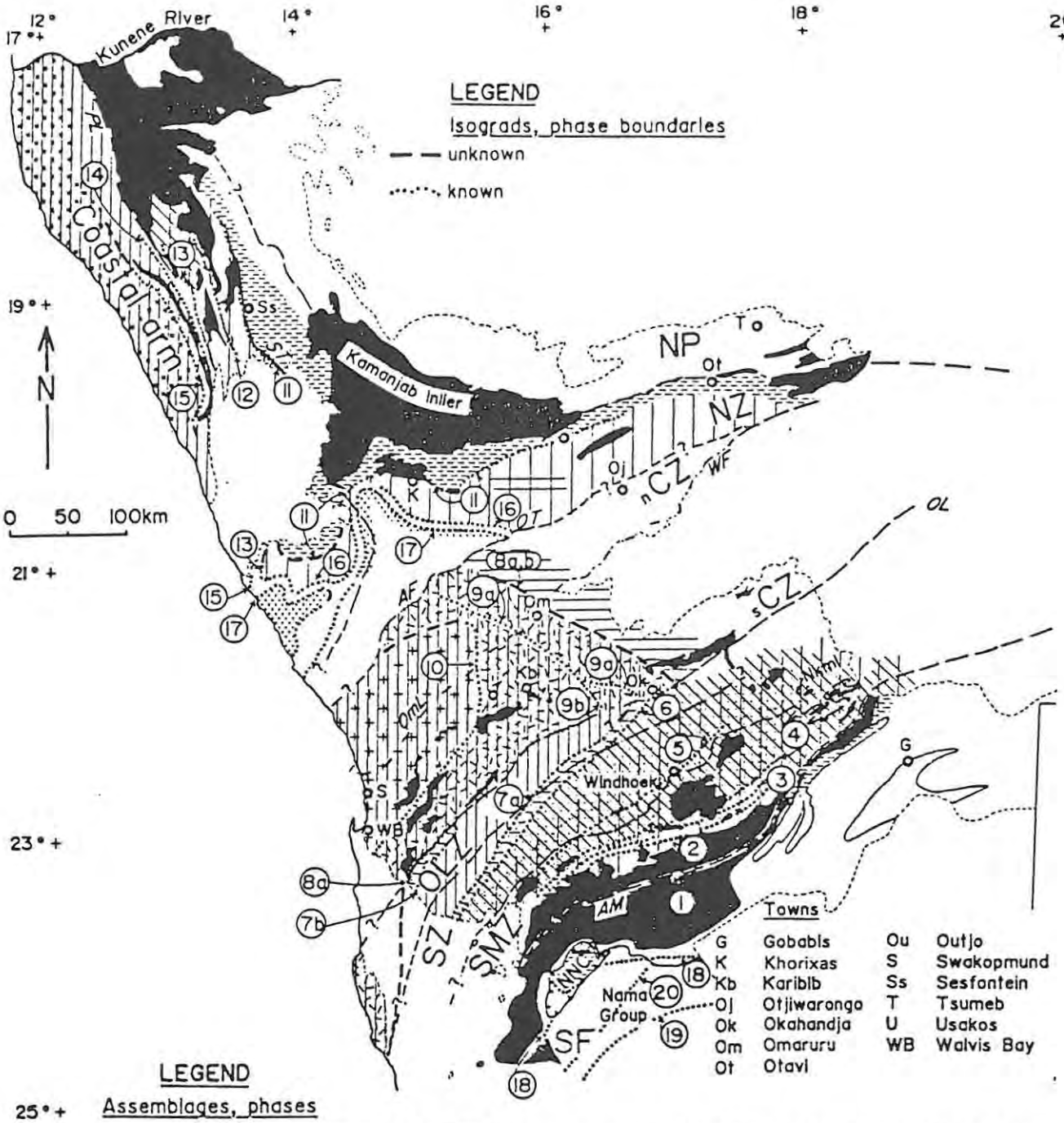

Figure 26

Isoreactiongrads, phase boundaries and isolines of illite crystallinity (after Guj, 1970a; Miller, 1973a, 1979, 1980; Blaine, 1977; Hoffer, 1977; Klein, 1980a; de Kock, in prep a; Ahrendt *et al.*, 1977; Miller *et al.*, 1975; Hartmann *et al.*, 1983).

1. Chl + Kspar = Bi + Stilp + Qtz + H_2O, approximately along Areb Mylonite.
2. Chl_{ss} + Plag = Ga + Chl_{ss} + Qtz + H_2O
3. Ga + Chl + Mus (Phengite) = St + Bi + Qtz + H_2O
4. St + Chl + Mus + Qtz = Ky + Bi + H_2O
5. Ky + Chl + Mus + Qtz = Cord + Bi + H_2O (rare)
6. Ky = And
7a. And = Sill
7b. St + Mus + Qtz = Sill + Bi + H_2O
8a. And = Sill
8b. Mus + Plag + Qtz + H_2O = melt + Sill
9a. Mus + Qtz = Sill + Kspar + Ab + H_2O
9b. Bi + Sill + Qtz = Cord + Kspar + H_2O
10. Bi + Kspar + Plag + Qtz ± Cord = melt + Ga
11. Main Bi-in boundary
12. Ga in
13. Chl + Mus out, oligoclase in, Hnbl in
14. Sill in
15. Feldspar blastesis in
16. Thermal metamorphism, Chl + Muse out
17. Thermal metamorphism, cordierite in
18. Illite crystallinity, Hb_{xl}<200
19. Illite crystallinity, Hb_{xl}<350; boundary between diagenesis and metamorphism
20. Southern limit of slaty cleavage in Nama rocks

Ab — albite, And — andalusite, Bi — biotite, Chl — chlorite, Cord — cordierite, Ga — garnet, Hnbl — hornblende, Kspar — potash feldspar, Ky — kyanite, Mus — muscovite, Plag — plagioclase, Qtz — quartz, Sill — sillimanite, St — staurolite, Stilp — stilpnomelane.

Figure 4.3.5(c): Millers' (1983) Metamorphic Map

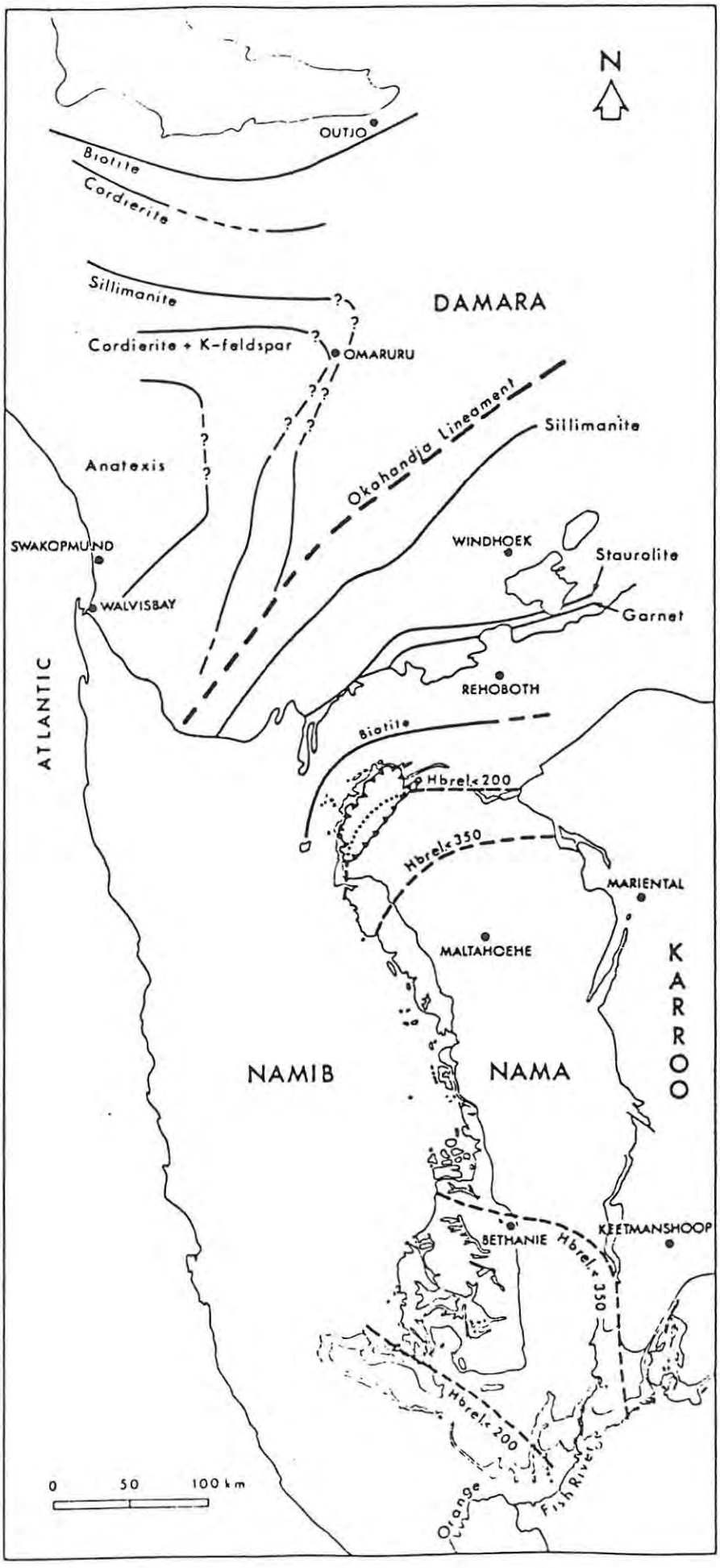

Figure 4.3.5(d): Ahrendts' et al. (1978) Metamorphic Map

4.4 GEOLOGICAL HISTORY OF THE NEURAS GRANT AREA

Although rifts have been extensively studied their origin is still the subject of controversy. Mechanisms for rifting generally fall into two classes - active and passive. Borg (1988) advocates an active model for the development of the Irumide rift which involves a stationary elongate asthenospheric plume over which the Kalahari plate migrated. Borg (op cit.) suggests a southwards migration of the plate over the stationary plume to account for the tectonogenesis of both the Irumide and Damara orogens (Figure 4.4.1).

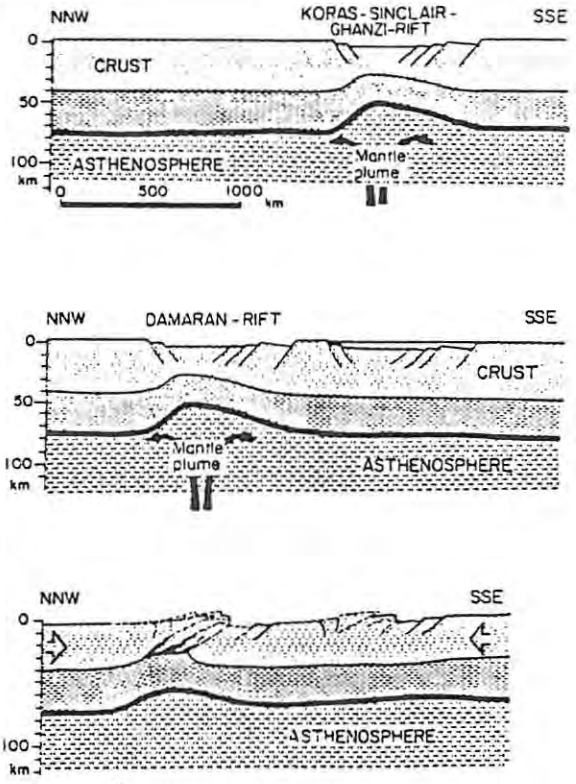

Figure 4.4.1: Schematic illustration of the evolution of the Koras-Sinclair-Ghanzi rift and early Damara Rift due to plate migration southwards over a stationary mantle plume (after Borg, 1989).

A passive model for rifting, ie. one that advocates mechanical thinning or lateral lithospheric stretching in response to a regional extension followed by the passive rise of asthenospheric material into shallower levels, is favoured by the author. It is well known that rifting throughout the African continent is preferentially developed at the margins of continental plates (Bailey, 1983). Rifting of the Irumide is broadly contemporaneous with the development of the 'Namaqua Orogen' suggesting that rifting may have well been collision induced (Figure 4.4.2).

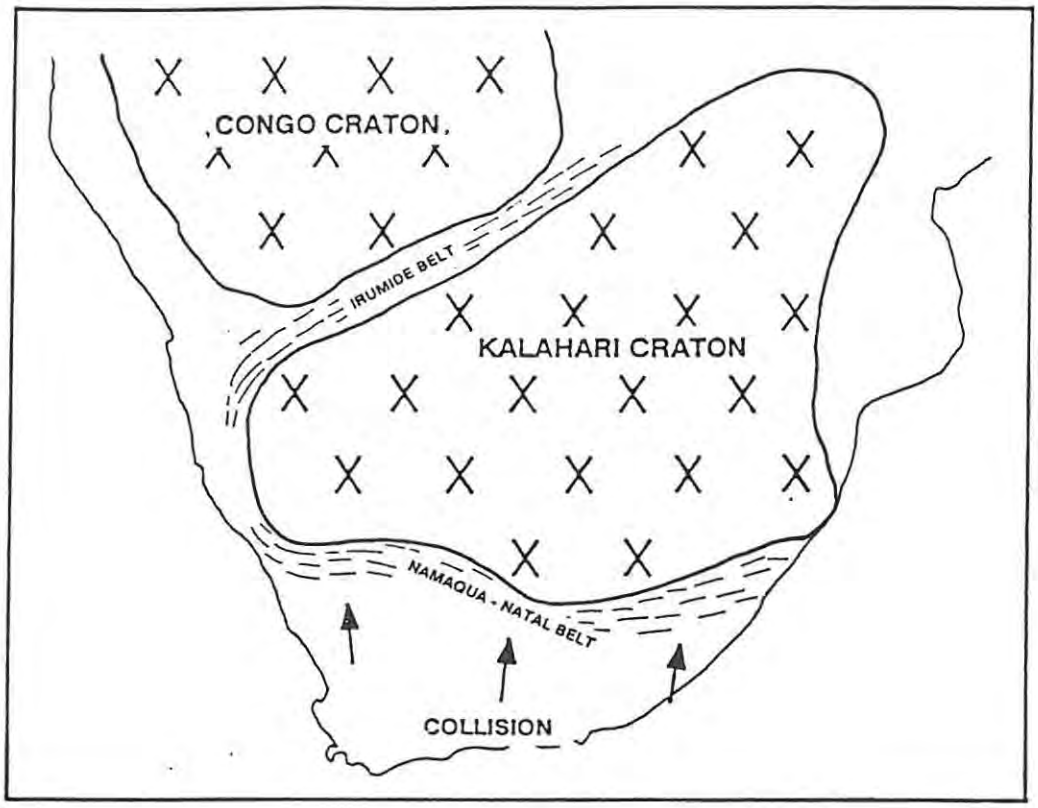

Figure 4.4.2: Schematic figure of the Namaqua Collisional event and formation of the Irumide Belt.

Initial extension of the lithosphere resulted in the development of narrow fault-bounded continental rift grabens whose structural and sedimentation patterns were strongly controlled by normal faulting. Sedimentation was accompanied by acid magmatism (rhyolite lavas, tuffs and ignimbrites), which is thought to reflect initial crustal melting in response to higher geothermal gradients and possible volatile fluxing from rising asthenospheric material (Figure 4.4.3).

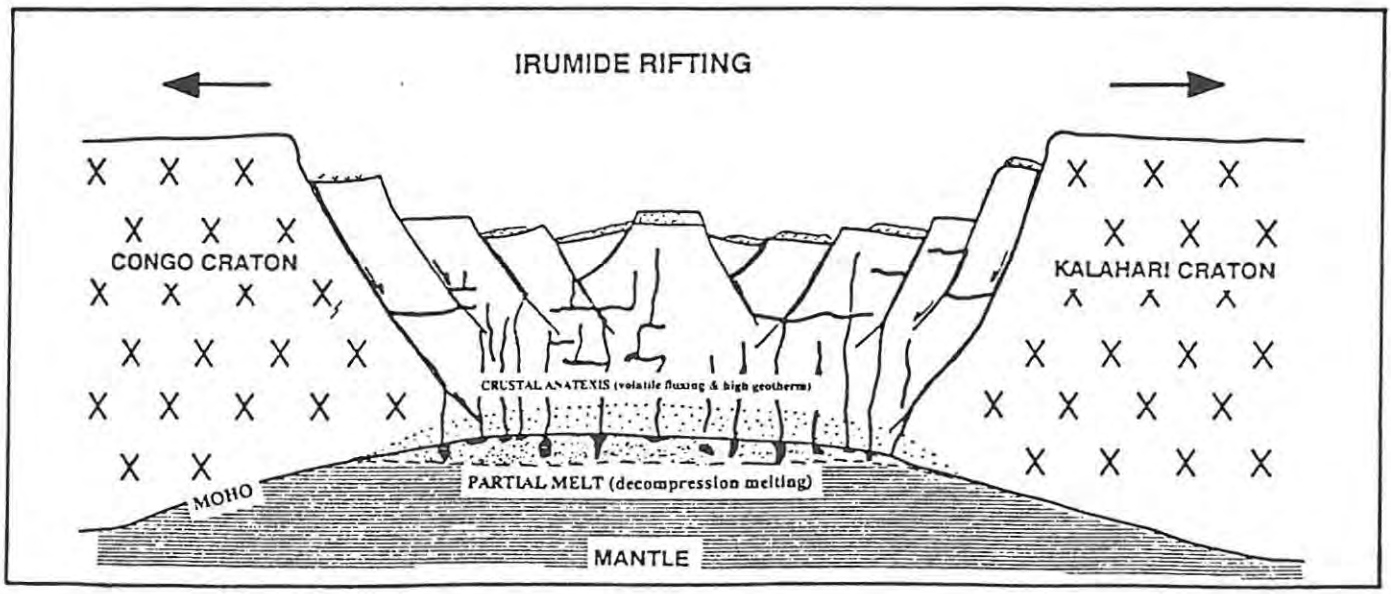

Figure 4.4.3: Schematic figure of initial rifting during formation of the Irumide Belt.

A later pulse of acid magmatism resulted in voluminous amounts of granitoid emplacement (Piksteel, Swartmodder, Swartskaap and Neuras Granites). Apart from the Piksteel Granodiorite, which is S-type in origin, all other granites have I-type and calc-alkaline affinities. Tectonic discrimination using immobile trace elements reveal dominant 'Volcanic Arc' signatures. The reader is referred to section 3.2 in which discussion of the 'anomalous' tectonic signatures is delt with (Figure 4.4.4).

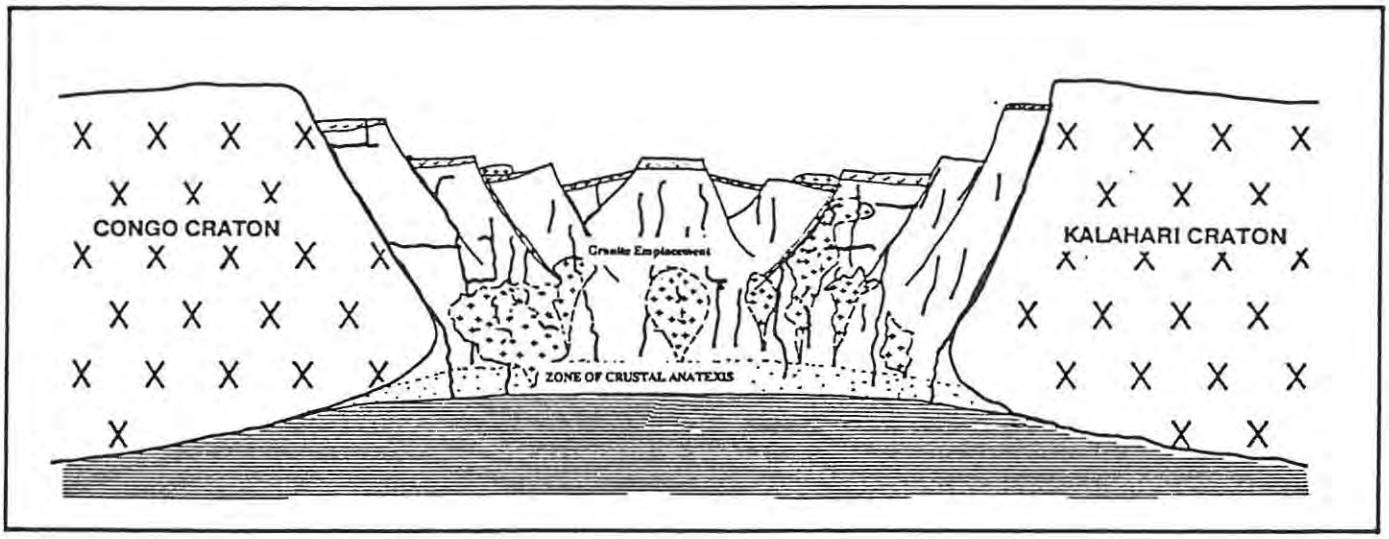

Figure 4.4.4: Schematic figure of granite formation as a result of increased geothermal gradients due to rifting.

With continued extension fractures penetrated through the attenuated crust and tapped partial melt formed during mantle uprise (decompression melting). The magma extracted from the 'fertile' mantle was enriched in incompatible trace elements, compared to later magmas, and emplaced as a swarm of mafic dykes whose trends parallel the rift axes. These dykes were undoubtedly feeders for flows higher up in the sequence (now eroded away).

Intrusion of quartz porphyry dykes and voluminous high level granite/quartz porphyry followed that of the mafic dyke swarm resulting in intence deformation of the dykes. The acid magmas are again I-type and calc-alkaline in character and suggested to have again been derived from lower crustal material. Closure of the Irumide rift basins appears to have been from the north and resulted in low grade metamorphism, intense foliation and mineralization (Figure 4.4.5). Thrust faults are propagated in a south-eastward direction confirming compressional stress from the north-

west. Studies of thin sections reveal a dominant fabric which has been kinked in places. K-Ar dating of the micas from the pelitic units indicate a metamorphic age of 530 Ma which is correlated with the peak metamorphic event of the Damara.

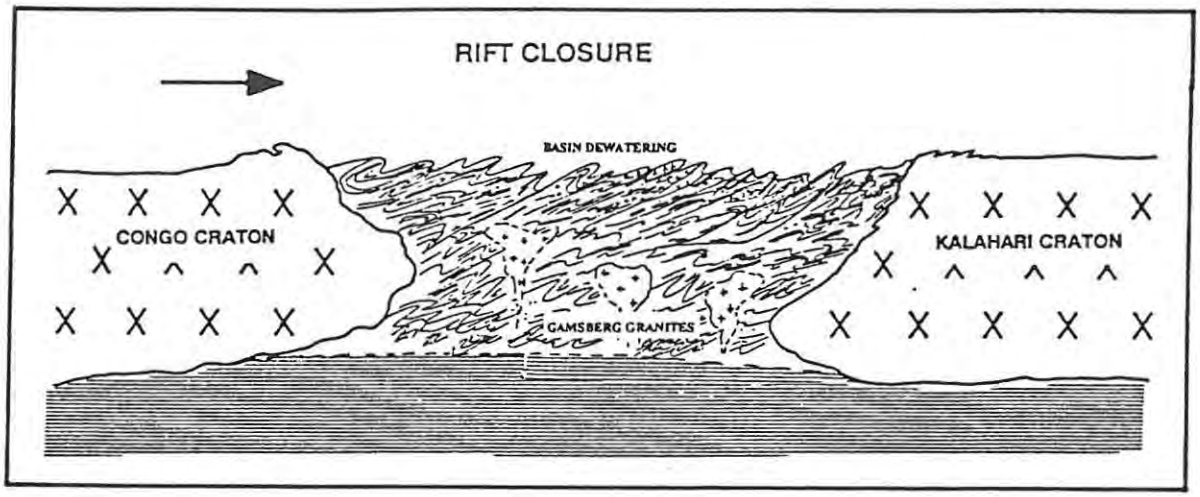

Figure 4.4.5: Schematic figure illustrating rift closure and basin dewatering.

Several studies have thus advocated a single deformation event for the Irumide as being syn-metamorphic. Regional field evidence suggests that the Irumide lithologies have undergone a pre-Damara deformation event. Hoffmann (pers comm., 1990) states that the Irumide lithologies are comparatively more deformed than the immediately overlying Damara lithologies and that the structural contact between the Damara and Irumide is in fact unconformable. Reactivation of various shears and faults by the Damara deformation event is not excluded to have occurred. Of all the lithologies in the study area, only two are undeformed, the Swartkoppies mafic dyke swarm and the Gamsberg Granite Suite (Figure 4.4.6). The Swartkoppies mafic dykes are intruded along similar trends to the Older sheared dyke swarm. Geochemistry of the Swartkoppies dykes shows them to be chemically more primitive than the former dyke swarm.

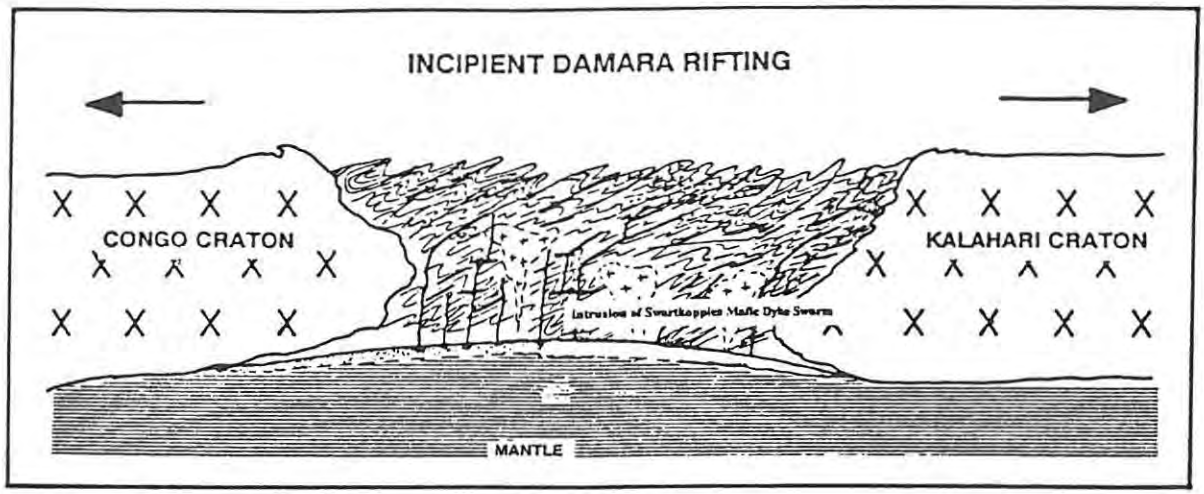

Figure 4.4.6: Schematic figure illustrating incipient Damara Rifting and intrusion of the Swartkoppies Mafic Dyke Swarm.

The lack of overlapping variation trends and relatively long time gap (49 Ma to 140 Ma) between the two dyke swarms precludes fractional crystallization as a viable petrogenetic model. The Older mafic dyke swarm may represent the initial partial melt formed during the Irumide rifting, depleting the upper mantle of incompatible elements. With the onset of initial Damara rifting, which developed partly on and adjacent to the Irumide Belt, partial melting again took place, giving rise to the Swartkoppies dyke swarm (Figure 4.4.6). This second partial melt would have been depleted in incompatible elements and thus comparatively more primitive than the Older sheared dyke swarm.

4.5 MINERALIZATION

4.5.1 TYPES AND OCCURRENCES OF MINERALIZATION

Gold was the only element analysed for on a routine basis. Samples were analysed by means of a commercial 'scanning technique' (Scientific Services) with lower limits of detection being < 40 ppb Au and upper limits of detection being > 5000 ppb Au. The 'gold scanning technique' employed is the Aqua Regia leach/Organic phase stripping method and concentrations are measured on AAS. Although only Au was analysed for, numerous copper showings were noted. The present study emphasises gold mineralization but copper mineralization is briefly covered were relevant.

4.5.2 COPPER MINERALIZATION

4.5.3 Swartmodder Copper Mine

The Swartmodder Copper Mine was brought into production by Oamites which purchased mining rights from Falconbridge in order to enrich and prolong the Oamites Mine situated further north (Plate 4.5.3(a)). The decision to mine was based on several borehole intersections of up to 3% Cu over several metres. Initial ore reserves were calculated at 340 000 t grading at 2.47% Cu and 4 g/t Ag over a width of 2 m. Once underground development and mining commenced it became obvious that mineralization was extremely patchy.

Mineralization consists essentially of chalcopyrite and pyrite with minor covellite , chalcocite , bornite and magnetite hosted in a relict schist enclave within the Swartmodder Granite (Plate 4.5.3(b)). The schist appears to have been sheared into an almost east-west undulating zone which pinches and swells along its 160m strike length. Three mafic dykes cut the shear zone resulting in local enrichment of sulphides.

Plate 4.5.3(a): Inclined shaft of the abandoned Swartmodder Copper Mine.

A combination of bad ground and a lack of ore-zone continuity forced the company to consider cut-and-fill mining methods instead of the conventional long-hole open stoping. Swartmodder produced ore for only 6 months, between August 1980 and Febuary 1981, before closing down. The main reason for closure was the lack of continuity which resulted in high waste extraction which effectively diluted the ore grade to less than 1% Cu over the entire period of production.

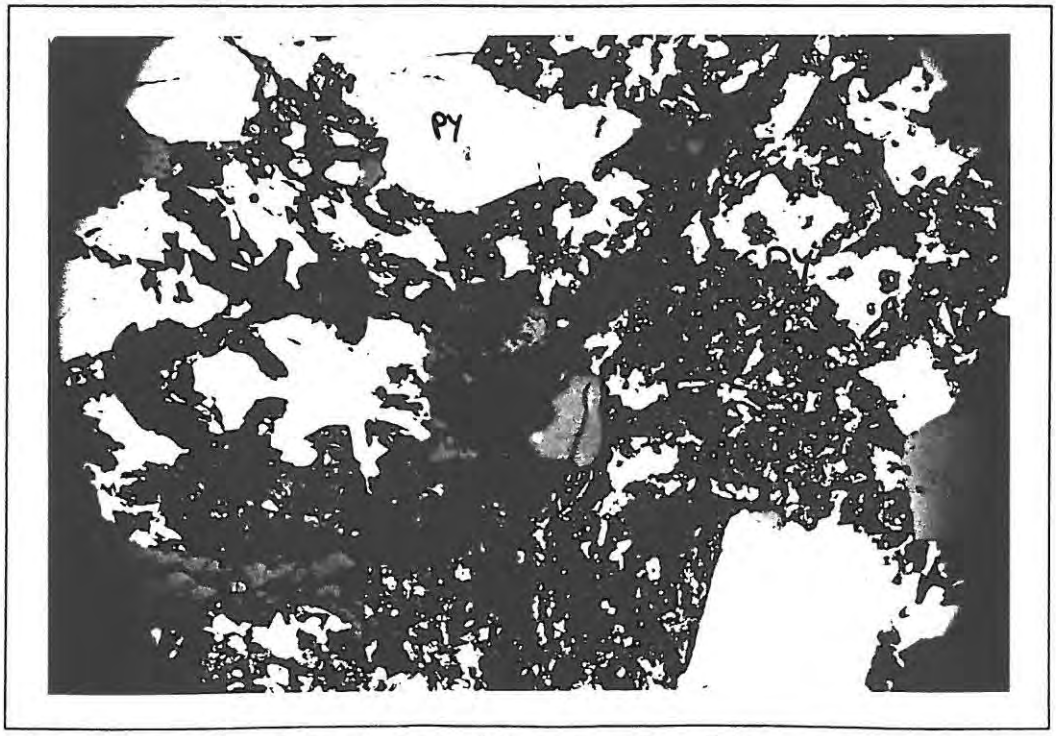

Plate 4.5.3(b): Photomicrograph of Swartmodder Ore:- cpy = chalcopyrite, py = pyrite, cc = chalcocite, FOV = 3 mm.

4.5.4 GOLD MINERALIZATION

Gold mineralization within the Neuras Grant area was recognised as far back as the ninteenth century. Several small mines namely, Neuras, Swartmodder and Blanks Mines operated in the early part of the twentieth century. The Mebi Mine, a small one-man operation, is currently still in production. The present study involved revisiting many of these old workings as well as other mineralized areas, with the aim of trying to formulate a model for the mineralization. Based on various geological features observed both in the field and in the laboratory, a model is proposed which accounts for the genesis, timing and controls of gold mineralization within the area studied. A comprehensive account of mineralized areas within the Neuras grant area precedes the proposed model.

4.5.5 Swartmodder Gold Mine

Extensive trenching along a mafic dyke and the contact zone between Marienhof Schist and Piksteel Granodiorite highlights the sites of previous mining activity (Plate 4.5.5). The mine area is reported to have yielded 32.5 kg of gold during its production (Cooke, 1965).

Plate 4.5.5: Inclined shaft at Swartmodder Gold Mine.

Gold mineralization is restricted to two areas of concentration :-

i) Gossanous quartz-haematite veins in the footwall of a sheared mafic dyke.

ii) Gossanous quartz-haematite veins at the contact margin between Piksteel Granodiorite and Marienhof Schist.

Both these contact areas have been extensively mined out along a strike distance of ± 250m. Mining occurred by means of inclined shafts along the mineralized contacts, figure 4.5.5 shows gold scan values associated with the contact between the schist and granodiorite.

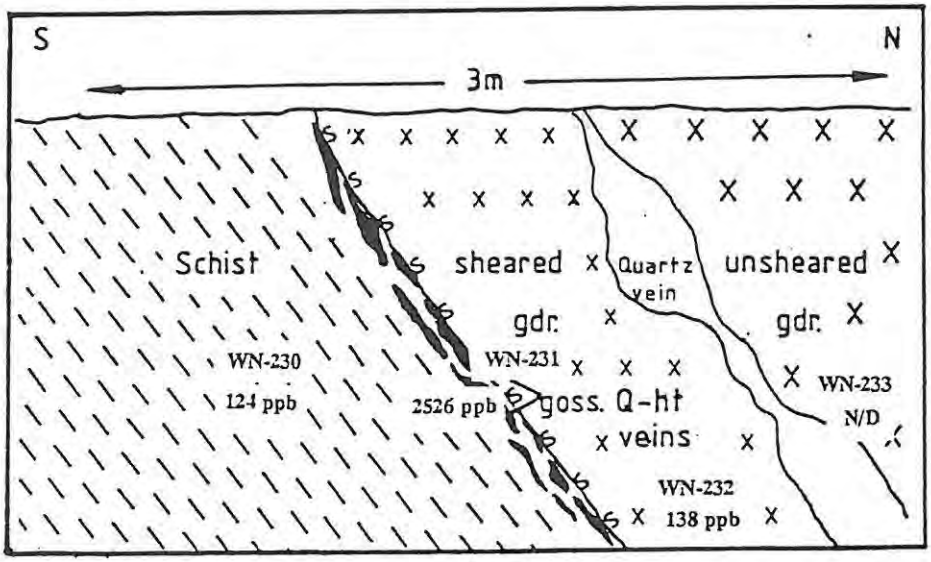

Figure 4.5.5: A field sketch of a section of trench depicting the mineralized contact at Swartmodder Gold Mine.

The ore mineral assemblage is devoid of sulphides, although limonitic boxworks after pyrite and chalcopyrite testify to their prior existence. Oxides such as haematite, magnetite and goethite dominate the mineralized veins. Alteration is restricted to narrow zones adjacent to the mineralization and is dominated by quartz and sericite. The control of the mineralization is clearly structural, with mineralizing fluids utilizing the various lithological contacts as conduits zones.

4.5.6 Neuras Gold Mine

The Neuras gold mine was the first operating gold mine within the Neuras grant area. Mining commenced in 1910 and lasted for a few years. Very little is documented in the way of tonnages and total gold recovered, although an average grade of the concentrate being 68.5 g/t Au was recorded.

Mining took place adjacent to two sheared mafic dykes which appear to have channelled and restricted mineralizing fluids. Gold mineralization is concentrated in narrow gossanous haematite-quartz veins adjacent to the dyke margins. Values of up to 463 ppb Au were recorded for altered mafic dykes; while unaltered dykes yielded below detection limits. Gossanous quartz-haematite veins yielded values consistently above 2000 ppb Au.

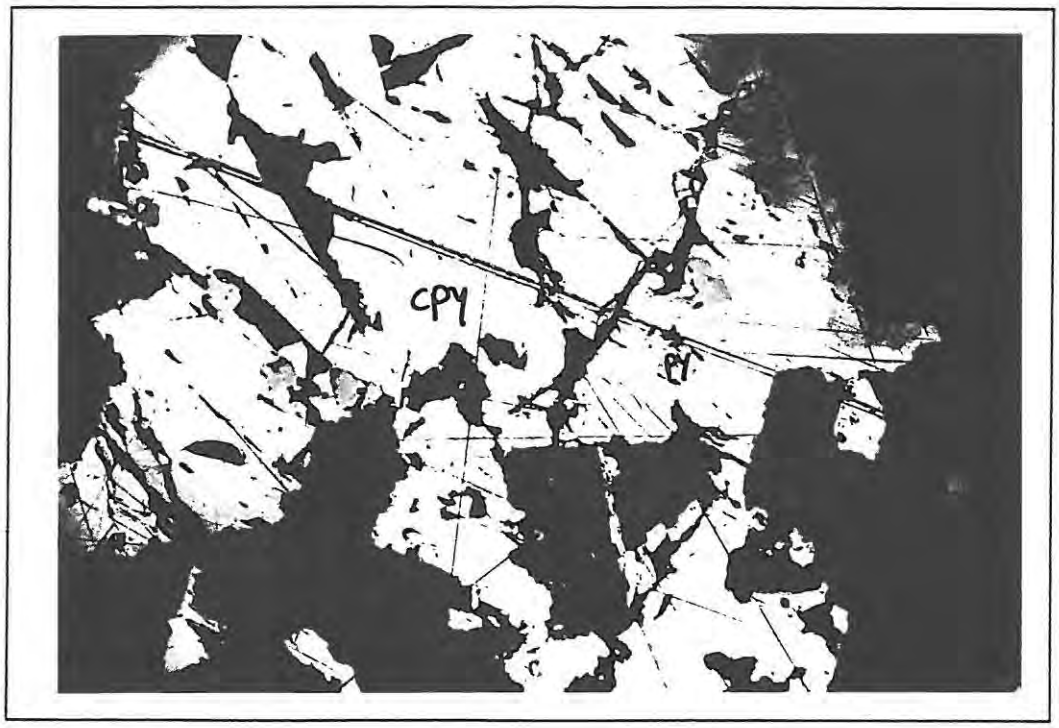

Plate 4.5.6(a): Photomicrograph of the mineralization at the Neuras Gold Mine, cpy = chalcopyrite, py = pyrite, FOV = 1 mm.

The Neuras host granite is intruded by both mafic dykes and quartz-porphyry. Mineralized gossanous quartz-haematite-sulphide veins are hosted in both the Neuras Granite and the quartz-porphyry (Plate 4.5.6(a)). Alteration of the host rocks is restricted to narrow areas adjacent to the mafic dykes and includes non-pervasive sericitic and chloritic alteration. Later epidotization, in the form of cross-cutting veinlets, is commonly evident (Plate 4.5.6(b)). Unaltered host rock is barren of any mineralization.

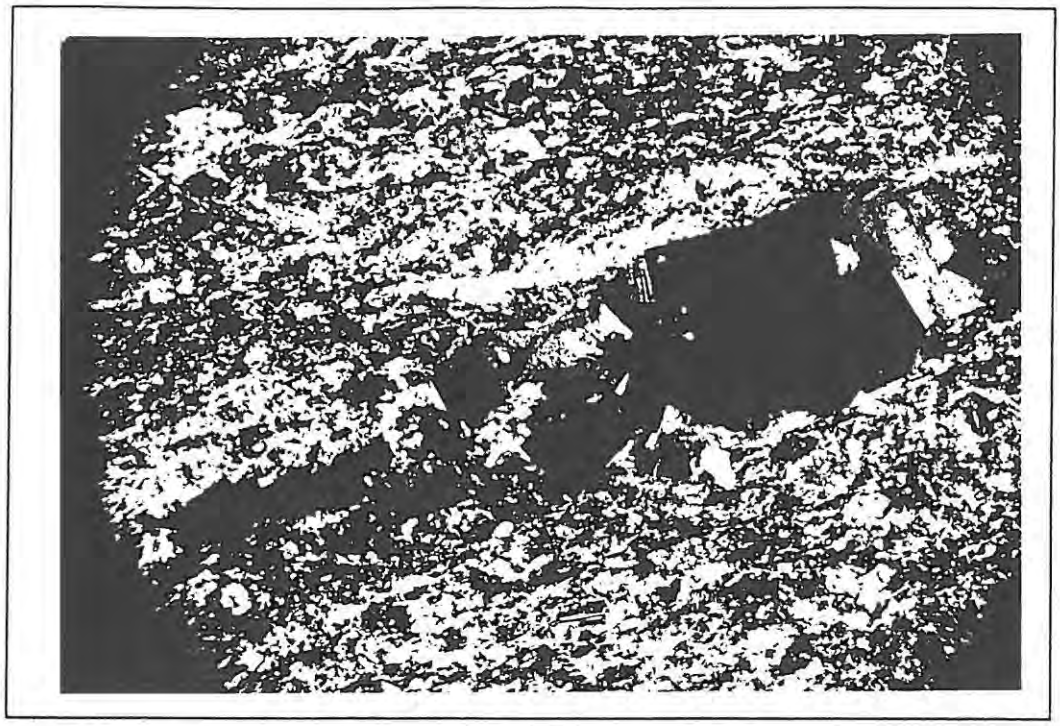

Plate 4.5.6(b): Photomicrograph of the alteration mineralogy at Neuras Gold Mine, FOV = 3 mm

4.5.7 Mebi Gold Mine

For a detailed account of the structure of the Mebi shear zone, the reader is referred to section 4.2.3. Mebi mine is reported as having been in production since 1979 and tonnage mined is roughly between 30 000 and 50 000 t with an average grade of 2.2 g/t Au (Siebeck, 1989 pers comm.).

Mineralization is confined to the Mebi shear zone within Piksteel Granodiorite and Marienhof schists. Gold mineralization is restricted to quartz veining within the zone of shearing however although some lower values were obtained in altered and less deformed islands of country rock (Plate 4.5.7(a)). Vein quartz is by far the most prominent constituent of the shear zone and hosts isolated pods of copper-sulphides as well as gossanous veinlets within the quartz. Highest gold values were obtained from such sulphide pods (Table 2).

Plate 4.5.7(a): The Mebi Shear Zone, 60 m below surface.

Table 2

Au Value (ppb)	Host lithology
N/D *	Raft of Piksteel Granodiorite
N/D	Quartz vein material
323	Ferruginised quartz
343	Ferruginised granodiorite
514	Quartz vein material
669	Sheared granodiorite
681	Quartz vein material
1559	Sulphide-bearing quartz vein
2966	Sulphide-bearing quartz vein
2967	Sulphide-bearing quartz vein
3199	Sulphide-bearing quartz vein
5000	Sulphide-bearing quartz vein

Table 2: Gold values for Mebi Mine. *N/D = not detected.

Ore mineralogy comprises chalcopyrite, covellite, chalcocite and oxides haematite and goethite. Secondary enrichment of the chalcopyrite to covellite and chalcocite is clearly evident in the photomicrograph below (Plate 4.5.7(b)).

Plate 4.5.7(b): Photomicrograph of ore from the Mebi Mine. FOV = 3 mm. py = pyrite, cc = chalcocite, cpy = chalcopyrite.

Petrographic examination of the host rock granodiorite reveals two generations of sulphide (pyrite ?) pseudomorphed by haematite; a pre to syn-deformation generation which has been rounded by deformation (D_1) and a post D_1, perhaps syn-D_2 introduction of the second haematite-generation which is characterised by its lack of deformation (Plate 4.5.7(c)).

Alteration of the granodiorite host rock is pervasive in areas which border on the major quartz veining and rapidly becomes non-pervasive further away. The granodiorite is altered to an assemblage of quartz-sericite-carbonate. In places a second generation of silicification accompanies a later stage carbonate alteration phase.

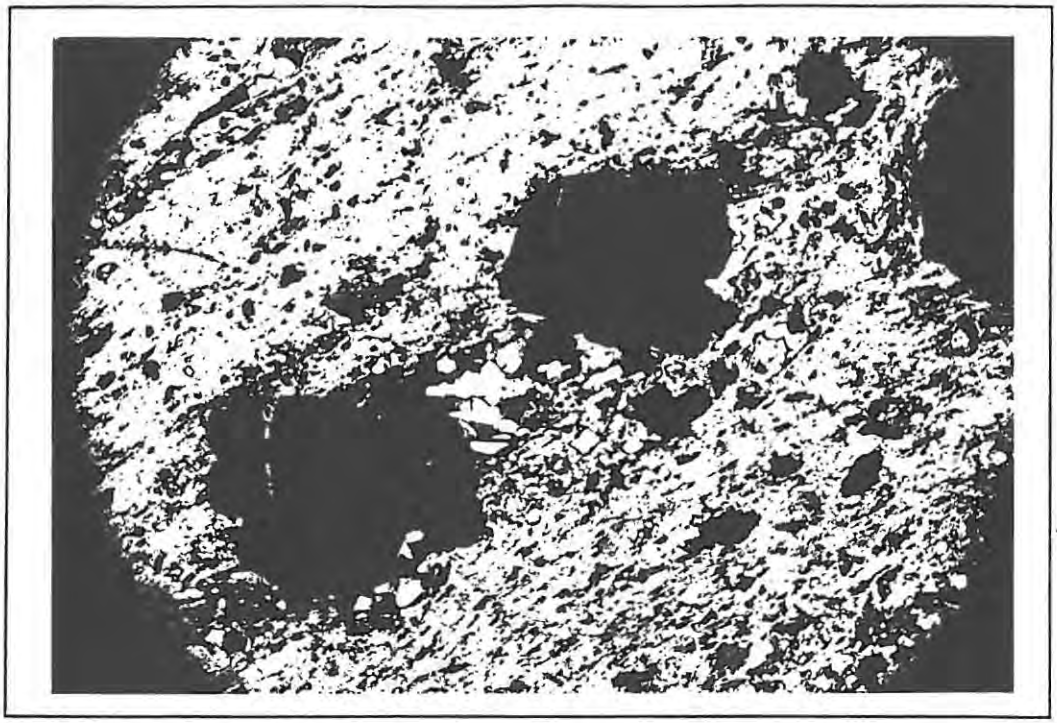

Plate 4.5.7(c): Haematite pseudomorphs after pyrite within the Mebi Shear Zone.

4.5.8 TARGET AREAS 1 - 20

Reconnaissance mapping at a scale of 1 : 10 000 identified several areas of anomalous gold mineralization (Smalley, 1989). Each target area was investigated by the author (present study) by means of detailed mapping and lithosampling at a scale of 1 : 1000. Maps of each target area showing sampling positions, gold values and lithological relations are presented along with brief descriptions. Gold is restricted to older, first order, gossanous-quartz-haematite veins while younger undeformed greasy-white veins, second-order, are barren of any mineralization.

KEY FOR DETAILED AREAS.

Alluvium

Quartz vein and scree.

Quartz porphyry dyke

Rhyolite (lava and tuff)

Quartz porphyry

Mafic dyke

Granite

Granodiorite

Schist

Phyllite

Quartzite

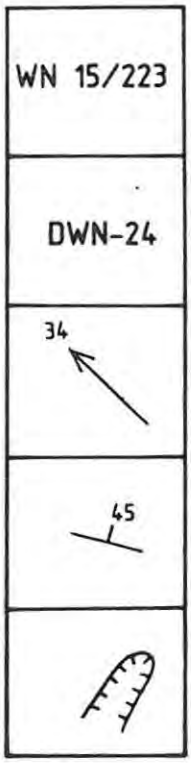

Sample No/Au ppb

Petrographic sample

Lineation

Foliation (dip and strike)

Workings

mt	magnetite
Fe	iron (limonite, gossan)
Cu	copper (malachite, chalcocite)
py	pyrite
ht	hematite

SCALE 1:1000

4.5.8.1. Area 1

The geology of the area comprises Piksteel Granodiorite intruded by the Older sheared mafic dyke swarm and quartz-feldspar porphyry dykes. Plate 4.5.6.1 shows a bifurcating sheared mafic dyke intrusive into the Piksteel Granodiorite, note the extreme degree of foliation.

Plate 4.5.8.1: Bifurcating sheared mafic dyke within Piksteel Granodiorite.

Anomalous gold values were recorded for gossanous-quartz-haematite veins whereas values generally fell below detection limits for host rock granodiorite. Mineralized veins were often noted adjacent to the contacts of sheared mafic dykes and consistently paralleled the regional foliation. Gold values for sheared mafic dykes ranged between 77 and 49 ppb Au.
Barren 'bull-quartz' veins with a constant 050° trend are late-stage and give rise to vast amounts of quartz scree (**Map 1**).

AREA 2

WN - 42	N/D	:	Q. - ht vein
WN - 43	148 ppb	:	Q. - vein
WN - 44	N/D	:	Q. - vein
WN - 45	N/D	:	Q. - po
WN - 46	N/D	:	Q. - porphyritic
WN - 47	565 ppb	:	Q. - veins (sheared Q.-po)
WN - 48	55 ppb	:	Q. - ht veins
WN - 49	N/D	:	Q. - ht veins
WN - 50	N/D	:	Q. - vein
WN - 51	52 ppb	:	Q. - vein

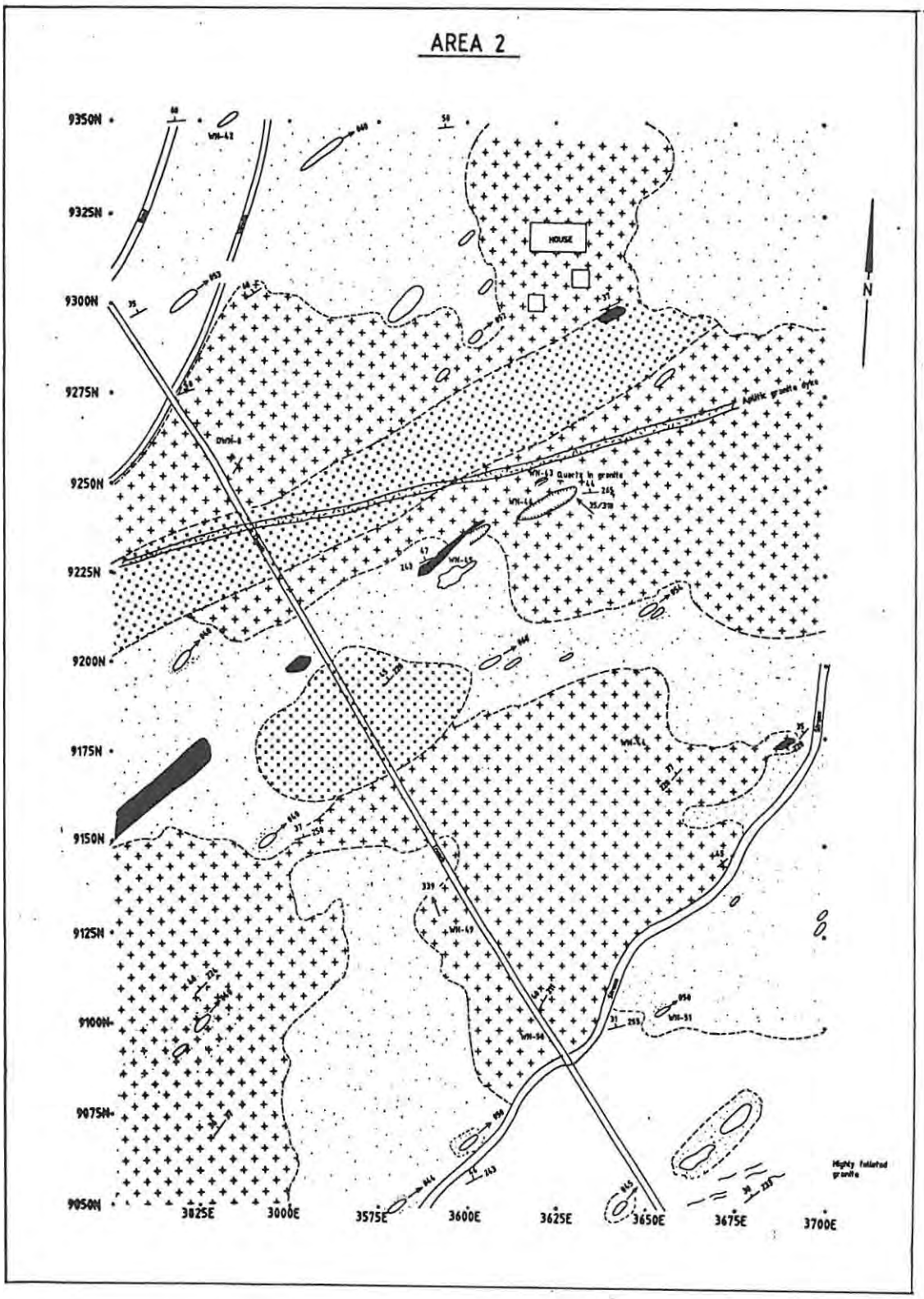

4.5.8.2 Area 2

The geology of this area is dominated by quartz porphyry with remnant islands of Piksteel Granodiorite (Plate 4.5.8.2.). Despite the area being adjacent to the Blanks Mining area little mineralization was noted. Mineralized gossanous quartz-haematite veins were recorded in the hangingwall of a sheared mafic dyke. A value of 565 ppb Au was recorded for the gossanous quartz-haematite vein while all other samples yielded below detection limits
(Map 2).

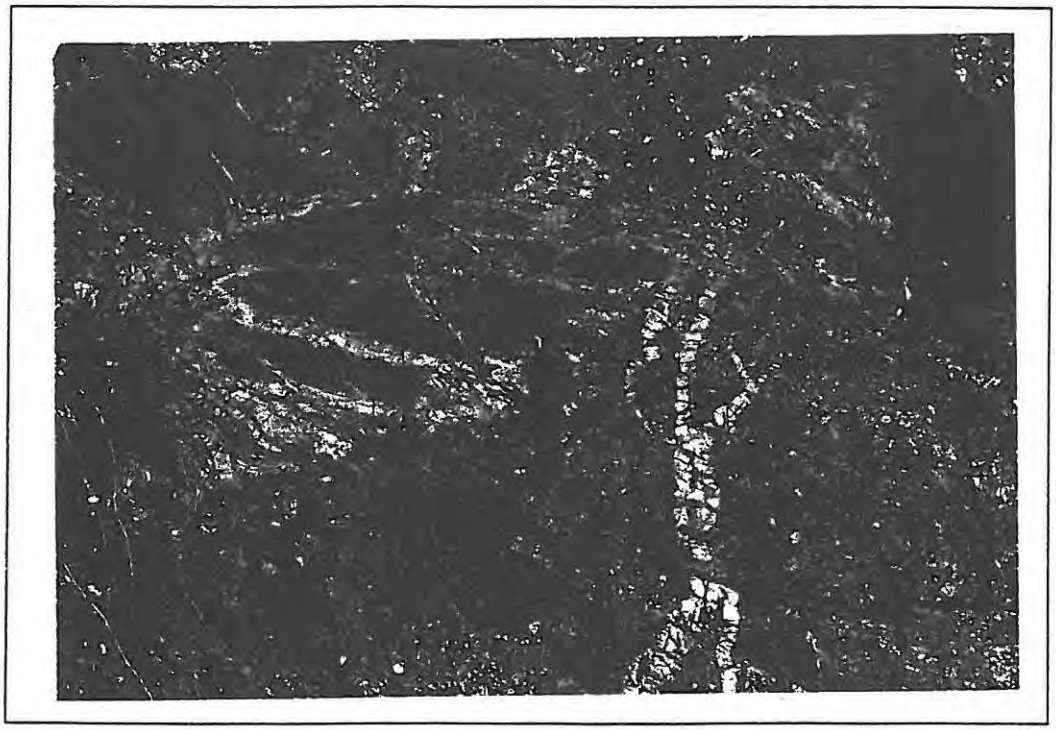

Plate 4.5.8.2: Intrusive relationships between younger Quartz porphyry and older Piksteel Granodiorite.

4.5.8.3 Area 3

The geology of Area 3 is relatively simple. Sheared mafic dykes have intruded the Piksteel Granodiorite along north-easterly trends. A series of unmineralized late-stage second-order quartz veins trend between 040° and 050°.

Mineralization is restricted to gossanous-quartz veins in minor shear zones within the Piksteel Granodiorite and isolated margins of some sheared mafic dykes. The profile of a trench at 3960E/9690N, depicted in figure 4.5.8.3, clearly depicts the spatial relationship between the mineralized gossanous quartz-haematite veins and the mafic dyke (Map 3).

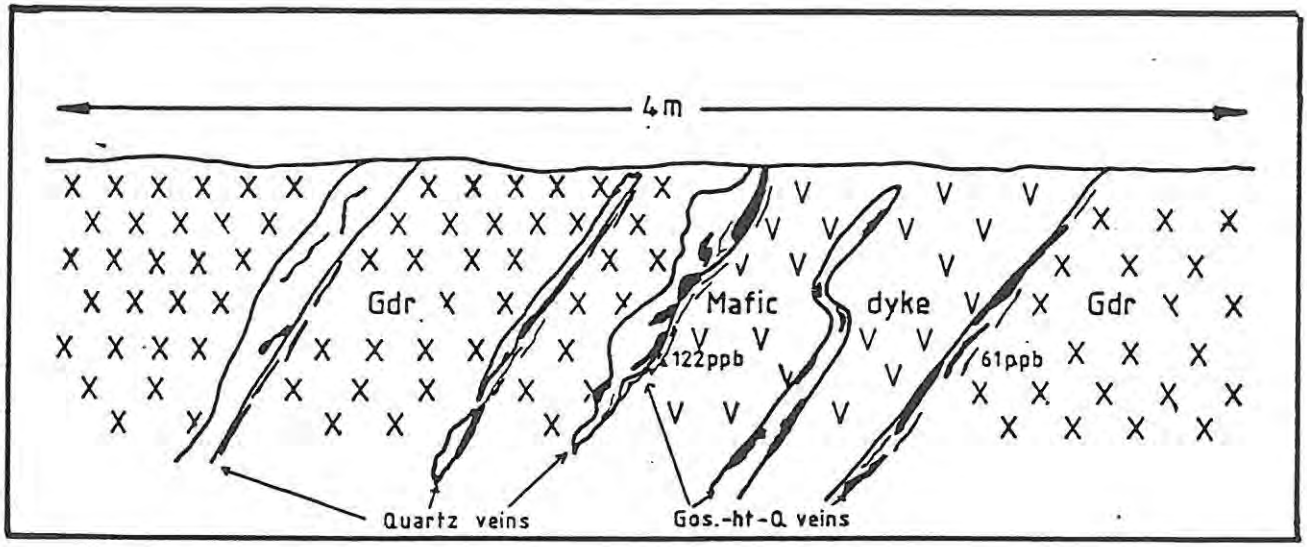

Figure 4.5.8.3: Field sketch of mineralization adjacent to a mafic dyke - Area 3.

A minor shear, trending 035°, within the Piksteel Granodiorite is well mineralized at depth and is less well mineralized closer to surface. Gold scan values range between 4362 ppb Au at -2.5m (below surface) to 353 ppb Au at -0.5m and finally < 40 ppb Au at surface for the same gossanous quartz-haematite vein within the shear. Plate 4.5.8.3(a) depicts the shear and gossanous vein mentioned above.

A shallow trench to the south of the large trench depicted in Map 3 again yielded gold values which increased with depth. Surface values yielded below the lower limit of detection (LLD) while the same gossanous vein yielded 4125 ppb Au at depth (Plate 4.5.3.8(b)).

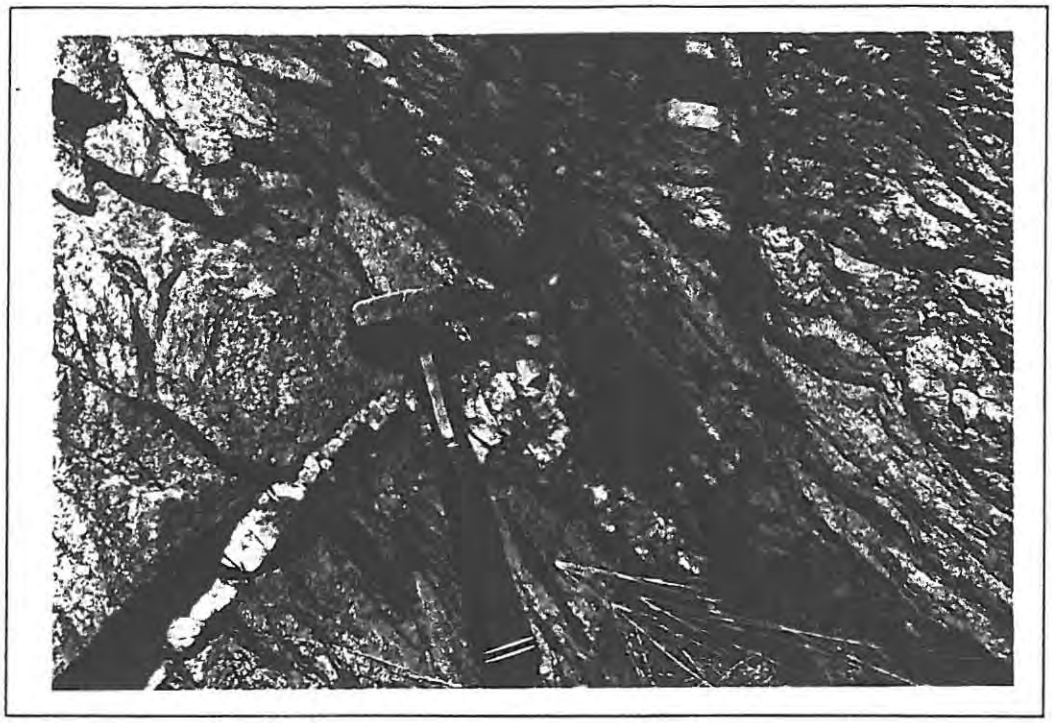

Plate 4.5.8.3(a): A mineralized shear plane within Piksteel Granodiorite, mineralized only at depth.

Plate 4.5.8.3(b): Mineralized gossanous quartz-haematite vein.

Mineralization was recorded within a sheared quartz vein at 4075E /9535N and yielded values of between 541 ppb Au and 4087 ppb Au.

WN-58

AREA 4

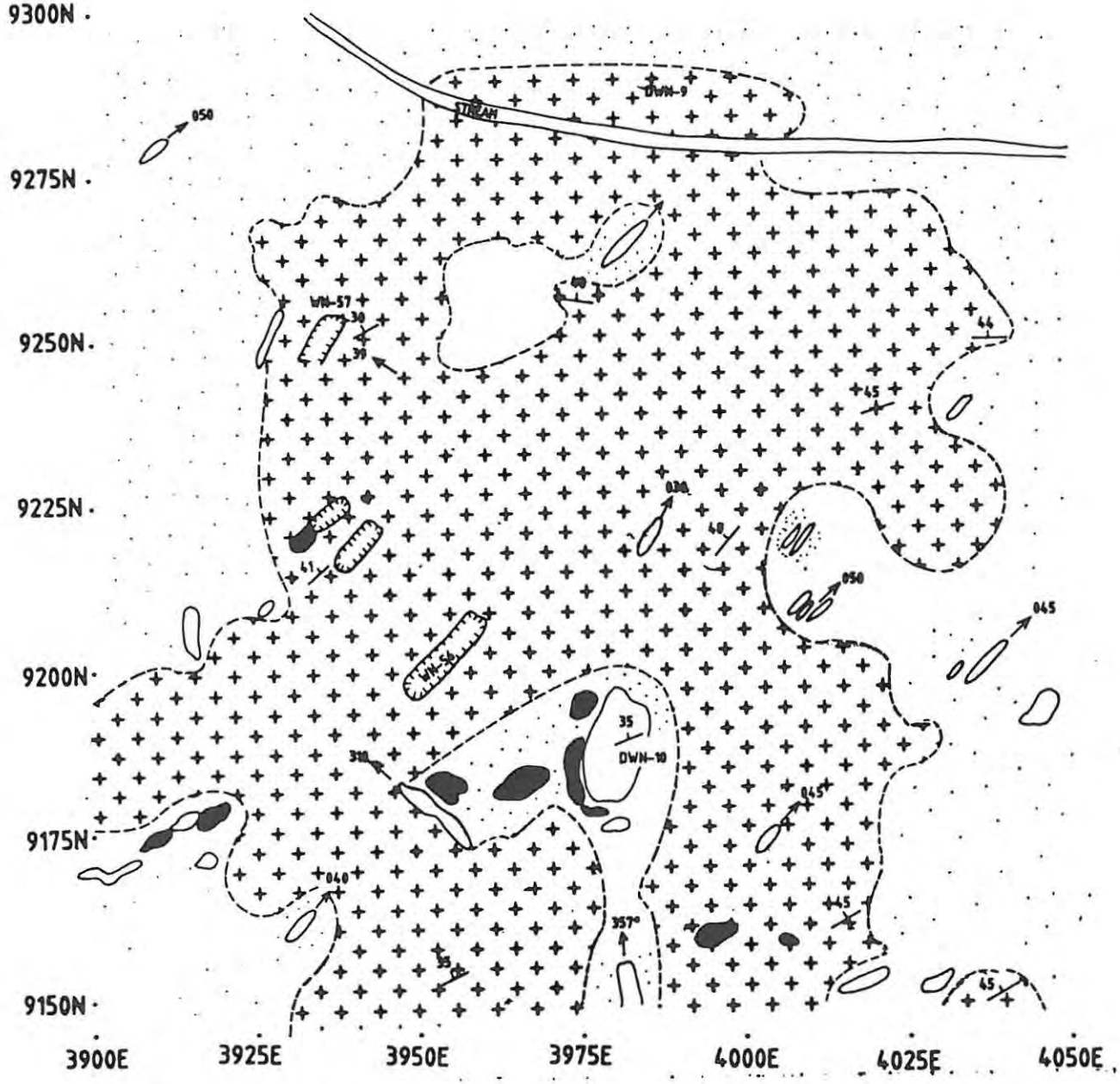

AREA 4

WN - 56	N/D	:	Q - vein
WN - 57	52 ppb	:	Q - ht vein

AREA 5

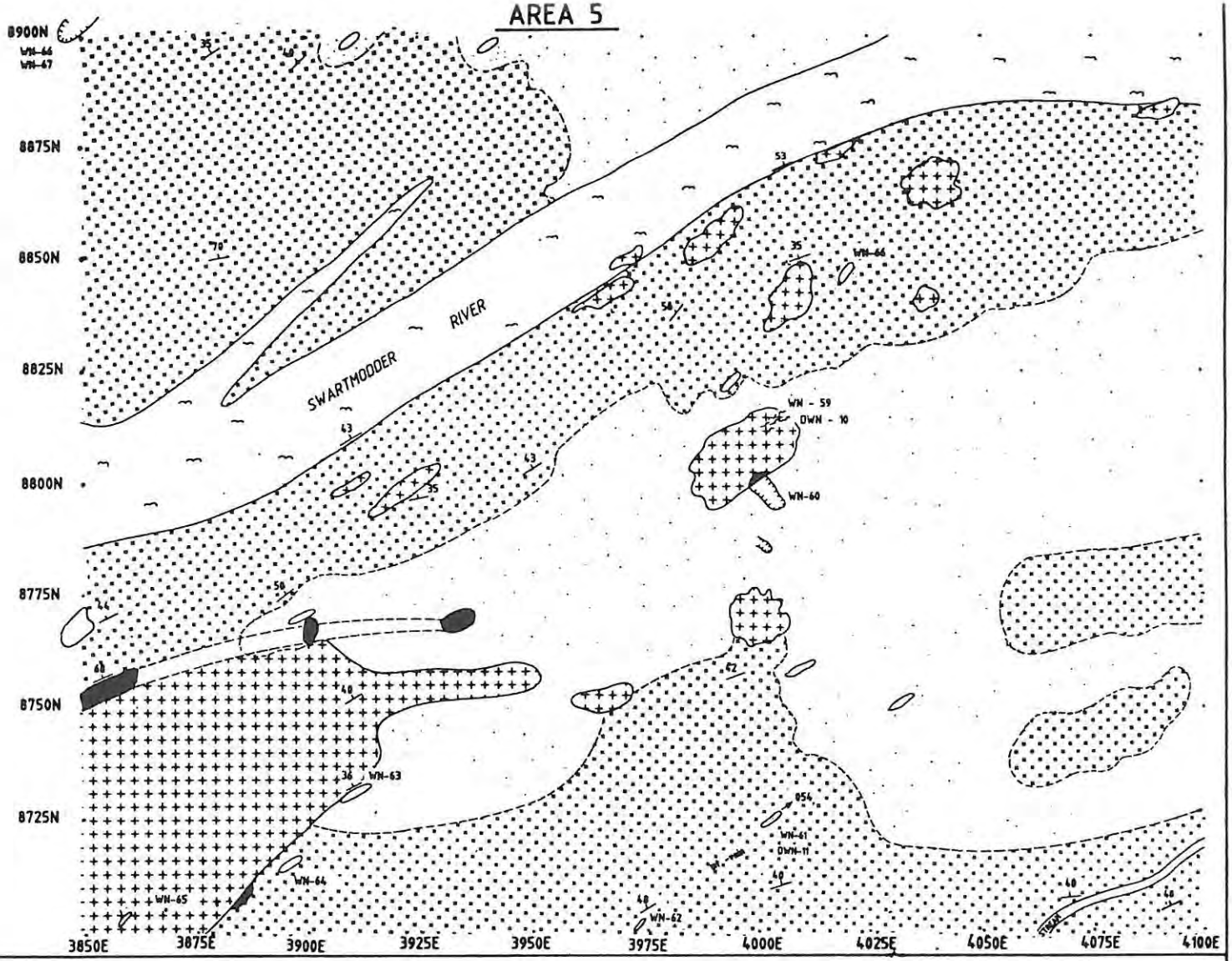

AREA 5

WN - 59	:	180 ppb	:	Q - ht vein
WN - 60	:	N/D	:	Q - ht vein
WN - 61	:	351 ppb	:	mt - vein
WN - 62	:	N/D	:	Q - vein
WN - 63	:	N/D	:	Q - vein
WN - 64	:	1104 ppb	:	Q - vein.
WN - 65	:	86 ppb	:	Q - ht vein
WN - 66	:	N/D	:	gdr
WN - 67	:	216 ppb	:	Q - ht vein

4.5.8.4 Area 4

Area 4 is comprises quartz porphyry, sheared mafic and quartz-feldspar porphyry dykes and numerous second-order quartz veins.

Despite the presence of four trenches within the area mapped, the highest gold value obtained was 52 ppb Au for a sample of Cu-stained quartz porphyry (**Map 4**). This area is barren of mineralization.

4.5.8.5 Area 5

Area 5 essentially comprises Piksteel Granodiorite intruded by apophyses of quartz porphyry and sheared mafic dykes.

Mineralization is confined to localized areas with narrow gossanous quartz-haematite veins (0.5 and 1cm wide) within the Piksteel Granodiorite. A persistent haematite vein (2cm wide) yielded 351 ppb Au (**Map 5**).

AREA 6

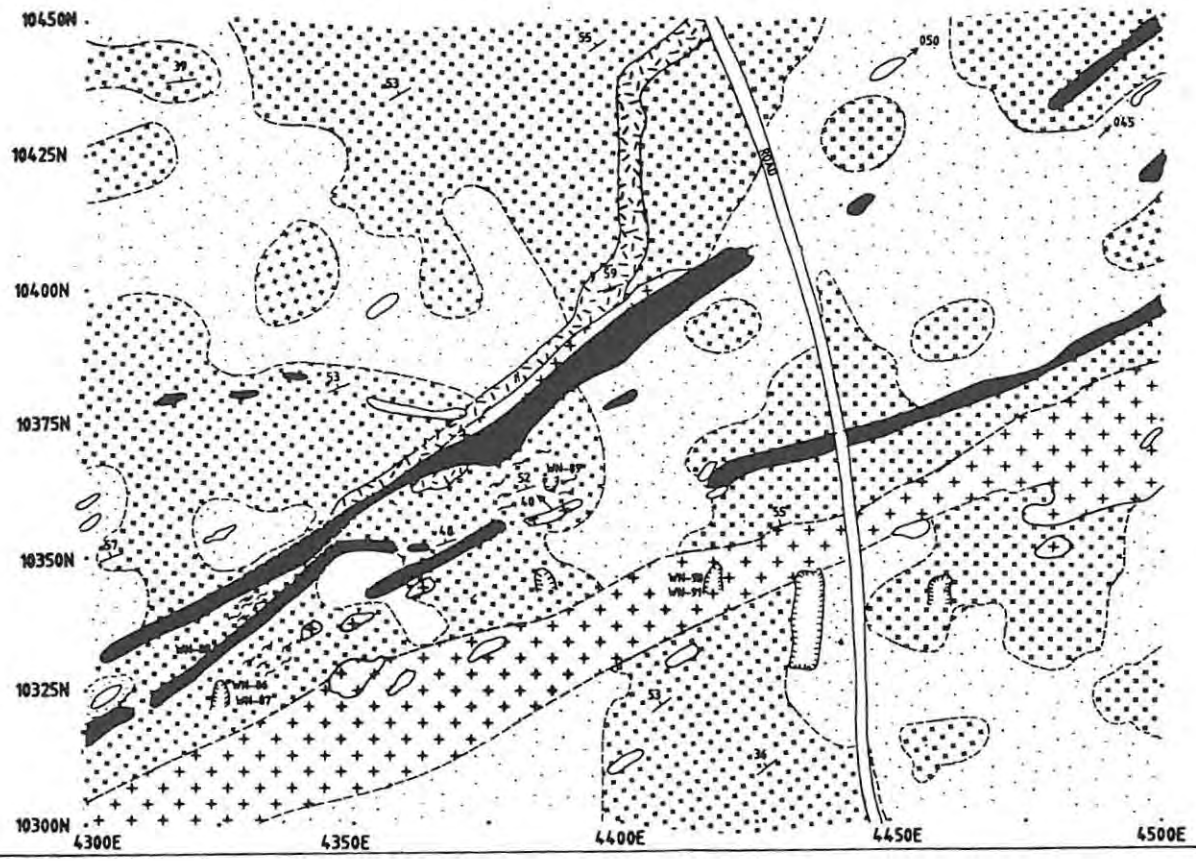

AREA 6

WN - 86	1565 ppb	:	Q - ht veins
WN - 87	N/D	:	host rock
WN - 88	N/D	:	mafic dyke (py)
WN - 89	827 ppb	:	Q - ht veins
WN - 90	586 ppb	:	Q - ht veins
WN - 91	N/D	:	host rock

4.5.8.6 Area 6

The Piksteel Granodiorite in this area is intruded by sheared mafic dykes and younger quartz porphyry. Numerous trenches within the area attest to the anomalous concentration of gold present within this area (**Map 6**).

Detailed mapping and sampling reveal that gold mineralization is confined to narrow gossanous quartz-haematite veins associated with margins of the sheared dykes. The mineralization is localized in the gossanous quartz veins (up to 1565 ppb Au) and samples of host rock taken 0.5 m away from the veins yield below the LLD. Although the sheared mafic dykes are rich in pyrite no Au values recorded above the LLD.

4.5.8.7 Area 7

Apart from small apophyses of quartz porphyry and second-order quartz veins the Piksteel Granodiorite in the area is devoid of any other intrusives (**Map 7**).

Again the mineralization is confined to narrow, 1 and 2 cm wide, gossanous quartz-haematite veinlets which yield scan values greater than the ULD (>5000 ppb Au). Host rock granodiorite 0.5 m away from the mineralized veins yielded gold scan values below the LLD.

4.5.8.8 Area 8

The detailed mapping of Area 8 highligted the extension of the Mebi Shear zone along strike from the Mebi mine eastwards into the schists. The geology of the area comprises the Piksteel Granodiorite and Marienhof Schist Formation which have been extensively foliated and in places sheared and intruded by mafic dykes (Map 8).

Surface outcrop of the Mebi Shear zone is poor and often non-existent. Good exposures were obtained in trenches along the strike of the shear. Where developed at surface, the Mebi shear is distinguished by the development of narrow gossanous veins trending virtually east-west. A good exposure of the shear zone within the schists occurs in a trench at 6670E/9151N (Map 8). Plate 4.5.8.8 and figure 4.5.8.8 depict the shear zone within the trench looking west.

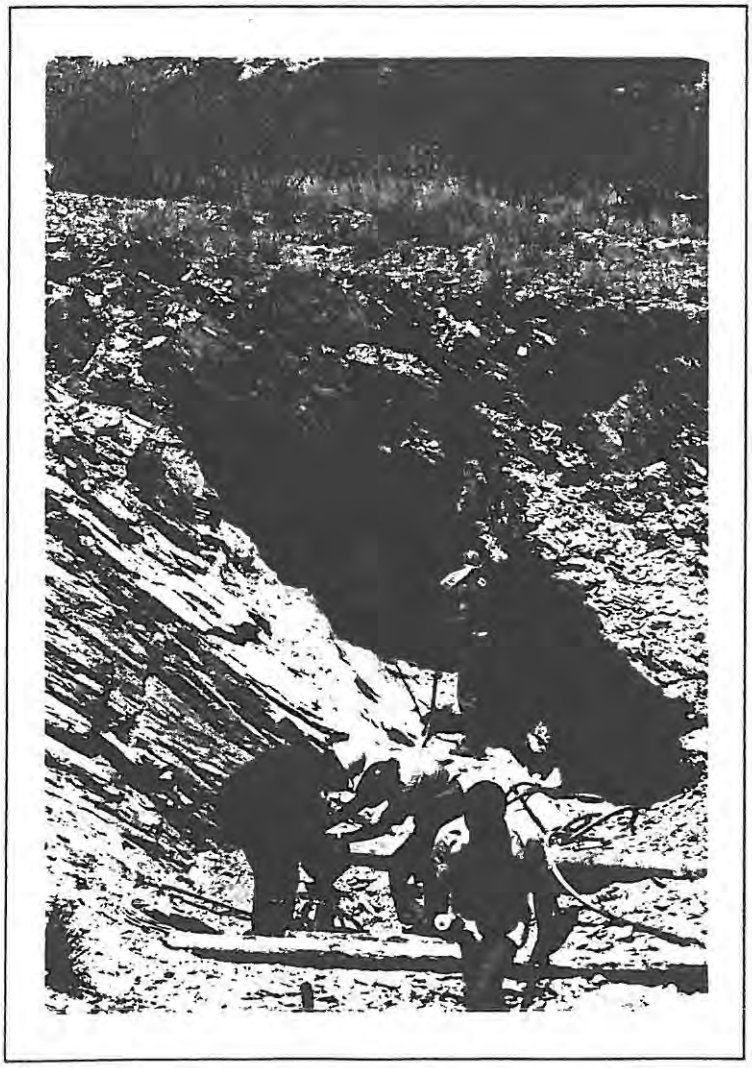

Plate 4.5.8.8(a): Mebi Shear Zone within Marienhof Schist.

Sampling of the vertical profile revealed a marked increase in gold scan values from below the LLD near surface to > 1500 ppb Au at -3m (Figure 4.5.8.8).

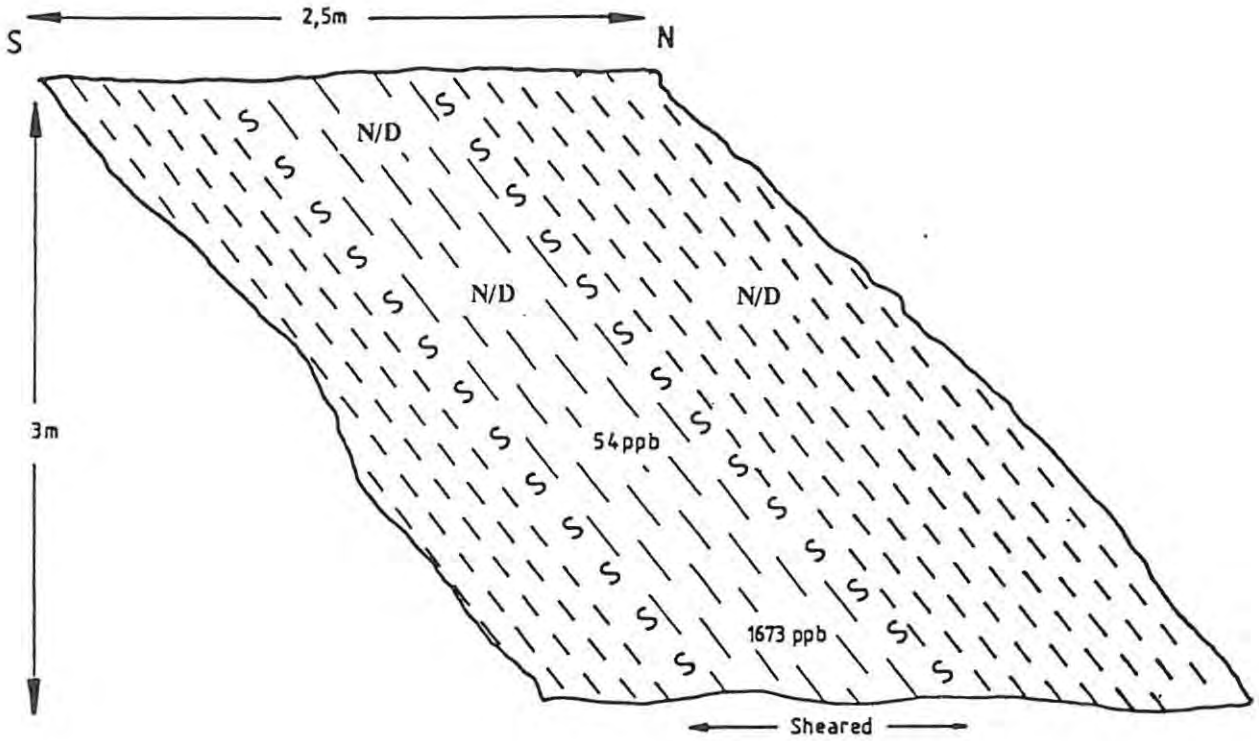

Figure 4.5.8.8: Field sketch of the Mebi Shear within schist.

The Mebi shear zone was traced intermittently from the mine area to a trench at 7150E/9151N after which it does not crop out. A trench in the Marienhof schists, at 7150E/9090N, revealed boudinaged pods of sulphides (pyrite and chalcopyrite) within the shear zone which analysed greater than the ULD. Alteration associated with the mineralization is dominantly sericitic with minor carbonate (Plate 4.5.8.8(b)). Alteration is restricted to narrow areas adjacent to the mineralized gossanous quartz-haematite veins.

Plate 4.5.8.8(b): Photomicrograph of hydrothermal alteration mineral assemblage in granodiorite adjacent to the Mebi Shear zone. Ht = haematite, CO_3 = carbonate, Cl = chlorite.

4.5.8.9 Area 9

The geology of Area 9 is relatively simple; Marienhof schists are intruded by north-east trending sheared mafic dykes. Mineralization within this area is restricted to gossanous quartz-haematite veins adjacent to the margins of some sheared mafic dykes (**Map 9**).

A detailed sampling profile, across a sheared mafic dyke with associated mineralization, was undertaken as a 'case study'. Plate 4.5.8.9 depicts the profile sampled in detail, and figure 4.5.8.9(a) depicts sample localities.

AREA 9

AREA 9

WN - 92	59 ppb	:	ft wall schist
WN - 93	109 ppb	:	Q-ht veins
WN - 94	52 ppb	:	mafic dyke
WN - 95	62 ppb	:	h/wall alt. contact
WN - 96	1623 ppb	:	Q - ht - mt - sulphide vein
WN - 97	336 ppb	:	h/wall schist contact
WN - 98	49 ppb	:	background schist value

Plate 4.5.8.9: Mineralization adjacent to a mafic dyke - Area 9.

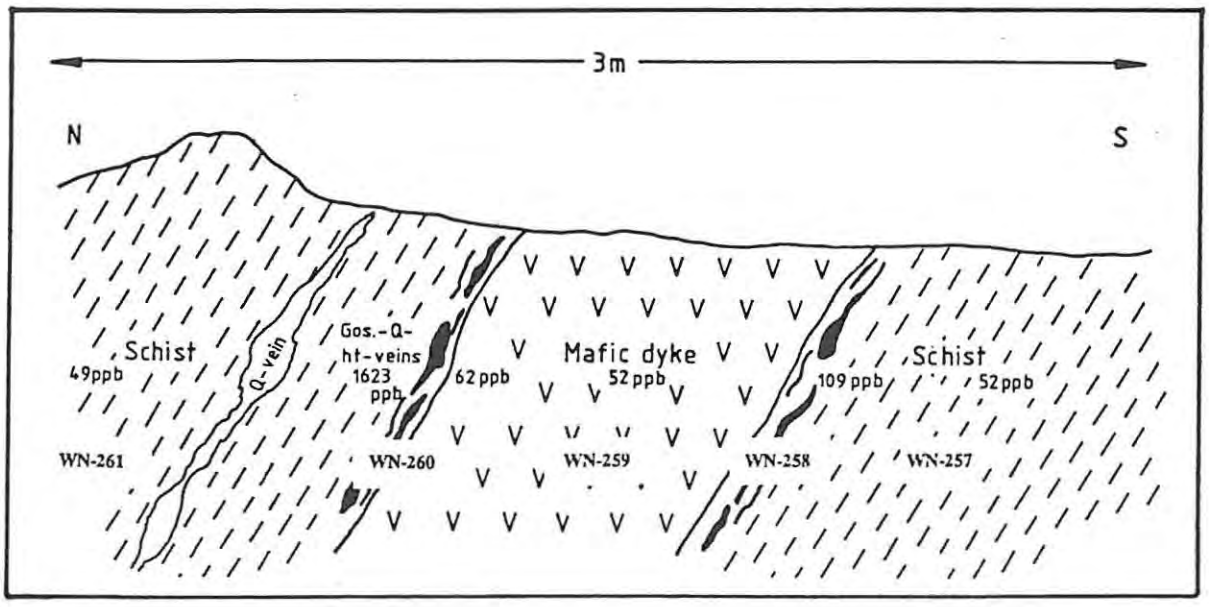

Figure 4.5.8.9(a): Field sketch and associated gold values.

Figures 4.5.8.9(b) and 4.5.8.9(c) graphically illustrate the relative concentrations of base and precious metal associated with each sample.

(B)

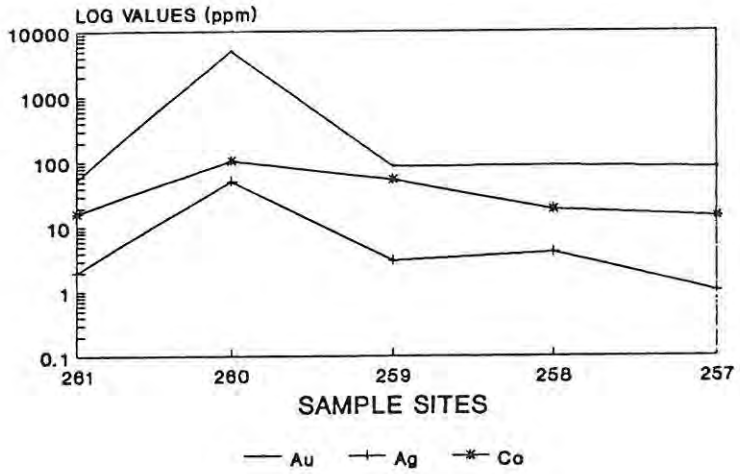

(C)

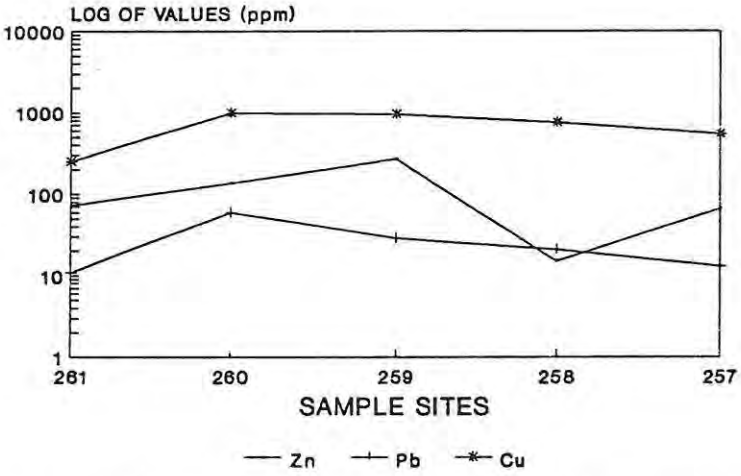

Figures 4.5.8.9(b) and 4.5.8.9(c): Graphical illustrations of various metals.

From the data presented above it is clear that the sheared mafic dyke has an important bearing on the localization of mineralization. It is inferred that mineralizing solutions rich in Cu, Au, Co and Zn were channelled up the contacts of the dyke and within the sheared dyke during metamorphic dewatering of the basin. Mineralization was precipitated as a result of changes in either temperature, pressure and/or chemical environments.

4.5.8.10 Area 10

Quartz porphyry dominates the rock types within this area. The older rocks occur as rafts of Piksteel Granodiorite and sheared mafic dykes (**Map 10**).

Gold mineralization in localized to narrow gossanous quartz-haematite veins within minor shear zones and adjacent to sheared mafic dykes. Plate 4.5.8.10 shows the localised nature of the mineralization adjacent to a mafic dyke at 8050E/8445N (picture taken looking west).

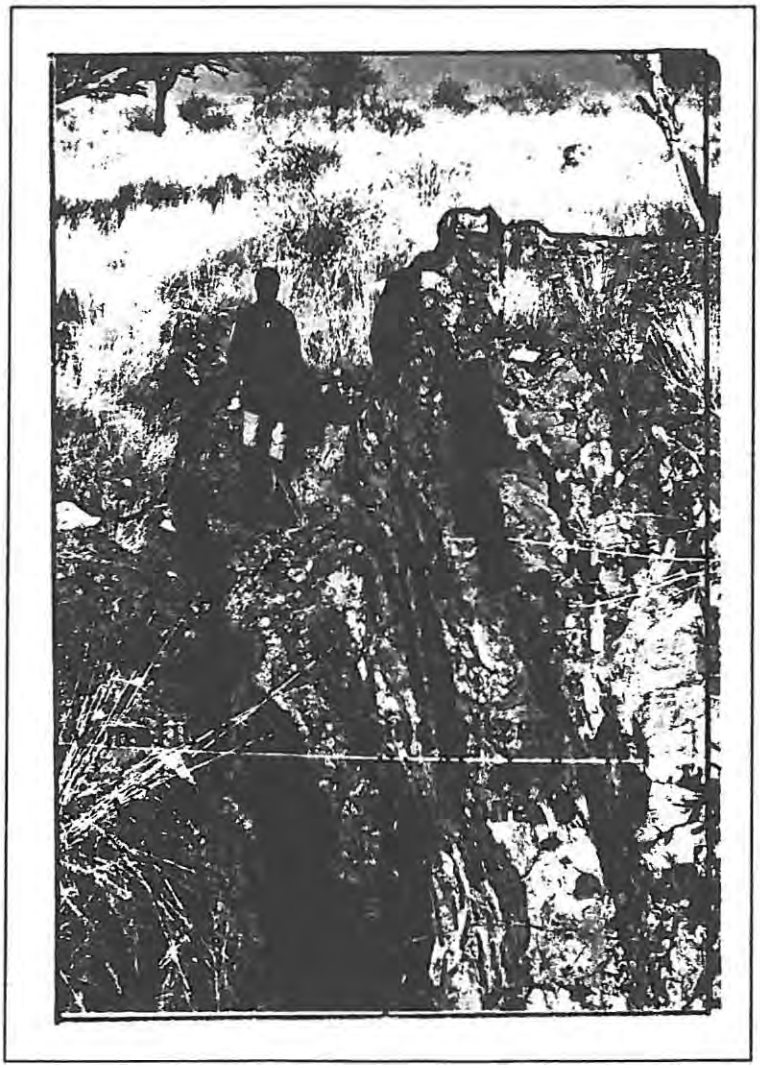

Plate 4.5.8.10: Mineralization adjacent to a mafic dyke - Area 10.

Apart from the few localised areas depicted on the map, no other mineralization was recorded.

4.5.8.11 Area 11

Area 11 consists of a series of contorted north-east trending sheared mafic dykes, numerous rafts of Marienhof schist and Piksteel Granodiorite enclosed within quartz porphyry (**Map 11**).

The sheared mafic dykes vary in size from about 1 m to 7 m in width and are all magnetic. Gold scan values for the dykes average 50 ppb Au. Gossanous quartz-haematite veins in the margin of the dykes peak at 3192 ppb Au and are generally always in excess of 1000 ppb Au. A large trench excavated at 8250E/9925N, revealed sericitic and argillic alteration haloes, in the quartz porphyry country rock, at both the foot- and hangingwall contacts of a sheared mafic dyke (Plates 4.5.8.11(a) & (b)).

Mineralization is restricted to narrow gossanous quartz-haematite veins in the altered quartz porphyry adjacent to the dyke margin (Plate 4.5.8.11(b)). Gold values of the gossanous veins consistently yield values of >1000 ppb Au.

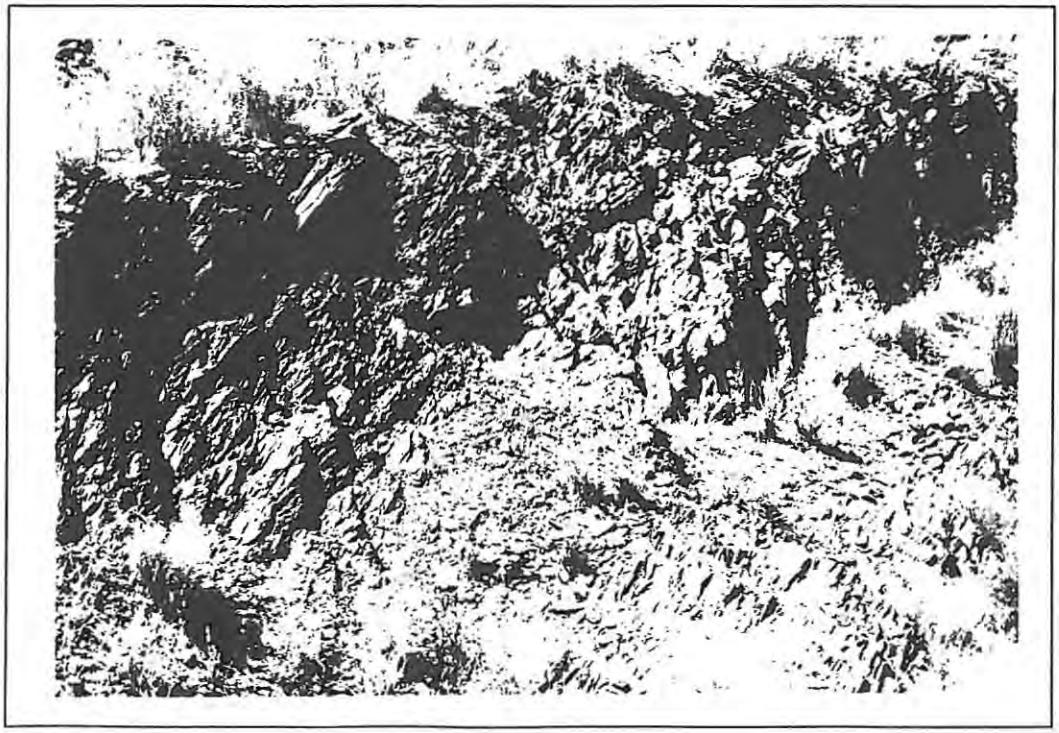

Plate 4.5.8.11(a): Argillic/Sericitic alteration adjacent to a mafic dyke - Area 11.

AREA 12

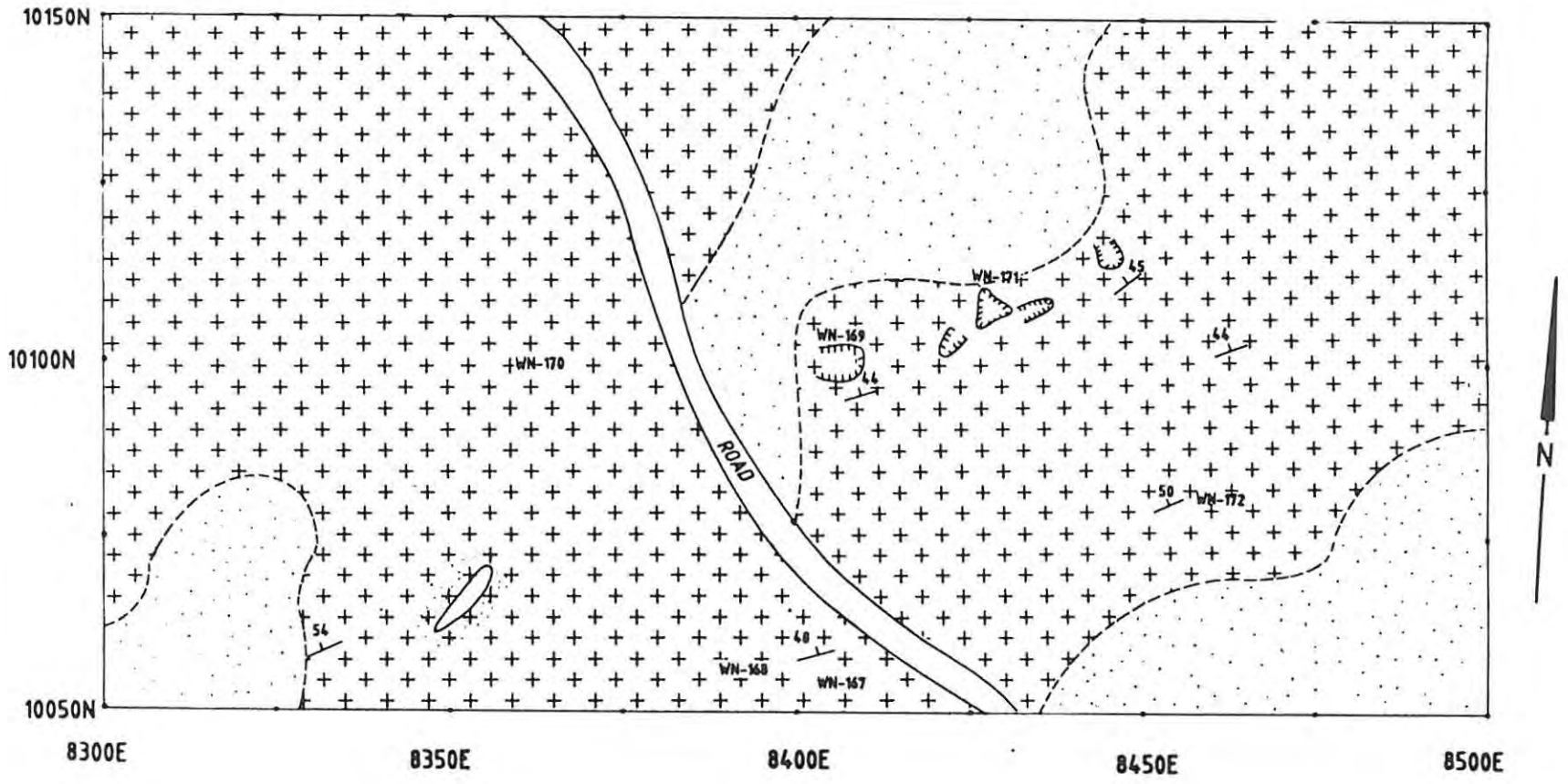

AREA 12

WN - 167	N/D	:	Q-S-P alt Q-po
WN - 168	—	:	(sample 18568)
WN - 169	69 ppb	:	Q-S-P alt Q-po
WN - 170	N/D	:	Q-S-P alt Q-po
WN - 171	102 ppb	:	Q-S-P ht alt Q-po
WN - 172	N/D	:	Q-S-P alt Q-po

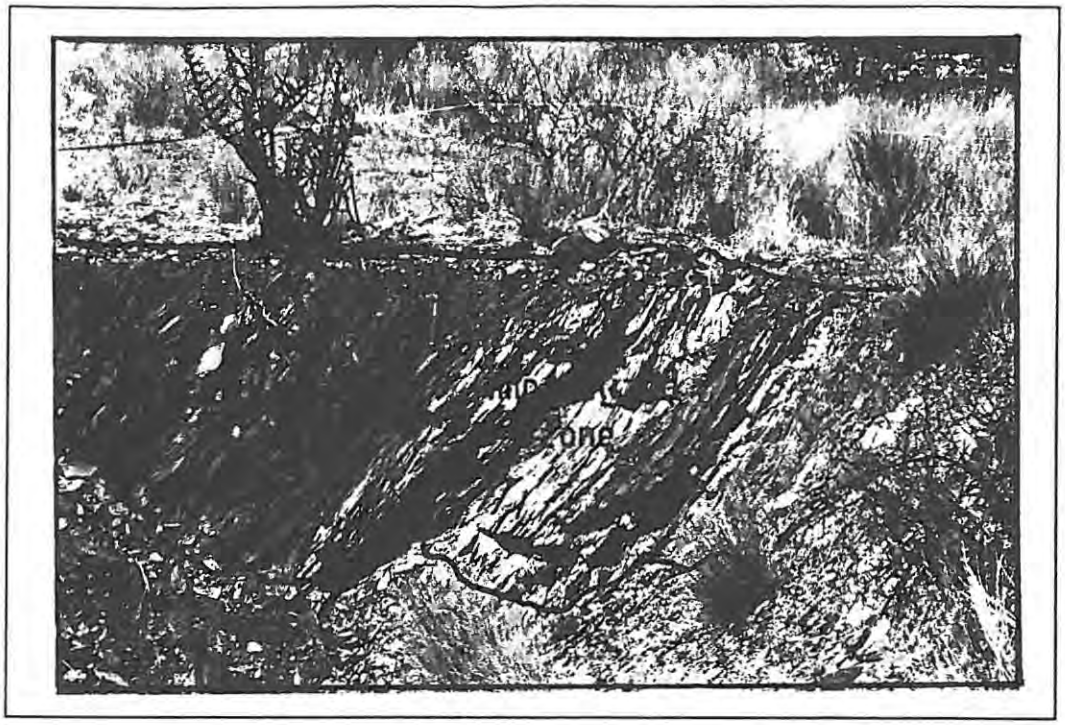

Plate 4.5.8.11(b): Mineralization within altered Quartz porphyry adjacent to a mafic dyke - Area 11.

4.5.8.12 Area 12

Foliated quartz porphyry crops out over the entire area 12. Despite the occurence of pyrite in some areas, gold scan values of lithochip samples peak at 102 ppb Au for a haematite stained sample of quartz porphyry (**Map 12**).

No other mineralization was recorded from this area.

4.5.8.13 Area 13

Quartz porphyry has intruded Marienhof schists and Piksteel Granodiorite in this area, leaving remnant islands of the former lithologies within a sea of quartz porphyry. Sheared mafic dykes are less deformed in the eastern portion of the area where the quartz porphyry has not intruded a sequence of rhyolite lavas as intensly (**Map 13**).

No mineralization was recorded from this area.

AREA 15

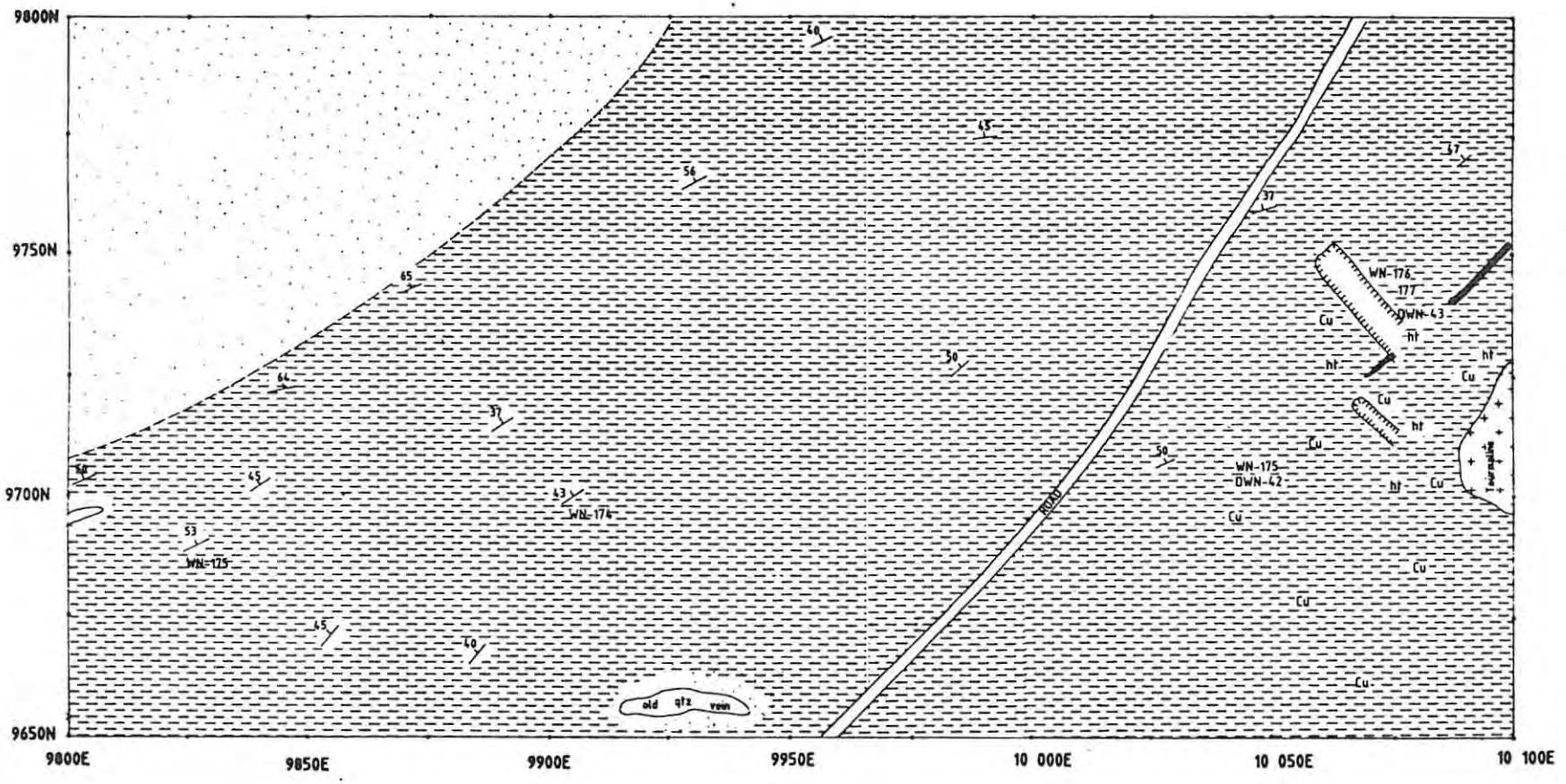

AREA 15

WN - 173	163 ppb	:	schist
WN - 174	79 ppb	:	schist
WN - 175	N/D	:	Cu - rich schist
WN - 176	46 ppb	:	ht - rich schist
WN - 177	41 ppb	:	ht - rich schist

AREA 14

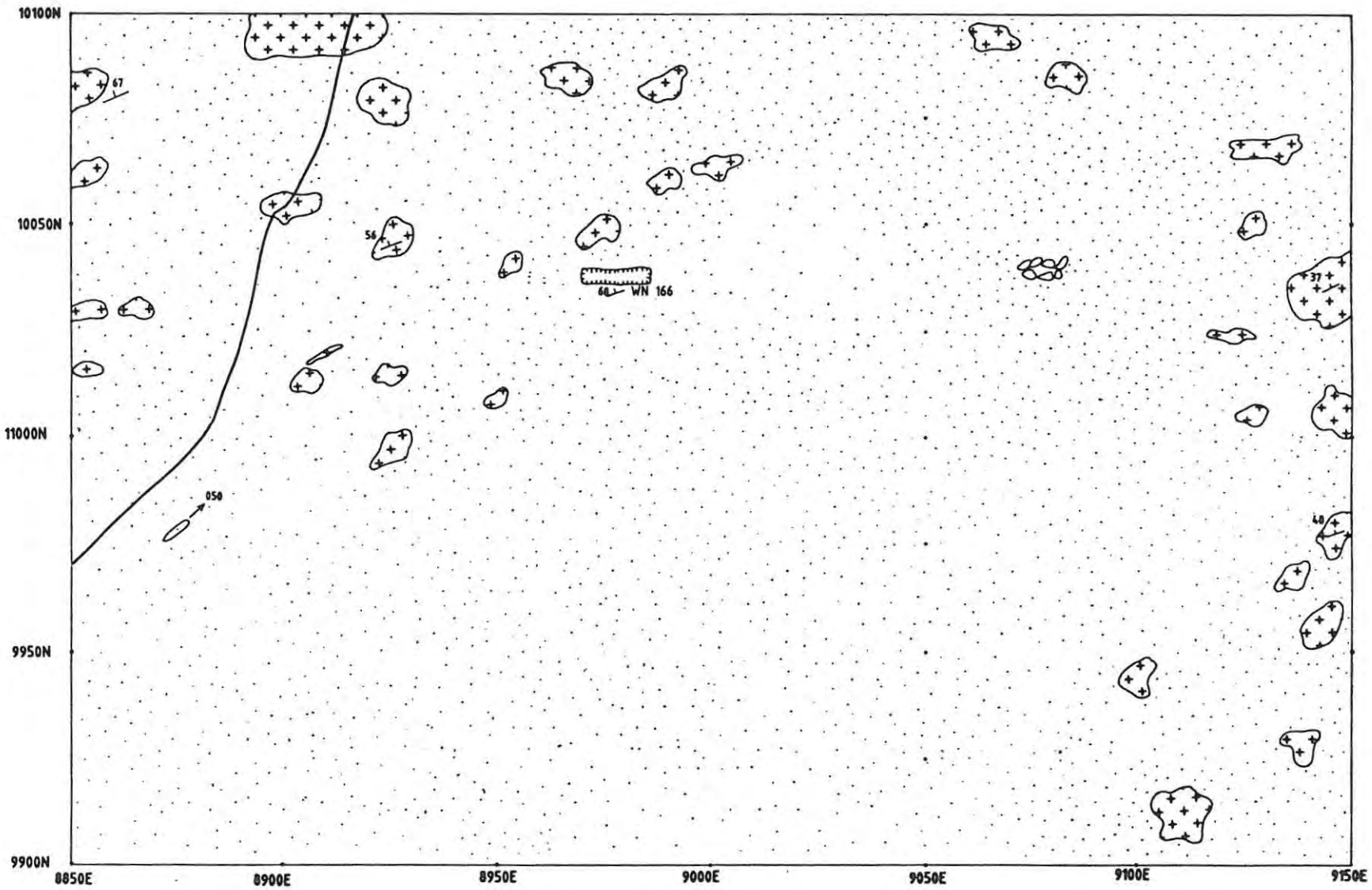

WN - 166 56 ppb : Q - po

4.5.8.14 Area 14

The area appears to be entirely underlain by quartz porphyry but is extensively covered with quartz scree derived from second-order quartz veins which trend 050° and are consistently barren of any mineralization (**Map 14**).

Only the trench within the centre of the area was sampled and a gold scan value of 56 ppb Au was recorded. The area appears devoid of any mineralization.

4.5.8.15 Area 15

Area 15 is underlain mainly by Marienhof Schists, intruded inplaces by an extremely porphyritic apophysis of quartz porphyry. Rosettes of tourmaline are common within the quartz porphyry apophysis indicating the collection of volatiles in the cupola regions of the Quartz-porphyry (**Map 15**).

The schists are malachite stained and the development of euhedral haematite crystals within the schist is localised to the margins of the intrusive apophysis (Plate 4.5.8.15). Gold values for the schists ranges from 163 ppb to 70 ppb Au whereas the haematite-rich schist yielded just above detection limits (41 ppb to 46 ppb Au).

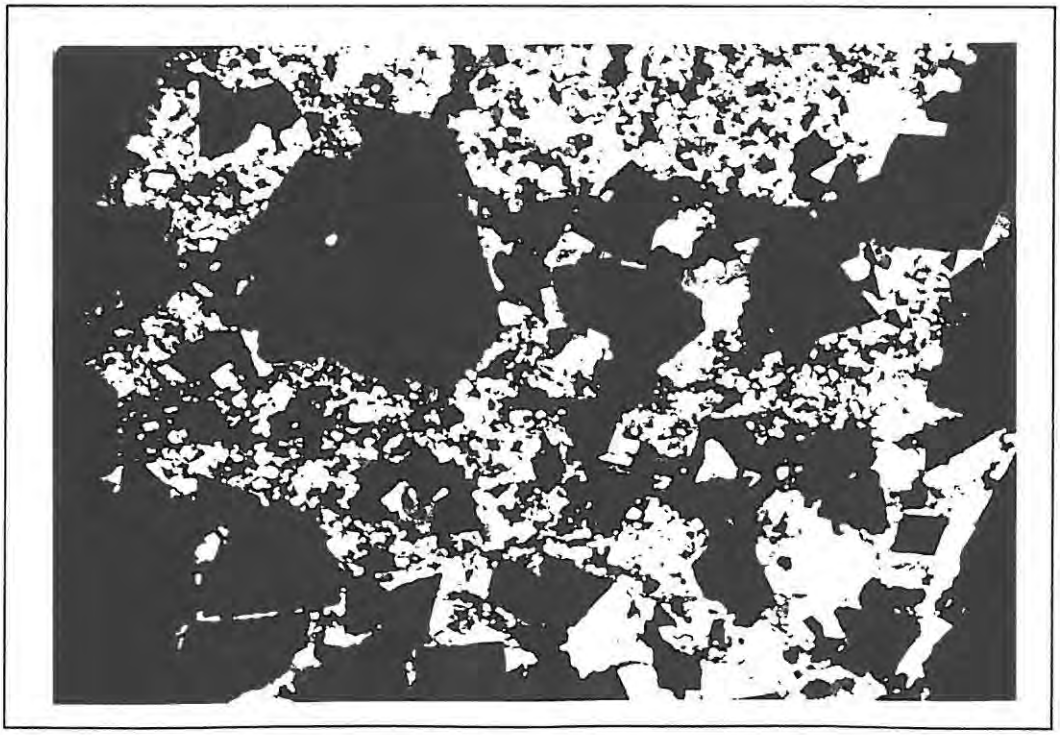

Plate 4.5.8.15: Photomicrograph of haematite within schist. FOV = 3 mm.

AREA 16

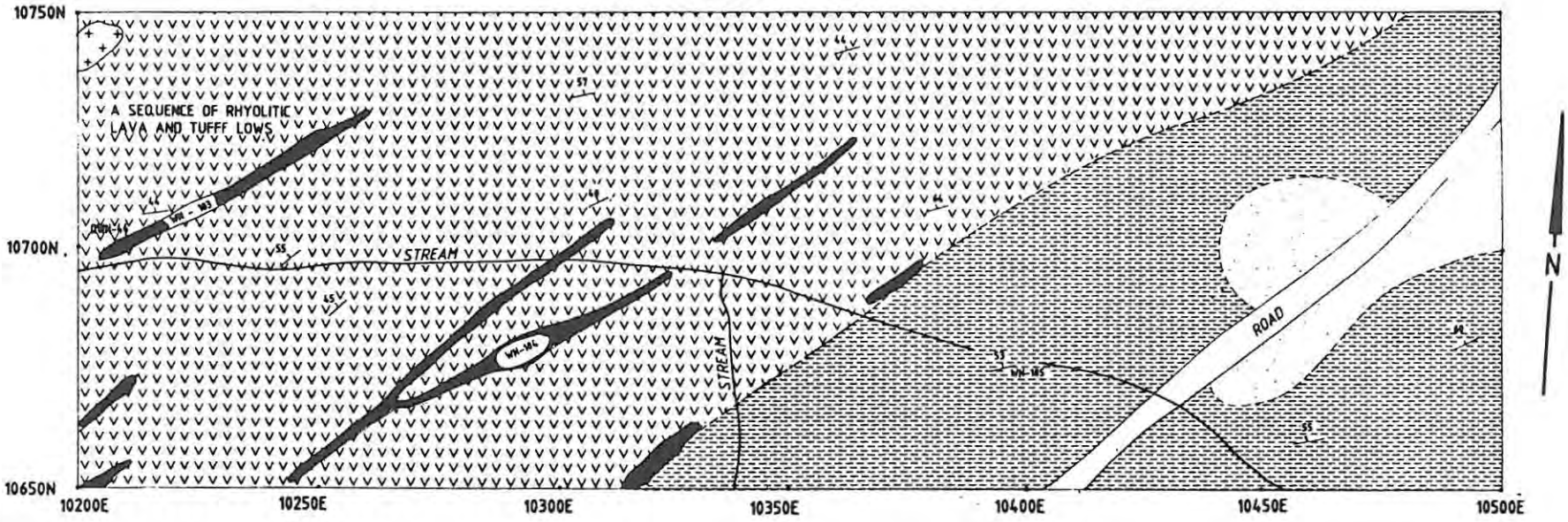

AREA 16

WN - 183	66 ppb	:	schist
WN - 184	61 ppb	:	mafic dyke
WN - 185	66 ppb	:	rhyolite

4.5.8.16 Area 16

Area 16 covers the contact between a sequence of rhyolite lavas and interbedded tuffs with Marienhof schists. Both these lithologies are intruded by the Older sheared mafic dykes. The bimodal volcanic association is well depicted within this area (**Map 16**).

No mineralization was recorded from this area.

4.5.8.17 Area 17 (Raabies Mine)

The geology of Area 17 consists of a series of rhyolitic lava flows which are intruded by sheared mafic dykes and a younger quartz porphyry (**Map 17**).

Two vertical shafts at the contacts between quartz porphyry mafic dyke and rhyolite constitute what is known as Raabies Mine. Copper was apparently mined although narrow gossanous quartz-haematite veins adjacent to the dyke and gossanous dump material yielded gold values of 553 ppb Au. Apart from the mine no other areas of mineralization were observed.

4.5.8.18 Area 18

Area 18 is entirely underlain by Swartmodder Granite. Besides liberal Cu-staining of the granite no other mineralization was detected (**Map 18**).

4.5.8.19 Area 19

In contrast with area 18, area 19 is geologically complex ; rafts of schist float within Swartmodder Granite which is later intruded by Piksteel Granodiorite (**Map 19**). The schist is extensively Cu-stained (malachite and azurite). Cu-stained schist at the contact with Piksteel Granodiorite appear anomalously rich in gold (80 ppb Au, Plate 4.5.8.19), while high values are again restricted to localised narrow gossanous quartz-haematite veins (1407 ppb Au).

Plate 5.5.8.19: Auriferous copper-stained schist.

AREA 20

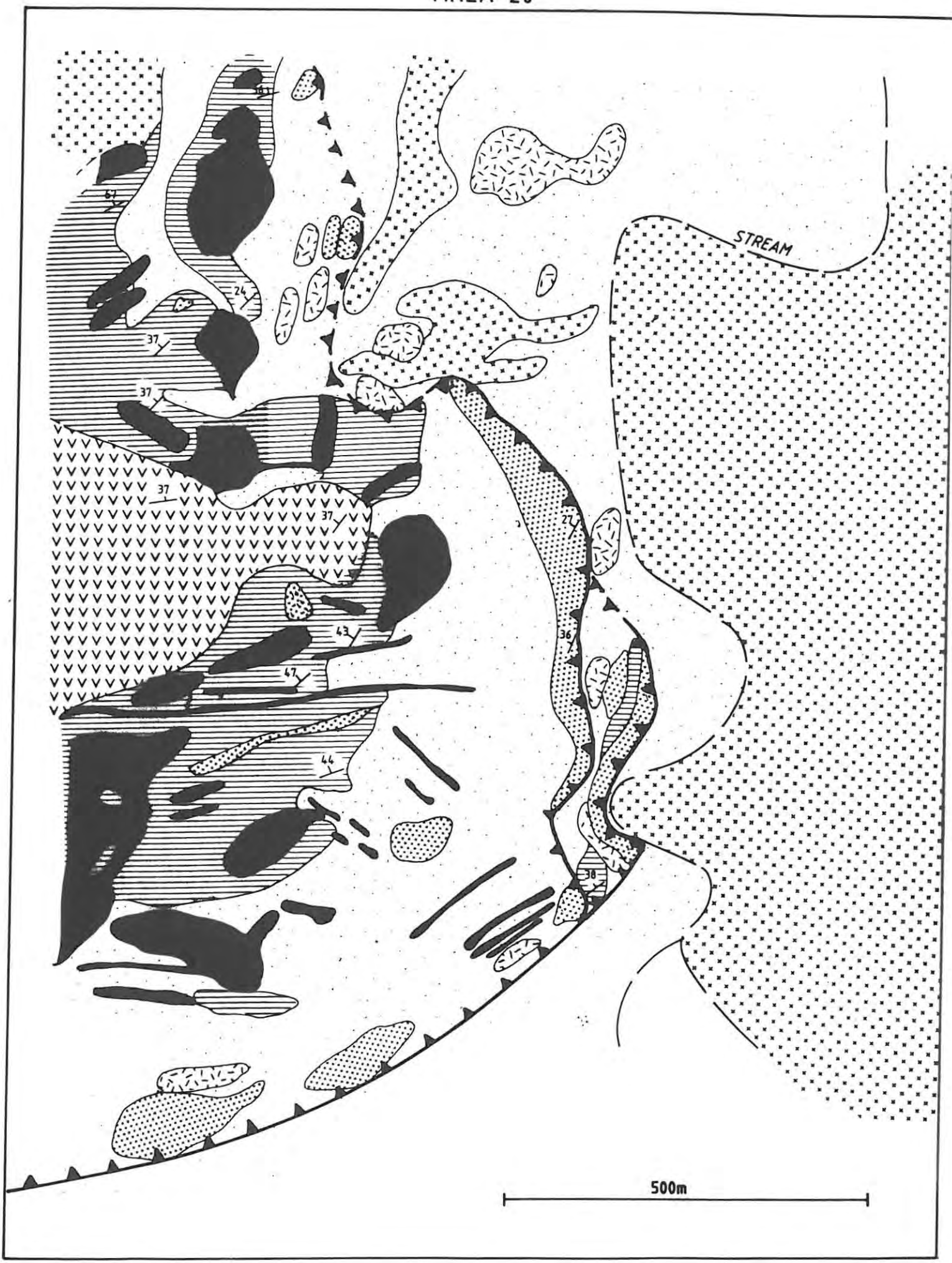

4.5.8.20 Area 20

Although area 20 was not initially demarcated as a target area, the presence of abundant haematite and limonite pseudomorphs (after pyrite) within the phyllites and a marked structural discontinuity necessitated detailed sampling and mapping (**Map 20**).

Area 20 consists of a series of deformed phyllites which are intruded by sheared mafic dykes and sills (gabbros) emplaced into a unit of rhyolitic ignimbrites (Plate 4.5.8.20). A series of contorted quartz veins and quartzites mark a thrust fault contact between the phyllites and adjacent quartz porphyry, Uitdraai Granite and Piksteel Granodiorite. Gold scan values of the phyllites average out at about 82 ppb Au, indicating that the phyllites have anomalously high background values. A graphic representation of the gold scan data is presented in figure 4.5.8.20.

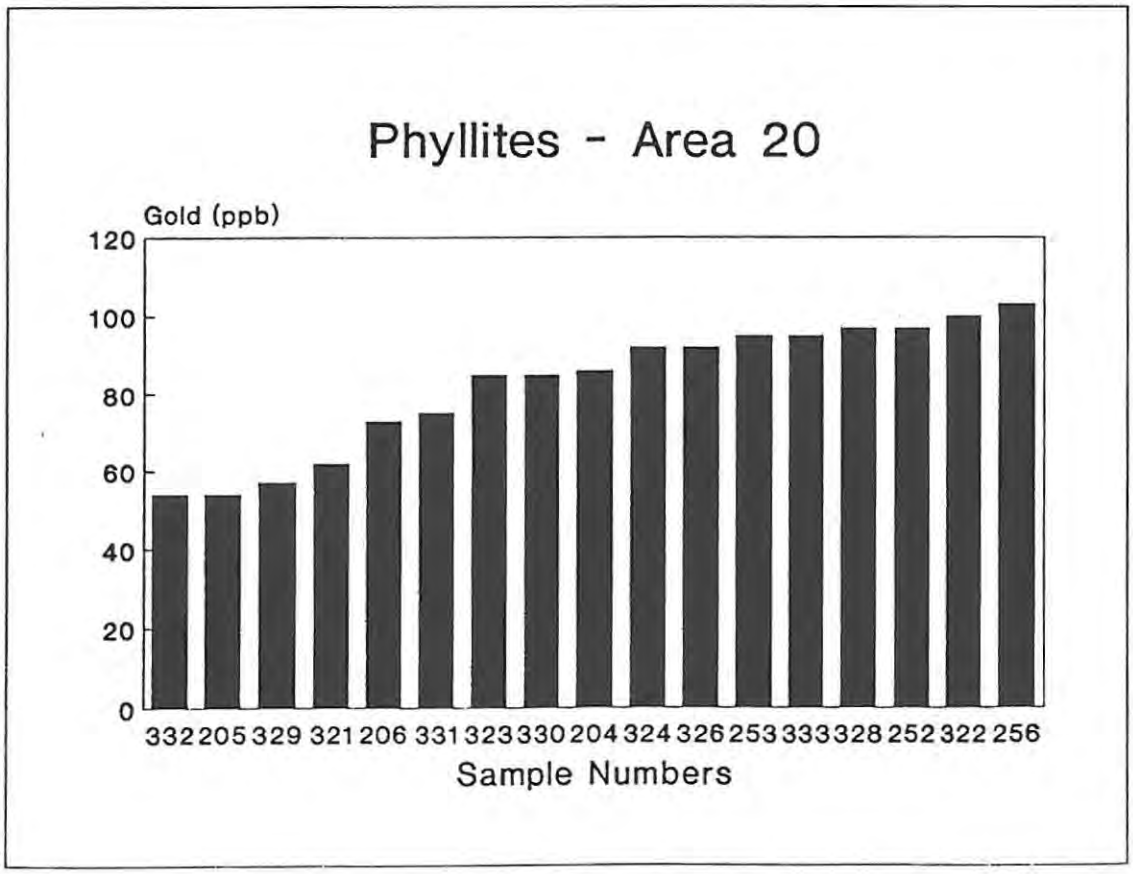

Figure 4.5.8.20: A graphical representation of gold values from the phyllites - Area 20.

Plate 4.5.8.20: Phyllites within Area 20. Note transposed foliation and remnant bedding planes.

4.5.9 DISCUSSION

The common factors emerging from all the areas examined in detail are :-

1) The gold mineralization occurs in narrow veinlets which are sulphide rich at depth and generally gossanous at surface.

2) The mineralized veins are hosted in all lithologies which have been tectonised (ie. strongly foliated).

3) Mineralization is geographically best developed in the northern sector of the grant area.

Histograms of all the lithological chip samples taken of the various lithologies show some lithologies to have inherently higher concentrations than others (Figure 4.5.7). A plot of gold values vs. host rock reveals that the greatest concentrations of gold occur in gossanous quartz-haematite veins.

The detailed mapping of the twenty target areas shows that two generations of quartz veins exist. The older generation, or first order, quartz veins are characteristically gossanous haematite-stained veins less than 5 cm in width, more or less parallel to the regional foliation cleavage and generally somewhat deformed. Gold mineralization is intimately associated with this generation of quartz vein. The younger set of quartz veins, 'second-order quartz veins', are characteristically coarse-grained 'greasy' white veins which consistently trend between 035° and 055°. These veins are barren of any mineralization and give rise to vast amounts of quartz scree.

The first-order quartz veins containing mineralization occur in all lithologies which exhibit the regional foliation. Only the Gamsberg Granites and the Swartkoppie Dykes are undeformed and are unmineralized. Areas of greatest gold mineralization (ie. areas where there is greatest development of first order gossanous quartz veins) within the Neuras Grant include lithological contact zones, regional foliation and zones of major shearing (Mebi Shear) except for thrust planes.

A clear relationship between gold mineralization and structural features is thus apparent.

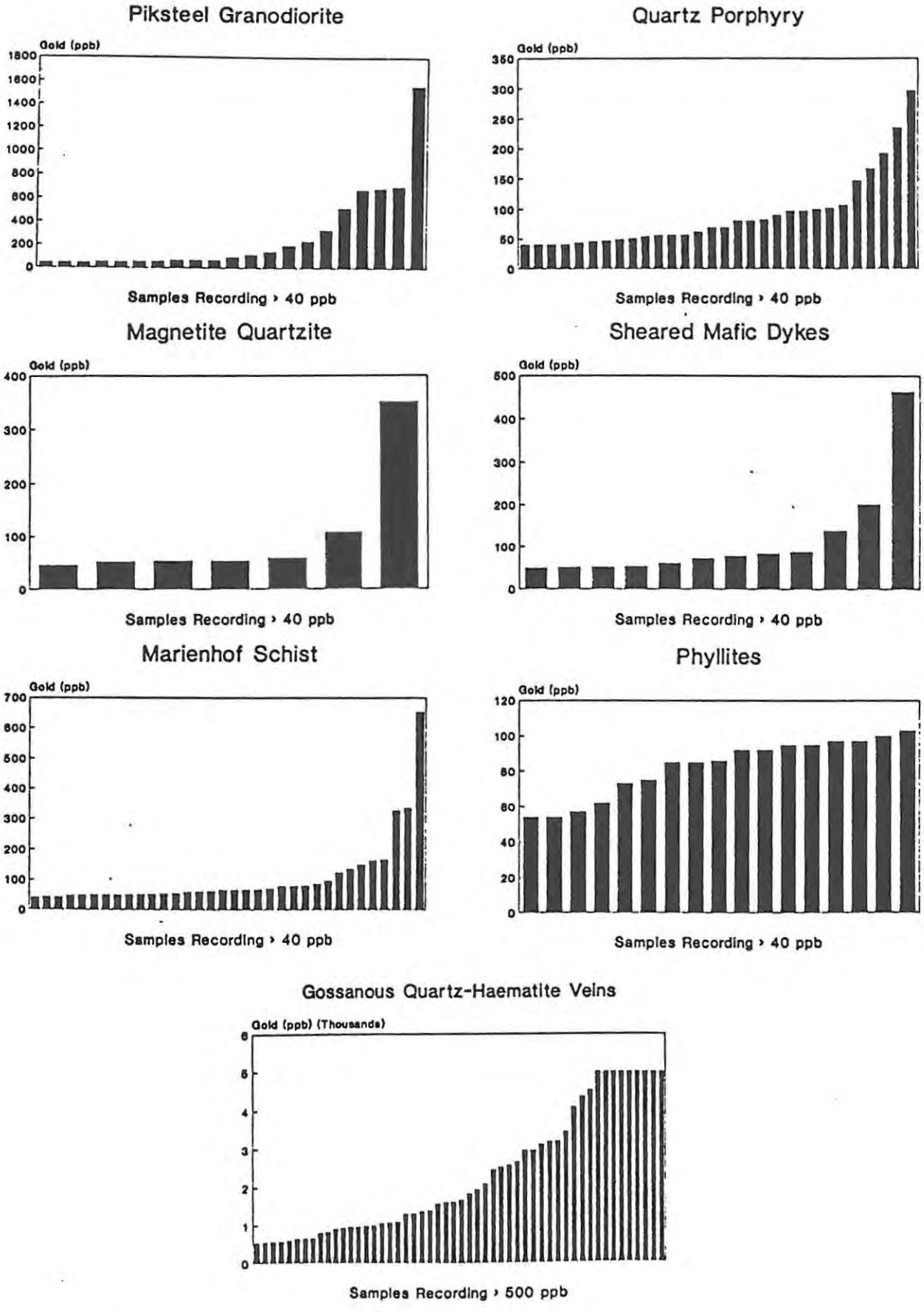

Figure 4.5.7 Graphical illustrations of various gold concentrations within the Neuras Grant rocks.

4.5.10 Proposed Model For Gold Mineralization

Findings of the present study support a growing concensus that the tectonic setting of the Irumide Belt is that of an intra-cratonic rift setting and not a consuming plate margin as previously advocated by Watters (1976).

Initial rifting of the basement led to the development of graben basins which were infilled by thick bimodal volcanic rocks and sedimentary sequences. Hydrothermal fluids circulating through the basin lithologies and along faults leached copper and gold out of the mafic volcanic rocks and redistributed them in various structural traps.. Mineralization resulted from metamorphic dewatering of the basin lithologies during the Irumide deformation D_1 and metamorphic events M_1. The distinct foliation which dips steeply to the north-west accompanied by south-eastward directed thrusting suggests that rift closure occurred from the north. The second deformation event was associated with the Damara event and only affected Irumide lithologies adjacent to the Damara - Irumide contact. Metamorphism associated with the Damara Orogen was however more widespread and resulted in resetting of isotopic ages within micas.

Fluids derived from deeper portions of the volcano-sedimentary pile were channelled efficiently by structural and lithological conduits alike. The Mebi Shear zone appears to host the largest single concentration of gold mineralization within the Neuras Grant area, and by no coincidence, the Mebi Shear zone also happens to be the largest shear within the area studied (excluding the thrust zones). The development of carbonate within unmineralized thrust planes suggests that fluids which carried carbonate were not mineralized.

Attention has been constantly drawn to the fact that gold mineralization within the Neuras Grant is spatially associated with lithological contacts. Mineralization has often been recorded adjacent to mafic and quartz porphyry dykes, particularly at the margins of these intrusives. The Older mafic dykes are sheared and altered suggesting that fluids migrating up through the basin fill sequences made use of these efficient conduits as well as their contact margins. The quartz-porphyry dykes are unfoliated compared to the mafic dykes and hence behaved more as aquicludes to the mineralizing solutions than aquifers. Consequently mineralization is absent from within the unaltered porphyry dykes and only occurs adjacent to their margins.

The mineralization at the Swartmodder Gold mine is restricted to a lithological contact zone between Piksteel Granodiorite and Marienhof Schist. Fluids have again made use of the greater permeability along the lithological contacts and precipitated mineralization during their passage.

All the factors for the development of a low-grade high tonnage gold and high-grade low tonnage deposit within the Neuras area are present except for a suitable mineralization trap. The metamorphic fluids that circulated through the various lithologies resulted in limited hydrothermal alteration and mineralization. Had a suitable trap such as an impermeable lithological unit (carbonate layer) or major shear zone, and greater fluid activity prevailed, the chances of mineralization being developed to orebody proportions would have greatly been enhanced.

5 EXPLORATION METHODOLOGY

Previous work in the area at the turn of the century involved small workings of quartz veins with relatively high gold grades. It is possible that the area holds potential for low-grade high-tonnage gold deposits and that these had been overlooked in the past. The present study was directed towards evaluating this possibility.

5.1 Mapping

Initial reconnaissance line mapping at a scale of 1 : 10 000 was done in the northern part of the grant area by Smalley (1989). The purpose of this mapping was to highlight target areas which revealed anomalous gold values. Twenty target areas were recommended for follow up work.

The follow up involved mapping at a scale of 1 : 1000 and detailed lithological chip sampling. On completion of the detailed follow up the remainder of the grant was mapped on a scale of 1 : 25 000 with the aid of air photos and topographic maps. The regional mapping revealed other areas of highly localized mineralization and proved invaluble in conceptualizing the broader geological framework within which the gold and copper mineralization occurs.

5.2 Geochemical Sampling

Geochemical sampling is an intrinsic part of any mineral exploration program. Lithological chip sampling involved the collection of 1 - 2kg samples from various sites. Sampling was carried out within the targeted areas. Samples were only analysed for gold on a routine basis, while selected samples were analysed for numerous other elements. Had elements such as Cu, Pb, Zn, Bi and W been analysed for on a routine basis, a zonational pattern may have been detected with differing styles of mineralization.

Figure 5.2: The lithosampling procedure undertaken for the Mebi Mine Grid is as follows : Litho samples were taken every 5m and composited every 25m on traverses 25m apart to form a 25m x 25m sampling grid. Gold scan results from 325 samples clearly define an anomalous trend of 094° and a second less well mineralized trend bearing 318°.

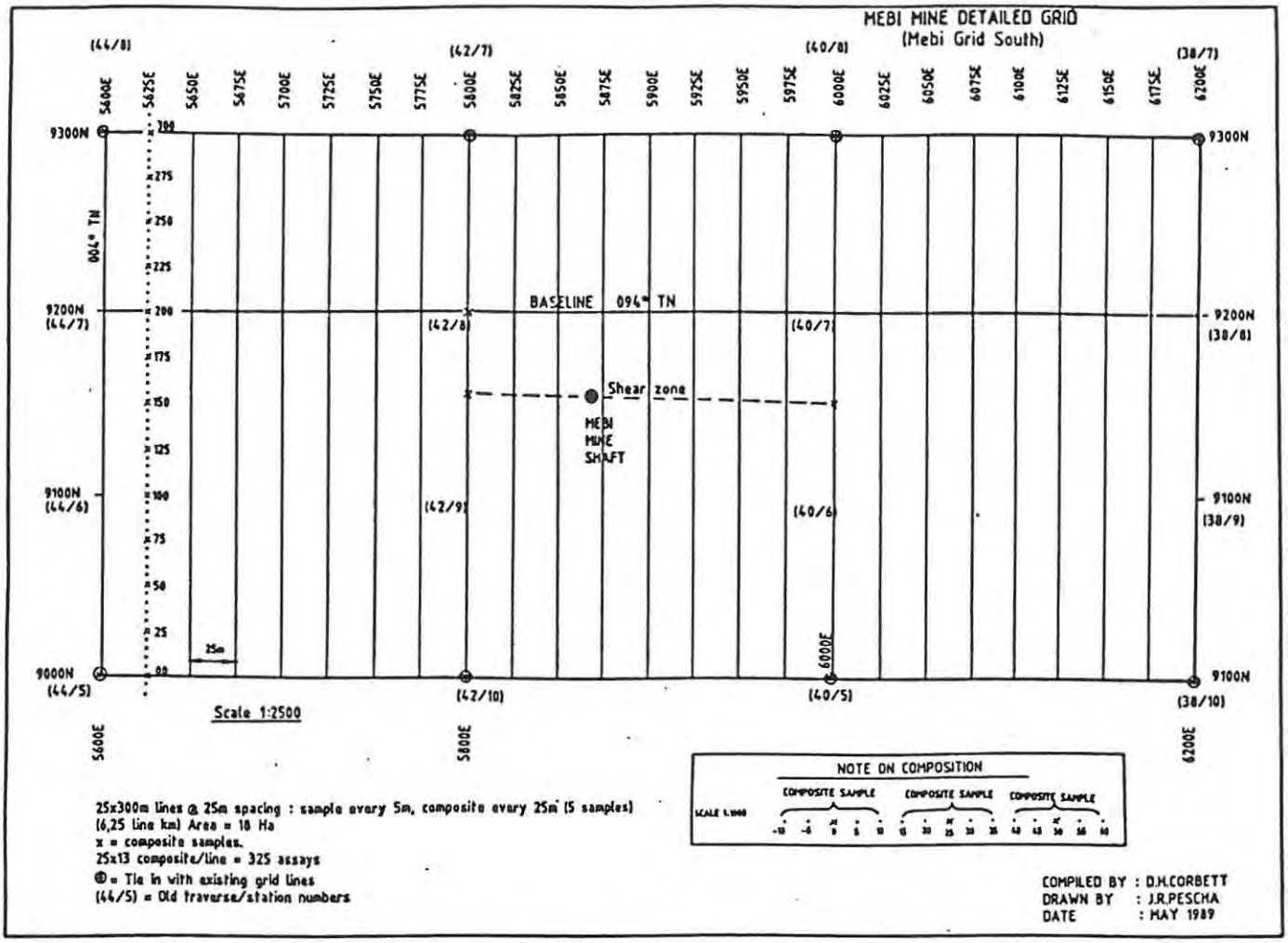
MEBI MINE DETAILED GRID
(Mebi Grid South)
(44/8)
(42/7)
(40/8)
(38/7)
5600E
5625E
5650E
5675E
5700E
5725E
5750E
5775E
5800E
5825E
5850E
5875E
5900E
5925E
5950E
5975E
6000E
6025E
6050E
6075E
6100E
6125E
6150E
6175E
6200E
9300N
9200N
9100N
9000N
094° TN
BASELINE 094° TN
(44/7)
(42/8)
(40/7)
(38/8)
Shear zone
MEBI MINE SHAFT
(44/6)
(42/9)
(40/6)
(38/9)
25m
(44/5)
(42/10)
(40/5)
(38/10)
Scale 1:2500
NOTE ON COMPOSITION
COMPOSITE SAMPLE
COMPOSITE SAMPLE
COMPOSITE SAMPLE
25x300m lines @ 25m spacing : sample every 5m, composite every 25m (5 samples)
(6,25 line km) Area = 18 Ha
x = composite samples.
25x13 composite/line = 325 assays
⊕ = Tie in with existing grid lines
(44/5) = Old traverse/station numbers
COMPILED BY : D.H.CORBETT
DRAWN BY : J.R.PESCHA
DATE : MAY 1989

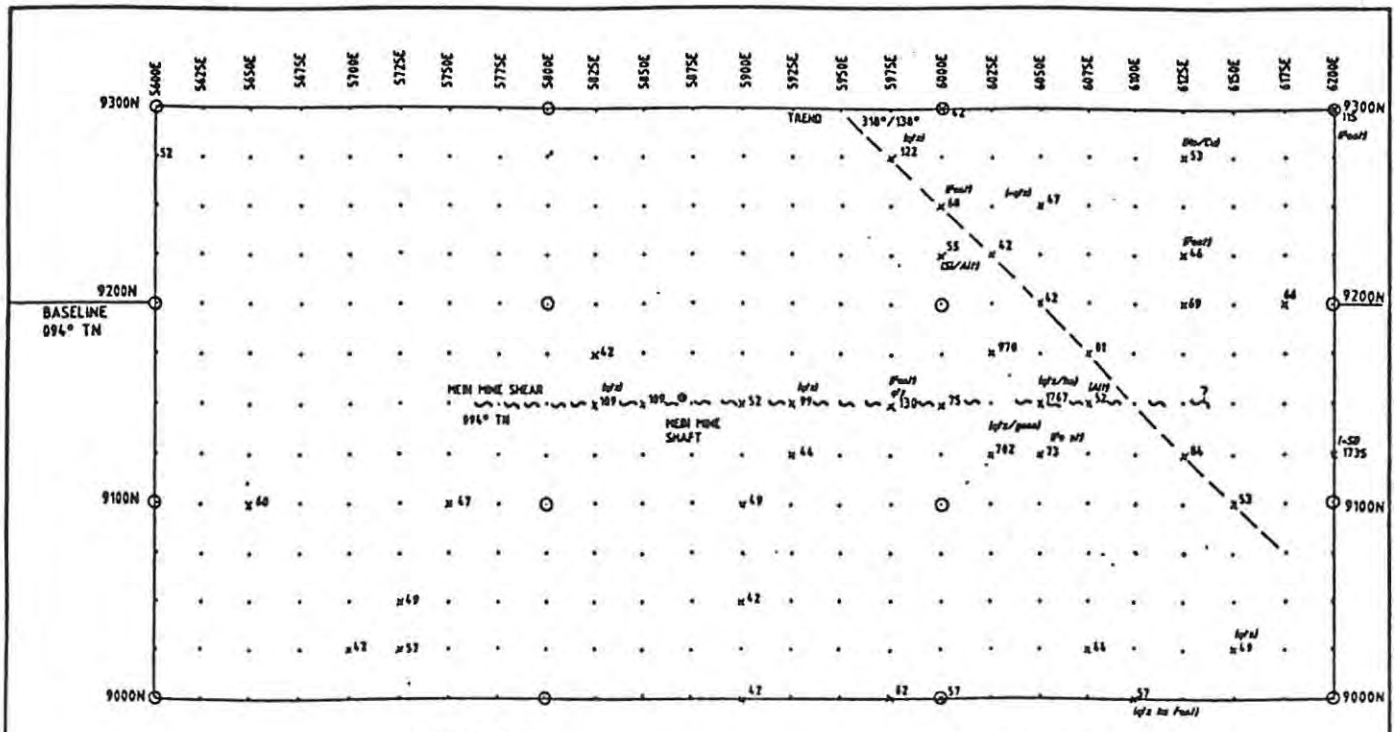
9300N
9200N
9100N
9000N
BASELINE
094° TN
MEBI MINE SHEAR
094° TN
MEBI MINE
SHAFT
TREND
318°/138°
ABBREVIATIONS:
he - hematite
qtz- quartz vein
Fest- iron staining
goss- gossanous
Si - Siliceous
Alt - Alteration?
Cu - Copper staining
T.N
MEBI MINE DETAILED GRID - RESULTS.
SCALE 1:2500
x 57 = Au (Scan) in ppb
. = Not detected
O = Old sample positions (Mebi Grid South)
COMPILED BY : D.H. CORBETT
DRAWN BY : J.R. PESCHA
DATE : MAY 1989.

A lithosampling program over the Mebi shear zone was implemented in order to determine the orientation of mineralization. Figure 5.2 illustrates the technique employed.

5.3 Evaluation of Shear Zone Gold Mineralization

A preliminary evaluation of shear zone gold mineralization was modelled using the aid of soft-ware developed for the Mineral Exploration Course, by C.A. Mallinson. The modelling revealed that grades typical of the Mebi Shear were insufficient to sustain mining operations economically. Keeping all factors the same, the grade was increased until hypothetical mining operations showed a profit. Grades upwards of 10 g/t Au within a shear zone similar to Mebi would prove to be economically viable. Such grades are excessively high for the Neuras Grant. The largest mineralized shear within the area is the Mebi Shear; this appears to have an average grade of 2.69 g/t, far below that of the 10 g/t required. It therefore appears that this area offers poor potential in proftabable Au mining; both for high-grade low-tonnage and high-tonnage low-grade mineralization.

5.4 Suggestions for Exploration

Two styles of mineralizing styles have become apparent during the present study. Sediment-hosted copper mineralization appears to have developed during the early stages of the envisaged rifting stage and shear zone gold mineralization during the dewatering of the rift basins.

Despite the lack of economically viable targets within the Neuras grant, work done in the area resulted in the formulation of a model which allows for a more defined mineral exploration program within in the Irumide basement rocks of Namibia. The noticeable feature of the Neuras grant area is the apparent lack of large scale 'mineralizing traps'. The largest 'trap' within the grant area is the Mebi Shear Zone.

Based on this study the following recommendations are suggested for gold exploration within the basement lithologies :-

1). Major structural features such as shear zones, faults and lineaments within the basement lithologies and particularly within the metasediments. The Areb Shear Zone comes to mind as an immediate target.

2) Thrusts within the various lithologies appear to have been conduits for fluids of compositions different from those responsible for the mineralization. In this area faults with quartz veins are mineralized but those with carbonate are barren.
Further work on other shear zones will verify or disprove the association of carbonate with a lack of mineralization both on local and regional scales.

3). Impermeable formations within the metapelitic lithologies such as carbonates or marls would act as mineralizing traps.

An analogy can be drawn with mineralization in the central zone of the Damara Belt. There, the Abbabis Formation contains mafic dykes with anomalously high Au at contacts (Steven, 1990). Remobilization of this during Damara metamorphism may have resulted eventually in concentration within overlying Karibib Formation marbles to form the Navachab Au deposit.

In addition to gold anomalous amounts of copper occur within the Irumide lithologies in the mapped area and general (eg. Klein Aub, Swartmodder, Natas, Jan Jonker Mines, Ghanzi etc..). It is therefore important to investigate the copper potential of Irumide lithologies, particularly if rifting mechanisms have been operative. Sawkins (1983) highlights the fact that most metal deposits formed within the Proterozoic times were generated in tectonic environments characterised by rifting. A brief study of all deposits between 1.5 Ga and 1.0 Ga reveal that the majority of base metal deposits are sediment-hosted accumulations from inferred rift settings (Sawkins, 1983). The reason that rift environments are so favourable for the generation of sediment-hosted copper deposits appears to stem from a combination of three factors :

1) the copper-rich nature of rift basalts;
2) sharp redox potential changes in rift sedimentary environments;
3) enhanced heat flow of rift environments.

6 SUMMARY AND CONCLUSION

The purpose of the study was to investigate the nature, controls and genesis of gold mineralization of the Neuras Grant area. In the light of a previous pegging boom, where earlier prospectors mined high-grade low-tonnage occurences of gold, it was thought that a low grade high tonnage target suitable for opencast mining could have been overlooked. Although the present study did not confirm an economically viable deposit it did develop a model which accounts for the geology and mineralization of the area. The model proposed is not intended as a definitive solution to the various geological problems within the area, but as a guide to future exploration for base- and precious metals in the Irumide Belt.

From regional mapping, lithological associations, geochemical data and metallogenic considerations it is concluded that the Irumide belt, in Namibia, evolved in an intra-continental rift setting.

Trace element data from two distinct mafic suites suggest fertile mantle characteristics for the older suite and depleted mantle characteristics for the younger. Mantle melting is attributed to passive thinning of the lithosphere during extension and resulted in decompression melting of the mantle. The continental crust deformed by creating faulting leading to fault bounded basin features which were filled by volcano-sedimentary sequences. The bimodality (acid - mafic) of the volcanic components, within the area studied, fits a rift model.

Copper mineralization within the Irumide belt is widespread, more so than gold, which is more localized to specific areas or basins. The dominance of base metals (in particular copper), within the Proterozoic sequences of the Irumide belt is similar to other Proterozoic deposits in rift tectonic settings. Gold is less well known from the Irumide belt and appears restricted to the Klein Aub - Rehoboth basin.

Detailed mapping and sampling of mineralized sites within the area studied revealed that gold mineralization is locally restricted to second-order gossanous quartz-haematite veins. Values of several thousand ppb Au were restricted to such veins while low (± 40 ppb) values are recorded for the host rock adjacent to the mineralization. Second-order veins are developed within all tectonised lithologies. The greatest concentrations of gold

mineralization within the area occur within the shear zones in the Blanks' and Mebi Mine areas, followed by the lithological contact areas at the Swartmodder and Neuras Mines. Findings from this study support a model which invokes metamorphic dewatering which led to syn-deformational mineralization strongly controlled by structure and lithological contacts.

Most of the ingredients for the previously conceived low-grade high-tonnage deposit are present. The lack of a suitable mineralizing trap/host, such as well developed shear zone and/or the presence of an impermeable layer (carbonate horizon), and limited hydrothermal activity are cited as the main reasons why no economically favourble accumulation of gold occurred.

APPENDIX - 1 DETAILED STRATIGRAPHY OF THE NEURAS GRANT AREA.

APPENDIX - 1 Detailed stratigraphy of the Neuras Lithologies.

TABLE 1.1: Stratigraphy of the Neuras Grant Area.

Formation	Lithology	Approx. Age (Ma)
Gamsberg Granite Suite	Uitdraai and Kobos Granite plutons. Reddish coloured, coarse grained & undeformed .	1010 - 1090
Swartkoppies Mafic Intrusives	Undeformed mafic dykes and metagabbros.	1021
Langberg Formation	Quartz porphyry/ Quartz-feldspar porphyry - High level Granite & Quartz porphyry dykes	1080
Older Sheared Mafic Intrusives	Sheared and altered mafic dykes and metagabbros.	
Neuras Granite	Coarse grained S-type granite.	
Swartskaap Granite	Possible I-type gneissic granite.	
Piksteel Granodiorite	Porphyritic, S-type granitoid. Most widespread intrusive in the area studied.	
Swartmodder Granite	Oldest intrusive within the area. Hosts rafts of Cu-mineralized schist	
Marienhof Formation	Reddish-brown Phyllites - intruded by numerous sheared mafic dykes. --- Quartzites - usually sheared --- Rhyolitic Ignimbrites, lavas & tuffs --- Reddish-brown Schists	1668
Elim Formation	Metagabbros & remnant basaltic lavas	>1668

Table 1.1 The stratigraphy of the Neuras Grant.

1.1 ELIM FORMATION CORRELATIVES

1.1.1 Remnant Basaltic Lava

Outcrop of this basaltic lava is extremely poor and constitutes nothing more than scree. Despite poor outcrop and being intruded by various younger granites, the lava is well displayed on satellite images as a dark patch (Plate 4.1.2).

Plate 1.1.1 Photomicrograph of remnant basaltic lava. FOV = 1 mm

1.1.2 Metagabbroic Intrusive

A single metagabbroic intrusive of possible Elim Formation was recorded in the study area. The metagabbro is intruded by the Swartmodder Granite to the east and by the Piksteel Granodiorite to the south and east, the two oldest granites in the area. The metagabbro is essentially undeformed, except for the margins which are strongly foliated. A competence contrast between the metagabbro and the less competent granodiorite resulted in the relative lack of deformation despite the older age.

The mafic intrusive is retrogressively metamorphosed to an assemblage of greenschist facies minerals. Rare remnants of plagioclase (labradorite) and clinopyroxene (diopsidic) show incipient alteration to the major mineral phases now present in the rock, namely epidote-clinozoisite and actinolite.

1.2 MARIENHOF FORMATION

The Marienhof Formation, was first studied on the farm Marienhof, more or less in the centre of Basterland, and comprises mainly metasediments and lesser sequences of volcanic and intrusive units. Acid volcanic rocks, namely rhyolitic ignimbrites, lavas and tuffs are interbedded within the pelites and intruded by mafic dykes and sills. The metapelites are limited in distribution to the northernmost sector of the Neuras Grant.

The metasediments consist of schists, phyllites and minor quartzites (typically sheared) and are discussed below.

1.2.1 Marienhof Schists

The schists form the lowest package of the metasediment lithologies, underlying both the quartzites and phyllites. Outcrop is excellent and the schists appear to be more resistant to weathering (compared to other lithologies) and thus tend to form hilly topography in an otherwise flat terrain.

Two distinct units can be recognised within the schists, a psammitic unit and a pelitic unit. The psammitic schist units weather a reddish - brown colour and the pelitic units vary in shades of green. The schists are foliated and apart from microscopic grading no internal structures are visible. The total thickness of the metasedimentary package within the Neuras grant is estimated at less 500 m.

Thin sections of the various units within the schists reveal varying composition and textural characteristics. The more pelitic units have internally graded units and the following mineralogy (in order of decreasing abundance) : sub-angular quartz grains which rarely exceeds 0.4 mm in length (despite deformation and recrystallization), sericite and chlorite exhibit a marked parallel orientation; calcite occurs as typically sub-angular grains and along with an iron oxide phase magnetite(?) makes up the remainder of the rock (Plate 1.2.1) . Internal grading within the psammitic schist units is absent and mineralogically the sediment appears more immature. Thin section studies reveal the following minerals in order of decreasing abundance : quartz grains (average size 0.7 mm) are sub-angular and largely recrystallized; sub-angular albite grains (sericitized); muscovite and chlorite laths are randomly dispersed and an

anhedral oxide magnetite (?) occurs as an accessory phase. On the whole the schists can best be described as being of greywacke in origin, the more psammitic units tending towards feldspathic wackes.

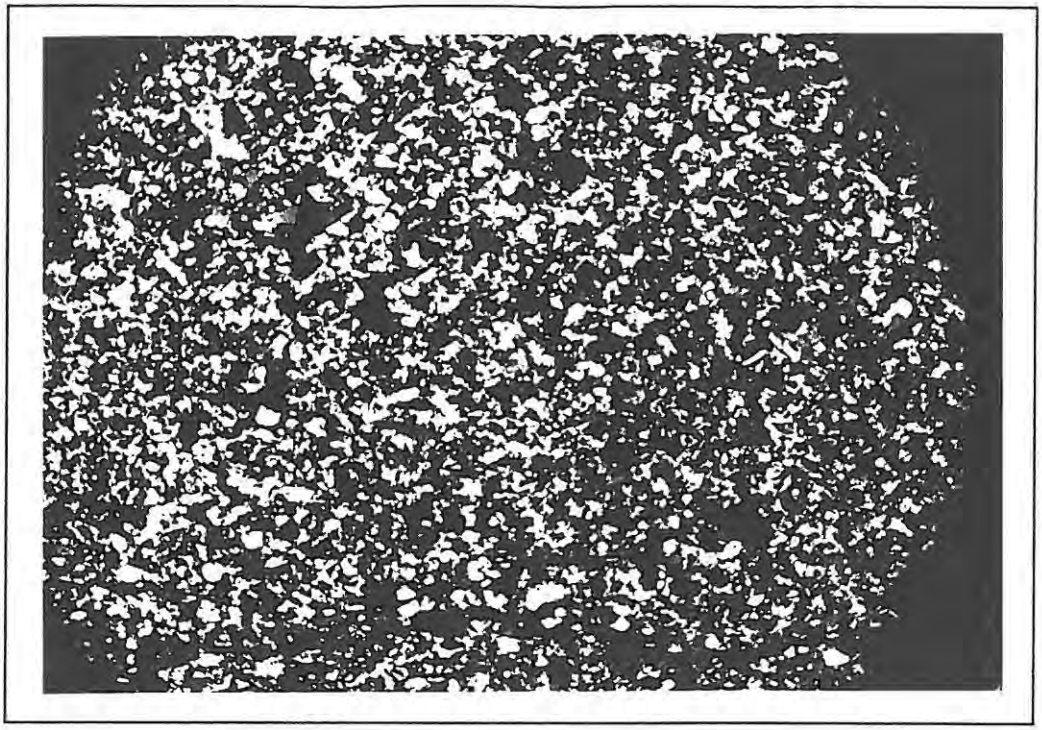

Plate 1.2.1: Photomicrograph of a pelitic schist unit. FOV = 3 mm.

1.2.2 Quartzites

The quartzites encountered in the study area occur as elongate lenses associated with the thrust faulted contact between the schists and phyllites. Thicknesses vary from a minimum of 2.5 m to a maximum of about 8 m. Shearing and recrystallization of the quartzites have resulted in the destruction of internal structures and the development of a strong tectonic fabric.

1.2.3 Phyllites

This fissile lithology has a deep purple colour in fresh outcrop and weathers to a deep maroon colour. The phyllites occur directly above the quartzites and are intruded by mafic dykes of the Older dyke swarm. The phyllites (and mafic dykes) are foliated and remnant bedding is visible in outcrops where the foliation transposes cuts it by a high angle and partly transpose it. The thickness of this unit is uncertain due to probable folding and duplication. In some areas the phyllite is magnetic and

detailed mapping revealed localized concentrations of small magnetite crystals. Limonite pseudomorphs after pyrite cubes are common throughout the phyllites and range in size from 0.4 mm to 20 mm in size.

Thin sections of phyllite typically show deformed quartz grains (about 0.1mm in length); laths of lepidoblastic sericite and a few percent of limonite. The nature of contact between the schists and phyllites, on the Neuras grant, is largely faulted except, near the north eastern grant boundary, where an unconformity separates the two units.

1.2.4 Rhyolitic Ignimbrites

This lithology is recorded as the "Spitskop Rhyolite" on the 1:50 000 Geological survey map of Rehoboth (unpublished). The ignimbrite is rhyolitic in nature and varies from a lithic- to crystal-dominated tuff. Lithic fragments within the tuff vary in composition from mafic through to pelitic fragments and rarely exceed 10cm in length. All the fragments are elongated in the down dip direction of the regional foliation a result of tectonic stretching.

In thin section the ignimbrite is holocrystalline and inequigranular porphyritic. Lithic fragments are commonly angular and crystal fragments vary from bipyramidal quartz fragments to anhedral feldspar (sanidine) fragments. Embayment of the various crystals is attributed to thermochemical dissolution during emplacement of the flow. Crystal phenocrysts range in size from 0.5 mm to 3 mm and are set in an aphanitic microcrystalline groundmass of plagioclase (albite) and quartz. This groundmass is thought to represent devitrification of previous volcanic glass. Welded pumice fragments (*fiamme*) have also devitrified to a quartz - feldspar aggregate,and are distinguished from the groundmass by their slightly coarser grain size and characteristic symmetry (Plate 1.2.4(a)). Strongly pleochroic biotite is the only ferromagnesian mineral recorded and accessory amounts of apatite, sphene, zircon, epidote and opaque oxides are present.

1.2.5 Rhyolite Lavas and Tuffs

The lavas and tuffs occur as discrete units within the schists. Each unit may comprise up to twenty individual lava flows and usually fewer tuff layers. The lava flows are well preserved and internal flow-banding is

clearly visible (Plate 1.2.5(a)). The interbedded tuffaceous units are less well perserved and tend to be more weathered and jointed (Plate 1.2.5(b)) In some areas, particularly around Raabies Mine, intrusion of a younger quartz porphyry gives rise to confusing relationships.

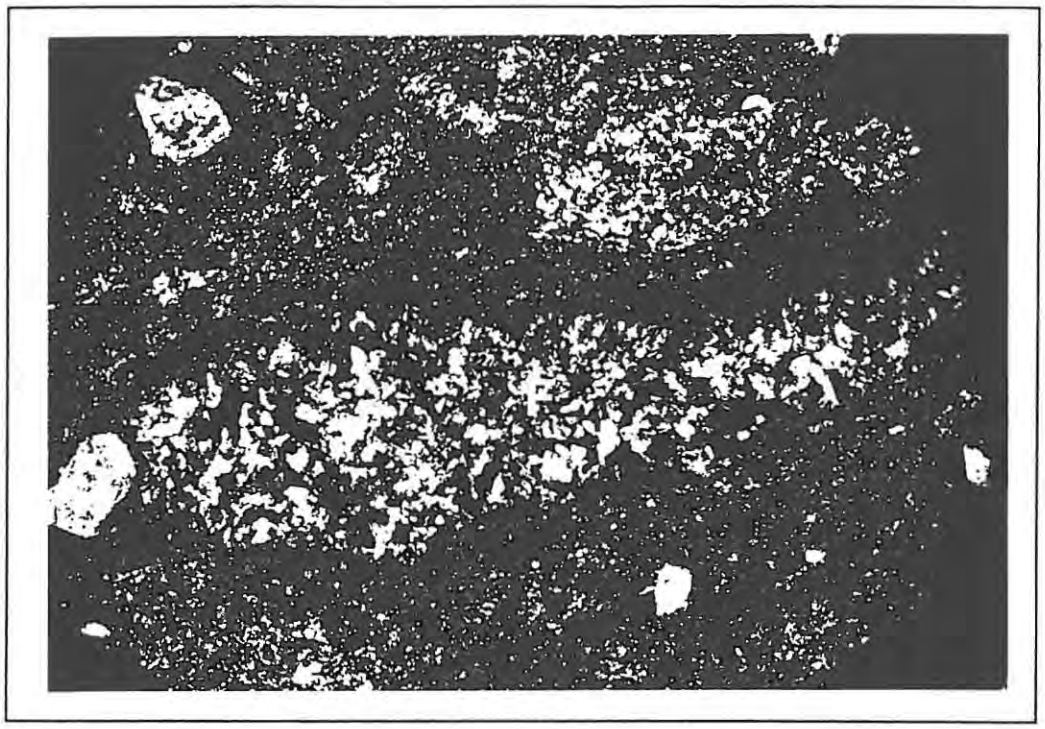

Plate 1.2.4(a) Photomicrograph of rhyolitic ignimbrite. Note elongate fiamme (welded pummice fragment) - F. FOV = 3mm.

Plate 1.2.5(a): Flow banding within rhyolitic lava flows.

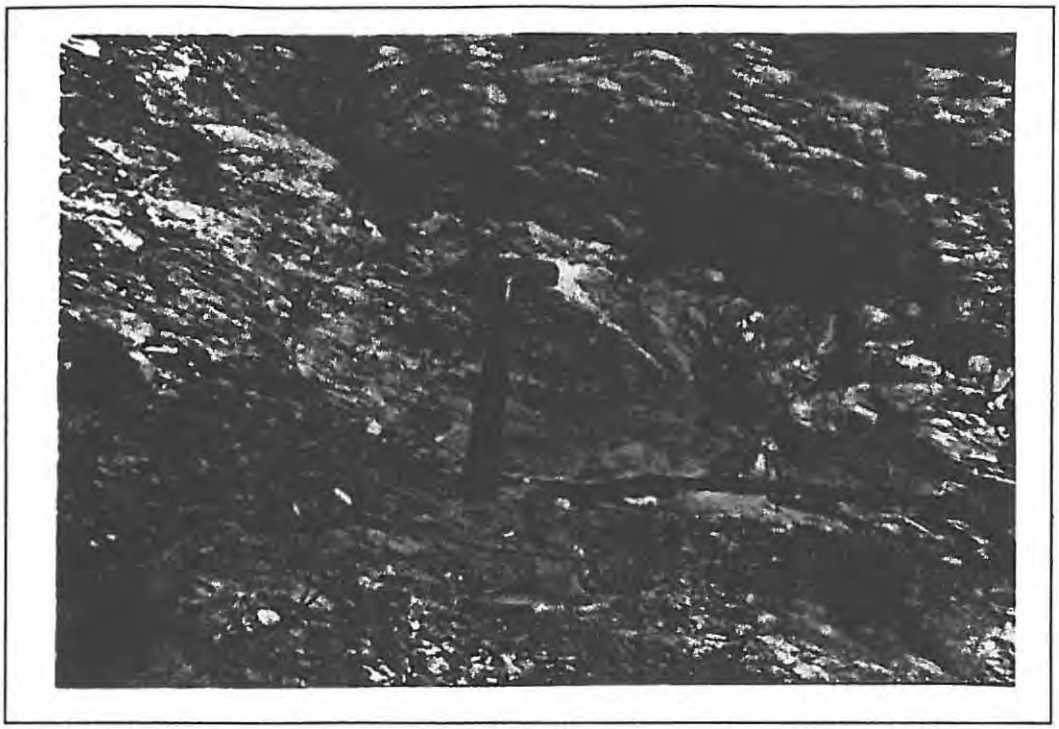

Plate 1.2.5(b): Jointed rhyolitic tuff units.

The expected petrography of a rhyolitic lava would generally be a hypocrystalline aphanitic textured rock. The rhyolites encountered within this study however, depict a somewhat different texture. The lavas are now holocrystalline and exhibit an allotriomorphic granular texture as a result of devitrification of a previously glassy rock. Glass is unstable and the lack of natural glasses older than Cretaceous (135 m.y.) suggests that given sufficient time it will devitrify (Lofgren, 1971). Quartz and feldspar (albite & oligoclase) crystals (>1 mm in size) comprise 96% of the rock and larger grains of epidote and cassiterite form less than 1%. Non-pervasive sericitic alteration of the plagioclase laths is thought to be a result of later hydrothermal activity.

The above fabric, compared to fresh rhyolite, has probably resulted from complete devitrification of previously holohyaline rock.

1.2.6 Geochemistry

The scope of the present study is not intended to include a detailed geochemical account of the the various igneous suites but rather a brief account of the geology within which Au mineralization occurs. Observations

and proposals are thus based on relatively few analyses, particularly for the mafic suites. A major problem in interpreting chemical analyses (Appendix 3) of altered volcanic rocks concerns the degree of element migration associated with contemporaneous post-eruptive alteration and low grade metamorphism. Data concerning mobile elements should thus be interpreted with caution. In figure 1.2.5(a), Nb (High Field Strength Element) is plotted against K_2O, SiO_2, and Zr to illustrate chemical modification which may have occurred. The Nb vs. Zr plot (Figure 1.2.5(a)) shows a tight cluster for both ignimbrites and rhyolites. By contrast the K_2O vs. Nb plot (Figure 1.2.5(a)) shows a distinct difference between the ignimbrites and lavas. The important fact to note, is that there is relatively little variation of K_2O within the individual rock types. This relationship reflects the lack of post-eruptive modification undergone by the rhyolites. The Nb vs. SiO_2 plot (Figure 1.2.5(a)) again shows a good grouping, indicating a lack of alteration (silicification). In view of the apparently insignificant alteration undergone by the rhyolites a petrogenetic interpretation can be extended to include the major-element constituents of the rhyolites.

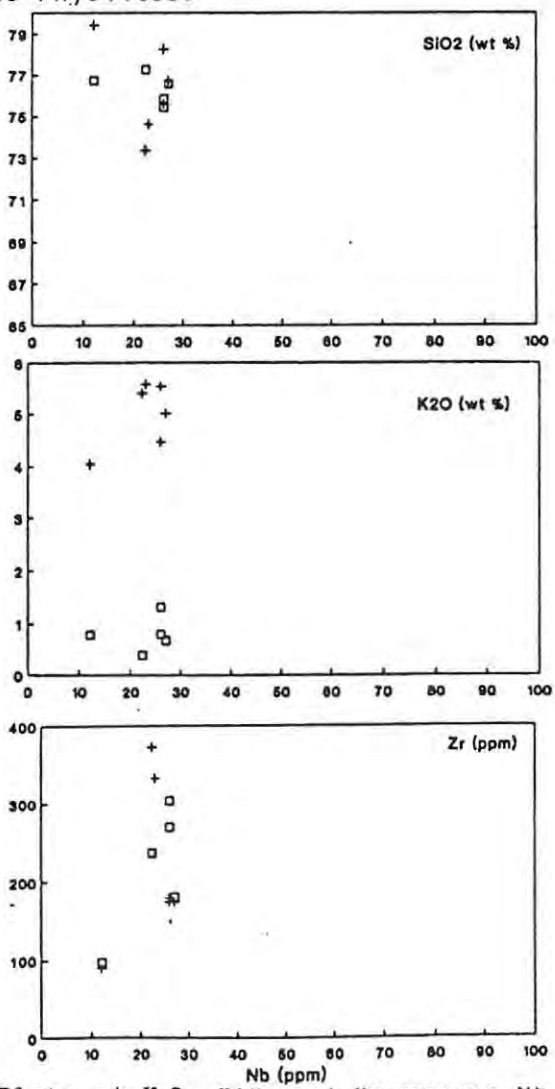

Figure 1.2.5(a): Plots of K_2O, SiO_2 and Zr versus Nb.

Major Element Variation

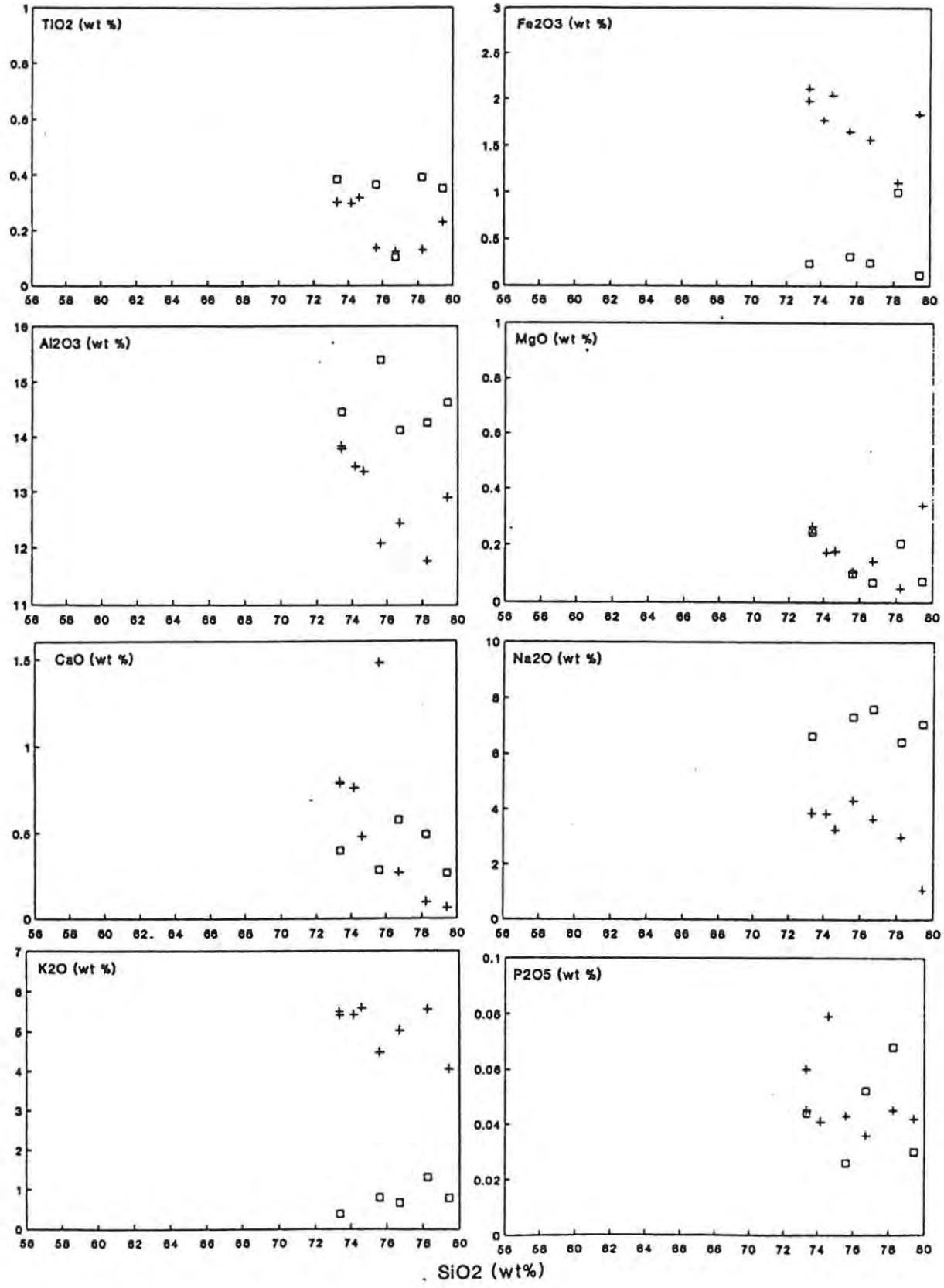

Figure 1.2.5(b): Harker variation diagrams for Rhyolitic Volcanics.

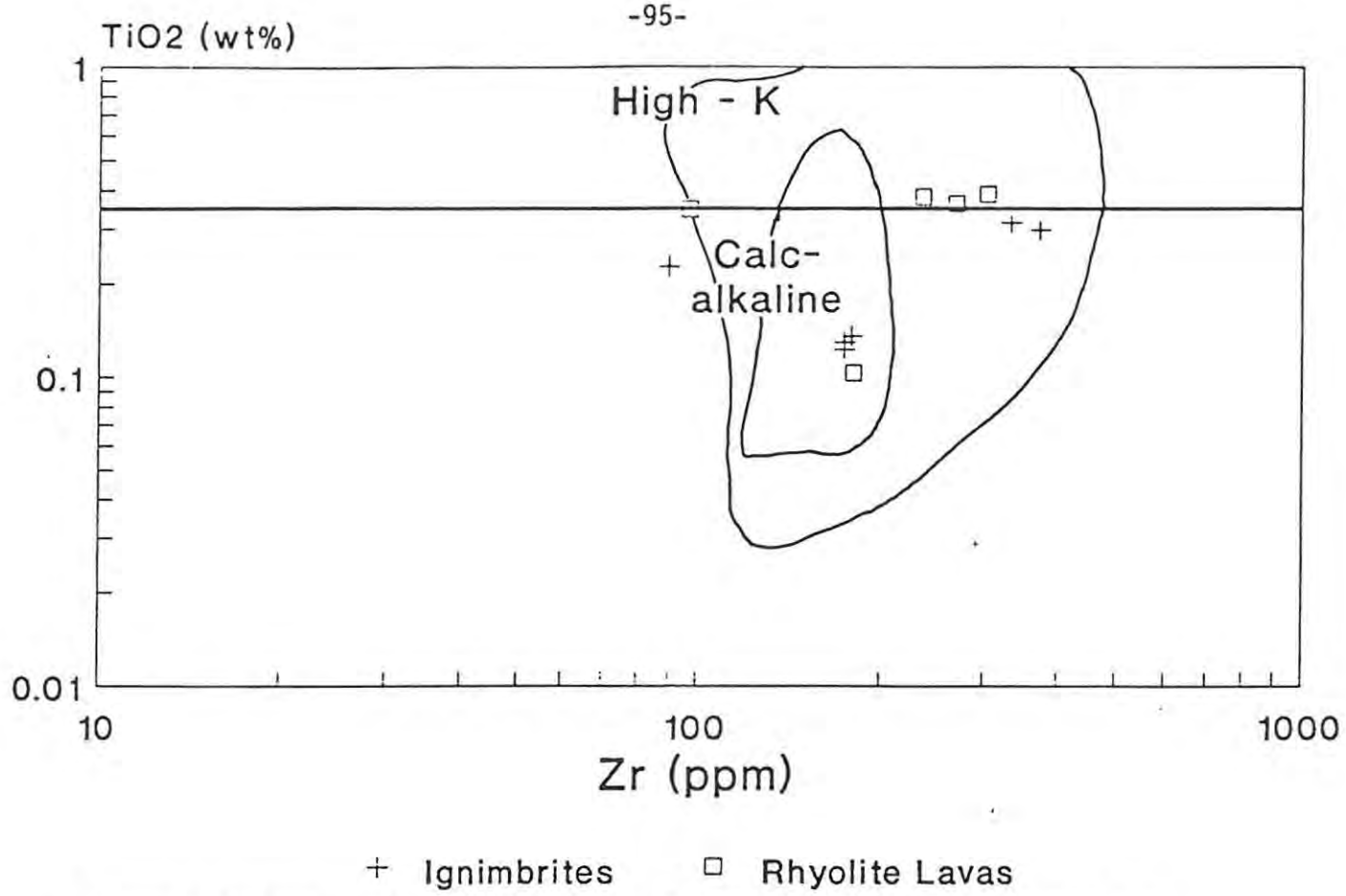

Figure 1.2.5(c): Plots of Zr versus TiO_2 showing fields of high-k and calc-alkiline lavas (Pearce, 1980)

Harker variation diagrams (Figures 1.2.5(b)) show that the fields occupied by the rhyolite lavas and ignimbrites overlap. In general the lavas tend to have slightly lower levels of $_{tot}Fe_2O_3$, TiO_2, P_2O_5 and Sr when compared to the ignimbrites. Both the lavas and the ignimbrites fall within the calc-alkaline and high - K field on the TiO_2 vs. Zr plot (Figure 1.2.5(c)). Also shown in this figure is the line (TiO_2 = 0.35%) that, according to Ewart (1979), separates rhyolites with more than 73% SiO_2, of both high-K and calc-alkaline types from less silicic volcanic rocks. All the samples plot below this line indicating that they are fairly evolved rhyolites.

Rhyolite lavas and ignimbrites plot within the peraluminous field, according to Shand (1927), which indicates that all samples have $Al_2O_3 > (Na_2O + K_2O + CaO)$. The high degree of alumina saturation (A/CNK > 1) suggests that these lavas were derived from melting of crustal sequences. Rhyolitic ignimbrites consistantly plot in the 'Within Plate Field' while rhyolite lavas plot within both 'Ocean Ridge' and 'Within Plate Fields' on tectonic discrimination diagrams, after Pearce et al. (1984) .

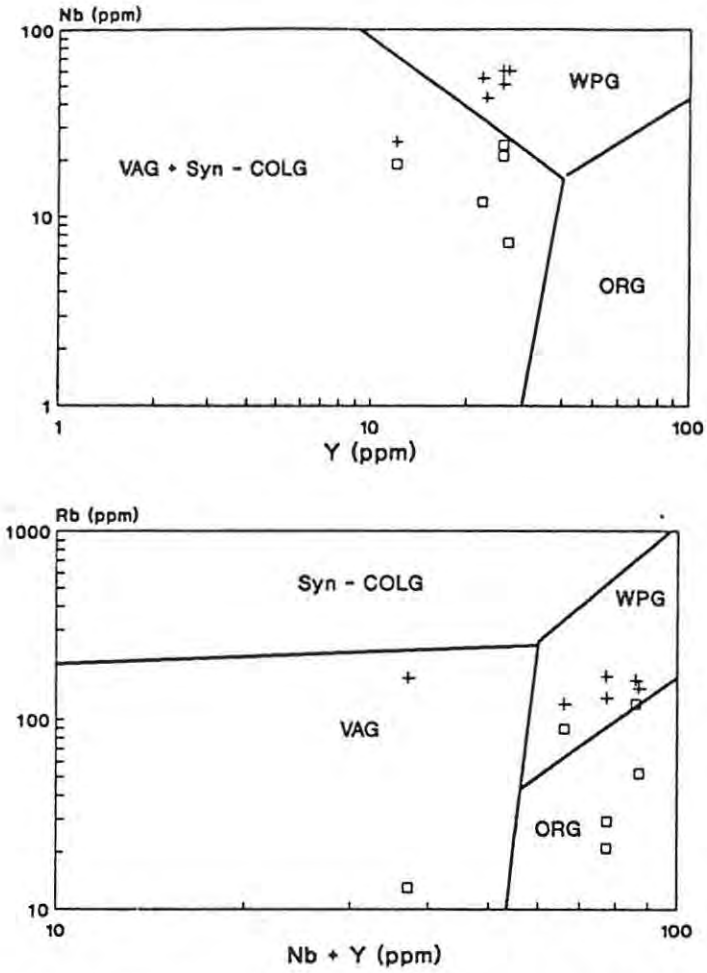

Figure 1.2.5(d): Tectonic discrimination diagrams of the rhyolitic lavas

The relatively low Nb, Y and Rb contents of the rhyolite lavas suggests either 'Volcanic Arc' or 'Syn-collisional' setting according to the data of Pearce et al. (1984). The ignimbrites however, have relatively higher Nb, Y and Rb concentrations and thus plot within the 'Within Plate Field'. A possible explanation for the differing tectonic signatures is that the ignimbrites, which represent the initial explosive eruption, depleted the magma of incompatible trace elements (Nb, Y & Rb) and hence the later lavas were relatively depleted in these elements. The reader is referred to section 3.2 where, discussion of tectonic discrimination diagrams highlights their application to acid rocks.

1.3 SWARTMODDER GRANITE

The Swartmodder Granite is the oldest intrusive within the area studied. Fresh samples obtained from underground workings yielded the following petrographic information. In thin section the granite is typically medium to fine grained with a hypidiomorphic granular texture (Plate 1.3). K-feldspar (perthite) is the dominant mineral and varies in size from <1 mm to 4 mm. The larger perthite grains characteristically have quartz and fewer albite inclusions. In places the abundance of inclusions give rise to a 'sieve-like' texture. Anhedral plagioclase grains are pervasively altered to sericite and quartz grains are sutured exhibiting strained extinction. Biotite is the dominant ferromagnesian mineral, followed by less hornblende and chlorite.

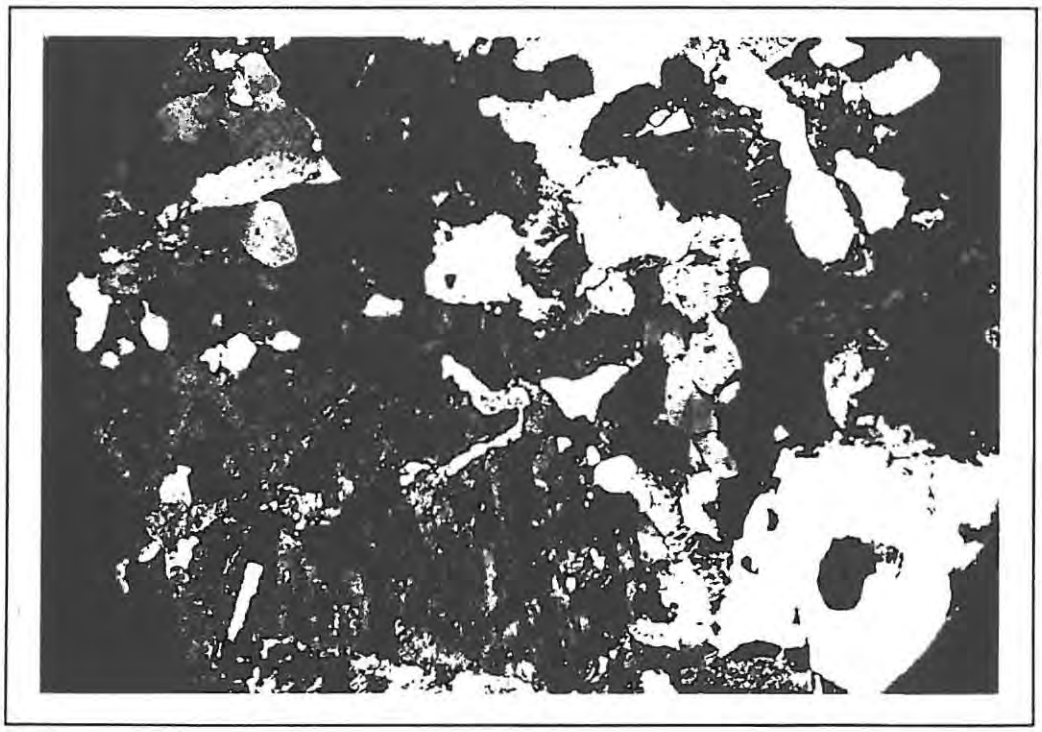

Plate 1.3: Photomicrograph of the Swartmodder Granite. FOV = 3 mm

1.4 PIKSTEEL GRANODIORITE

The Piksteel Granodiorite is the most widespread rock type encountered within the entire Neuras grant (Plate 1.4(a)). The granodiorite intrudes the Marienhof meta-volcanic pile and is itself intruded by later granites.

In its undeformed state the granodiorite is characteristically porphyritic but locally it may be equigranular (Plate 1.4(b)). Deformation of this lithology results in the progressive reduction and elimination of the feldspar phenocrysts. In thin section the large feldspar phenocrysts were found to be K-feldspar (perthite) which often included exsolved laths of plagioclase (albite). The rock has an allotriomorphic-inequigranular texture with perthite grains varying from 5 - 25 mm in diameter. Quartz occurs as aggregates of sutured grains exhibiting strained extinction. Plagioclase occurs as albite and K-feldspar as microcline both of which are pervasively altered to sericite. Chlorite and hornblende are the dominant ferromagnesian minerals, and biotite, sphene, zircon and opaque oxides comprise accessory phases.

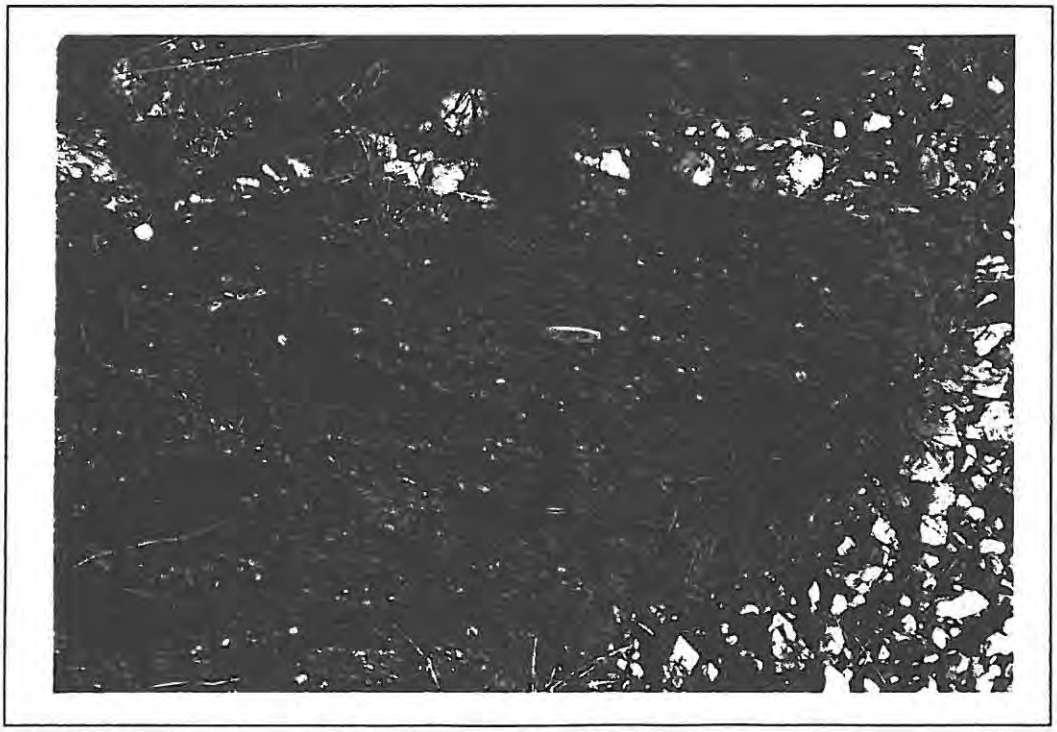

Plate 1.4(a): Weathered outcrop of Piksteel Granodiorite.

Plate 1.4(b): Photomicrograph of Piksteel Granodiorite. FOV = 3 mm.

1.4.1 Geochemistry

Tight clusters for all the Piksteel samples on Harker variation diagrams (Figure 1.4(b)) reflect a consistent chemical uniformity across the grant area. All samples analysed were unaltered in outcrop and slight variations in mobile elements such as K_2O are attributed to regional low grade metamorphism (Figure 1.4(a)). The modal Q-A-P contents of the Piksteel place it within the granite field of Streckeisen (1976), while a normative An-Ab-Or plot reveals a granodioritic composition. Of all the granitoids within the Neuras Grant area, only the Piksteel is corundum normative (ie. > 1% Co). On a Al_2O_3 - CaO - (Na_2O + K_2O) ternary diagram (Figure 1.4(c)) the Piksteel plots within the peraluminous field and a A/CNK ratio of 2.19 classifies the Piksteel Granodiorite as an S-type granitoid. The low Rb values, high initial $^{87}Sr/^{86}Sr$ ratios which range between 0.707 and 0.709 (Reid et al., 1988) and peraluminous nature suggest a crustal origin for the Piksteel.

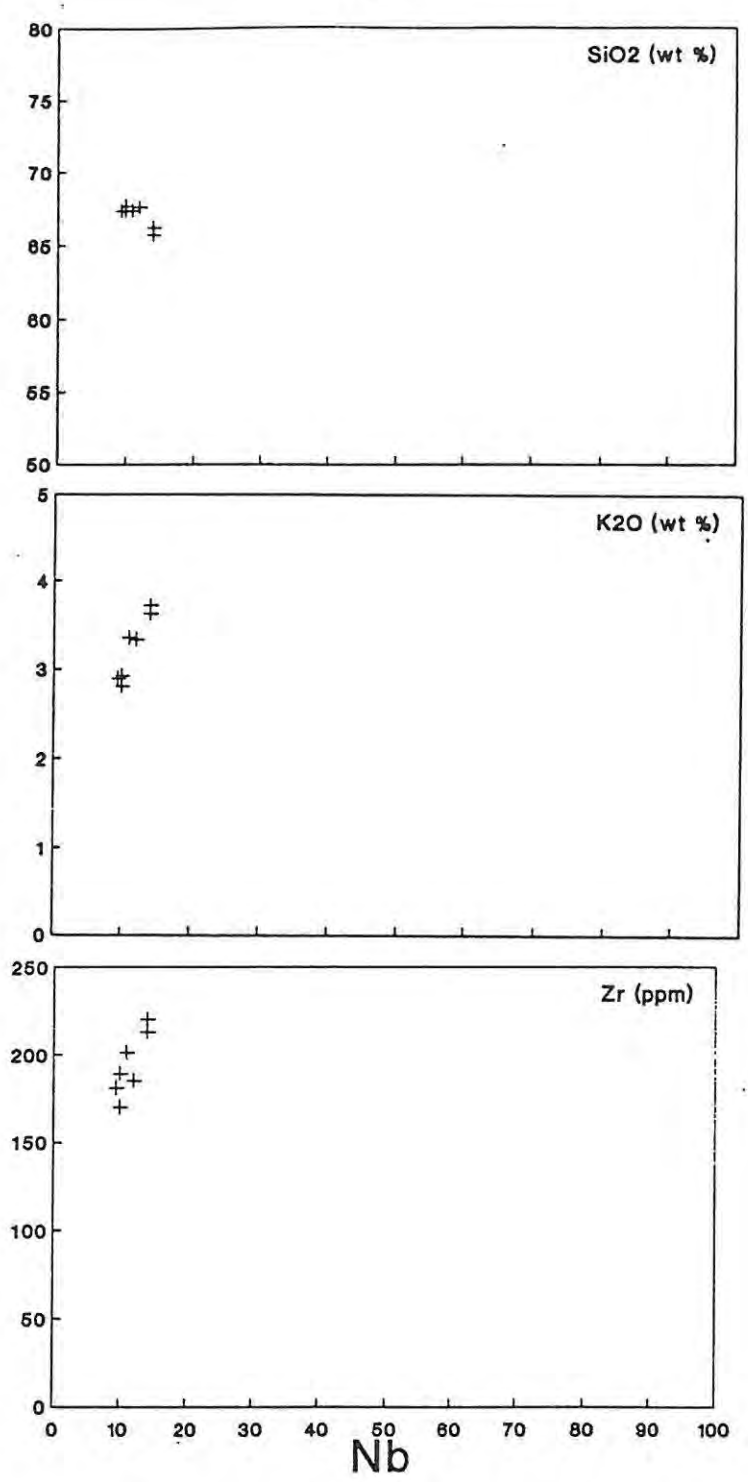

Figure 1.4(a): Plots of K_2O, Na_2O and Zr versus Nb.

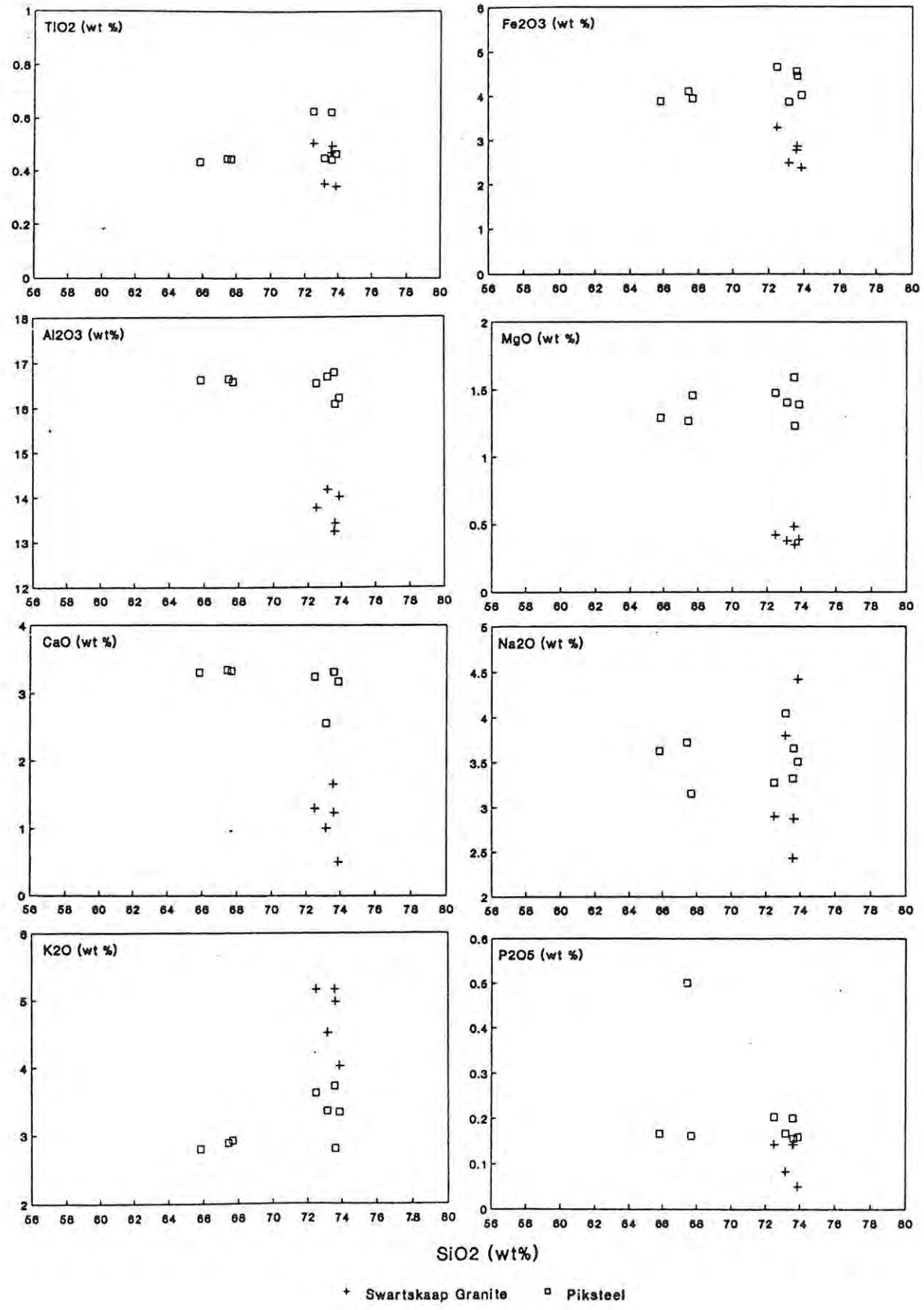

Figure 1.4(b): Harker variation diagrams for the Piksteel Granodiorite and Swartskaap Granite.

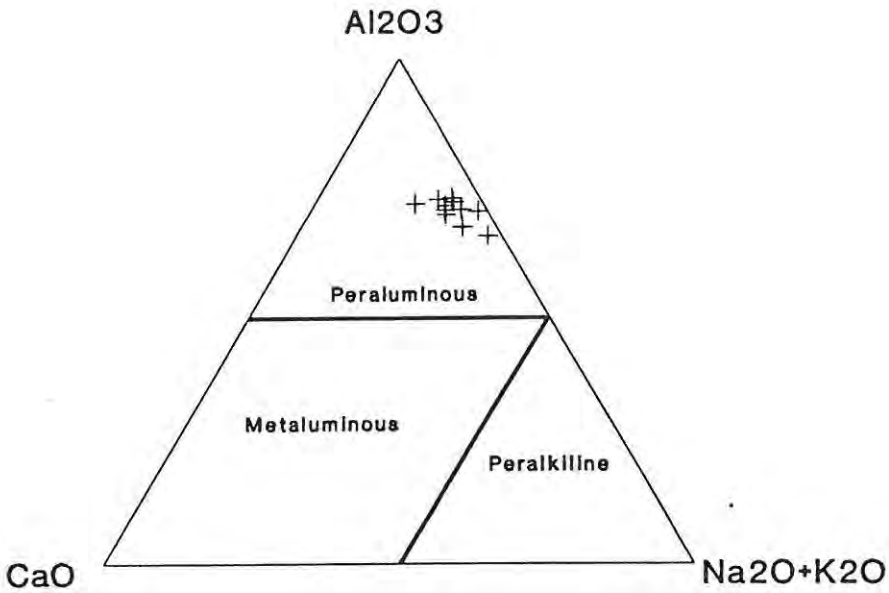

Figure 1.4(c): Ternary diagram depicting the Peraluminous nature of the Piksteel Granodiorite

The low Rb, Y and Nb values place the Piksteel within the 'Volcanic Arc ' field on the Nb-Y-Rb tectonic discrimination diagrams depicted in figure 1.4(d).

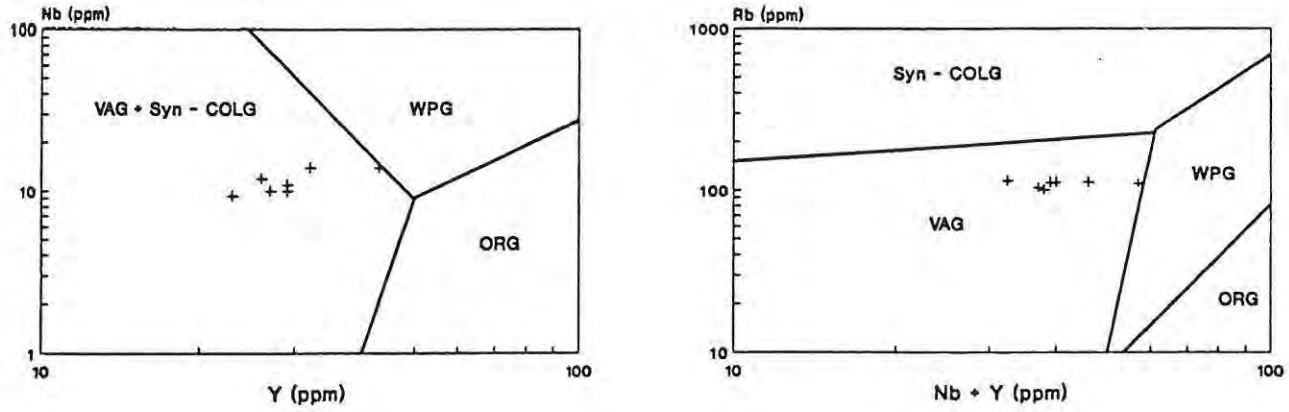

Figure 1.4(d): Tectonic discrimination diagrams for the Piksteel Granodiorite.

The Piksteel is interpreted as having been, the first voluminous crustal melt to have occurred during initial stages of rift development. The volcanic-arc trace-element signatures do not reflect the tectonic setting into which the Piksteel intruded but rather those inherited from the basement lithologies during melting.

1.5 SWARTSKAAP GRANITE

The Swartskaap Granite was recorded on the eastern-most boundary of the Neuras grant in an area of particularly poor outcrop. The granite is weathered, leucocratic and exhibits a gneissic texture in outcrop.

In thin section the rock is phaneritic, medium grained and displays an allotriomorphic-granular texture. Anhedral grains of strained quartz have sutured boundaries and in places have recrystallized giving rise to a poorly developed mortar texture. Anhedral laths of plagioclase (albite) and K-feldspar (microcline) are variably altered to sericite, and less common K-feldspar (perthite) appears unaltered. Biotite occurs as small (>1 mm) platy laths making up between 1 and 3% of the rock. Accessory mineral phases include epidote - clinozoisite, chlorite and an opaque oxide.

1.5.1 Geochemistry

A plot of mobile (K_2O), semi-mobile (SiO_2) and immobile (Zr) element variation vs. an immobile element (Nb) reveals that there has been post-emplacement alteration (Figure 1.5.1(a)). Major element variations (Figure 1.4(c)) reveal the effect of post-emplacement alteration.

Immobile trace element ratios plot as a spread between 'Volcanic Arc' and 'Within Plate Granite' fields on tectonic discrimination diagrams (Figure 1.2.5(c)) (Pearce et al., 1984).

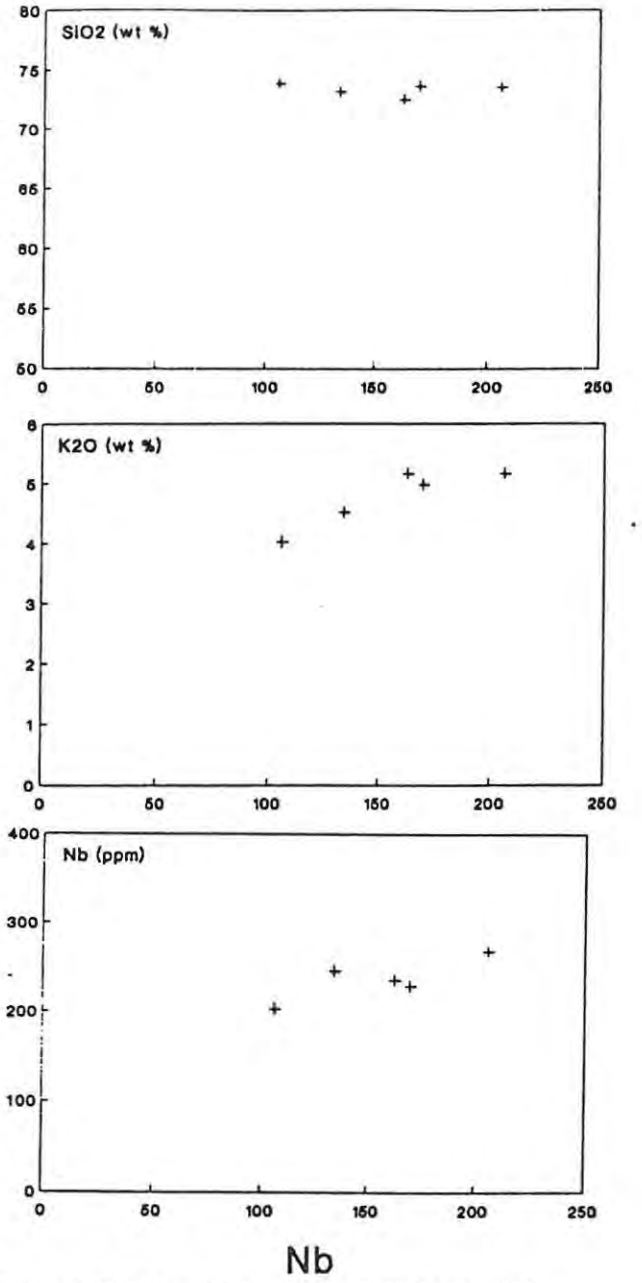

Figure 1.5.1(a): Plots of K_2O, SiO_2 and Zr versus Nb.

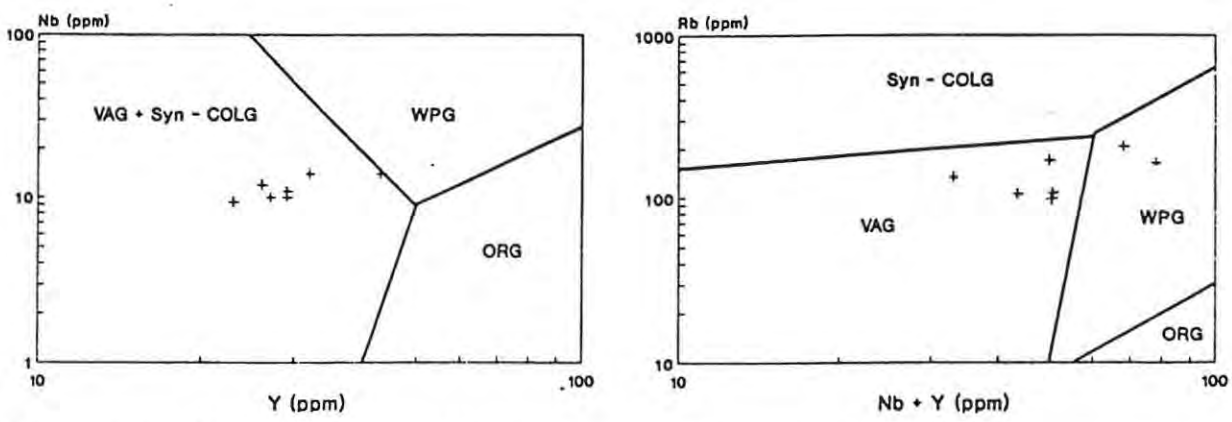

Figure 1.5.1(b) Tectonic discrimination diagrams of the Swartskaap Granite

1.6 NEURAS GRANITE

Outcrop of the Neuras Granite is generally poor and locally restricted to areas adjacent to the abandoned Neuras Gold Mine. In outcrop the granite is leucocratic and displays a faintly gneissic texture (Plate 1.6(a)). Alteration of the granite is restricted to areas adjacent to mafic dykes which cross cut the granite. A later quartz porphyry has in turn intruded both the granite and mafic dykes.

In thin section the rock is phaneritic fine- to medium grained with an allotriomorphic-granular texture (Plate 1.6(b)). Deformation has resulted in a gneissic fabric not clearly discernible in thin section. Quartz appears to have recrystallized to form polycrystalline sutured aggregates of strained quartz. In places a mortar texture has developed around the larger quartz grains. Plagioclase (albite) is the dominant feldspar and occurs as euhedral laths which vary in size from 0.2 - 5 mm. Grains characteristically exhibit deformed twin lamellae and alteration to sericite is generally non-pervasive. Perthite is less common and tends to occur as large (< 3 mm) anhedral grains. Epidote is common throughout the granite and in places forms late-stage cross cutting veins. Lesser amounts of chlorite and sphene generally accompany epidote. Calcite occurs as single grains generally less than 1 mm in size, although rims of calcite on other grains were noted sporadically.

Plate 1.6(a): Neuras Granite Outcrop.

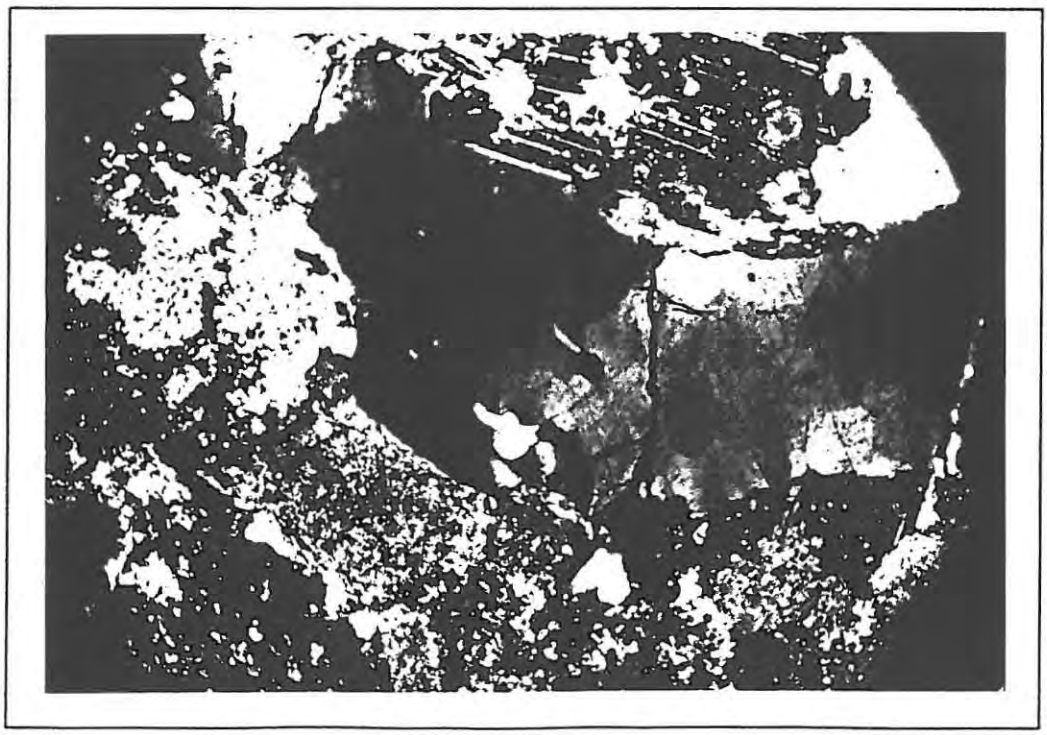

Plate 1.6(b): Photomicrograph of the Neuras Granite. FOV = 3 mm.

1.7 SHEARED MAFIC DYKE SWARM

The Older mafic dykes encountered within the study area are characteristically foliated, altered and laterally impersistent. The dyke swarm has been subjected to deformation during intrusion of granites, and by regional deformation. The average orientation of the dykes is 045° which is sub-parallel to the regional foliation. In outcrop the dykes are greenish - brown in colour and they tend to anastomose and bifurcate along strike before terminating abruptly. Gold mineralization is spatially associated to the contacts of this swarm of dykes.

In thin section the mafic dykes are completely altered to a mass of lepidoblastic chlorite and anhedral epidote - clinozoisite grains (Plate 1.7). Sulphides and oxides form up to 20 % of the rock in places. Brecciated quartz veins have been recemented by microcrystalline quartz indicating more than one generation of fluid activity.

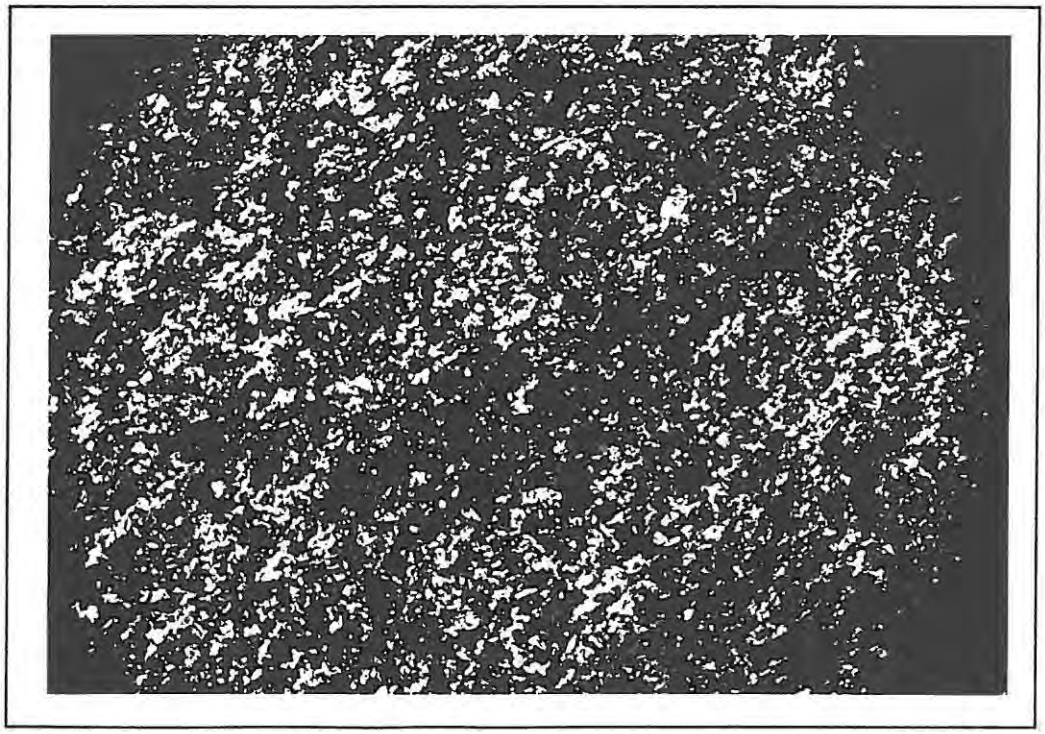

Plate 1.7: Photomicrograph of the sheared mafic dykes.

1.7.1 Geochemistry

The geochemistry of the Sheared Mafic Dyke swarm is discussed in conjunction with the Swartkoppies Mafic Dyke swarm in section 1.9.2.

1.8 HIGH LEVEL GRANITES

A series of quartz-feldspar porphyry dykes, flow-banded quartz porphyry and quartz-feldspar porphyry lithologies is collectively termed the High Level Granite Suite in this study.

1.8.1 Quartz Feldspar Porphyry Dykes

The porphyry dykes in the Neuras Grant are only recorded as having intruded some of the older formations within the study area, namely the Marienhof Formation and Piksteel Granodiorite. Geographically the older formations occur in the northern part of the grant area, consequently outcrop of the porphyry dykes is also restricted to this area. Width of the dykes varies from 0.5 - 5 m and an average trend of 050° was recorded. Dykes are clearly porphyritic in hand specimen and exhibit a marked tectonic fabric (Plate 1.8.1).

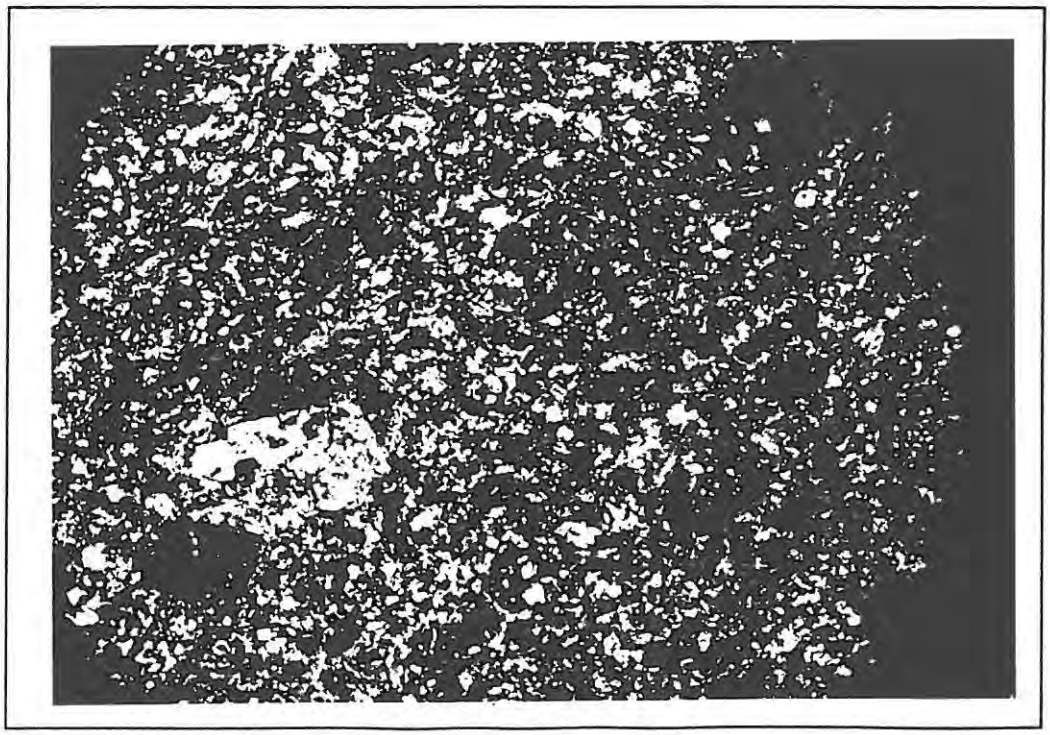

Plate 1.8.1: Photomicrograph of the Quartz porphyry dykes.

In thin section the dykes are holocrystalline and phaneritic, fine grained with an inequigranular porphyritic texture. Anhedral phenocrysts of quartz and K-feldspar (perthite) ranging between 1 and 2 mm in diameter are set in a fine-grained equigranular matrix of quartz, plagioclase (albite), K-feldspar (microcline) and calcite. Sericite, muscovite and epidote occur as accessory phases throughout the rock.

The quartz porphyry dykes have a similar geochemistry to the quartz porphyry. Nowhere in the area studied were quartz porphyry dykes observed to intrude the quartz porphyry. The dykes are suggested to have been derived from the High Level Granite / quartz porphyry and intruded ahead of the main pluton.

1.8.2 Quartz-Feldspar Porphyry

The quartz-feldspar porphyry intrudes almost all the lithologies within the Neuras grant. The unit becomes flow banded towards the contacts of the pluton and in general the texture varies from being equivalent to a granite (equigranular) in the southern portion of the grant to being porphyritic towards the north.

In thin section the quartz-feldspar porphyry texture is similar to the quartz porphyry described above. Phenocrysts of quartz sericitized plagioclase and perthite (1.5 mm on average) are set in a fine (>1 mm) groundmass of quartz and plagioclase. The perthite phenocrysts are generally subhedral and zoned while the quartz grains are anhedral and show strained extinction. Plagioclase phenocrysts are pervasively altered to sericite and epidote. The groundmass consists of a mass of fine-grained quartz and plagioclase. Epidote is a common mineral phase making up 3 - 5% of the rock, in places as late cross cutting veins. Biotite occurs as small sub-parallel laths at grain rims. Acessory opaque oxides appear spatially related with larger concentrations of sericite and epidote.

Interpretation of the textural variation of this unit is as follows. A high level granitic magma is emplaced into the near surface environment where it crystallizes rapidly. The granitic texture observed in the southern area of the grant represents crystallization of the lower portion of the pluton while the upper portions of the pluton are characterised by the porphyritic texture. On one particular outcrop in the

northern sector of the grant an exceptionally porphyritic apophysis was observed to contain rosettes of tourmaline. Boron-rich volatiles are incompatible in granitic melts and will tend to concentrate in the upper cupola regions of a pluton. This particular outcrop could represent a remnant of the highest portions of the granitic intrusion.

1.8.3 Geochemistry

Major element variations of the flow-banded quartz porphyry, quartz-feldspar porphyry and quartz-feldspar porphyry dykes are illustrated in figures 1.8.3(a). The quartz-feldspar porphyry, in general, has higher TiO_2, Fe_2O_3, MgO, K_2O and P_2O_5 and lower Al_2O_3, CaO and Na_2O than the quartz-feldspar porphyry dykes. The flow-banded quartz porphyry appears rather more silicified than the other two porphyries and in general has similar major element concentrations. Alteration resulted in some mobilization of elements as depicted by figure 1.8.3(b), where K_2O, SiO_2 and Zr are plotted against Nb (immobile HFSE). All the porphyries are peraluminous (Figure 1.8.3(c)) and an average A/CNK value of 1.51 results in this suite being classified as an S-type granite according to Chappell and White (1974).

On the tectonic discrimination diagram Nb vs. Y (Pearce et al., 1984) both the quartz-feldspar porphyry and quartz-feldspar porphyry dykes plot within the 'Volcanic Arc' and 'Syn-Collision Granite' fields. The discrimination diagram using Nb + Y vs. Rb, however separates the 'Volcanic Arc' field from 'Syn-Collision Granites'and it is within this latter field that both dykes and quartz porphyries plot (Figure 1.8.3(c)). These High Level Granites were deformed during the Irumide deformation event and hence must have been intruded either before or during the Irumide deformation. A plausible explanation favours the intrusion of the High Level Granites as being related to lower crustal melt formed prior to closure of the rift basins.

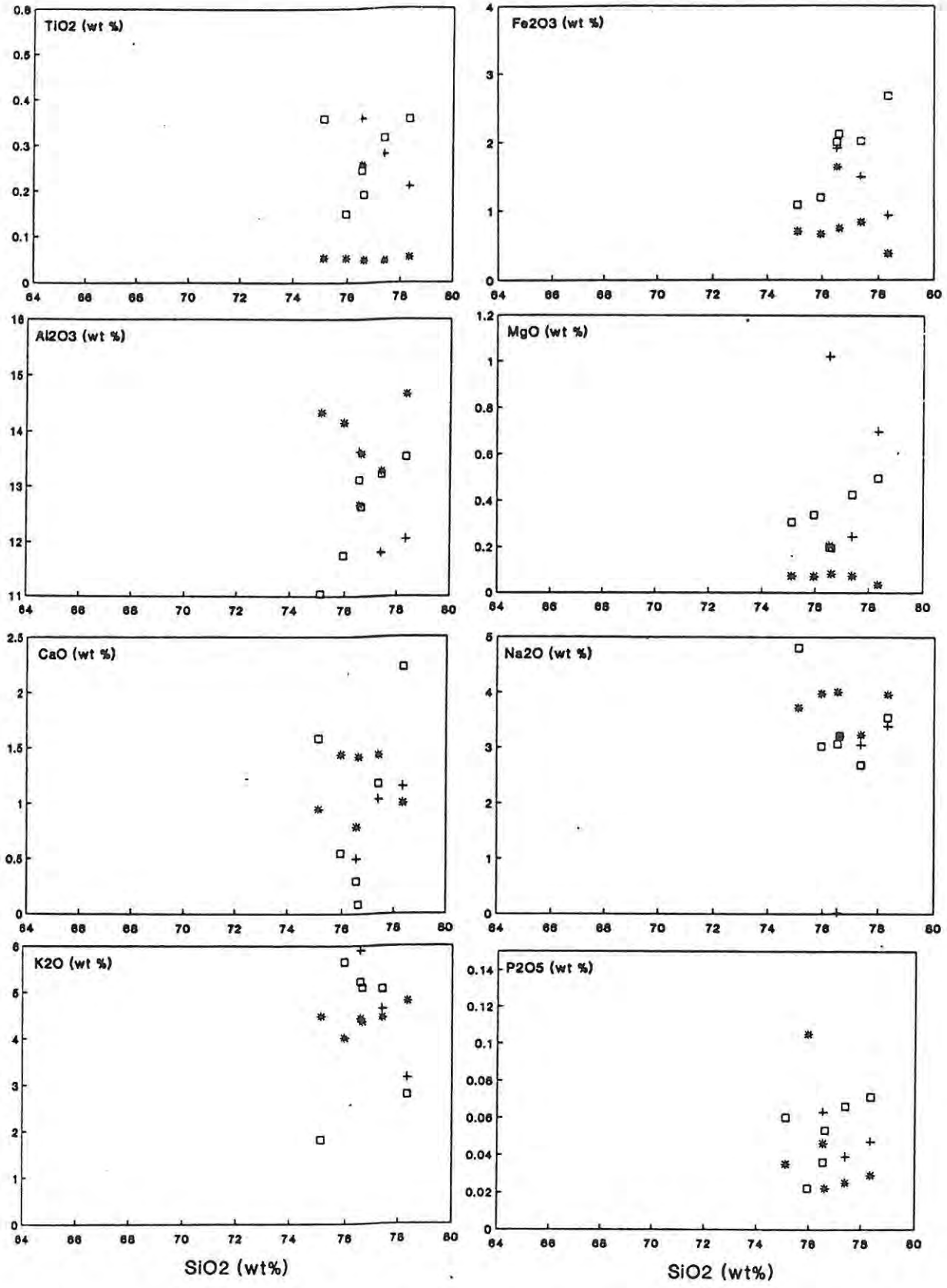

Figure 1.8.3(a): Harker variation diagrams of the High Level Granites.

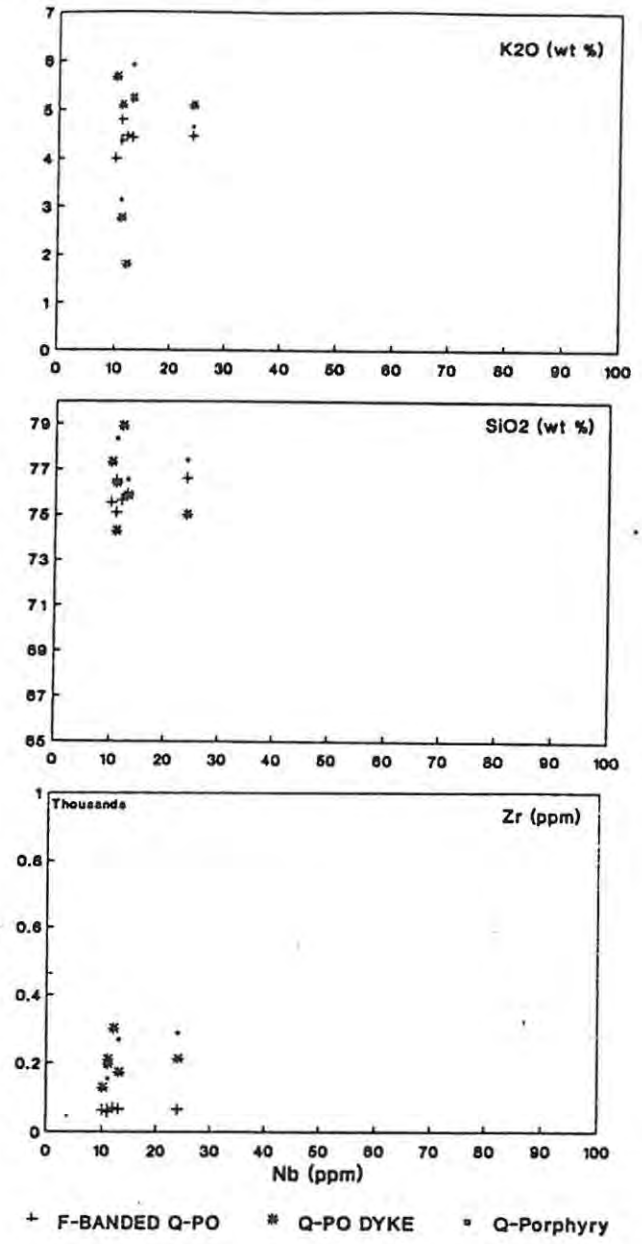

Figure 1.8.3(b): Variations of semi-mobile SiO_2, mobile K_2O and effectively immobile Zr

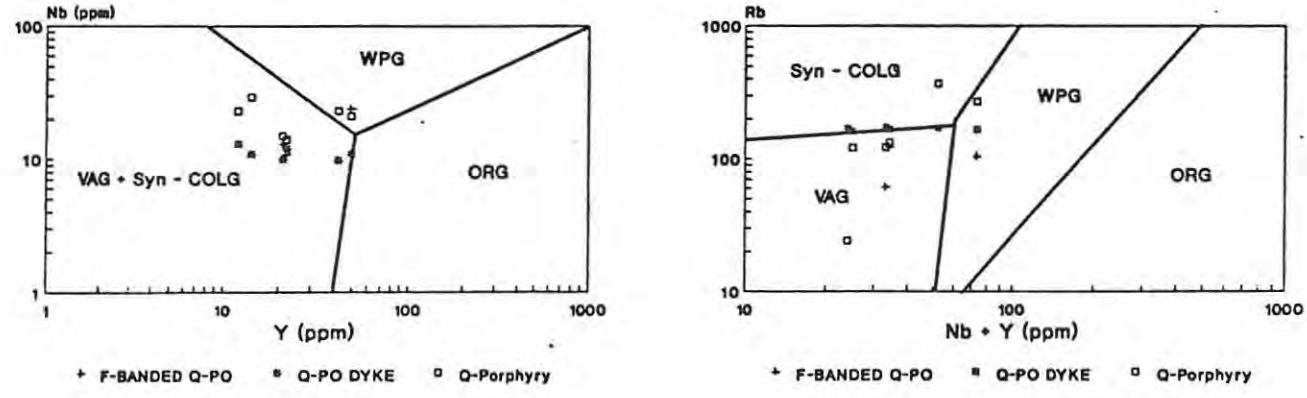

Figure 1.8.3(c): Tectonic discrimination diagrams of the High level Granites.

1.9 SWARTKOPPIES MAFIC SUITE

1.9.1 SWARTKOPPIES MAFIC DYKE SWARM

In the field the Swartkoppies mafic dyke swarm is characterized by its 'fresh' appearance and lack of deformation. Dykes vary in thickness from 1 to 4 m and are laterally more extensive than the Older mafic dyke swarm. No mineralization is associated with this swarm of dykes. The dykes are unfoliated and largely restricted in outcrop to the southern portion of the grant (Plate 1.9.1(a). The age of the dyke swarm, 1030 ± 185 Ma was determined by K/Ar dating (Reid et al., 1988).

Petrographic studies reveal the dykes to be uniform in texture and retrogressively modified by low-grade regional metamorphism. In thin section the rock is holocrystalline and phaneritic fine grained with a hypidiomorphic-inequigranular texture. Relatively larger laths of anhedral clinopyroxene (variably altered to actinolite) are set in a finer grained matrix of acicular plagioclase (albite), chlorite and epidote-clinozoisite after a more calcic plagioclase precursor. An opaque oxide (magnetite) forms 2 - 3% of the rock in places (Plate 1.9.1(b)).

Plate 1.9.1(a): Undeformed Swartkoppie Mafic Dyke.

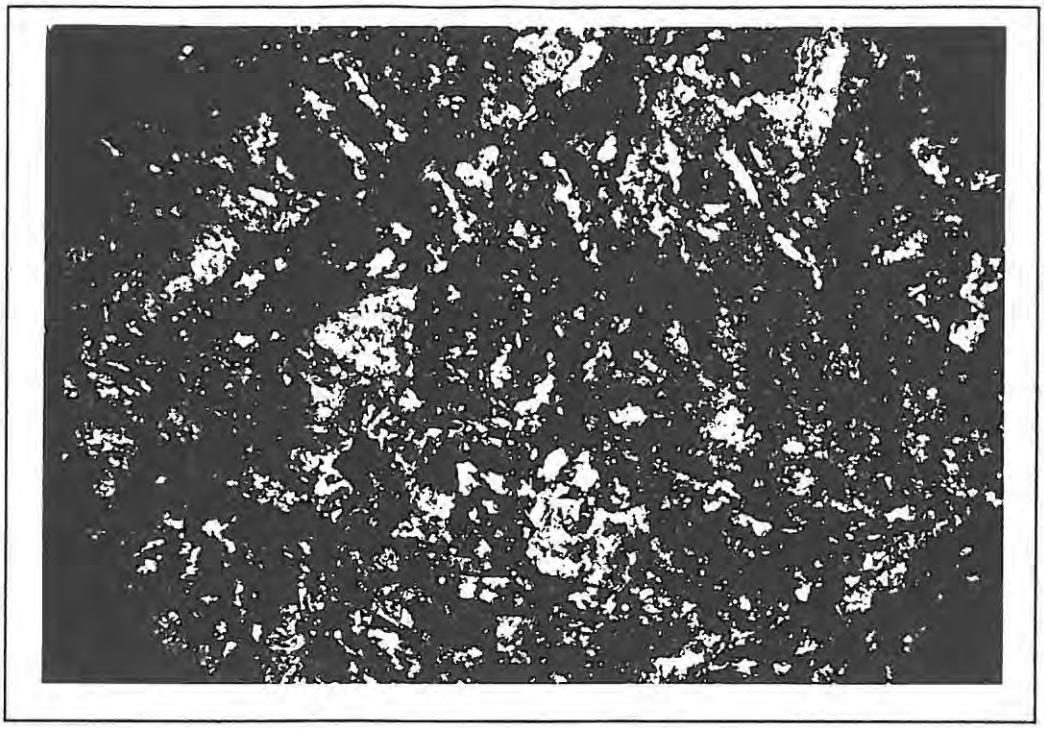

Plate 1.9.1(b): Photomicrograph of a Swartkoppie Mafic Dyke. FOV = 3 mm.

1.9.2 SWARTKOPPIE METAGABBRO

Several quantitatively significant masses of metagabbro are correlated with the later phase of mafic intrusive activity. Similarly to the Swartkoppies dykes, the metagabbros show little deformation and are also retrogressively metamorphosed. It is suggested that the emplacement of these metagabbros occurred concurrently with the emplacement of the Swartkoppies mafic dyke swarm. Surficial weathering of these metagabbros gives rise to the wide spread development of calcrete.

The mineral assemblage of these metagabbros is dominated by hornblende, clinopyroxene (diopsidic), actinolite, epidote - clinozoisite and plagioclase (altered labradorite). In thin section the rock is phaneritic inequigranular with a porphyroblastic texture. Subidioblastic porphyroblasts of hornblende, with an average size of 1 cm, are set in a finer grained matrix of anhedral clinopyroxene and epidote - clinozoisite crystals. Accessory minerals include quartz, apatite and sphene.

1.9.3 Classification of the Mafic Igneous Rocks

Metamorphic recrystallization and varying degrees of hydrothermal alteration have prohibited the proper use of petrographically based classification schemes.

In applying geochemical classification schemes to the metamorphosed mafic rocks, it has been taken into account that mobilization of certain elements, in particular the alkalies (Na_2O & K_2O), has occurred. Many of the classification schemes presently in use tend to use the alkalies, in some form, as the basis for subdivision. Although some of these schemes are presented, one cannot apply them with rigour. The broad characteristics of a suite, i.e., whether it is alkaline, tholeiitic or calc-alkaline, are more helpful than the precise naming of the rocks.

Irvine & Baragar (1971) and Mac Donald (1968) distinguish between alkaline and sub-alkaline volcanic rocks by plotting alkalies against silica. Although plots are widely scattered (Figure 1.9.3(a)) all the mafic rocks plot within the subalkaline field. *Note, that 'Swartkoppie mafics' include dykes and sills.

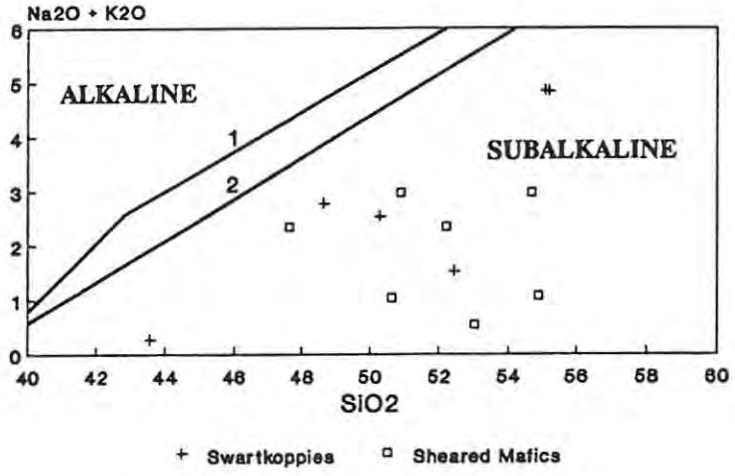

Figure 1.9.3(a): Alkalies versus silica diagram with dividing lines proposed by Irvine and Baragar (1971) and Mac Donald (1969).

Although a wide spread is observed on figure 1.9.3(b), the majority of the samples plot on the boundary between the subalkaline basalt field and the andesite/basalt field.

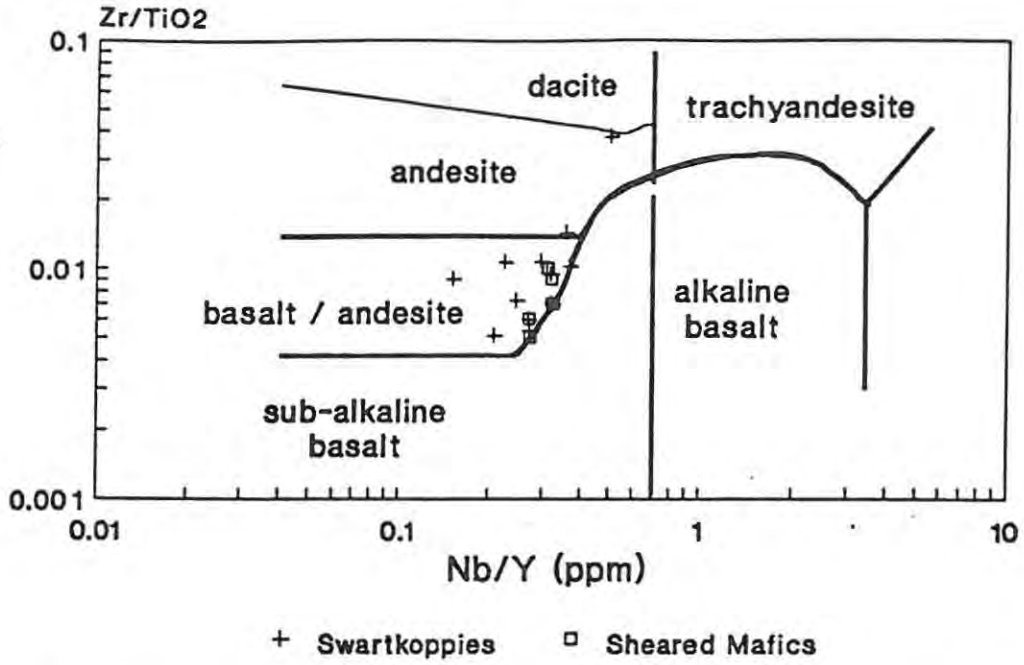

Figure 1.9.3(b): Zr/TiO_2 versus Nb/Y volcanic rock discrimination diagram (after Winchester and Floyd, 1977)

An AFM plot of the mafic rocks again depicts a scatter of points although a slight iron enrichment is evident, a characteristic of tholeiites (Figure 1.9.3(c)).

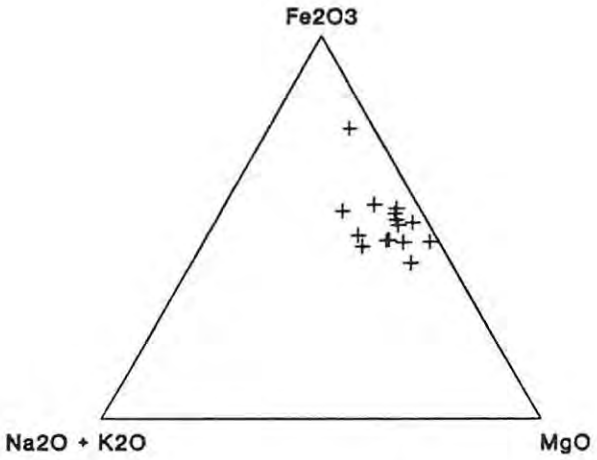

Figure 1.9.3(c): AFM diagram illustrating a slight iron enrichment trend in the Neuras Mafic rocks.

An alternative method for classifying subalkaline volcanic rocks is proposed by Jensen (1976), which makes use of the less mobile major elements Al_2O_3, $Fe_{(total)}$ + TiO_2 and MgO. Figure 1.9.3(d) shows that the Swartkoppie dyke swarm and related gabbros are typical high Fe-tholeiitic basalts while the Older sheared dyke swarm are more Mg-rich.

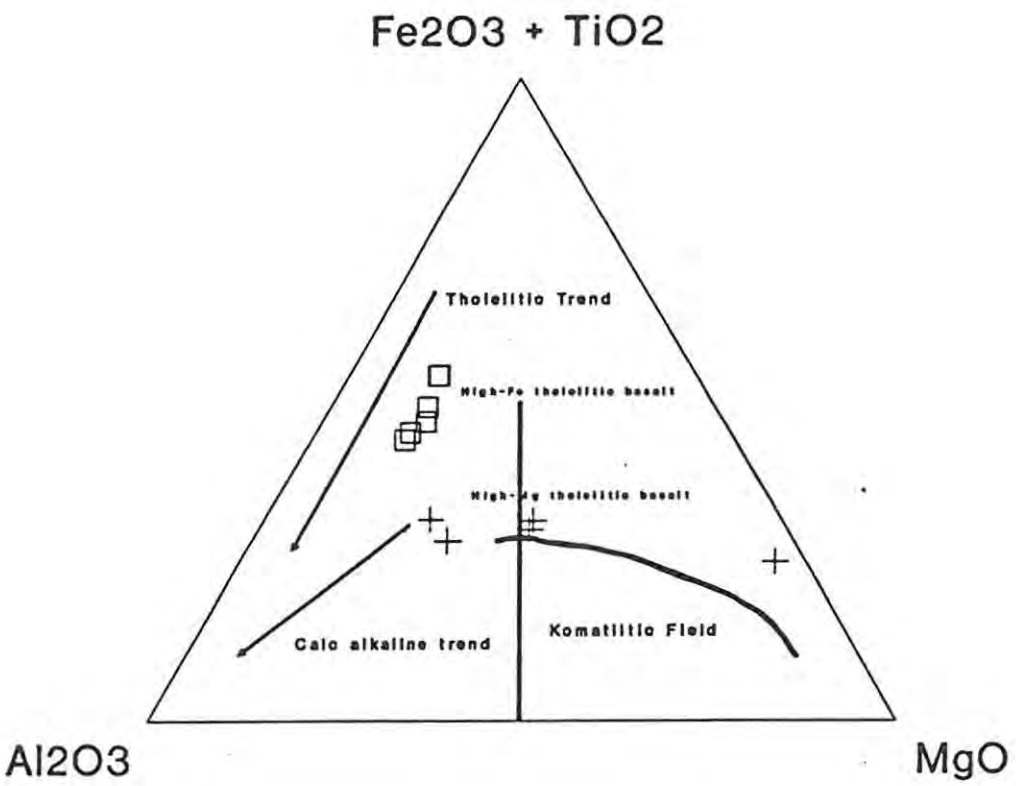

Figure 1.9.3(d): Jensen Cation Plot illustrating the tholeiitic trend in the Dordabis metabasalts (after Jensen 1976).

Plots of immobile trace elements Nb/Y vs. Zr/P_2O_5 (after Winchester & Floyd, 1975) are used to distinguish between oceanic and continental tholeiites and alkali basalts. Unfortunately an overlap exists between the oceanic and continental tholeiites. The mafic rocks of Neuras plot in an area which straddles both the oceanic- and continental-basalt fields (Figure 1.9.3(e)).

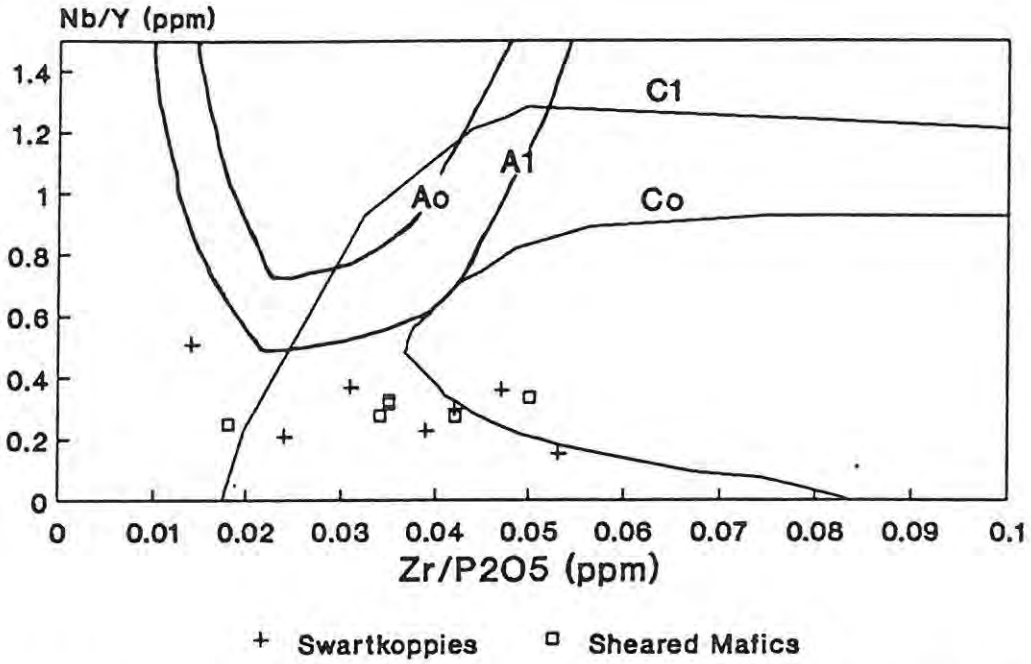

Figure 1.9.3(e): Nb/Y versus Zr/P_2O_5 discrimination diagram where oceanic alkali basalts are represented by fields enclosed by line A_o, continental alkali basalts by A_1, oceanic tholeiitic basalts by C_o and continental tholeiitic basalts by C_1 (after Floyd and Winchester, 1975).

The above plot, Nb/Y vs. Zr/P_2O_5, does not distinguish between oceanic and continental tholeiites, although it does discriminate well between alkali, basaltic and tholeiitic fields. Ternary tectonomagmatic plots, after Pearce (1975 & 1977), of Neuras mafic rocks indicate that they are of continental affinity.

Based on the above-mentioned information it appears that both mafic dyke swarms have characteristics of continental tholeiitic basalts.

1.9.4 Geochemistry of the Neuras Mafic Suites

Whole-rock analyses of sixteen basic intrusives from the Neuras grant area are presented in Appendix 4. Samples are limited to eight from each of the Swartkoppie Mafic dyke swarm and associated metagabbros and eight of the Older Sheared Mafic dyke swarm and associated metagabbros.

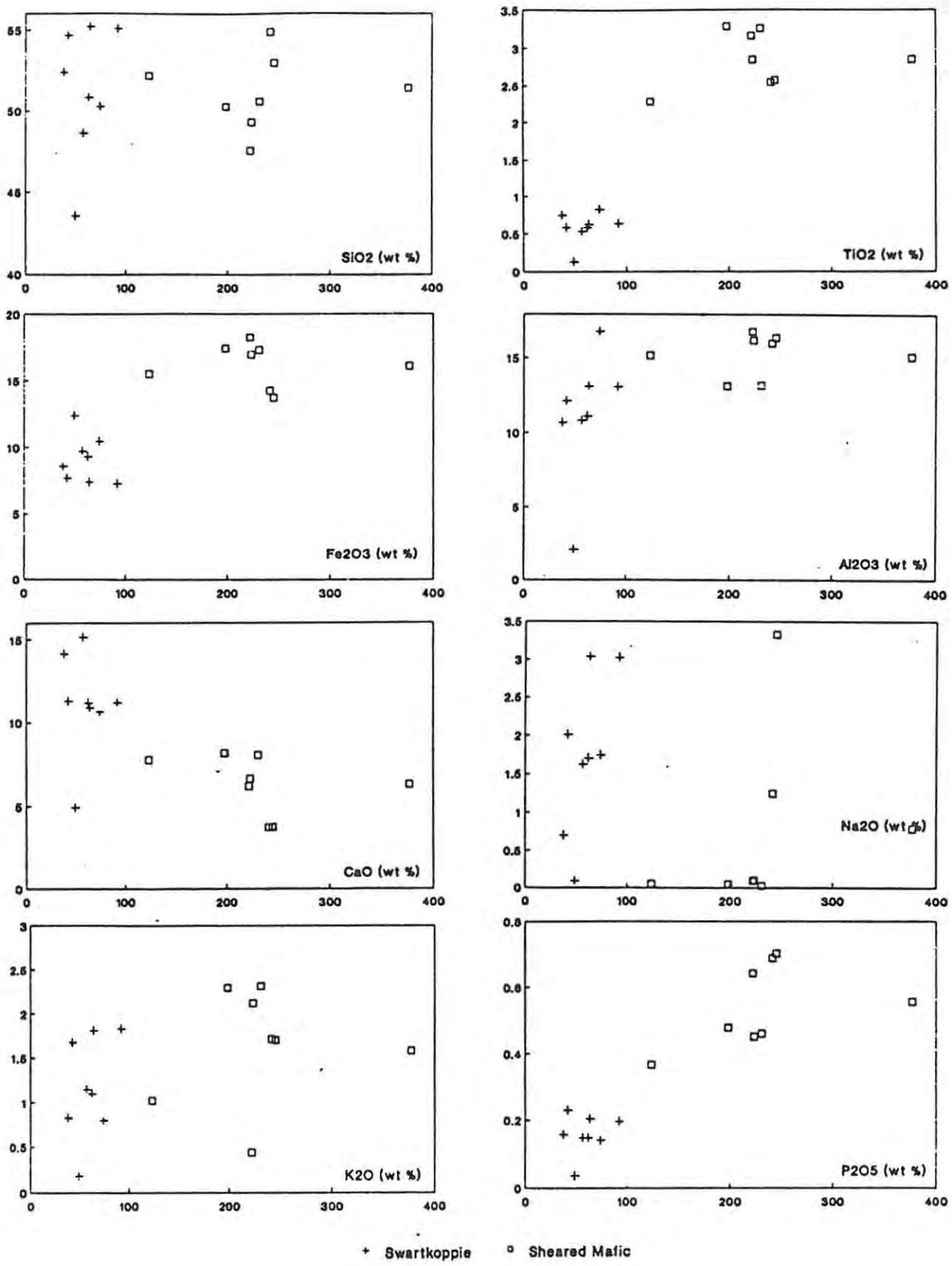

Figure 1.9.4(a): Harker variation diagrams for the Neuras Mafic Rocks.

The rocks analysed have undergone low grade metamorphism, varying degrees of hydrothermal alteration and weathering. It is thus important to distinguish between the effects of alteration and those of primary petrogenetic processes.

Various studies, Pearce et al. (1973, 1977, 1982, 1984), Winchester & Floyd, (1976) have shown zirconium to be relatively immobile during secondary alteration processes. It is however known to be extremely sensitive to primary igneous processes. Based on this knowledge, major-element variations are presented as plots of the various elements vs. Zr (the abscissa). Figures 1.9.4(a) and (b) reveal the major- and trace-element concentrations in relation to Zr for the Neuras mafic rocks.

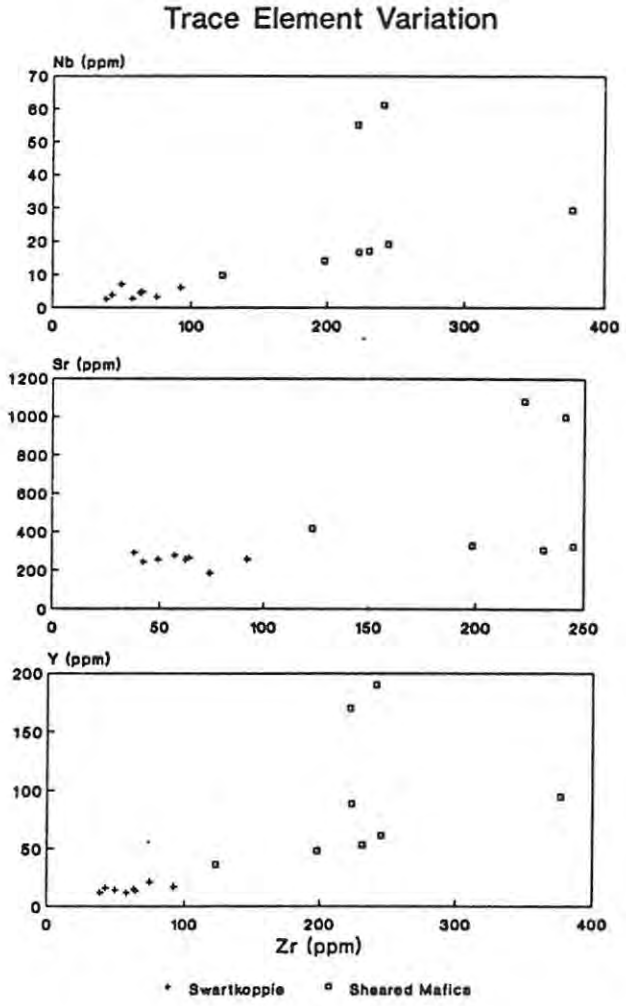

Figure 1.9.4(b): Trace element variation diagrams for the Neuras Mafic Rocks.

TiO_2 and P_2O_5 (Figure 1.9.4(a)) are the only major oxides to exhibit coherent variation trends with Zr. Al_2O_3, MgO and CaO contents generally decrease (Figure 1.9.4(a)) while TiO_2, Fe_2O_3 and P_2O_5 contents increase (Figures 1.9.4(a)). These variations are similar to those which accompany the evolution of a magma by differentiation. Swartkoppie basalts generally have lower TiO_2, Al_2O_3, Fe_2O_3 and P_2O_5 concentrations and higher MgO, CaO and Na_2O contents than the Older basalts. Variation diagrams of the major elements suggest that the older basalts are more differentiated and hence compositionally more evolved than the Swartkoppies metalavas.

The trace element Sr appears to have been mobilized in the older metabasalts and displays no trend when plotted against Zr (Figure 1.9.4(b)). However, in the Swartkoppie basalts it plots as a cluster indicating the relatively unaltered nature of these younger metabasalts. Although Rb is commonly considered as a mobile element, it appears to have acted essentially as an immobile element within the Neuras metabasalts. Nb, Y and Zr all occur in greater concentrations in the Older sheared metabasalts than the Swartkoppie metabasalts indicating that the Older dyke swarm is relatively enriched (more evolved) than the latter.

1.9.5 Petrogenetic Models

Age differences and lack/ or development of deformation in the various mafic suites precludes petrogenetic models such as crustal contamination, magma mixing and fractional crystallization. These are nevertheless evaluated before discussing the proposed model.

If either of the first two models, crustal contamination or magma mixing, are to be attributed to describing the observed variation trends (Figure 1.9.4(a)) then the two mixing components must have compositions that fall at extreme opposite ends of the variation trends. Either of these are unlikely compositions of crustal or mantle melts. Thus the first two models are eliminated as possible petrogenetic processes that resulted in the observed variation trends.

Trace-element and to a lesser degree major-element data for the two mafic dyke swarms plot in distinctly separate fields. Overlapping of variation trends is only observed for mobile elements and is ascribed to secondary alteration processes. The lack of overlapping trends suggests that the two dyke swarms need not necessarily be cogenetic (by fractional

crystallization of a common parent magma). With the limited number of samples analysed it is possible, although not likely, that sampling resulted in a biased data set, which did not include 'intermediate compositions'. Perhaps inclusion of such compositions could have resulted in overlapping variation trends - confirming a fractional crystallization petrogenetic model for the two dyke swarms.

Based on morphology and stratigraphic relations the sheared dyke swarm is conclusively older than the Swartkoppies dyke swarm. An age of 1030 ± 185 Ma is reported for 'post-Gamsberg mafic dykes' (Reid et al., 1988). On the basis of their undeformed character, post-Gamsberg age, similar trends and mafic compositions author concludes that Reid's (op cit.) 'post-Gamsberg dykes' are infact Swartkoppies dykes. No age for the Older sheared mafic dykes is published. However, field relationships show that they intrude the Piksteel Granodiorite (1170 Ma) and are pre-Irumide deformation and pre-Gamsberg (1079 Ma) in age. A time span of between 49 Ma and 140 Ma therefore separated the two swarms. It is suggested that the Older mafic dyke swarm is of Sinclair age and associated with initial Irumide rifting and the younger Swartkoppies dyke swarm reflects mantle melting - possibly as a result of incipient Damara rifting?

The Older sheared dyke swarm with its higher incompatible element concentrations may have resulted from initial partial melting of a 'normal' (undepleted) mantle. Melting occurred in response to decompression of the mantle as it rose into higher levels as a result of crustal thinning during the Irumide. Incompatible elements, such as TiO_2, Nb, Zr and Y may have been extracted from the mantle by this initial partial melt which intruded the attenuated crust along trends which are parallel to the rift axis. A fairly lengthy period of time elapsed (between 49 and 140 Ma) in which no extraction of mantle material occurred. Melting of the lower crust which resulted in emplacement of the various granites may have took place during this time. Closure of the rift resulted in deformation and thickening of the crust. The fact that the Damara Orogen is situated partly on and adjacent to the Irumide lithologies and assumes a simmilar trend suggests that the crust was weakened by the initial Irumide rifting. Incipient rifting of the Damara is suggested to have occurred as early as between 900 and 1000 Ma ago (Martin, 1965; Martin and Poroda, 1977; Poroda, 1979). Again partial melting of the mantle may have occurred resulting in a melt relatively depleted in incompatible elements compared to the initial melt formed during Irumide rifting. The emplacement of the second generation melt was structurally controlled by the pre-existing Irumide fabric.

1.10 GAMSBERG GRANITE SUITE

The Uitdraai and Kobos Granite plutons are included within the Gamsberg Granite Suite in this study. Both these granites are undeformed and have intruded the older rocks post-tectonically. Geochemically both granites are similar and are discussed in more detail in the following section.

1.10.1 Uitdraai Granite

The Uitdraai Granite pluton has an elongate shape within the area studied. The granite is melanocratic, medium to coarse grained and undeformed (Plate 1.10.1(a)). The northern boundary of the granite borders on a thrust and appears to be slightly tectonised. The thrust fault and shear zone post-date the emplacement of the pluton and affect its northern margin.

In thin section the rock is phaneritic coarse-grained and exhibits a hypidiomorphic-granular texture. Large (5-7 mm) subidioblastic perthite grains, the dominant mineral, commonly contain exolved albite laths. Anhedral quartz grains along with stumpy laths of albite constitute the dominant minerals in the rock. Unlike the older granites, plagioclase is essentially unaltered in the Uitdraai pluton. Chlorite is the only ferromagnesian mineral phase and is commonly associated with an accessory opaque oxide (magnetite). Epidote and zircon also form accessory phases. The Uitdraai Granite differs petrographically from the Kobos Granite in that it lacks sphene and biotite (Plate 1.10.1(b)).

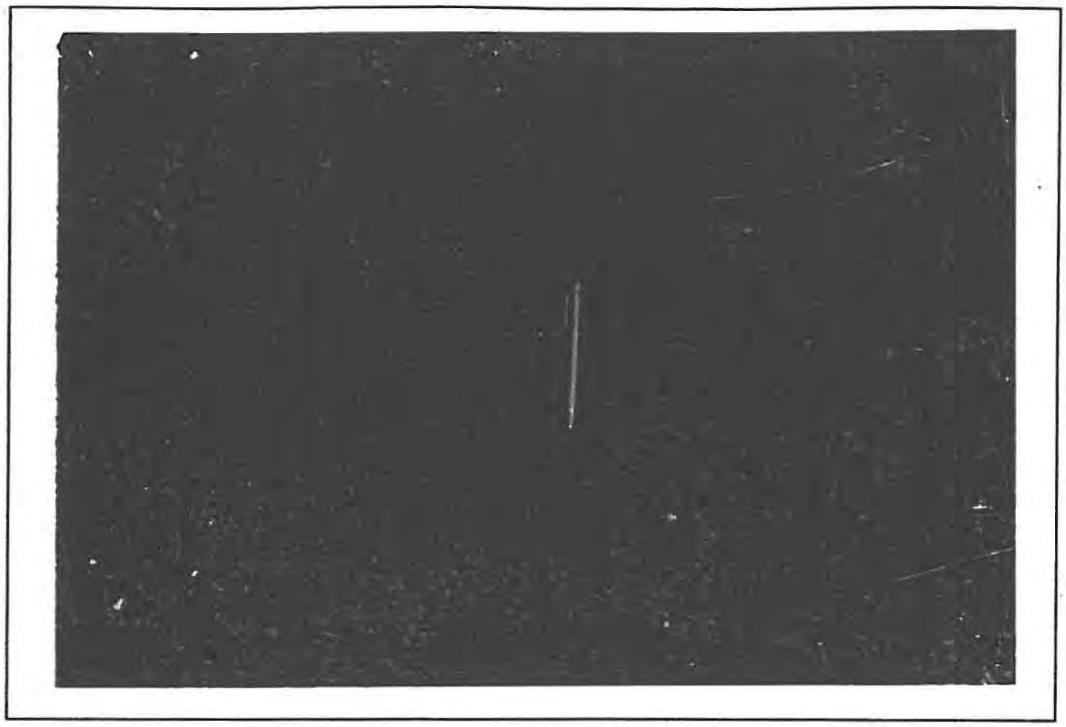

Plate 1.10.1(a): Uitdraai Granite outcrop.

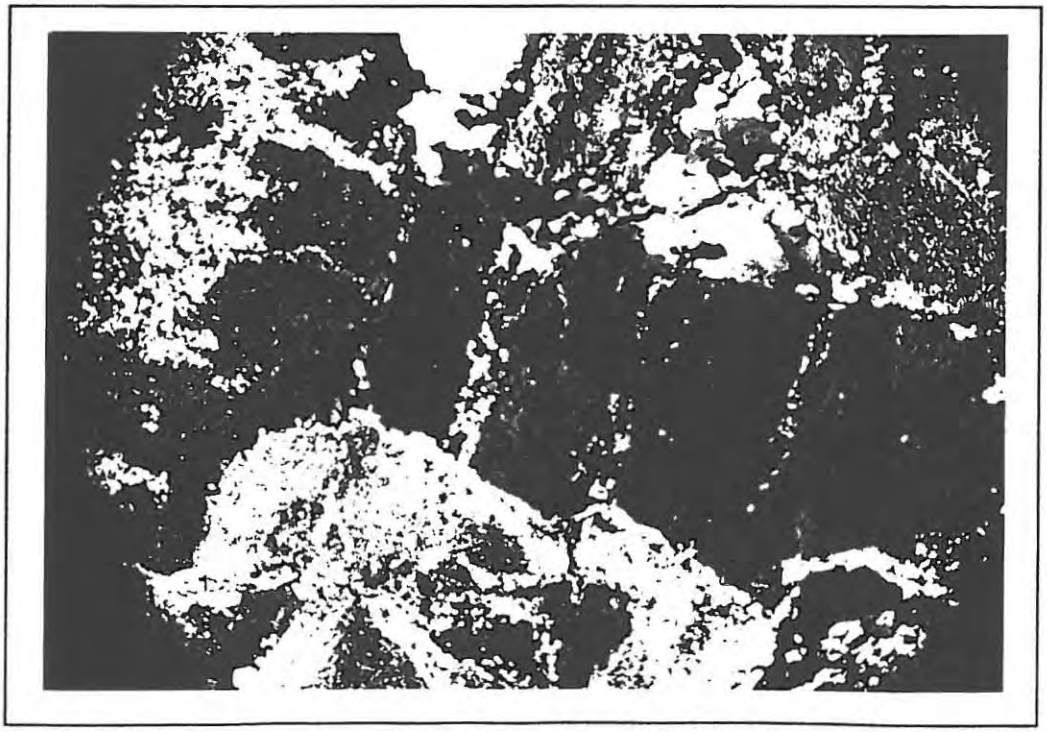

Plate 1.10.1(b): Photomicrograph of the Uitdraai Granite. FOV = 3 mm.

1.10.2 Kobos Granite

The Kobos Granites occur in the southern most part of the study area. Their undeformed nature support the proposal that the Gamsberg Suite represents the youngest magmatic event in the area studied. Xenoliths within the Kobos plutons range in composition from quartz porphyry to schist and metagabbro. Intrusive breccias are formed at the contact of the Kobos Granite front (Plate 1.10.2(a)).

In thin section the Kobos Granite is hypidiomorphic and inequigranular. K-feldspar (perthite) is the dominant mineral phase and subhedral crystals range from 5 - 8 mm in size. Plagioclase (albite) is the next most dominant mineral and is variably altered to sericite. Anhedral quartz grains are typically 5 mm or less in size, they exhibit strained extinction and have sutured boundaries. Platy laths of biotite are abundant while lesser amounts of chlorite and hornblende make up the remainder of the ferromagnesian minerals. Accessory minerals include euhedral sphene and magnetite (Plate 1.10.2(b)).

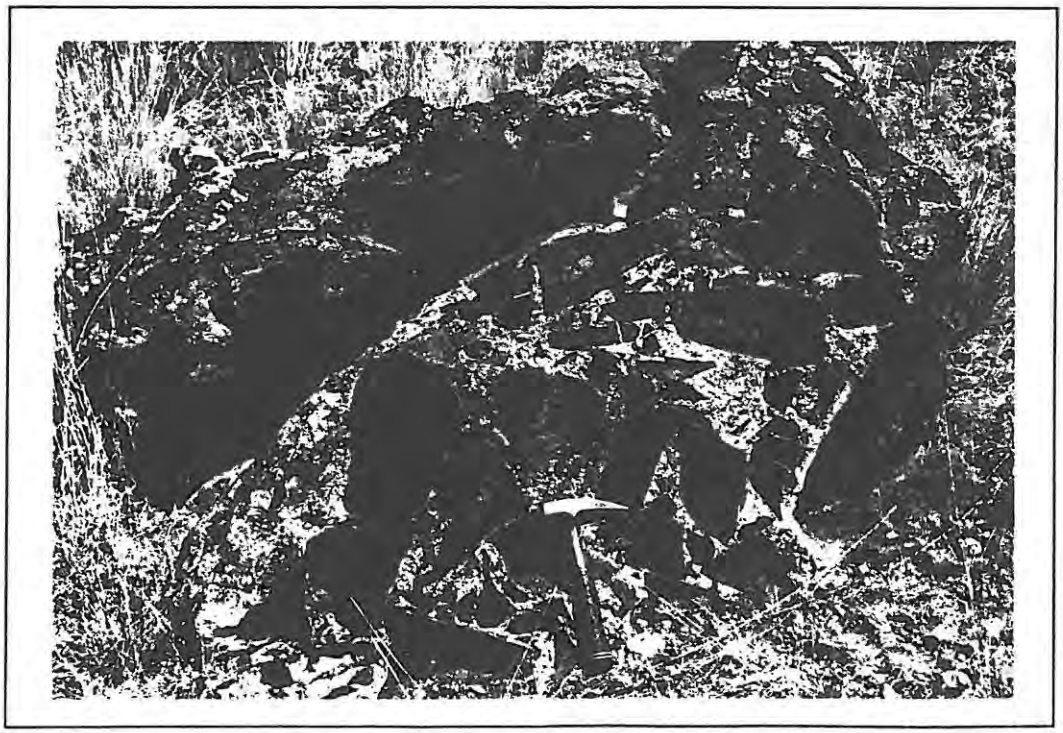

Plate 1.10.2(a): Intrusive breccia contact of the Kobos Granite.

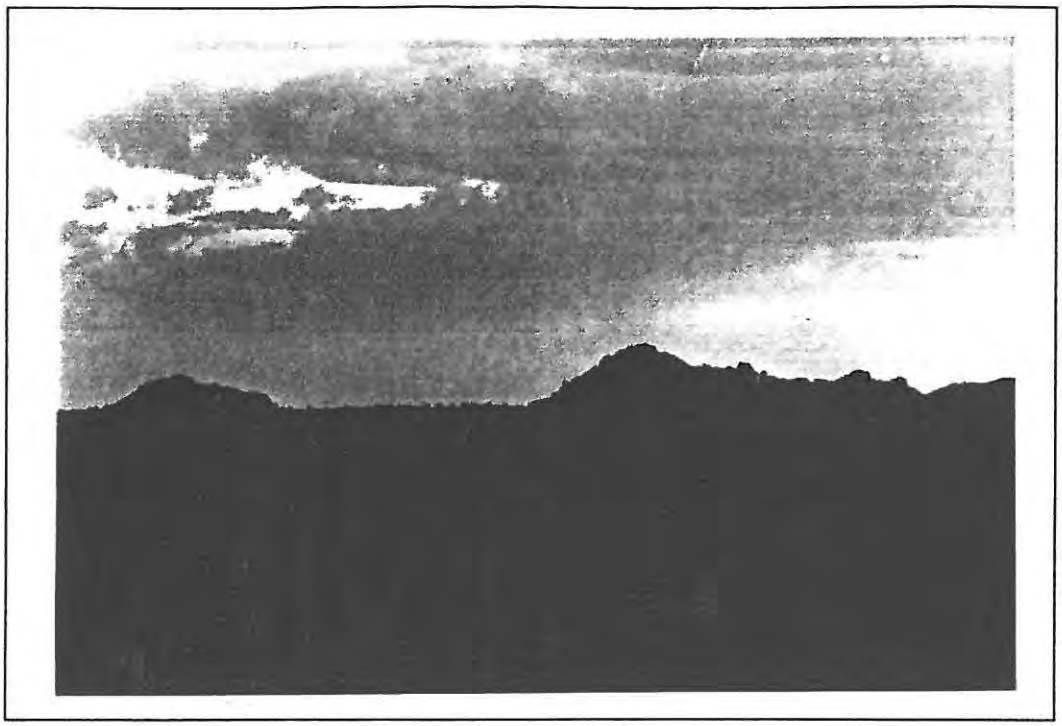

Plate 1.10.2(b): Kobos Granite outcropping in the southern portion of the grant Neuras Grant.

Plate 1.10.2(b): Photomicrograph of the Kobos Granite. FOV = 3 mm.

1.10.3 Geochemistry

The relatively linear plots depicted on Harker variation diagrams (Figure 1.10.3(b)) probably reflect original magmatic processes. MgO, CaO and K_2O plots show variations which are attributed to regional low-grade metamorphism. Both Gamsberg granitoids are peraluminous with average A/CNK values of about 1.45 classifying them as S-type granitoids. The low $^{87}Sr/^{86}Sr$ initial ratios of between 0.700 and 0.702, reported by Siefert (1986a & b) suggest lower crustal sources for this magmatism.
The two plutons, Uitdraai and Kobos, are easily distinguishable on their relative Sr and Rb contents as shown in figure 1.10.3(a). The Kobos plutons consistently have higher Sr and Rb values than the Uitdraai pluton, while Zr is virtually identical for both granites.

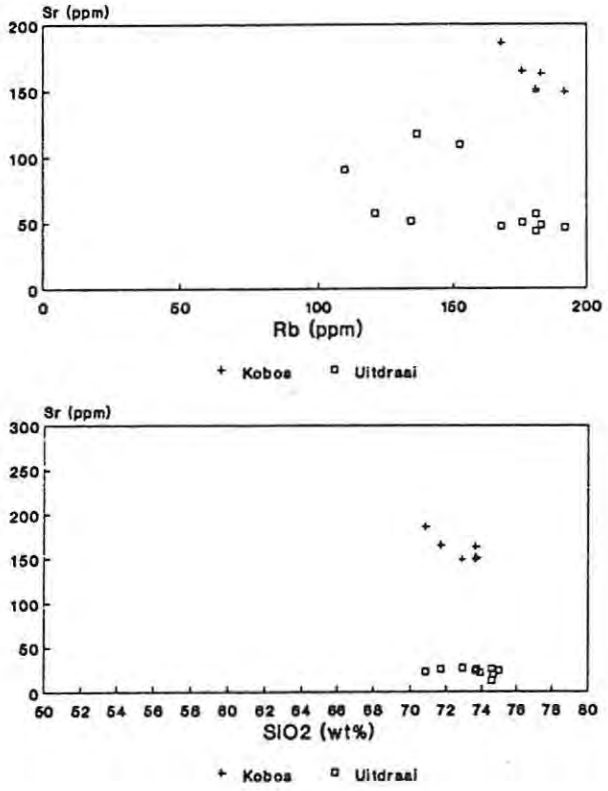

Figure 1.10.3(a): Sr versus SiO_2 and Rb.

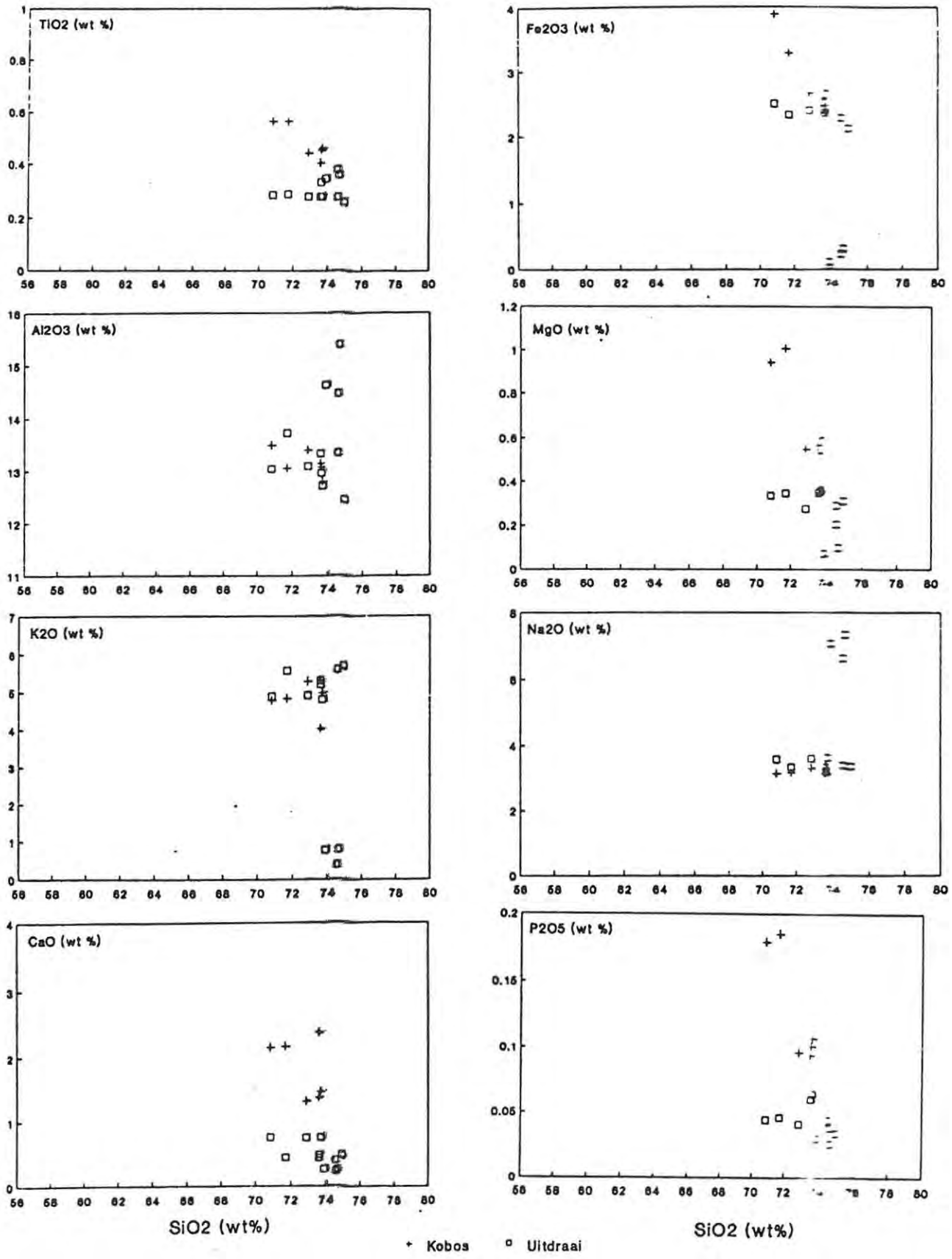

Figure 1.10.3(b) Harker variation diagrams of the Gamsberg Granites

In tectonic discrimination diagrams of Pearce et al. (1984), the Uitdraai pluton consistently plots within the 'Within Plate Granite' field while the Kobos Granite plots on the boundary between the 'Volcanic Arc Granites' and 'Within Plate Granites' fields (Figure 1.10.3(c)). As mentioned earlier, the Gamsberg plutons, within the area studied, are undeformed and thus must have intruded after the Irumide deformation. Ages of some other Gamsberg Plutons in the vicinity yielded ages of 1079 ± 29 Ma (Reid et al., 1988), which roughly correlates with the incipient development of the Damara rift partly over and adjacent to the Irumide Belt.

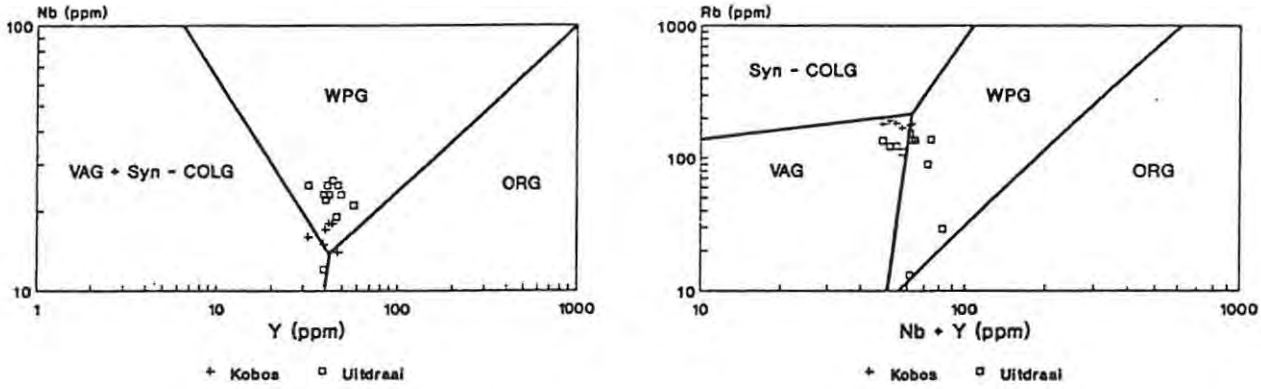

Figure 1.10.3(c): Tectonic discrimination diagrams of the Gamsberg Granites.

APPENDIX 2 : X-RAY FLUORESCENCE SPECTROMETRY

Whole rock analyses were carried out by XRF wavelength dispersive techniques using a Phillips 1410 X-ray spectrometer. The major elements, apart from sodium, were determined using duplicate fusion discs, prepared according to the method of Norrish and Hutton (1969). All iron was determined as Fe_2O_3. Sodium and trace elements were determined from pressed powder pellets. Mass absorbtion coefficients used in the processing of trace element data were derived from major element data using Heindrich's (1966) values.

H_2O and loss on ignition (LOI) were determined gravimetrically by heating samples for eight hours at 110° and 95° respectively. Standard departmental computer programs were used to process data. Corrections were made for deadtime, background, instrumental drift, spectral line interference and position factors. Details of analytical conditions for major and trace elements are provided in Table A. Working curves were calculated using the international and in-house rock standards presented in Table B.

TABLE A. X-RAY FLOURESCENCE ANALYTICAL CONDITIONS

ELEMENT	EMISSION LINE	TUBE	kV	mA	CRYSTAL	TIME	COUNTER	COLLIMATOR	SPECIMEN
Si	K_α	Cr	55	40	PET	40	FLOW	COARSE	FUSION DISC
Ti	K_α	Cr	55	40	LIF(200)	10	FLOW	FINE	FUSION DISC
Al	K_α	Cr	55	40	PET	40	FLOW	COARSE	FUSION DISC
Fe	K_α	Cr	55	40	LIF(200)	20	FLOW	FINE	FUSION DISC
Mn	K_α	Cr	55	40	LIF(200)	20	FLOW	COARSE	FUSION DISC
Mg	K_α	Cr	55	40	TLAP	100	FLOW	FINE	FUSION DISC
Ca	K_α	Cr	55	40	LIF(200)	10	FLOW	FINE	FUSION DISC
Na	K_α	Cr	55	40	TLAP	100	FLOW	FINE	POWDER PELLET
K	K_α	Cr	55	40	LIF(200)	10	FLOW	FINE	FUSION DISC
P	K_α	Cr	55	40	Ge	20	FLOW	COURSE	FUSION DISC
Nb	K_α	W	55	40	LIF(200)	200	SCINT	FINE	POWDER PELLET
Zr	K_α	W	55	40	LIF(200)	200	SCINT	FINE	POWDER PELLET
Y	K_α	W	55	40	LIF(200)	200	SCINT	FINE	POWDER PELLET
Sr	K_α	W	55	40	LIF(200)	200	SCINT	FINE	POWDER PELLET
Rb	K_α	W	55	40	LIF(200)	200	SCINT	FINE	POWDER PELLET

TABLE B. International and in-house rock standards used

ELEMENTS	SAMPLES
Major Elements	GSP-1, AGV-1, DTS-1, BCR-1
	PCC-1, JG-1, NIM-D, NIM-N
Na	BCR-1, G-2, GSP-1, AGV-1
	JB-1
Nb, Zr, Y, Sr, Rb	GSP, BCR, BHVO, AGV, RGM

APPENDIX 3 : WHOLE ROCK AND SELECTED TRACE ELEMENT GEOCHEMICAL ANALYSES.

Note

Major element analyses within 1% of 100% total are recalculated to 100% while analyses within 0.5% of the total 100% are not recalculated.

Table 3.1. Geochemical Analyses of the Neuras Igneous Rocks

	FLOW-BANDED QUARTZ PORPHYRY			Quartz Porphyry Dykes					
	DWN127	DWN156	FTN135	DWN101	DWN98	DWN140	DWN101A	DWN98A	DWN140A
SiO2	78.34	76.53	77.39	75.09	75.93	76.61	75.63	75.53	76.51
TiO2	0.21	0.36	0.28	0.05	0.26	0.05	0.05	0.05	0.05
Al203	12.05	13.63	11.80	14.65	12.67	13.27	14.32	14.14	13.58
Fe203	0.93	1.91	1.49	0.38	1.63	0.83	0.70	0.66	0.74
MnO	0.05	0.07	0.04	0.02	0.05	0.05	0.03	0.03	0.06
MgO	0.70	1.02	0.25	0.03	0.21	0.07	0.07	0.07	0.08
CaO	1.15	0.50	1.04	1.00	0.79	1.43	0.95	1.43	1.41
Na20	3.39	0.02	3.05	3.96	4.01	3.22	3.72	3.98	3.20
K20	3.14	5.90	4.63	4.79	4.42	4.44	4.47	4.00	4.36
P205	0.05	0.06	0.04	0.03	0.05	0.03	0.04	0.11	0.02
TOTAL	100.00	100.00	100.00	100.00	100.00	100.00	99.97	100.00	100.00
Nb	11.00	13.00	24.00	12.00	10.00	11.00	13.00	9.80	11.00
Zr	153.00	269.00	289.00	58.00	65.00	65.00	68.00	62.00	64.00
Y	22.00	21.00	49.00	12.00	42.00	14.00	16.00	11.00	13.00
Sr	264.00	120.00	179.00	153.00	202.00	145.00	160.00	156.00	140.00
Rb	61.00	122.00	104.00	172.00	166.00	166.00	169.00	170.00	161.00

	QUARTZ PORPHYRY				IGNIMBRITES					
	DWN125	DWN128	DWN112	DWN119	DWN123	DWN103	DWN170	DWN171	DWN106	DWN157	DWN90
SiO2	74.28	75.82	74.99	78.90	77.30	76.39	78.25	76.71	75.61	73.36	74.631
TiO2	0.36	0.25	0.32	0.36	0.15	0.19	0.13	0.12	0.14	0.30	0.314
Al203	13.53	13.12	13.21	11.04	11.75	12.63	11.77	12.44	12.08	13.78	13.372
Fe203	2.67	2.00	2.02	1.08	1.19	2.12	1.10	1.56	1.65	2.11	2.034
MnO	0.04	0.02	0.06	0.05	0.04	0.04	0.04	0.08	0.13	0.09	0.058
MgO	0.50	0.20	0.42	0.31	0.34	0.20	0.05	0.14	0.10	0.27	0.177
CaO	2.23	0.29	1.17	1.58	0.55	0.08	0.09	0.27	1.48	0.78	0.477
Na20	3.54	3.06	2.69	4.81	3.02	3.21	2.99	3.64	4.31	3.87	3.281
K20	2.77	5.21	5.06	1.81	5.65	5.09	5.54	5.01	4.47	5.40	5.578
P205	0.07	0.04	0.07	0.06	0.02	0.05	0.05	0.04	0.04	0.05	0.079
TOTAL	99.98	100.00	100.00	100.00	100.00	100.00	100.00	100.00	100.00	100.00	100.001
Nb	14.00	15.00	21.00	23.00	23.00	29.00	26.00	27.00	26.00	22.30	23
Zr	209.00	172.00	212.00	300.00	128.00	195.00	174.00	174.00	179.00	373.00	333
Y	37.00	31.00	47.00	40.00	72.00	152.00	60.00	60.00	51.00	55.00	43
Sr	128.00	76.00	100.00	185.00	23.00	56.00	33.00	35.00	36.00	46.00	37
Rb	121.00	132.00	269.00	24.00	367.00	120.00	162.00	147.00	170.00	130.00	121

	RHYOLITES				PIKSTEEL GRANODIORITE					
	DWN104	DWN172	DWN169	DWN167	DWN-174	FTN42	DWN120	DWN100A	DWN100B	DWN115	DWN130
SiO2	75.83	76.54	75.42	77.25	76.71	67.43	67.67	65.81	66.28	67.43	67.726
TiO2	0.39	0.10	0.36	0.38	0.35	0.45	0.46	0.62	0.62	0.44	0.443
Al2O3	14.26	14.11	15.39	14.45	14.62	16.68	16.21	16.78	16.54	16.08	16.575
Fe2O3	1.00	0.25	0.31	0.24	0.12	3.86	4.01	4.55	4.64	4.44	3.936
MnO	0.05	0.03	0.01	0.00	0.01	0.06	0.08	0.10	0.09	0.07	0.09
MgO	0.20	0.07	0.10	0.24	0.07	1.40	1.39	1.59	1.48	1.23	1.457
CaO	0.49	0.57	0.28	0.39	0.26	2.56	3.18	3.32	3.25	3.32	3.331
Na2O	6.42	7.61	7.32	6.63	7.07	4.04	3.51	3.32	3.27	3.65	3.154
K2O	1.30	0.66	0.78	0.38	0.78	3.36	3.34	3.72	3.63	2.81	2.927
P2O5	0.07	0.05	0.03	0.04	0.03	0.17	0.16	0.20	0.20	0.16	0.161
TOTAL	100.00	100.00	100.00	100.00	100.00	100.00	100.00	100.00	100.00	99.62	99.8
Nb	24.00	7.30	21.00	12.00	19.00	11.00	12.00	14.00	14.00	10.00	10
Zr	303.00	180.00	269.00	236.00	97.00	201.00	185.00	220.00	213.00	170.00	189
Y	5.70	11.00	8.90	7.20	26.00	29.00	26.00	43.00	32.00	27.00	29
Sr	133.00	116.00	109.00	90.00	117.00	581.00	621.00	558.00	566.00	691.00	610
Rb	52.00	21.00	29.00	13.00	89.00	112.00	100.00	110.00	112.00	103.00	111

	KOBOS GRANITE						SWARTSKAAP GRANITE			
	DWN132	DWN130	DWN118	DWN131	DWN131A	DWN130A	DWN134	DWN141	DWN113	DWN114A
SiO2	73.58	73.69	72.89	70.81	71.70	73.62	73.15	73.86	73.56	73.606
TiO2	0.41	0.46	0.44	0.57	0.56	0.45	0.35	0.34	0.47	0.495
Al2O3	13.15	12.79	13.40	13.50	13.05	13.07	14.18	14.02	13.24	13.431
Fe2O3	2.37	2.70	2.66	3.89	3.28	2.59	2.48	2.37	2.78	2.857
MnO	0.05	0.09	0.08	0.50	0.04	0.06	0.06	0.02	0.07	0.028
MgO	0.57	0.60	0.55	0.94	1.01	0.53	0.38	0.39	0.48	0.347
CaO	1.37	1.46	1.31	2.14	2.16	2.37	1.01	0.50	1.66	1.242
Na2O	3.16	3.11	3.30	3.14	3.17	3.17	3.80	4.42	2.43	2.874
K2O	5.31	4.99	5.28	4.79	4.84	4.03	4.51	4.02	5.16	4.977
P2O5	0.09	0.11	0.10	0.18	0.19	0.10	0.08	0.05	0.14	0.143
TOTAL	100.05	100.00	100.00	100.45	100.00	100.00	100.00	100.00	100.00	100
Nb	18.00	16.00	18.00	17.00	14.00	15.00	15.00	12.50	18.00	16
Zr	243.00	269.00	290.00	284.00	258.00	248.00	245.00	203.00	268.00	229
Y	42.00	32.00	44.00	40.00	47.00	39.00	18.00	31.00	50.00	34
Sr	149.00	151.00	149.00	186.00	165.00	163.00	198.00	97.00	106.00	119
Rb	192.00	181.00	181.00	168.00	176.00	183.00	134.00	106.00	206.00	170

UITDRAAI GRANITE										
	DWN162	DWN163	DWN163	DWN163	DWN162	DWN164	DWN160	DWN161	DWN169	DWN167
SiO2	74.55	74.97	74.66	74.56	73.88	74.69	74.55	75.25	75.42	77.29
TiO2	0.28	0.28	0.28	0.29	0.29	0.33	0.28	0.26	0.36	0.38
Al2O3	13.33	12.71	13.09	13.04	13.72	12.96	13.34	12.45	15.39	14.45
Fe2O3	2.41	2.36	2.40	2.50	2.33	2.53	2.28	2.12	0.31	0.24
MnO	0.06	0.07	0.00	0.02	0.05	0.05	0.03	0.05	0.01	0.00
MgO	0.35	0.36	0.27	0.33	0.34	0.35	0.29	0.31	0.10	0.20
CaO	0.44	0.76	0.75	0.75	0.44	0.49	0.23	0.49	0.26	0.39
Na2O	3.22	3.62	3.60	3.58	3.34	3.34	3.39	3.36	7.34	6.63
K2O	5.30	4.81	4.91	4.89	5.56	5.20	5.58	5.68	0.78	0.38
P2O5	0.06	0.06	0.04	0.04	0.05	0.06	0.04	0.03	0.03	0.04
TOTAL	100.00	100.00	100.00	100.00	100.00	100.00	100.00	100.00	100.00	100.00
Nb	23.00	25.00	26.00	22.00	25.00	23.00	25.00	23.00	19.00	12.00
Zr	267.00	274.00	280.00	232.00	273.00	236.00	301.00	266.00	97.00	7.20
Y	41.00	49.00	46.00	39.00	57.00	42.00	46.00	49.00	26.00	237.00
Sr	46.00	43.00	56.00	47.00	50.00	48.00	57.00	51.00	117.00	90.00
Rb	121.00	134.00	136.00	110.00	152.00	123.00	135.00	137.00	89.00	13.00

Swartkoppie Mafic Rocks

	DWN101	DWN151	DWN153	DWN109	DWN95	DWN95A	DWN-110	DWN-111
SiO2	43.56	52.45	48.65	50.29	55.09	55.20	50.87	54.69
TiO2	0.13	0.75	0.53	0.82	0.64	0.62	0.58	0.58
Al2O3	2.10	10.69	10.83	16.83	13.08	13.12	11.11	12.14
Fe2O3	12.38	8.57	9.71	10.45	7.25	7.37	9.29	7.67
MnO	0.18	0.19	0.20	0.17	0.19	0.20	0.19	0.19
MgO	36.40	11.53	12.02	8.12	7.52	7.56	13.86	9.53
CaO	4.94	14.14	15.15	10.64	11.19	10.88	11.16	11.29
Na2O	0.09	0.70	1.63	1.74	3.02	3.03	1.70	2.01
K2O	0.19	0.83	1.15	0.80	1.84	1.81	1.10	1.68
P2O5	0.04	0.16	0.15	0.14	0.20	0.21	0.15	0.23
TOTAL	100.00	100.00	100.00	100.00	100.00	100.00	100.00	100.00
Nb	7.10	2.50	2.70	3.20	6.10	4.80	4.40	3.90
Zr	49.00	38.00	57.00	74.00	92.00	64.00	62.33	42.13
Y	14.00	12.00	12.00	21.00	17.00	13.00	14.83	15.78
Sr	254.00	291.00	276.00	183.00	258.00	264.00	254.33	243.55
Rb	35.00	7.80	27.00	38.00	43.00	32.00	30.47	34.21

Sheared Mafic Rocks

	JSM109	DWN102	JSM6	JSM110	JSM108	JSM108	DWN05	DWN06
SiO2	53.02	54.89	47.60	52.21	50.62	50.29	51.44	49.34
TiO2	2.57	2.54	3.16	2.28	3.26	3.28	2.85	2.84
Al2O3	16.40	16.02	16.81	15.17	13.19	13.15	15.12	16.21
Fe2O3	13.68	14.22	18.19	15.49	17.23	17.34	16.03	16.89
MnO	0.15	0.16	1.07	0.23	0.21	0.21	0.33	0.30
MgO	4.69	4.80	5.80	5.42	4.66	4.74	5.02	5.10
CaO	3.76	3.73	6.21	7.77	8.05	8.17	6.28	6.65
Na2O	3.33	1.25	0.09	0.05	0.03	0.05	0.80	0.10
K2O	1.70	1.72	0.44	1.02	2.31	2.30	1.58	2.12
P2O5	0.70	0.69	0.64	0.37	0.46	0.48	0.56	0.45
TOTAL	100.00	100.00	100.00	100.00	100.00	100.00	100.00	100.00
Nb	19.00	61.00	55.00	9.80	17.00	14.00	29.30	16.60
Zr	245.00	241.00	222.00	123.00	231.00	198.00	376.67	223.10
Y	61.00	190.00	170.00	36.00	53.00	52.00	93.67	88.30
Sr	322.00	998.00	1080.00	414.00	305.00	325.00	524.15	607.69
Rb	154.00	67.00	75.00	57.00	130.00	145.00	104.67	93.80

REFERENCES

Ackerman, E., 1960. Strukturen im Untergrund eines interkratonischen Doppel-Orogens (Irumiden, Nordrhodesien). Geol Rundschau, 50, 538 - 553.

Ahrendt, H., Huntziker, J.C. and Weber, K., 1978. Age and degree of metamorphism and time of nappe emplacement along the southern margin of the Damara Orogen /Namibia (SW Africa). Geol. Rundsch, 67(2), 719 - 742.

Anhaeusser, C.R., and Button, A., 1974. A review of Southern African Stratiform Ore Deposits - Their Position in Time and Space. Econ. Geol Res Unit Univ Witwatersrand Inf Circ No. 85, 1 - 48.

Arculus, R.J., 1987. The Significants of Source versus Process in the Tectonic Controls of Magma Genesis. Journal of Volcanology and Geothermal Research, 32, 1 - 12.

Bailey, D.K., 1983. The chemical and thermal evolution of rifts. Tectonophysics, 94, 585-597.

Bloomfield, K., 1981. The Pan-African Event in Malawi and Eastern Zambia. In Hunter, D.R., (Ed.), Precambrian of the Southern Hemisphere, Elsevier Publ. Co., Amsterdam, 743 - 754.

Boocock, C., 1968. Ann. Rep. Geol. Surv. Botswana for 1967. 40p.

Borg, G. and Maiden, K.J., 1986a. A preliminary appraisal of the Tectonic and Sedimentological environment of the Sinclair Sequence in the Klein Aub area. Comms. Geol. Surv. SWA/Namibia 2, 65 - 73.

Borg, G. and Maiden, K.J., 1986b. Stratabound copper-silver-gold-mineralization of late Proterozoic age along the margin of the Kalahari Craton in SWA/Namibia and Botswana. Can. Mineral., 24 :178

Borg, G and Maiden, K.J., 1987a. Alteration of late Middle Proterozoic volcanics and its relation to stratabound copper-silver-gold mineralization along the margin of the Kalahari Craton in SWA/Namibia and Botswana. J.Geol. Soc. London, in press.

Borg, G and Maiden, K.J., 1987b. The Kalahari Copper Belt of SWA/Namibia and Botswana. Geol Assoc. Can., Spec. Pap., in press.

Borg, G. 1988. The Koras-Sinclair-Ghanzi rift in Southern Africa. Volcanism, sedimentation, age relationships and geophysical signature of a late middle Proterozoic rift system. Precambrian Research, 38, 75-90.

Cahen, L., 1970. Igneous activity and mineralization episodes in the evolution of the Kibaride and Katangide Orogenic Belts of Central Africa. (In) Clifford, T. N. and Gass, I. G., (Eds.), African Magmatism and Tectonics. Oliver and Boyd, Edinburgh, 97 - 118.

Cahen, L. and Leppersonne, J., 1967. The Precambrian of the Congo, Rwanda, and Burundi. In K. Rankhama (Ed), The Precambrian, 3. Interscience Publ., London, 143 - 290.

Cahen, L and Snelling, N.J. 1984. The Geochronology and Evolution of Africa. Clarendon Press, Oxford, 512 pp.

Chappell, B.W. and White, A.J.R., 1974. Two contrasting granite types. Pacific Geol.,8, 173 - 174.

Cook, E.F., 1966. Palaeovolcanology. Earth Sci. Reviews., 1, 155-174.

Cooke, R., 1965. A preliminary report on the Gold occurrences of Swartmodder and Kobos 321, Rehoboth. Report Geol. Surv. S.W.A. (Unpubl.)

De Kock, W.P., 1934. The Geology of the Western Rehoboth, an explanation of Sheet F33-W3. Mem. Dep. Mines. S.W.Afr., 148 pp.

Floyd, P.A. and Winchester, J.A., 1975. Magma type and tectonic setting discrimination using immobile elements. Earth Planet. Sc. Lett., 27, 211-218.

Grobler,N.J., Botha, B.J.V. and Smit, C.A., 1977. The tectonic setting of the Koras Group. Trans. Geol. Soc. S. Afr., 80, 167-176.

Handley, J.R.F., 1965. General Geological succession on the farm Klein Aub 350 and environs, Rehoboth District, South West Africa. Trans. Geol. Soc. S Afr. LXVIII, 211 - 224.

Hartman, O., Hoffer, E., and Haack, U., 1983. Regional metamorphism in the Damara Orogen: interaction of crustal motion and heat transfer. Geol Soc S Afr Spec Publ No 11, p 515.

Hartnady, C., Joubert, P and Stowe, C., 1985. Proterozoic Crustal Evolution in Southwestern Africa. Episodes 8, 236 - 244.

Heindrich, K.F.J., 1966. X-ray absorption uncertainty. In McKinley, T.D., Heindrich, K.F.J. and Whittry, D.B., (Eds.), The electron microprobe

Hoal, B.G., 1989. Isotopic evolution of the Middle to Late Proterozoic Awasib Mountain Terrain in Southern Namibia. Precambrian Research, 45, 175-189.

Hoal, B.G., 1989. Proterozoic crustal evolution of the Awasib Mountain Terrain, Southern Namibia, with special reference to the volcanic Haiber Flats Formation. Ph.D thesis (unpubl.) Univ. Cape Town (251 pp.)

Irvine, T.N. and Baragar, W.R.A., 1971. A guide to the chemical classification of the common volcanic rocks. Can. J. Earth Sc., 8, 523-548.

Jensen, L.S., 1976. A new cation plot for classifying subalkalic volcanic rocks. Geochem. et Cosmochim., 38, 611-627.

Kröner, A., 1976. Proterozoic crustal evolution in parts of Southern Africa and evidence for extensive sialic crust since the end of the Archaean. Phil Trans. R. Soc. Lond. A280, 541 - 544.

Kröner, A., 1977. The Sinclair aulacogen - a late Proterozoic volcano-sedimentary association along the Namib Desert of southern Namibia (SWA). 9th Colloquium Afr. Geol., Göttingen: 82-83 (abstract)

Kuno, H., 1968. Differentiation of basaltic magma. 632-688. In: Hess, H.H. and Poldervaart, A (Eds.), Basalts. Wiley, Intersciences New York.

Lofgren, G., 1971. Textures in natural rhyolitic glass. Geol. Soc. Am. Bull., 82, 111-124.

Mac Donald, G.A., 1968. Composition and origin of Hawaiian lavas. Geol. Soc. Am. Mem., 116, 477-522.

Malling, S., 1975. Some aspects of the Lithostratigraphy and tectonometamorphic evolution in the Nauchas - Rehoboth Area SWA/Namibia, 13th Ann. Rep. Precamb. Res Unit, Univ of Cape Town, pp 159.

Martin, H., 1965. The Precambrian Geology of South West Africa and Namaqualand. Precambrian Res. Unit, Univ. Cape Town., 159 pp.

Martin, H. and Porada, H. 1977. The intracontinental branch of the Damara orogen in South West Africa. 1. Discussion of geodynamic models. Precambrian Research: 5, 311-338.

Mason, R., 1981. Mobile Belts. (In) Hunter, D.K. (Ed.), Precambrian of the Southern Hemisphere. Elsevier Sci. Pub. Co. Amsterdam, 754 - 781.

Miller, R McG (Ed.), 1983. Evolution of the Damara Orogen of South West Africa/Namibia. Geol Soc S Afr Spec Publ No 11, p 515.

Norrish, K. and Hutton, J.T., 1969. An accurate X-ray spectrographic method for the analysis of a wide range of geologic samples. Geochim. et Cosmochim., 33, 431-453.

Pearce, J.A., 1976. Statistical analysis of major element patterns in basalts. J. Petrol., 17, 15-43.

Pearce, J.A., 1982. Trace element characteristics of lavas from destructive plate boundaries. In : R.S. Thorpe (editor), Andesites. John Wiley & Sons, New York, N.Y., pp. 525-548.

Pearce, J.A. and Cann, J.R., 1973. Tectonic setting of basic volcanic rocks determined using trace element analyses. Earth Planet. Sci. Lett., 19, 290-300

Pearce, T.H., Gorman, B.E. and Birkett, T.C., 1975. The TiO_2-K_2O-P_2O_5 diagram: a method of discriminating between oceanic and non-oceanic basalts. Earth Planet Sci. Lett., 24: 419-426.

Pearce, T.H., Gorman, B.E. and Birkett, T.C., 1977. The relationship between major element chemistry and tectonic environment of basic and intermediate volcanic rocks. Earth Planet. Sci. Lett., 36, 121-132.

Pearce, J.A., Harris, N.B.W. and Tindle, A.G., 1984. Trace element discrimination diagrams for the tectonic interpretation of igneous rocks. J. Petrol., 25, 956-983.

Pirajno, F. and Jacob, R.E., 1984. A review of Archaean, Proterozoic Tectonic Provinces, and patterns of Crustal Evolution in Southern Africa. Unpubl M.Sc Course notes. Dept Geol Rhodes University, Grahamstown.

Piper, J.D.A., 1974. Proterozoic crustal distribution, mobile belts and apparent polar movements. Nature, 251, 381 - 384.

Porada, H., 1979. The Damara-Ribera orogen of the Pan African-Brazilliano cycle in Namibia (South West Africa) and Brazil as interpreted in terms of continental collision. Tectonophysics, 57, 237-265.

Pretorius, D.A., 1984. The Proterozoic basins of Southern Africa : Tectonic Settings, pattern of evolution and distribution of gold mineralization. Course notes; M.Sc Min. Expl. Rhodes University, Grahamstown.

Reeves, C.V., 1978. Reconnaisance Aeromagnetic Survey of Botswana II: Its contributions to the geology of the Kalahari. Bull 22 Geol Surv Dept Botswana, 67 - 92.

Reid, D.L. 1984. Some aspects of Proterozoic Igneous activity in the West Namaqua Province, lower Orange River Region. (Abst.) Conference on Middle to late Proterozoic lithosphere evolution. Precamb Res. Unit. Univ Cape Town.

Reid, D.L., Malling, S., and Allsopp, H.L., 1988. Rb-Sr ages of granitoids in the Rehoboth-Nauchas Area, South West Africa/Namibia. Comms. Geol. Surv. S.W.Africa/Namibia. 4, 19 - 27.

Reuning, E., 1937. Die Goldfelder von Ondundu, Südwestafrika. Gold Runchsch, **28**, 229-239.

Ruxton, P.A., 1981. The sedimentology and diagenesis of copper-bearing rocks of the southern margin of the Damara Orogenic Belt. Unpubl. Ph.D thesis Univ Leeds.

Ruxton, P.A., 1986. Sedimentology, isotopic signature and ore genesis of the Klein Aub Copper Mine, South West Africa/Namibia. (In) Anhauesser, C. R., Maske, S., (Eds.), Mineral Deposits of Southern Africa II, 1726 - 1738.

Ruxton, P.A. and Clemmey, H., 1986. Late Proterozoic stratabound and red bed-copper deposits of the Witvlei area, South West Africa/Namibia. (In) Anhauesser, C.R., Maske, S., (Eds.), Mineral Deposits of Southern Africa II, 1726 - 1738.

Sanderson - Damstra, C.G., 1982. Geology of the Central and Southern Domains of the Koras Group, Northern Cape Province. Unpubl. M.Sc thesis, Rhodes University, Grahamstown.

Sawkins, F.J., 1984. Metal deposits in relation to plate tectonics. Berlin, Springer, 325p.

Shackleton, R.M., 1973. Correlation of structures across Precambrian Orogenic Belts in Africa. In D.H. Tarling and S.K. Runcorn (Eds.), Implication of Continental Drift to the Earth Sciences, 2. Academic Press, London, 1091 - 1095.

Shand, S.J., 1927. **Eruptive rocks.** Wiley, New York, 488 pp

Siefret, N.L., 1986a. (In) Geochemistry of the Rehoboth basement Granitoids, SWA/Namibia. Stoessel, G.U.F. and Ziegler, U.R.F., 1988. Comms. Geol Surv. S.W.Africa/Namibia, 4, 71 - 81 .

Siefret, N.L., 1986b. (In) Geochemistry of the Rehoboth basement Granitoids, SWA/Namibia. Stoessel, G.U.F. and Ziegler, U.R.F., 1988. Comms. Geol Surv. S.W.Africa/Namibia, 4, 71 - 81 .

Smalley, T.J., 1989. A reconnaysance mapping of the Northern Portion of the Neuras Grant M143/43. Gold Fields of Namibia in House Report.

South African Committee for Stratigraphy (SACS), 1980. Stratigraphy of South Africa. Part 1: (Comp L E Kent) Lithostratigraphy of the Republic of South Africa, South West Africa/Namibia and the Republics of Boputhatswana, Transkei and Venda. Handb. Geol. Surv. S. Afr. 8.

Steven, N. 1990. Gold mineralization in the central belt, Namibia. Provisional title, Ph.D Thesis (in prep.) Univ. Cape Town.

Stoessel, G.F.U. and Ziegler, U.R.F., 1988. Geochemistry of the Rehoboth Basement Granitoids, SWA/Namibia. Comms. Geol. Surv. S.W.Africa/Namibia, 4, 71 - 81.

Streckeisen, A. 1976. To each plutonic rock its proper name. Earth Sci. Rev., 12: 1-33.

Thomas, C.M., 1973. Brief explanation of the geology of South Ngamiland (quarter degree sheet 2022D with parts of 2022C and 2023C). Geol. Surv. Botswana.

Toens, P.D., 1975. Geology of part of the foreland of the Damara Orogenic Belt in South West Africa and Botswana. Geol. Rundsch., 64, 175 - 192.

Turner, F.J., 1981. Metamorphic Petrology: mineralogical, field and tectonic aspects. 2nd edition, McGraw-Hill, Washington.

Twist, D. and Harmer, R.E.J., 1987. Geochemistry of contrasting siliceous magmatic suites in the Bushveld Complex; genetic aspects and implications for tectonic discrimination diagrams. Journal of Volcanology and Geothermal Research, 32, 83 - 89.

Watters, B.R., 1974. Stratigraphy, igneous petrology and evolution of the Sinclair Group in southern South West Africa. Bull. 16, Precamb. Res. Unit, Univ. Cape Town, 235p.

Watters, B.R., 1976. Possible late-Precambrian subduction zone in South West Africa. Nature, 259, 471 - 473.

Watters, B.R., 1977. The Sinclair Group : definition and regional correlation. Trans. Geol. Soc. S. Afr., 80, 9 - 16.

Watters, B.R., 1982. A Sr-isotopic study of a suite of Precambrian Shoshonites from the Sinclair Group in Southern Namibia. Trans. Geol. Soc. S. Afr., 85, 81 - 86.

Winchester, J.A. and Floyd, P.A., 1976. Geochemical magma type discrimination: application to altered and metamorphosed basic igneous rocks. Earth Planet Sci. Lett., 28: 459-469.

Winchester, J.A. and Floyd, P.A., 1977. Geochemical discrimination of different magma series and their differentiation products using immobile elements. Chem. Geol., 22, 325-343.

Winkler, H.G.F., 1979. Petrogenesis of metamorphic rocks. 5th edition, Springer-Verlag, New York.

Ziegler, U.R.F. and Stoessel, G.F.U., 1988. K-Ar dating of the Marienhof and Billstein Formations in the Rehoboth Basement Inlier, SWA/Namibia. Comms. Geol. Surv. S.W.Africa/Namibia, 4, 45 - 50.

ACKNOWLEDGEMENTS

I would like to express my sincere gratitude to the following people and organizations for their help and time during the course of this project:

1. Gold Fields Namibia - for setting up the project, financial help and logistical assistance in the field. In particular I would like to thank Dudley Corbett for his assistance and dedicated supervision as well as my field crew Paulas Hamukwaya and Silvanus for their assistance. Mr John Pescha is also thanked for drafting of the many maps.

2. My supervisors, Prof. R.E. Jacob, Prof. F. Piranjo and C.A. Mallinson, for their guidence and advice throughout my studies. Prof. J.S. Marsh is kindly thanked for his help with the XRF work and stimulating discussions.

3. The technical staff of the Geology Department, Rhodes University, for their assistance, namely Able Roman.

4. My fellow students, Mike Brennen, Ian De Klerk, Tom Nowicki, Fabrice Matheys, Marilena Moroni, Warwick Bullen and Link Linklater for companionship throughout the duration of this degree.

5. Charlie Hoffmann of the Geological Survey of Namibia, and Tim Smalley for thought provoking discussions.

6. My parents and girlfriend, Fiona Taylor, for their constant support and encouragement.

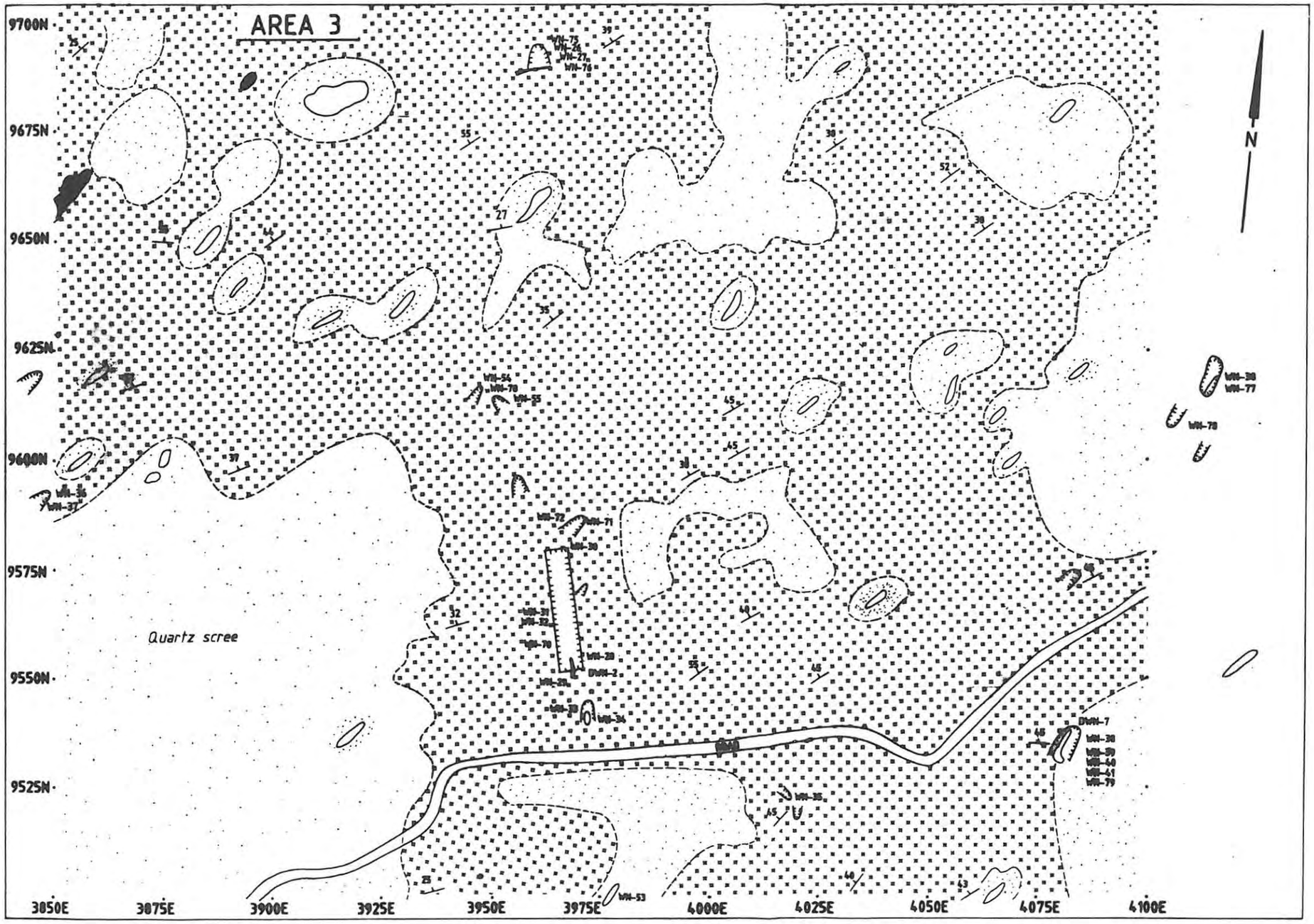

AREA 3

WN - 26	61 ppb	:	Q. - veins adj. mafic dyke
WN - 27	122 ppb	:	Q. - veins adj. mafic dyke
WN - 28	1323 ppb	:	Q. - ht - mt vein
WN - 29	63 ppb	:	Q. - vein
WN - 30	4362 ppb	:	goss - Q. - vein (-3m)
WN - 31	353 ppb	:	goss - Q. (-1m)
WN - 32	N/D	:	goss - Q. - vein
WN - 33	4521 ppb	:	Q. - ht - vein
WN - 34	5000 ppb	:	Q. - ht - py vein (-2.5m)
WN - 35	300 ppb	:	Q. - ht vein
WN - 36	43 ppb	:	Q. - ht - goss. vein
WN - 37	650 ppb	:	Q. - ht - py vein
WN - 38	1303 ppb	:	goss. - Q. - vein
WN - 39	4087 ppb	:	Q. - ht -py vein
WN - 40	541 ppb	:	Q. - ht - vein
WN - 41	N/D	:	Q. - ht - py vein
WN - 53	N/D	:	Q. - vein
WN - 54	370 ppb	:	Q. - ht - vein
WN - 55	N/D	:	Q. - ht - vein
WN - 71	52 ppb	:	host. gdr.
WN - 72	5000 ppb	:	Q. - ht - vein
WN - 75	N/D	:	gdr.
WN - 76	49 ppb	:	host. gdr.
WN - 77	44 ppb	:	host. gdr.
WN - 78	49 ppb	:	alt. gdr.
WN - 79	N/D	:	alt. gdr

AREA 7

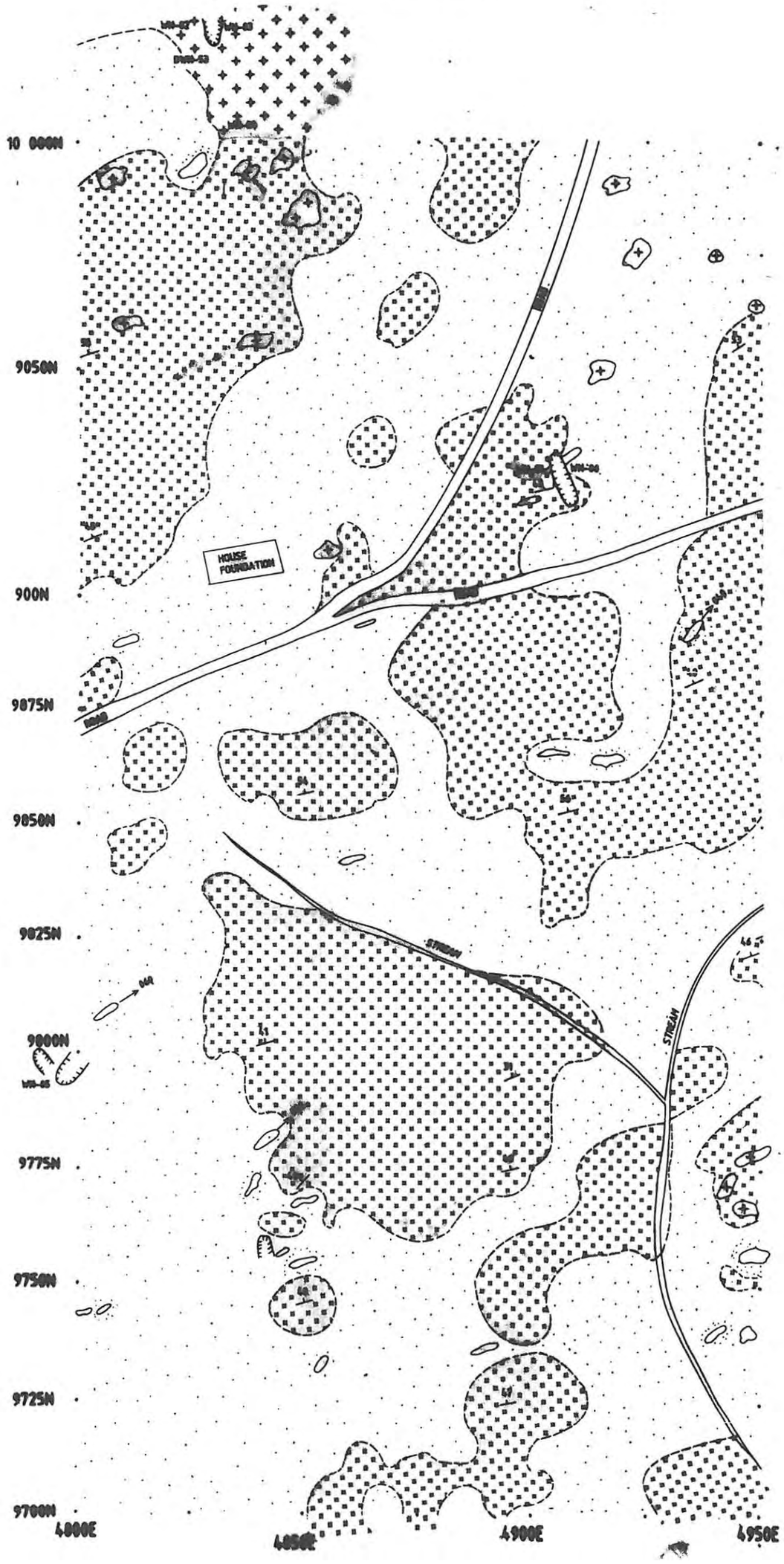

N

AREA 7			
WN - 80	44 ppb	:	alt. gdr
WN - 81	65 ppb	:	ferrug. gdr
WN - 82	5000 ppb	:	Q - ht - goss v
WN - 83	N/D	:	host. Q-po
WN - 84	235 ppb	:	py-rich granite
WN - 85	N/D	:	Q - ht vein

AREA 17

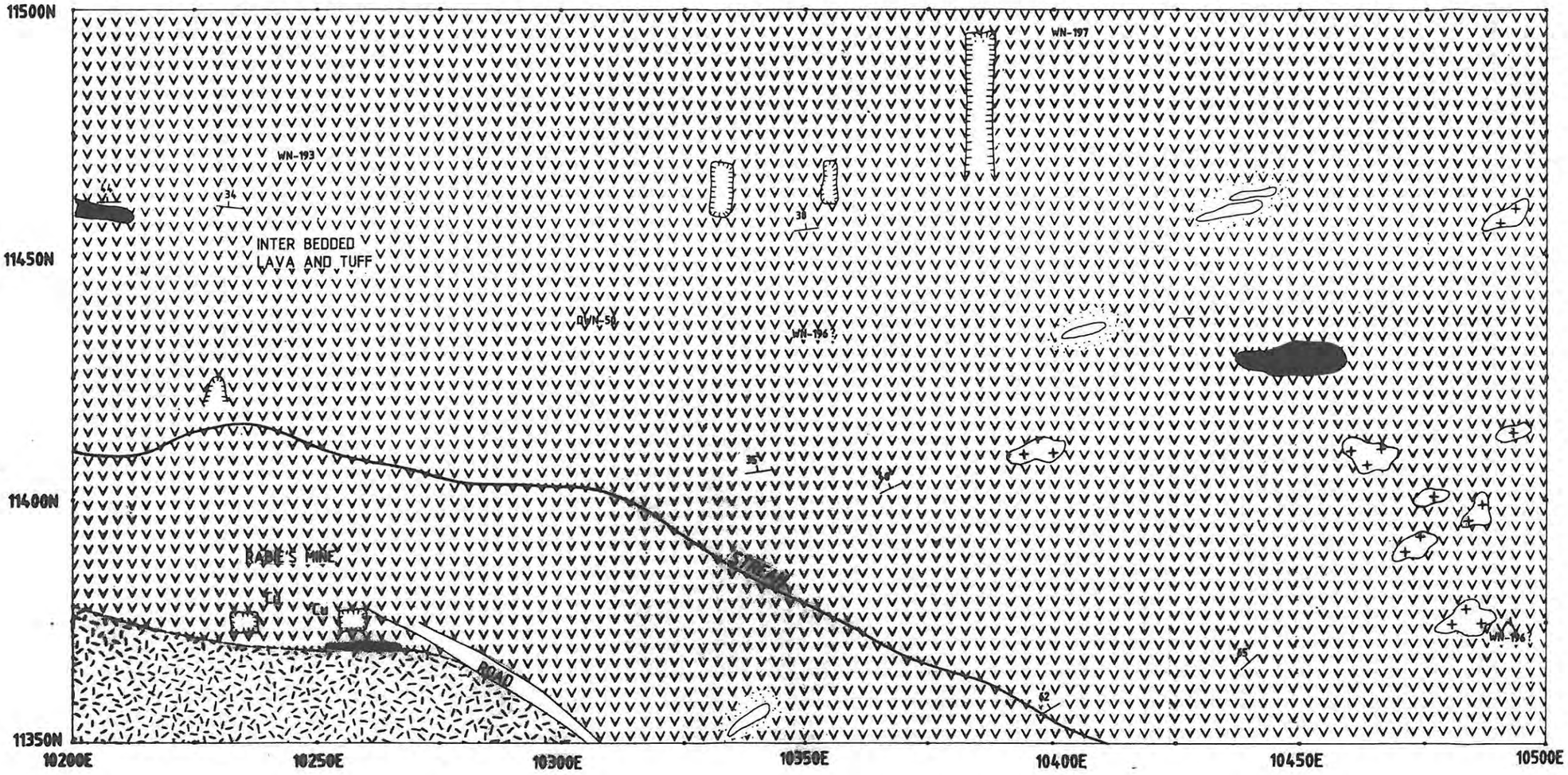

AREA 17

WN - 193	N/D	:	rhyolite
WN - 194	533 ppb	:	Q - ht veins
WN - 195	42 ppb	:	host rhyolite to veins
WN - 196	67 ppb	:	rhyolite

AREA 18

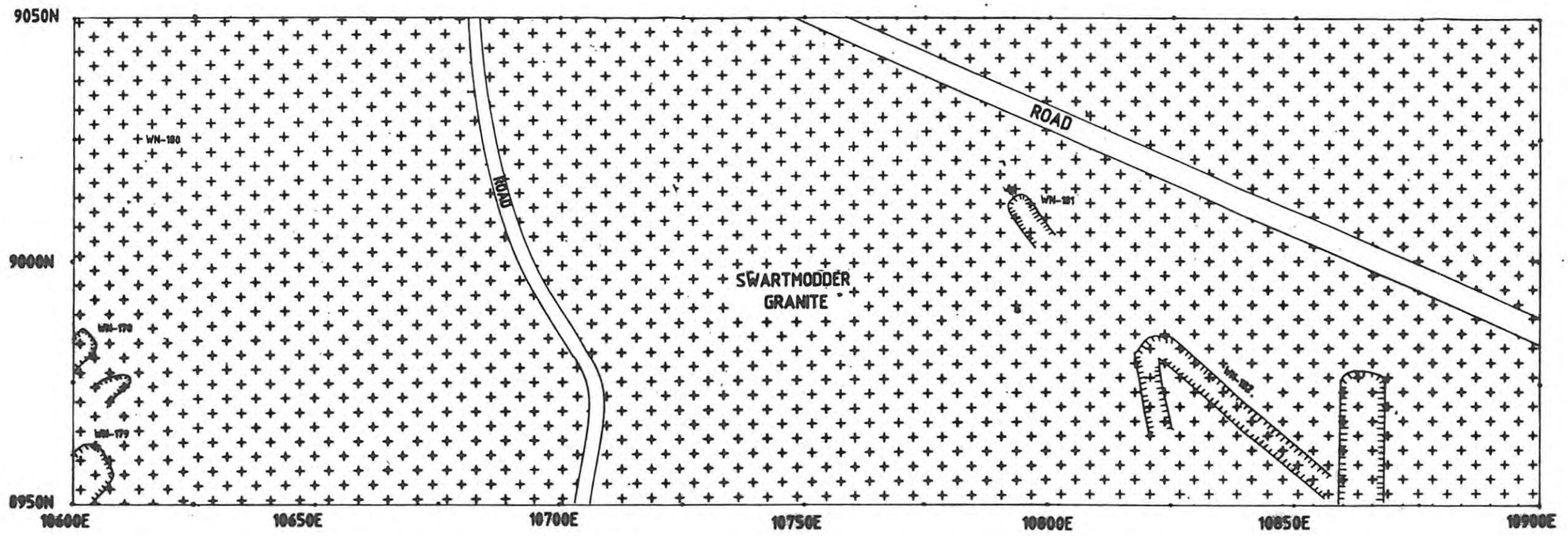

AREA 18

WN-178	46 ppb	:	ferrug. Sm - granite
WN-179	69 ppb	:	ferrug. Sm - granite
WN-180	N/D	:	Sm. - granite (Un. alt.)
WN-181	107 ppb	:	ferrug. Sm - granite
WN-182	41 ppb	:	ferrug. Sm. - granite

AREA 19

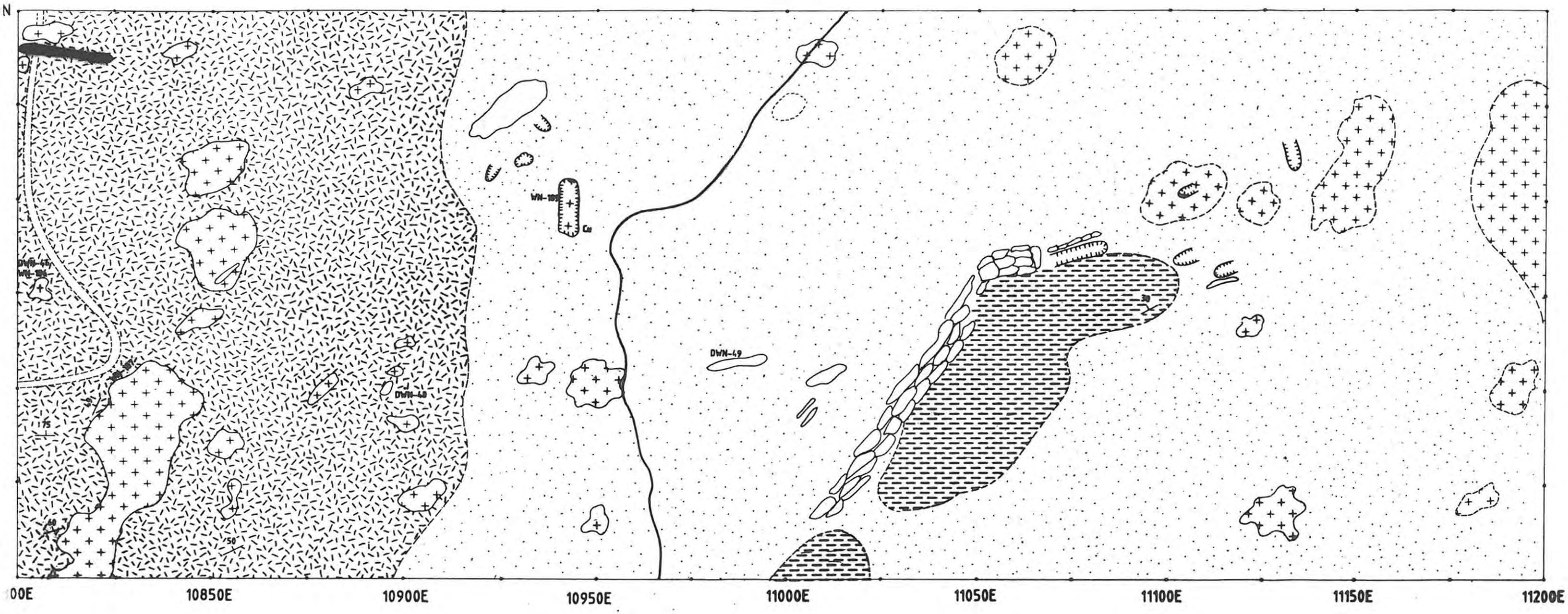

AREA 19

WN - 186	57 ppb	: ferrug. Sm. - granite
WN - 187	97 ppb	: ferrug. Sm. - granite
WN - 188	80 ppb	: Cu - rich schist
WN - 189	1407 ppb	: composite sample ferrug. Sm-granite